Role of the nucleotide oligomerization domain-like receptor protein 7 in the pathology of recurrent hydatidiform moles

Elie Akoury

Department of Human Genetics
McGill University
Montreal, Quebec, Canada

February 2016

A thesis submitted to McGill University in partial fulfillment of the requirements of the degree of Doctor of Philosophy

TABLE OF CONTENTS

ABSTRACT

A molar pregnancy or hydatidiform mole (HM) is a human pregnancy with no embryo, but cystic degeneration of chorionic villi and excessive proliferation of the trophoblast. Mutations in *NLRP7,* a member of the nucleotide-binding domain and leucine-rich repeat-containing receptors family of proteins with roles in inflammation and apoptosis, are responsible for recurrent hydatidiform moles (RHMs). In previous studies, we demonstrated that *ex vivo* stimulated peripheral blood mononuclear cells (PBMCs) from patients with *NLRP7* mutations secrete lower levels of interleukin 1 beta (IL1B) and tumor necrosis factor (TNF) than control cells despite the fact that patients' cells have normal to slightly higher intracellular levels of IL1B. **We hypothesized that *NLRP7* mutations do not alter IL1B synthesis or processing but affect the microtubules and consequently intracellular cytokines trafficking**. To address this hypothesis, I first characterized the expression and subcellular localization of NLRP7 in PBMCs. Using immunofluorescence, I showed that NLRP7 is expressed in all PBMC subpopulations before and after LPS stimulation including monocytes, which are the main cells that express and secrete IL1B and TNF in response to LPS stimulation. Additionally, I found that NLRP7 localizes to the microtubule organizing center (MTOC) and the Golgi apparatus in various hematopoietic cell lines. The localization of NLRP7 to the MTOC and Golgi drew our attention to check for any possible dependence of NLRP7 signal on microtubules at these two locations. Toward this goal, I treated Epstein Barr Virus transformed B-lymphocytes (EBV) cells from control subjects with nocodazole, a microtubule disrupting agent, and found that this treatment disrupts the NLRP7 signal, which became more diffuse and fragmented around the nucleus. These results suggest that *NLRP7* mutations impair cytokine secretion by affecting microtubules. The identification of *KHDC3L* as the second gene for RHMs prompted us to investigate the expression and subcellular localization of its protein in hematopoietic cells. Using immunofluorescence, I found that KHDC3L co-localizes with NLRP7 to the MTOC and Golgi apparatus in control EBV cells (data not shown). The similarities in the subcellular localization of NLRP7 and KHDC3L suggested that they may share a common function in IL1B and TNF secretion. To understand the role of NLRP7 and KHDC3L in RHMs, I sought to determine their subcellular localization in control human oocytes and early cleavage embryos, stages at which the disease starts. Using confocal immunofluorescence and electron microscopies, I found that NLRP7 co-localized with KHDC3L mainly to the cortical region in oocytes from the germinal

vesicle (GV) until the formation of the zygote. Within the cortex, electron and high resolution confocal microscopies confirmed the co-localization of NLRP7 and KHDC3L between cortical granules, mitochondria, and other organelles on oocyte cytoskeletal structures subsequently identified as the human subcortical maternal complex (SCMC). Additionally, we found that NLRP7 co-localizes with OOEP, another member of the SCMC and depends on alpha tubulin microtubules and filamentous actin networks. Between 2-cell and morula stages, both NLRP7 and KHDC3L signals were restricted to the outer cortical regions and absent from the cell-to-cell contact region. At the blastocyst stage, NLRP7 and KHDC3L relocate to the cytoplasm and nucleus, respectively, of the inner cell mass (ICM) and the trophectoderm. Collectively, our data implicate roles for NLRP7 and KHDC3L directly or indirectly in the cytoskeleton and open up new areas of research to investigate the role of these two maternal-effect proteins in the manifestation of HM.

RÉSUMÉ

La grossesse molaire ou môle hydatiforme (HM) est une pathologie de la grossesse humaine caractérisée par l'absence du développement embryonnaire, la dégénérescence kystique des villosités choriales et la prolifération excessive du trophoblaste. Des mutations du gène *NLRP7*, membre de la famille NLRP jouant un rôle dans l'inflammation et l'apoptose, sont responsables de môles récurrentes (RHMs). Nous avons auparavant démontré que les cellules mononucléées du sang périphérique (PBMCs), isolées de patientes ayant des mutations de *NLRP7,* sécrètent des interleukines 1 bêta (IL1B) et des facteurs de nécrose tumorale (TNF) à un taux inférieur à celui des cellules contrôles alors même que le taux intracellulaire d'IL1B est normal ou légèrement augmenté dans les cellules de patientes. **Suite à ces observations, nous avons émis l'hypothèse que les mutations de *NLRP7* ne modifient pas la synthèse ou le processus de maturité d'IL1B mais affectent les microtubules et par conséquence le trafic intracellulaire des cytokines.** Pour vérifier cette hypothèse, j'ai d'abord caractérisé l'expression et la localisation cellulaire de NLRP7 dans les PBMCs par immunomarquage. NLRP7 est exprimée dans toutes les sous-populations de PBMCs avant et après la stimulation par LPS, y compris les monocytes, les principales cellules sécrétant IL1B et TNF après stimulation. En outre, j'ai trouvé que NLRP7 se localise au niveau du centrosome et de l'appareil de Golgi dans plusieurs lignées hématopoïétiques. Cette localisation nous a incités à vérifier une éventuelle dépendance du signal de NLRP7 sur les microtubules à ces deux endroits. Dans ce but, j'ai traité des cellules EBV contrôles avec du nocodazole, un agent de dépolymérisation microtubulaire, et constaté que ce traitement perturbe le signal de NLRP7, qui devient plus diffus et fragmenté autour du noyau. Ces résultats suggèrent que les mutations du *NLRP7* altèrent la sécrétion de cytokines en affectant les microtubules. J'ai également caractérisé l'expression et la localisation de KHDC3L*,* la protéine du second gène responsable de RHM, dans les cellules hématopoïétiques. J'ai montré la co-localisation de KHDC3L et de NLRP7 au centrosome et l'appareil de Golgi dans des cellules EBV contrôles (résultats non montrés). La similitude dans la localisation cellulaire de NLRP7 et KHDC3L suggère que ces deux protéines peuvent partager une fonction commune dans la sécrétion d'IL1B et de TNF. Pour comprendre le rôle de NLRP7 et KHDC3L dans les RHMs, j'ai caractérisé leurs localisations cellulaires dans des ovocytes et des embryons humains contrôles, les stades de développement au cours desquels la maladie commence. En utilisant l'immunomarquage et le microscope confocal, j'ai

trouvé que NLRP7 co-localise avec KHDC3L principalement à la région corticale dans les ovocytes au stade de vésicule germinale (GV) jusqu'à celui de la formation du zygote. En utilisant la microscopie électronique et le confocal à haute résolution, j'ai confirmé la localisation de NLRP7 et de KHDC3L au niveau du cortex entre les granules corticaux, les mitochondries et différents organites. J'ai également constaté que NLRP7 s'attache sur des structures ovocytaires identifiées par la suite comme le complexe maternel sous-cortical (SCMC), co-localise avec OOEP, un autre membre de la SCMC et dépend des microtubules et des filaments d'actine. Au stade embryonnaire de deux cellules et morula, NLRP7 et de KHDC3L étaient présentes à la région corticale externe et exclues des zones de contact entre blastomères. Au stade du blastocyste, NLRP7 et KHDC3L se déplacent dans le cytoplasme et le noyau, respectivement, du bouton embryonnaire et du trophectoderme. Au total, nos données impliquent NLRP7 et KHDC3L directement ou indirectement dans le cytosquelette et ouvrent de nouveaux horizons de recherche pour étudier le rôle de ces deux protéines à effet maternel dans la physiopathologie des grossesses molaires.

LIST OF FIGURES

Chapter 1

Chapter 2

Chapter 3

LIST OF TABLES

Chapter 1

Chapter 2

Chapter 3

Chapter 4

-NA-

Chapter 5

Chapter 6

-NA-

LIST OF ABBREVIATIONS

AGBL3	ATP/GTP binding protein-like 3
Alu-Yb8	Arthrobacter luteus Yb8 subfamily
AR	Androgen receptor
ATP	Adenosine 5′-triphosphate binding motif
BF-1	Brain factor 1
BhCG	Beta human chorionic gonadotropin
BSA	Bovine serum albumin
CDKN1C	Cyclin dependent kinase inhibitor 1C
CDKN2A	Cyclin dependent kinase inhibitor 2A
CHM	Complete hydatidiform mole
CPL	Cytoplasmic lattice
DAPI	4,6-diamidino-2-phenylindol-2-HCl
D&C	Dilatation suction and curettage
DMEM	Dulbeco's modified Eagle's medium
DMR	Differentially methylated region
DMSO	Dimethyl sulfoxide
EBV	Epstein Barr virus transformed B-lymphocyte
ELISA	Enzyme-linked immunosorbent assay
ESC	Embryonic stem cell
FBS	Fetal bovine serum
FBXO4	F-Box only protein 4
FIGO	International federation of gynecology and obstetrics
GLIS3	GLI-similar zinc finger 3
GNAS	Guanine nucleotide binding protein (G Protein), alpha stimulating
GNAS-1A	Guanine nucleotide binding protein(G Protein), alpha stimulating exon 1A
GNAS-AS	Guanine nucleotide binding protein(G Protein), antisense RNA
GNAS-XLαS	Guanine nucleotide binding protein (G Protein) extra-large alpha subunit
GNAS-NESP55	Guanine nucleotide binding protein (G Protein) neuroendocrine secretory protein 55
GTD	Gestational trophoblastic diseases
GTN	Gestational trophoblastic neoplasia
GV	Germinal vesicle
H19	H19 imprinted maternally expressed transcript
HEK293	Human embryonic kidney 293 cell
HIC-1	Hypermethylated in cancer 1
HM	Hydatidiform mole
ICM	Inner cell mass
ICSI	Intracytoplasmic sperm injection
IG	Intergeneic

IL1B	Interleukin 1 beta
IVF	*In vitro* fertilization
KCNQ1OT1	Potassium channel, voltage gated KQT-like subfamily Q member 1
KH	K homology domain
KHDC1	KH homology domain containing 1
KHDC3L	KH domain containing 3-like
L3MBTL1	Lethal (3) malignant brain tumor-like protein 1
LIN28B	Lin-28 Homologue B
LINE-1	Long interspersed nuclear elements 1
LPS	Lipopolysaccharide
LRR	Leucine-rich repeats
MEG3	Maternally expressed 3
MCCC1	Methylcrotonoyl-CoA Carboxylase 1 (Alpha)
mRNA	Messenger RNA
MTOC	Microtubule organizing center
NACHT	NAIP, CIITA, HET-E, and TP1 family
NAD	NACHT-associated domain
NAP1L5	Nucleosome assembly protein 1-like 5
NLRP7	Nucleotide oligomerization domain-like receptor protein 7
NLS	Nuclear localization signal
NSV	Nonsynonymous variant
PBMC	Peripheral blood mononuclear cell
PBS 1x	Phosphate buffered saline
PCR	Polymerase chain reaction
PDI	Protein disulfide isomerase
PEG1	Paternally expressed gene 1
PEG3	Paternally expressed gene 3
PEG10	Paternally expressed gene10
PFA	Paraformaldehyde
PGK1	Phosphoglycerate kinase 1
PGD	Preimplantation genetic diagnosis
PGS	Preimplantation genetic screen
PHM	Partial hydatidiform mole
PKC	Protein kinase C
PKM	Protein kinase M
POC	Product of conception
PYD	Pyrin domain
RISC	RNA-induced silencing complex
RT-PCR	Polymerase chain reaction after reverse transcription
SCMC	Subcortical maternal complex
siRNA	Small interfering RNA

SNRPN	Small nuclear ribonucleoprotein polypeptide N
SUCGL2	Succinate-CoA ligase GDP-forming, Beta subunit
THP1	Monocytic cell line
TNFα	Tumor necrosis factor alpha
WHO	World health organization
YY1	Yin Yang 1
ZAC	Zinc finger protein which regulates apoptosis and cell cycle arrest
ZBDF2	Zinc finger, DBF-type containing 2
ZBTB16	Zinc finger and BTB domain containing 16
ZFP42	Zinc finger protein 42
ZNF261	Zinc finger protein 261
ZNF597/NAA60	Zinc finger protein 597/N(alpha)-acetyltransferase 60

FORMAT OF THE THESIS

This is a manuscript-based thesis, which conforms with the "Guidelines for Thesis Preparation" of the Faculty of Graduate Studies and Research at McGill University. This thesis is comprised of six chapters, of which three chapters are in the form of manuscripts that were published. Chapter 1 is a literature review/general introduction that recapitulates the background material for this thesis. Chapter 2 is a manuscript that was published in the Journal of Biological Chemistry, 2011 (PMID: 2202561). Chapter 3 is a manuscript that was published in the journal of Human Reproduction in 2014 (PMID: 25358348). Chapter 4 is a manuscript in preparation. Chapter 5 is a manuscript that was published in Reproductive Biomedicine Online (PMID: 25982095). Preface for chapters 3, 4 and 5 are used to connect between the chapters and to ensure the continuity of the thesis. Chapter 6 contains a general overview of the findings from this thesis and discusses them in greater detail, alongside possible future experiments.

The references of all the chapters are provided at the end of the thesis. The appendix of each chapter contains supplemental data that are available on the journal site for the original published chapter. The annex at the end of the thesis contains a) one publication I have worked on during my PhD but not included in the thesis along with the permission of the journal for the four publications (the ones included or the one added as an annex) and b) the certification of ethical acceptability for research involving human subjects.

LIST OF ORIGINAL PUBLICATIONS (INCLUDED IN THE THESIS)

The present thesis is based on the following original publications. It comprises six chapters, three of which are manuscripts that are written in the format they were submitted and one that is in preparation.

(1) **Messaed C*, Akoury E*,** Djuric U, Zeng J, Saleh M, Gilbert L, Seoud M, Qureshi S, Slim R. NLRP7, a nucleotide oligomerization domain-like receptor protein is required for normal cytokine secretion and co-localizes with the Golgi and the microtubule organizing center. J Biol Chem. 2011 Oct. PMID: 22025618.*** The two authors contributed equally to this paper.**

(2) **Akoury E,** Zhang L, Ao A, Slim R**.** NLRP7 and KHDC3L, the two maternal-effect proteins responsible for recurrent hydatidiform moles, co-localize to the oocyte cytoskeleton. Hum Rep.2014 Oct 9. PMID: 25358348.

(3) **Akoury E**, Ao A, Slim R. NLRP7, responsible for recurrent hydatidiform moles, is a possible regulator of the microtubules and filamentous actin networks in human oocytes (manuscript in preparation).

(4) **Akoury E**, Gupta N, Bagga R, Brown S, Déry C, Kabra M, Srinivasan R, Slim R. Live births in women with recurrent hydatidiform mole and two *NLRP7* mutations. Reproductive Biomedicine Online 2015 Apr 16. PMID: 25982095.

<u>Annex</u>

(1) **Akoury E**, El Zir E, Mansour A, Mégarbané A, Majewski J, Slim R. A Novel 5-bp Deletion in Clarin 1 in a Family with Usher Syndrome. Ophthalmic Genet 2011 Nov. 32(4):245-9. PMID: 21675857.

CONTRIBUTION OF AUTHORS

This thesis is based on the following original manuscripts that were published.

Chapter 2

NLRP7, a nucleotide oligomerization domain-like receptor protein, is required for normal cytokine secretion and co-localizes with Golgi and the microtubule-organizing center

Christiane Messaed, Elie Akoury, Ugljesa Djuric, Jibin Zeng, Maya Saleh, Lucy Gilbert, Muhieddine Seoud, Salman Qureshi, and Rima Slim

Manuscript published in the Journal of Biological Chemistry 24 October 2011

I produced the experiments of figures 2.1C, 2.3 and 2.4, supplemental figure 2.1, and contributed to the writing of the manuscript. Christiane Messaed contributed to the generation of the data in figure 2.1 (A, B and D), produced the experiments of figures 2.5, 2.6 and 2.7, supplemental figure 2.2 and 2.3, and contributed to the writing of the manuscript; Ugljesa Djuric contributed majorly to the experiments of figure 2.1 (A, B and D); Jibin Zeng produced the experiment of figure 2.2. Lucy Gilbert and Muhieddine Seoud provided samples for the study. Maya Saleh and Salman Qureshi were involved in the implementation and troubleshooting of some methods and the analysis of the results and in providing us access to equipments in their laboratories. Rima Slim supervised the work and wrote the manuscript.

Chapter 3

NLRP7 and KHDC3L, the two maternal-effect proteins responsible for recurrent hydatidiform moles, co-localize to the oocyte cytoskeleton

Elie Akoury, Li Zhang, Asangla Ao, and Rima Slim

Manuscript published in Human Reproduction 29 October 2014

I designed the study, performed immunofluorescence, confocal and electron microcopy, analyzed the data, coordinated the work, produced all figures and the supplemental table 4.1, and wrote

the manuscript. Li Zhang and Asangla Ao consented patients, collected oocytes and embryos, manipulated oocytes and embryos in all experiments. Rima Slim supervised the design of the study, provided financial support, and wrote the manuscript.

Chapter 4

Elie Akoury, Asangla Ao, and Rima Slim

Manuscript in preparation

I designed the study, performed immunofluorescence, confocal and electron microcopy, analyzed the data, coordinated the work, produced all figures and the supplemental table 4.1, and wrote the manuscript. Asangla Ao consented patients, collected oocytes and embryos; Rima Slim supervised the design of the study and provided financial support, and wrote the manuscript.

Chapter 5

Akoury E, Gupta N, Bagga R, Brown S, Déry C, Kabra M, Srinivasan R, Slim R.

Manuscript published in Reproductive Biomedicine Online 16 April 2015

I reviewed the mutations and their associated reproductive outcomes and wrote the manuscript. Neerja Gupta N.G and Madhulika Kabra referred 2 cases, 626 and 748. Rashmi Bagga and Radhika Srinivasan referred one case 678 and examined the placenta. Stephen Brown referred one case 1077. Christine Déry, cloned the mutations of 678 and established the phase. Rima Slim supervised the mutation analysis and cloning and wrote the manuscript.

ACKNOWLEDGMENTS

I would like to extend my gratitude to my PhD supervisor Dr. Rima Slim for giving me the opportunity to pursue my PhD in her laboratory and her unwavering guidance, help, support and patience.

I am also indebted to my supervisory committee members, Drs. Asangla Ao, Loydie Jerome-Majewska and Yojiro Yamanaka for the invaluable guidance and advice all through my work. I cannot thank you enough Dr. Asangla Ao for your support, wisdom and collaboration during the five years of my Ph.D. Many thanks go as well to my examining committee and to my student advisor Dr. Patricia Tonin.

I would like also to thank Dr. Li Zhang and Xiao Yun Zhang for their support, technical assistance and help in collecting the spare human oocytes and embryos from the patients

I would like to thank my friends and colleagues in Rima's Lab, past and present, for their help and with whom I spent pleasant times in the laboratory. I have been fortunate to work with Wafaa Chebaro, Christiane Messaed, Ramesh Reddy, Florence Grégoire-Briard, Yassemine Khawajkie, Nawel Mechtouf and Pierre Adrien Bolze. I wish you all the best in life because you deserve the best.

I am also grateful to all the people (researchers, physicians, nurses…..) who contributed to this work and especially the patients for donating samples for research purposes.

I acknowledge the financial support granted by the McGill University Health Centre Research Institute (MUHC-RI) and the Réseau Québecois en Reproduction (RQR). I am also indebted and grateful to the department of Human Genetics and the faculty of Medicine for the excellence and travel awards I have been granted during my PhD.

Finally, I would like to express my heartfelt thanks to my family for their support, motivation and love and without whom I probably would never realize my dreams. I am very lucky and grateful to have you in my life.

CHAPTER 1

LITERATURE REVIEW

1.1. Hydatidiform mole

1.1.1. Overview on the history of hydatidiform mole

Hydatidiform mole (HM) is one of the gestational trophoblastic diseases (GTD) that implicate abnormal development of trophoblastic cells, which form the trophectoderm layer of the blastocyst. GTD also includes invasive moles, choriocarcinomas, placental-site trophoblastic tumors and epitheloid trophoblastic tumors. The etymology of HM emerged from the word Hydatisia (Greek ”a drop of water”) pointing to the watery contents of the cysts and the word mole (Latin “mola”) which means millstone and indicates a mass in a woman’s womb (Sebastian, 1999). Hydatidiform mole is an ancient human disease that has puzzled mankind from the earliest times. In one of the modern medical books entitled “Outlines of Greek and Roman Medicine”, the author, James Elliott, indicates that this condition was initially documented in Hippocrates’ treatise (470-410 BC) on “Airs, Water and Places” as dropsy of the uterus resulting from drinking impure water (Elliott, 1971). Almost 1000 years after Hippocrates, Aetius of Amida, a Byzantine Greek physician and medical writer (502-575 AD), described this disease using the expression “mola hydatidosa” in his writings on Greeko-Roman traditions of medicine (Ricci, 1950). According to Aetius, HM may result from an inflammation or local ulcer. A thousand years later, Christophe of Vega, in 1564 in his book "Ars Medendi" indicated the expulsion of “a twelve pound hydatid mole” (Taussig, 1907). At around the same period of time, Schenk of Grafenberg in 1565 and Valleriola in 1573 described spontaneously expelled vesicles from patients and suggested that this phenomenon originates from unfertilized ova, not impregnated by male semen (Taussig, 1907). The descriptions of HM became even more accurate in the book of Lamzweerde from Amsterdam “The Historia Naturalis Molarum Uteri” (Lamzweerde, 1686). This physician described moles as having the same composition of normal embryos and forming after impregnation. According to Lamzweerde, this entity encompasses three principles: a germinal, a milky and a bloody one and is directly caused following either the

absence, lack of complete, or misplacement of elements that are indispensable for the construction of the heart along with some external factors preventing the development.

Towards the latter half of the eighteenth century, many documented observations on this condition including Mauriceau in his "Maladie des femmes" in 1712 (Taussig, 1907). He described moles as a fleshy mass with irregular shape that arose after coitus and was deprived of bones, joints and limbs. According to Mauriceau, moles are formed because of increased frequency of intercourse which results in weakened seeds and consequently an organism with incomplete development. Almost a decade later, Friedrich Ruysch of Amestrdam in 1721 explained that moles can persist in women's womb for months without causing injuries (Taussig, 1907). Thirty years later, Smellie (1752) ascribed molar structures as "bunch of grapes of different sizes" (Brews, 1939). The abnormal accumulation of fluids in the dilated chorionic villi (the grapes) was perceived by Velpeau and Boivin in the first half of the nineteen century in 1827 (Sebastian, 1999). At the end of the nineteenth century, Marchand and shortly afterwards Langhans uncovered the cellular nature constituting moles and explained that the proliferation of the trophoblast is at the origin of the molar manifestation (Langhans, 1901; Marchand, 1895). In the twentieth century, Zondeck (1929), Aschheim (1930) and Meyer (1930) demonstrated that these abnormal entities produce high levels of gonadotropin, a pregnancy hormone, in the urine of patients experiencing moles (Aschheim, 1930; Meyer, 1930; Zondek, 1929).

1.1.2. Clinical presentation

The most common clinical manifestation of HM is the irregular vaginal bleeding which manifests in 80-90% of patients during the second trimester of gestation (Berkowitz and Goldstein, 1996). This sign is often accompanied by the passage of grape like tissues through the vagina. Upon physical examination, clinicians detect an excessive uterine enlargement in nearly half of the patients (Goldstein and Berkowitz, 1994). The other classic clinical signs and symptoms may comprise hyperemesis (severe vomiting), toxemia (high blood pressure, albuminuria, edema), hyperthyroidism, pulmonary embolism (Berkowitz and Goldstein, 2009a) and preeclampsia (pregnancy-induced hypertension). Additionally, ovarian bilateral enlargement of theca lutein cysts (Figure 1.1A-C) may also occur in approximately 30% of the cases (Szulman, 1984; Szulman and Surti, 1978b).

In modern clinical practice (over the last two decades), clinicians started to rely more on ultrasonography and serum Beta human chorionic gonadotropin (BhCG) tests which made important initial inroads in the early detection and diagnosis of HMs. Patients presenting with severe bleeding or severe vomiting during early pregnancy are first subjected to ultrasound examination which, in cases of moles, detects mixed echogenic patterns (vesicles) and absence of a fetal heart beat and fetal development. Thereafter, these patients undergo a hormonal test which, reveals a markedly elevated levels of serum BhCG overstepping 100,000 mIU/ml (Berkowitz et al., 1989) in cases of typical molar pregnancies.

1.1.3. Clinical management and follow-up

After suspecting the presence of a non-viable pregnancy with molar changes, the clinician interrupts and evacuates the abnormal conception by dilatation suction and curettage (D&C) (Berkowitz and Goldstein, 2009b). Uterine evacuation is an important procedure that allows almost eighty percent of women with HM to be cured (Elias et al., 2010). Clinicians may also indicate hysterectomy for women who are almost close to getting past the childbearing period or suffering from a life-threatening hemorrhage (Elias et al., 2010). After evacuation of the molar tissue, the patients are followed-up and monitored on a regular basis to ensure that the levels of BhCG in blood keep decreasing until they reach normal, non-pregnant values. According to the International Federation of Gynecology and Obstetrics (FIGO) and the World Health Organization (WHO) guidelines, a plateaued BhCG after four consecutive values over 3 weeks, or a rise of BhCG levels of ≥10% for three consecutive values over 2 weeks or a persistently raised BhCG at 6 months after molar evacuation indicate that the patient has a persistent trophoblastic disease or a gestational trophoblastic neoplasia (GTN) (Khoo et al., 2010; Lurain, 2011; Seckl et al., 2010). The term GTN is also used for a trophoblast that persists in cases of invasive HM, a choriocarcinoma, a placental site trophoblastic tumour and an epithelioid trophoblastic tumour. Additional tests, including imaging and histopathology of a biopsy are therefore conducted to distinguish between the four entities. Based on the classification of GTN according to the FIGO and WHO scoring system, each patient developing a GTN is subject to a specific chemotherapy regimen that consists of either a single or a combination of the following agents, methotrexate, actinomycin D and

cyclophosphamide. Adjuvant radiation therapy may also be used to control GTN that metastasizes either to the central nervous system, the liver, or rarely, to other sites (Lurain, 2011).

1.1.4. Gross morphology

Two types of HMs exist: complete HM (CHM) and partial HM (PHM), both of which may be in some cases macroscopically distinguishable (Figure 1.2). The evacuated product of conception (POC) of a well-developed CHM consists of an enlarged bloody tissue associated with grossly traceable and abnormal edematous villi but lacks detectable fetal parts. The hydropic changes affect most chorionic villi, which appear as transparent vesicles of variable sizes resembling grape- like clusters (Figure 1.2A). Grossly, a PHM consists of a bloody tissue that is usually smaller than complete moles and often displays some chorionic villi of normal appearance. Occasionally, villi with hydropic patterns may also be observed. Depending on the gestational age of the POC, a PHM may contain a gestational sac, fetal parts, or even a fetus with mild to moderate symmetrical intrauterine growth restriction and/or malformations. After evacuation dilatation suction and curettage, the POC specimen is then submitted for histological evaluation.

1.1.5. Histopathology

Histopathological analysis provides a more accurate but not final classification of CHM and PHM, and is based on the presence of morphological features that are exclusive for each entity (Stone and Bagshawe, 1976; Vassilakos and Kajii, 1976; Vassilakos et al., 1977). Microscopically, CHMs have massive and hydropic villi that appear to be budding, and have circumferential trophoblastic proliferation involving a significant percentage of chorionic villi. CHMs do not contain fetal nucleated red blood cells, fetal parts or extraembryonic membranes such as an amnion, yolk sac and chorion (Table 1.1 and Figure 1.3B). PHMs have mild hydropic and irregular chorionic villi intermixed with small, normal appearing or fibrous villi (Figure 1.3C). Some of the villi show scalloped edges and demonstrate focal trophoblastic proliferation.

These villi are generally vascularized unlike those in CHM. PHM may also contain a normal or abnormal fetus or embryonic tissues and structures (cartilage, bones, amnion, cord, fetal nucleated red blood cells inside the chorionic villi) (Table 1.1 and Figure 1.3D and E).

The classical histopathological examination of moles is a qualitative descriptive approach that lacks quantitative measurements. Hence distinguishing between both HM entities has been challenging due to some continuous variation in the molar degeneration (Vassilakos et al., 1977) and the current early diagnosis and evacuation of moles which occurs before the full manifestation of their distinguishable histopathological features. A misdiagnosis can also occur between a PHM and a miscarriage (Fukunaga et al., 2005; Gupta et al., 2012; Howat et al., 1993), which is a non-molar arrested pregnancy that may contain embryonic or extra embryonic tissues but do not have circumferential trophoblastic proliferation. Therefore, to establish an accurate diagnosis, pathologists nowadays rely not only on histopathological examination but also on additional tests, such as karyotype, flow cytometry, immunohistochemistry for $p57^{KIP2}$, fluorescent *in situ* hybridization, and DNA genotyping, that contribute to a more reliable classification of the three entities of spontaneously arrested pregnancies.

1.2. Mechanisms of hydatidiform mole formation

1.2.1. Diploid androgenetic hydatidiform mole

In the late seventies, the advancement of molecular and genetic studies allowed researchers to gain more insight about the etiology of HMs (Kajii and Ohama, 1977; Szulman, 1984; Vassilakos et al., 1977). Using karyotype and banding analysis, Kajii and Ohama were the first to demonstrate that chorionic villi of most complete moles have diploid genomes, predominantly 46,XX, that inherited only the paternal chromosomes, each in a duplicate fashion and are therefore of androgenetic nature (Kajii and Ohama, 1977). Their observation was based on the fact that in the paternal karyotype, the homologue chromosomes were heterozygous for banding polymorphisms whereas those of the moles were homozygous. The androgenetic phenomenon was subsequently validated using the same or different approaches (Hoshina et al., 1984; Jacobs et al., 1980; Kajii, 1986; Lawler et al., 1982; Yamashita et al., 1979). Further investigations provided more insights on the molecular content of the genome of complete moles

and showed that these tissues, similar to normal pregnancies, also carry maternal mitochondrial DNA (Azuma et al., 1991; Edwards et al., 1984; Wallace et al., 1982). Among diploid androgenetic moles, around 80% are monospermic and 20% dispermic (Baasanjav et al., 2010; Furtado et al., 2013; Kovacs et al., 1991; Lai et al., 2004; Lipata et al., 2010). The suggested mechanism underlying the formation of complete moles at this period of time involved the fertilization of an egg in which the maternal genome is inactivated or lost (Kajii and Ohama, 1977; Wake et al., 1978) with either a) one spermatozoon followed by the duplication of its genome for those with 46,XX (46,YY are non-viable) (Jacobs et al., 1980; Kajii, 1986; Lipata et al., 2010; Ohama et al., 1981; Szulman, 1984) or b) a diploid spermatozoon resulting from failure of the second meiotic division (46,XX) (Jacobs et al., 1980), or c) two spermatozoa for those with 46,XX or 46,XY (46,YY are non-viable) (Sebire et al., 2003b).

All the above suggested mechanisms for androgenetic moles remain under debate between investigators since empty oocytes have never been proven to exist or observed as a regular feature of oogenesis. A more plausible and interesting mechanism was proposed by Golubovsky (Golubovsky, 2003) to explain not only the formation of complete moles but also the occurrence of other conceptions with various chromosomal abnormalities including mixoploidies, trisomies and aneuploidies. This mechanism implies a dispermic fertilization followed by postzygotic diploidization.

1.2.2. Triploid diandric hydatidiform mole

Complete androgenetic moles are not the only genotypic entities of this condition. Partial moles, a milder form of the disease, also exist mostly with a triploid diandric monogynic genome. Of these, the majority are dispermic with 70% being 69,XXY, 27% 69,XXX and 3% 69,XYY (Jacobs et al., 1982b; Lawler et al., 1991; Redline et al., 1998; Szulman and Surti, 1978a). The mechanism governing the formation of these dispermic moles implies the fertilization of a haploid egg with two haploid spermatozoa (69,XXX, 69,XXY and 69,XYY). Only a few cases of triploid monospermic moles have been reported with two possible karyotypes 69,XXX and 69,XYY (Jacobs et al., 1982b; Kajii and Niikawa, 1977; Lawler et al., 1982). The mechanism leading to the formation of these monospermic moles would be the

fertilization of a haploid egg with one spermatozoon followed by the duplication of its genome (69,XXX, 69,XYY).

1.2.3. Diploid biparental hydatidiform mole

In addition to the above major genotypic types of moles, there are some which are found to carry a diploid biparental genome (46,XX or 46,XY) containing a single haploid genome from each parent (monogynic and monoandric) (Jacobs et al., 1982a; Ko et al., 1991; Kovacs et al., 1991; Sunde et al., 1993; Vejerslev et al., 1991). These HMs were found to be histopathologically either complete or partial. Some of these biparental moles may occur repeatedly in the same patients and are therefore known as biparental recurrent hydatidiform moles. Among these, few are familial since they occur in sisters or related women from the same family. Such a biparental diploid genomic constitution suggests the presence of a common mechanism underlying the etiology of these molar pregnancies in the family (Helwani et al., 1999), and which is transmitted according to the autosomal recessive mode of inheritance with the recessive mutations being in the patients who have the recurrent hydatidiform moles (RHMs) and hence recessive mutations in a maternal-effect gene.

1.3. The genomic imprinting defect in hydatidiform mole

Diploid androgenetic and triploid diandric are, respectively, the two major genotypes that constitute most sporadic non-recurrent complete and partial moles. Although these two entities share common histopathological features, they differ in the severity of trophoblastic proliferation, the presence of embryonic tissues, and the extent of hydropic degeneration of the chorionic villi. In an attempt to understand the nature of the defect leading to the manifestation of complete and partial moles, investigations were initiated in the eighties based on the theory that implicates an abnormal genomic imprinting. The theory proposes that the absence of imprinted, maternally expressed genes in diploid androgenetic HM underlies the absence of embryonic tissues in the androgenetic moles whereas the expression of two doses of imprinted, paternally expressed genes is responsible for the excessive proliferation of the trophoblast. This hypothesis was in agreement with observations made from pronuclear transfer studies. Two groups looked at the development of mouse embryos that were derived from reconstituted

fertilized mouse eggs with two male (androgenetic) or two female (gynogenetic) pronuclei (Barton et al., 1984; Solter, 1988). While both reconstituted embryos did not develop to term, gynogenetic embryos displayed underdeveloped extraembryonic tissues (trophoblast and yolk sac) and androgenetic ones had excessive trophoblast proliferation mimicking the features seen in diploid androgenetic moles (Barton et al., 1984). In addition, studies on chimeric embryos resulting from the aggregation of androgenetic and parthenogenetic embryos demonstrated, by mid-gestation, the restriction of androgenetic cells to the trophoblast and primitive endoderm lineages and the presence of parthenogenetic cells preferentially in the embryo and yolk sac mesoderm (Solter, 1988; Surani et al., 1988). Collectively, these observations demonstrated the differential roles of parental genomes in mammalian development and lineage specifications. These observations also suggested that an imbalance between the two parental genomes underlies the manifestation of the distinct phenotypical features of diploid androgenetic and triploid moles. While plausible for androgenetic and triploid moles, the above hypothesis is also applicable for the subset of rare identified moles with diploid biparental genomes, containing one haploid genome from each parent and whose histopathological features are indiscernible from their androgenetic and triploid dispermic counterparts. Because both genomes are present in the diploid biparental moles, a derivative hypothesis suggesting the involvement of abnormal expression of imprinted genes in the pathogenesis of moles is more plausible and could explain part of a common mechanism leading to all entities of moles (diploid androgenetic, biparental and triploid dispermic).

1.4. Epidemiology

Epidemiological studies have mainly evaluated CHM rather than PHM, due to an underdiagnosis of the latter in routine histopathological evaluation (Berkowitz and Goldstein, 2009a; Genest, 2001). The incidence of molar pregnancy varies between continents across the globe. For instance, estimates from studies conducted in North America (Atrash et al., 1986; Douglas, 1957; Hayashi et al., 1982; Hertig and Sheldon, 1947; Slocumb and Lund, 1969), Western Europe (Bagshawe et al., 1986; Flam et al., 1992; Franke et al., 1983; Mazzanti et al., 1986; Ringertz, 1970; Stevenson et al., 1959; Womack and Elston, 1985), New Zealand and Australia (Duff, 1989; Olesnicky et al., 1985; Paksoy and Reich, 1989; Steigrad, 1969) have

shown that the incidence of HM ranges from 0.5 to 1.84/1000 pregnancies whereas in South America the incidence of HM varies between 0.23 to 0.9 per 1000 pregnancies (Aguero et al., 1973; Rolon and de Lopez, 1977; Rolon et al., 1990). Available reports in Pubmed indicate an incidence averaged at 5/1000 pregnancies in Central Africa, mainly in Nigeria and Uganda (Agboola, 1979; Ayangade, 1979; Diejomaoh et al., 1984; Egwuatu and Ozumba, 1989; Ogunbode, 1978). In Southeast Asia, the incidence of HM per 1000 pregnancies is much higher than the previously described continents with rates ranging from 3.8 in Japan, 5 in Philippines and China, 8 in Taiwan and reaching 13 in Indonesia (Acosta-Sison, 1959; Buckley, 1984; Honda et al., 1982; Nakano et al., 1980; Shang, 1982; Song and Wu, 1987; Takeuchi, 1987; Wei and Ouyang, 1963). The above reported frequencies do not reflect the exact numbers of HM in all countries. Such inaccuracies occurred because some studies documented epidemiological data based only on the number of live births while others took into consideration the total number of pregnancies including live births, stillbirths, ectopic pregnancies, induced abortions and miscarriages. Additionally, some accurate information with respect to the number of spontaneous and induced abortions may not be recorded in all countries and may have led to variations in the frequencies in different studies and countries. Despite all these factors, these epidemiological studies demonstrated a global trend for the incidence of HM being the lowest in North America and the highest in South-East Asia.

1.5. Risk Factors for HM

The risk factors for HMs have been essentially described for complete hydatidiform moles.

1.5.1. Maternal and paternal ages

Maternal age is an established risk factor for the development of HM in different ethnic groups and regions across the globe. Women over the age of 35 and teenagers are at significantly higher risks of having HM than women in other age groups. The risk is 1.5-2 fold higher in women under the age of 20 years (Reyes, 1993), 2.5 fold higher in women over the age of 35 years, (Hayashi et al., 1982; La Vecchia et al., 1985) and 5-10 fold higher in women over 40 years (Bagshawe et al., 1986; Bandy et al., 1984; Yen and MacMahon, 1968). Few hypotheses have been suggested to explain the high incidences of HM. Among these, the quality of women's

ova (Smith and Kim, 2003) described as premature or postmature at the extremes of woman's reproductive lifespan as well as hormonal fluctuations during menarche or menopause (Teoh et al., 1971).

Paternal age was also investigated but all studies failed to demonstrate its association with the development of HM (Brinton et al., 1989; Matsuura et al., 1984; Yen and MacMahon, 1968) with the exception of one study that demonstrated an increased risk for HM estimated at 2.4, in women whose partners were between 40 to 44 years old. This risk was even higher and reached 4.2 for those whose partners were above 45 years (La Vecchia et al., 1985). However, to date, no additional studies replicated these observations. Thus, considering the paternal age as a risk for HM remains far from being established and further studies are needed to clarify this point.

1.5.2. Previous pregnancies

Past obstetric history is an important risk factor for the development of hydatidiform moles. HMs are usually sporadic not recurrent. Patients who experienced a previous HM are more prone to develop another one (MacGregor et al., 1969; Matalon and Modan, 1972; Sand et al., 1984; Yen and MacMahon, 1968) with estimated risks between 5 and 40 times compared to that of the general population (Bagshawe et al., 1986; Berkowitz et al., 1998; Eagles et al., 2015; Lorigan et al., 2000; Matalon and Modan, 1972; Matsui et al., 2001; Savage et al., 2013; Sebire et al., 2003a).

This risk increases significantly in women with more than one molar pregnancy (Bagshawe et al., 1986; Berkowitz et al., 1998; Lorigan et al., 2000; Matsui et al., 2001; Savage et al., 2013; Sebire et al., 2003a; Vargas et al., 2014). For instance, an independent study in the United Kingdom documented an estimated risk of 1/76 for developing a second HM in women with a prior mole. This risk increases to 1/6.5 (=12 fold) after two HMs (Bagshawe et al., 1986). However, this risk disappears in women who have had one or more normal pregnancies following a prior HM (Bagshawe et al., 1986).

A previous HM is not the only risk for a woman to develop a HM, a history of repeated miscarriages is also a well-established risk factor. One study reported an estimated risk of 1.9 to 3.1 times higher for developing a partial and complete HM respectively in women with a history

of two or more miscarriages compared to women from the general population (Parazzini et al., 1991). Other investigations even reported higher risks of having a HM estimated at 6 (Coulam, 1991) and 32.1 (Acaia et al., 1988) for women with a history of two or more miscarriages.

1.5.3. Ethnicity

The role of maternal or paternal ethnicities has been proposed as a potential risk factor for the development of moles and for the wide variations in their global incidences. To address this proposal, epidemiological studies followed two approaches. The first one was to investigate whether women originating from countries with high incidences of HM keep the same incidences of HM in the new hosting country located in a different geographical region. This study was possible in Hawaii with large multi-ethnic groups (Matsuura et al., 1984; Natoli and Rashad, 1972). Japanese and Filipino women, both from countries with well-documented high incidences of HM, kept the same high frequencies of moles, 1.75 and 1.65/1000 pregnancies, after living in Hawaii for several years. However, their compatriots, whites and native Hawaiians, of different genetic background and studied at the same period of time had low incidence of HMs, 0.80/1000. The role of ethnicity was confirmed in a second study showing that Hawaiians of Filipino origin have a five times higher risk of developing HM compared to Hawaiians of Caucasians origin (Jacobs et al., 1982a). The same applies for Hawaiians of oriental origin, another group with well-documented high incidence of HM. These women were shown to have higher rates of HM than Caucasians living in Hawaii during the same period of time (McCorriston, 1968).

The second approach was to check the rates of HM in various ethnic groups living together in the same geographical region and sharing the same environment. A report from Malaysia, a multiethnic country, documented the occurrence of molar pregnancies per 1000 pregnancies at an incidence of 2.43 for Malays, 2.66 for Chinese and 3.29 for Indians (Cheah et al., 1993). Also, a report from Singapore, another multiethnic country, revealed that the risks of having molar pregnancy in Malaysians, Chinese, and Indians were much higher than those found in Caucasians or Whites (Teoh et al., 1971). Up North in China, the Han population had lower rates of HM than those in the Zhang and in Inner Mongolian populations (Song H, 1981). In

Alaska, the frequency of HM in native Alaskans was found to be 3 to 4 times higher than the frequency of HM in Caucasian Americans living in the same area (Martin, 1978).

The above epidemiological data clearly demonstrate the involvement of genetic factors in the predisposition to HM within some ethnic groups but do not describe the level at which such susceptibility occurs and functions in these women with high rates of HM. However, Steigrad proposed an interesting explanation and postulated a genetic basis either for a high incidence of abnormal fertilization and/or an increased capacity to allow implantation of a genetically aberrant pregnancy (Steigrad, 2003).

1.5.4. Diet

Dietary deficiency as a probable risk factor for HM has been evoked initially at a time when the population in South East Asia, known to be at high risk for this condition was poor with limited nutritional resources. This brought up the idea postulating that nutritional deficiencies may increase the risk or predispose to developing HM. Early studies in the seventies went on investigating protein deficiency in the blood of patients prior to HM evacuation and focused on analyzing proteins that are obtained from animal sources and which are known as the first class category of proteins (such as meat, eggs, milk and cheese) (Pour-Reza et al., 1974). These investigations demonstrated significant low amounts of total protein and serum albumin but increased levels of serum creatinine and urea in patients with HMs as compared to normal matched subjects (Pour-Reza et al., 1974). These observations were formerly suggestive of an increased catabolism of body protein reserves due to malnutrition consequently favouring the occurrence of HM. The implication of protein deficiencies with the formation of HM was addressed in additional studies, of which some found associations (Berkowitz et al., 1985; Pascasio et al., 1970) and others did not (Martin, 1978). In addition, several investigators looked at other nutritional deficiencies such as vitamin A (Andrijono and Muhilal, 2010; Berkowitz et al., 1985; Craighill and Cramer, 1984; Parazzini et al., 1988), folate (vitamin B9) (Kokanali et al., 2008; Reynolds, 1976) and fat consumption and found them to be associated with high incidence of developing molar pregnancy (Berkowitz et al., 1985; Parazzini et al., 1988). Other studies have also tried to check for associations between diet or nutritional status (measured in very general terms) and the occurrence of HM but did not find any significant association

(Llewellyn-Jones, 1965; MacGregor et al., 1969; McCorriston, 1968; Shang, 1982; Yen and MacMahon, 1968). Although some of these findings are established as risk factors for HMs, the above-described dietary associations are not causative for moles but rather considered as contributing external factors. This is specifically true for sporadic complete moles of androgenetic origin, as demonstrated in a recent study by Coullin et al. on Senegalese and Moroccan population (Coullin et al., 2015). This study showed a high incidence of CHM in women whose mothers, during their first three months of pregnancy, received limited nutritional resources. Additionally, the authors suggested that the lack of necessary nutritional elements in the mother entails inappropriate DNA and protein synthesis and/or methylation, therefore affecting oocyte development of the female embryo (the future mother=patient) who will experience CHM in her future pregnancies. According to Coullin et al. a defective oocyte could lead to a) a damaged maternal pronucleus and consequently its loss and b) an abnormal cortical reaction favouring dispermic fertilization. The absence of the maternal pronucleus (inactivated/lost) and the fertilization by two spermatozoa are two key events that are needed to meet the description of one of a threefold mechanism previously proposed for CHMs.

1.5.5. Contraception

Oral contraceptives are hormones-based drugs that interfere with the natural cyclical hormones in a woman to prevent ovulation and consequently pregnancy. Such exogenous hormonal interference is believed to increase the risk for developing HM. Two studies looked for association between the use of oral contraception and the development of HMs. The reported risk was estimated at 1.9 (Palmer et al., 1999) to 2.6 (Brinton et al., 1989) in women who were on long-term use of oral contraceptives before conception and at 2 for women who used oral contraceptives during the menstrual cycle that preceded the HM (Palmer et al., 1999). The use of non-hormonal contraceptive methods has also been investigated as these were also hypothesized to cause HM as a result of enhanced inflammation in the endometrium. Three studies tried to look for association with antecedent use of an intrauterine device and HMs but gave inconsistent data with some finding associations and others not (Berkowitz et al., 1985; Brinton et al., 1989; Matsuura et al., 1984).

1.5.6. Various additional risk factors

Several additional factors have been examined for their possible association with HM. Data with regard to gravidity, parity and viral infection, presence of parasites, blood types and low socio-economic level showed no association; however, investigations on herbicides and smoking were conflicting, demonstrating either significant or no association with the development of HMs (Bracken et al., 1984; Matalon et al., 1972; Palmer, 1994; Parazzini et al., 1991; Yen and MacMahon, 1968). The data on smoking and viral infection are worth investigating for validation in additional series of case-control studies as both factors were previously studied and established as increasing the likelihood for spontaneous abortions/miscarriages during the first semester (Chatenoud et al., 1998; Giakoumelou et al., 2015; Ness et al., 1999).

1.6. Genes responsible for RHMs

1.6.1. Identification of *NLRP7*: the first causative gene responsible for RHMs

In 1999, the group of Dr. Slim initiated a linkage analysis on two families with RHMs and mapped a locus on chromosome 19 to q13.3-13.4 (Moglabey et al., 1999). Thereafter, Hodges et al. refined the locus to 1.1 Mb (Hodges et al., 2003). On the basis of these data, Dr. Slim's lab screened candidate genes from the candidate region and identified *NLRP7*, a nucleotide oligomerization domain-like receptor protein 7, as the first causative gene for this condition (Murdoch et al., 2006). Soon after, studies from various groups were conducted and demonstrated that *NLRP7* is a major gene for this rare condition since its mutations underlie about 48-80% of the cases (Estrada et al., 2013; Hayward et al., 2009; Qian et al., 2011; Slim et al., 2009). Different mutations in *NLRP7* were identified in women with RHMs. The identified mutations affected mostly both alleles either in a homozygous or a compound heterozygous state. To date, reported biallelic *NLRP7* mutations have reached a total of 50 of which 17 missenses and 33 that result in premature protein truncations (nonsense, splicing, small or gross deletion or insertion and complex rearrangement) (Akoury et al., 2015a; Milhavet et al., 2008). Several mutations were found in unrelated patients from the same population and were shown to be due to a founder effect (Kou et al., 2008; Slim et al., 2009). Most of the missense mutations were

reported to cluster within the leucine-rich repeat of the NLRP7 protein (Messaed et al., 2011b; Wang et al., 2009b). Additionally, reports described the presence of single heterozygous missenses (Deveault et al., 2009; Dixon et al., 2012; Landolsi et al., 2012; Messaed et al., 2011b) and protein-truncating mutations (Qian et al., 2011) in patients experiencing sporadic or low number of recurrent moles (2 to 3). Single heterozygous *NLRP7* mutations or rare variants were also found in some women with recurrent miscarriages (Qian et al., 2007). Women with one *NLRP7* defective allele manifested a less severe abnormal reproductive history with more live births and miscarriages but fewer HMs compared to those bearing two defective alleles, who were more prone to recurrent molar pregnancies but can exceptionally have live births in approximately 1% of their pregnancies (Akoury et al., 2015a; Messaed et al., 2011b). Interestingly, two males with normal reproductive history were found to carry biallelic *NLRP7* mutations (Court et al., 2013; Qian et al., 2007; Wang et al., 2009b). Albeit the small number of cases, these observations suggest that *NLRP7* mutations do not affect male reproduction.

1.6.1.1. *NLRP7* expression

NLRP7 does not have a murine orthologue and is thought to have arisen through a duplication of the ancestral gene *NLRP2/7* in primates (Duenez-Guzman and Haig, 2014; Tian et al., 2009). NLRP7 consists of 11 exons and is spliced into 6 isoforms (Okada et al., 2004) (http://www.genecards.org/). At least one of these transcripts is detected by polymerase chain reaction after reverse transcription (RT-PCR) in several human tissues, including endometrium, placenta, hematopoietic cells, all stages of oocytes and preimplantation embryos (Murdoch et al., 2006). In these stages, NLRP7 shows two main transcriptional time points. The first one is when *NLRP7* transcripts decline to reach their lowest levels at day 3 post-fertilization. The second one is when the amount of its transcripts increases strongly from day 3 to day 5, which concurs with the process of transcriptional activation of the embryonic genome (Zhang et al., 2008). Furthermore, *NLRP7* was reported to be highly expressed in testicular (Okada et al., 2004) and endometrial (Ohno et al., 2008) cancers. At the protein level, *NLRP7* was also shown to be expressed in human oocytes during folliculogenesis by immunohistochemistry (Wang et al., 2009a). My work on the localisation of NLRP7 in human oocytes and early embryos is described in Chapter 3.

1.6.1.2. NLRP7 protein structure

NLRP7 encodes 1037 amino acids including all coding exons of all splice isoforms. NLRP7 is one of the 14 NLRP proteins, a family of proteins that is principally involved in the regulation of autoinflammation, apoptosis and pathogen-induced inflammation (Tschopp et al., 2003). NLRP7 consists of three main domains (Figure 1.4A): 1) an amino-terminal Pyrin (PYD); 2) a central NACHT [i.e. found in the neuronal apoptosis inhibitor protein (NAIP), class II, major histocompatibility complex, transactivator (CIITA), incompatibility locus protein from *Podospora anserina* (HET-E), and mammalian telomerase-associated proteins (TP1) family proteins]; and 3) a carboxy-terminal region of 10 leucine-rich repeats (LRR). The Pyrin domain which is an adaptor domain interacts with other domains including the death domain (DD), the death effector domain (DED) and the caspase activation and recruitment domain (CAD) and subsequently triggers a cascade of signals implicated in cell death pathways (Aravind et al., 1999). The NACHT domain is found in proteins with apoptotic and anti-apoptotic functions. This domain encompasses three small domains: a conserved adenosine/guanidine 5′-triphosphate binding motif ATP/GTPase-specific P-loop domain, a NACHT-associated domain (NAD) and a nuclear localization signal (NLS). The ATP/GTPase-specific P-loop domain of the NACHT was originally described in prokaryotes, plants and eukaryotes. This domain initiates oligomerization by binding ATP and triggering ATPase activity (Radian et al., 2015). It controls programmed cell death mediated via cytochrome c mitochondrial outflow and consequently promotes apoptosome assembly (Koonin and Galperin, 2003; Tschopp et al., 2003). The NAD that resides also within the NACHT was recently described to act as a mediator for the oligomeric assembly of the NLRP7 protein (Singer et al., 2014). The LRR is present in proteins with versatile functions including Ran GTPase activating proteins, RNase inhibitor proteins and toll-like receptors. The Ran GTPases modulate the nucleo-cytoplasmic transport of RNAs and proteins across the nuclear envelope and are also crucial for mitotic spindle assembly and post-mitotic nuclear envelope assembly (Gruss and Vernos, 2004; Harel and Forbes, 2004; Hetzer et al., 2002; Macara, 2001). The RNase inhibitors are ribonuclease proteins that inhibit RNase A, an endonuclease (Blackburn and Gavilanes, 1982), eosinophil-derived neurotoxin, a protein found in eosinophil granulocytes (Hofsteenge et al., 1989; Shapiro and Vallee, 1991) and angiogenin also known as ribonuclease 5 (Fett et al., 1985) in order to control RNA degradation, RNA activity and neovascularization (Kobe and Deisenhofer, 1996). Toll-like receptors are key-

molecules of the innate immune system that recognize pathogen-derived molecules, sense the extent of tissue damage and determine the class of immune response (innate immune system versus the adaptive immune system) (Dembic, 2005).

1.6.1.3. NLRP7 subcellular localization

NLRP7 was initially described to localize homogeneously to the cytoplasmic compartment of human embryonal carcinoma cells, Tera-1 (Okada et al., 2004). My work on the localization of NLRP7 is detailed in Chapter 2. During my PhD, other studies have also looked at the localization of overexpressed wtNLRP7 in Human Embryonic Kidney 293 cells (HEK293) and found that this protein mainly localizes to the cytoplasm with occasional accumulation as an aggregate near the nucleus (Khare et al., 2012; Singer et al., 2015; Singer et al., 2014).

1.6.2. Identification of *KHDC3L*: a second causative gene responsible for RHMs

In 2011, a British group identified KHDC3L, KH domain containing 3-like, as a second gene responsible for RHMs (Parry et al., 2011). This gene consists of three exons and maps to chromosome 6q13. *KHDC3L* is a minor gene for RHMs because its mutations account for 10–14% of patients with RHMs who are negative for *NLRP7* mutations (Fallahian et al., 2013; Parry et al., 2011; Reddy et al., 2013). To date, available reports documented four mutations in *KHDC3L* in patients with two defective alleles (Parry et al., 2011; Reddy et al., 2013). *KHDC3L* codes for 217 amino acids (Figure 1.4B) and is a component of KHDC1 (KH homology domain containing 1) family of structurally related proteins that includes DPPA5 and FLOPPED (OOEP) (Pierre et al., 2007) characterized by the presence of a KH domain that interacts with RNA (Garcia-Mayoral et al., 2007). *KHDC3L* is transcribed in various human tissues and cell lines including hematopoietic cells (http://biogps.org/) (Parry et al., 2011; Reddy et al., 2013). Additionally, *KHDC3L* was reported to be also expressed at the RNA level in human oocytes at the germinal vesicle (GV) and to a lesser extent at metaphase II stages but not at the morula or the blastocyst stages (Parry et al., 2011). However, my investigations at the protein level showed

that KHDC3L is expressed in all oocyte and early cleavage-stages embryos and the data are described in Chapter 3.

1.6.3. Functional Roles of *NLRP7*

1.6.3.1. Role of NLRP7 in IL1B secretion in *in vitro* models

Over the course of the last 10 years after the identification of *NLRP7*, two studies investigated the effect of its overexpression in transient transfections on the intracellular level of interleukin 1 beta (IL1B), an important mediator of the inflammatory response. The study of Kinoshita et al. was the first to establish a relationship between NLRP7 and IL1B, and demonstrated that NLRP7 interacts with pro-caspase-1 and pro-IL1B, inhibits their processing and consequently downregulates IL1B secretion in transiently transfected HEK293 (Kinoshita et al., 2005). A few years later, the work from our laboratory by Messaed et al. concurred with the inhibitory function of NLRP7 on IL1B secretion. However, in this study, we unveiled that this inhibition is due to the downregulation of pro-IL1B synthesis in transiently transfected HEK293 and implicates concomitantly the three domains of NLRP7, albeit to a different extent (Messaed et al., 2011a). Recently, the study of Khare et al. (Khare et al., 2012) also implicated NLRP7 in IL1B release; however, this study indicated that NLRP7 and to a greater extent three of its HM-linked mutations (R693W, R693P and D657V) enhanced IL1B secretion in transiently transfected HEK293 cells after stimulation with mycoplasma derived lipopeptides. Additionally, the authors demonstrated a physical interaction between NLRP7 and ASC, an adapter protein that activates caspase 1 in a multiprotein complex of the innate immune response known as the inflammasome. In summary, available data concur on the requirement of wtNLRP7 for normal levels of IL1B secretion by HEK293 cells, but it remains unclear whether NLRP7 regulates the intracellular synthesis or processing of IL1B and further investigation is needed to clarify this point.

1.6.3.2. Role of NLRP7 in IL1B secretion in *ex vivo* models

The involvement of NLRP7 in IL1B secretion was also investigated in *ex vivo* cellular models by our group. We investigated the effect of some *NLRP7* mutations or variants on IL1B secretion in peripheral blood mononuclear cells (PBMCs) from patients with two *NLRP7* mutations or rare or low frequency *NLRP7* variant (Messaed et al., 2011a). This study showed that lipopolysaccharides (LPS)-stimulated PBMCs from these patients secrete lower levels of IL1B than PBMCs from control subjects despite the fact that the same stimulated cells have normal to slightly higher intracellular levels of pro- and mature-IL1B (Messaed et al., 2011a). This suggested that normal NLRP7 in these cells is required for IL1B release into the extracellular milieu. This role was further supported in a second study showing that silencing the expression of *NLRP7* after transfection with small interfering RNA (siRNA) in acylated-lipopeptides-stimulated human monocytic cell line (THP1) inhibits IL1B secretion (Khare et al., 2012). These observations on *ex vivo* models are in line with those obtained from the *in vitro* model and confirm that wtNLRP7 is indeed indispensable for normal IL1B secretion.

1.6.3.3. NLRP7 is implicated in cellular growth

Two studies revealed another interesting role for this protein in cellular growth. While Okada et al. (Okada et al., 2004) demonstrated that knocking down *NLRP7* with siRNA suppresses the growth of Tera-1 cells, Khare et al. (Khare et al., 2012) demonstrated that the same process prompted intracellular growth of *Staphylococcus aureus* and *Listeria monocytogenes*, in infected human primary macrophages. In conclusion, the role of NLRP7 in cellular growth is not clear but it is surprising to see that its knockdown inhibits cellular growth because the opposite is seen in molar tissues from patients with *NLRP7* mutations, which are characterized by hyperproliferation of the trophoblast. Thus, further investigations are required to address the exact role of NLRP7 in cellular proliferation.

1.6.3.4. NLRP7 is implicated in cellular differentiation

To the above described roles for NLRP7, two interesting ones were recently added by Mahadevan et al. (Mahadevan et al., 2014). The authors of this study examined the consequence of *NLRP7* inactivation in transduced human embryonic stem cells (ESC) and found that its knockdown accelerates trophoblast lineage differentiation and increases the amount of secreted BhCG. The latter observation is interesting because HMs are associated with an enhanced production of BhCG in the patients' blood.

1.6.3.5. NLRP7 and KHDC3L are involved in DNA methylation at imprinted genes

Genomic imprinting mainly through DNA methylation is a reversible epigenetic phenomenon independent of the classical Mendelian inheritance which leads to the exclusive expression of specific genes from only one parent. In other words, only one of the two parental alleles will be expressed and the other one will be imprinted or silenced. The methylation process adds a methyl group via DNA methyltransferase at the cytosine followed by guanine of the CpG dinucleotides (Illingworth and Bird, 2009). These imprinted loci are partially regulated by differentially methylated regions (DMR) (Prickett and Oakey, 2012). Genomic DNA methylation patterns are primarily established during either spermatogenesis or oogenesis designated as primary imprint or later during embryogenesis termed as secondary imprint reviewed in (Delaval and Feil, 2004). After the identification of recurrent moles containing diploid biparental genomes and which are transmitted following Mendelian modes of inheritance, researchers postulated that the causative genes for these RHMs would regulate the expression of imprinted, maternally expressed genes in recurrent diploid biparental moles. To address this hypothesis, six studies investigated DNA methylation in diploid biparental moles from patients with either *KHDC3L* or *NLRP7* biallelic mutations. Judson et al. was the first to demonstrate methylation defects at DMRs of imprinted genes in one diploid biparental CHM from a familial case with two *KHDC3L* mutations (Judson et al., 2002). In this study, the authors described that the methylation marks were lost at the following analyzed DMRs: *KCNQ1OT1, SNRPN, PEG1, PEG3, GNAS-1A, GNAS-AS*, with the exception of *GNAS-XLαS*, all known to be maternally methylated either during gametogenesis or embryogenesis. Additionally, two normally paternally

methylated DMRs were examined and showed contrasting behavior: while *GNAS-NESP55*, whose methylation is normally established at the blastocyst stage, acquired additional methylation marks, *H19* DMR, whose methylation is normally acquired during male gametogenesis, appeared unaffected. Later, the study of Hayward et al. corroborated the existence of such methylation defects on two analyzed DMRs, *KCNQ1OT1* and *GNAS-NESP55*, in two additional molar tissues from the same above mentioned patient with *KHDC3L* mutations (Hayward et al., 2009). The same study also demonstrated that *ZAC* and *PEG10* DMRs, which are normally maternally methylated during gametogenesis, display loss of and normal methylation, respectively.

To the list of familial biparental HMs from patients with two *KHDC3L* defective alleles, a total of five from patients with two *NLRP7* mutations have also been assessed in three studies for DNA methylation at the same aforementioned well-characterized imprinted genes (El-Maarri et al., 2003; Hayward et al., 2009; Kou et al., 2008). These studies demonstrated an aberrant loss of methylation marks on DMRs (*KCNQ1OT1, SNRPN, PEG3, GNAS-1A* and *ZAC*) of the imprinted genes, when tested, with the exception of the *GNAS-NESP55* DMR, which displayed a gain of methylation in all analyzed tissues.

Another study previously conducted by our laboratory analyzed diploid biparental tissues from patients with recessive *NLRP7* mutations in order to assess the extent of DNA methylation at CpG regions (Djuric et al., 2006) in major repetitive DNA and long interspersed nuclear elements (LINES), around *PEG3* DMR, as well as in the promoters of three genes at the inactive X chromosome (*AR, ZNF261* and *PGK1*) and three cancer related genes (*CDKN2A, CDH1* and *HIC-1*). In all four categories, the methylation is known to occur between fertilization and implantation or after implantation during early embryogenesis (Bird, 1986; Mann and Bartolomei, 2002; Reik and Walter, 2001; Yoder et al., 1997). Although performed on a small number of genes, the analysis demonstrated normal postzygotic DNA methylation patterns and therefore excluded the possibility of DNA demethylation or *de novo* methylation occurring at the described CpG sites in biparental HMs.

Recently, Delgado et al. analyzed five additional molar tissues from four patients with biallelic *NLRP7* mutations. This study demonstrated again a lack of methylation at several additional imprinted DMRs including *NAP1L5* and *L3MBTL1* both of which methylation is normally established in the female germline. However, paternally methylated DMRs which

normally acquire their methylation pattern in the male germline *H19*, *IG* and *MEG3* or during early development *ZNF597/NAA60, ZBDF2* maintained their normal methylation marks. The same molar tissues presented also with loss of methylation at many placenta specific imprinted DMR including *MCCC1, LIN28B, GLIS3, DNMT1 and AGBL3,* all of which are normally maternally methylated. Methylation analysis on *LINE-1* alpha-satellites and *Alu-Yb8* sequences demonstrated an unaffected methylation profile in the diploid biparental HMs from patients with recessive *NLRP7* mutations. Additionally, the authors pointed out the presence of methylation differences between different RHMs from the same patient or from two sisters carrying the same mutation (Sanchez-Delgado et al., 2015).

All these observations demonstrate an abnormal lack of methylation that occurs only at imprinted genes in diploid biparental moles from patients carrying either *NLRP7* or *KHDC3L* recessive mutations and thus implicate both genes in this process. Additionally, while the above-described data do not establish nor deny a causative relationship between abnormal methylation and molar manifestation, they raise another possibility that such a defective methylation pattern might be the consequence of an upstream event caused by *NLRP7* and *KHDC3L* mutations occurring in the oocyte or during early zygotic cleavages and lineage specification.

1.6.3.6. NLRP7 is involved in DNA methylation at non-imprinted genes

Recently, Mahadevan et al. investigated the potential implication of NLRP7 in setting up DNA methylation at imprinted DMRs (Mahadevan et al., 2014). The authors demonstrated that silencing *NLRP7* in differentiated human ESCs did not affect DNA methylation at the analyzed imprinted DMRs, including those previously described to be aberrantly methylated in diploid biparental molar tissues. According to Mahadevan et al., this observation could be due to the high degree of epigenetic stability and resistance to perturbation at imprinted loci in human ESC. In the same NLRP7-knockdown cells, the authors depicted, however, a new picture of aberrant DNA methylation at many non-imprinted genes, including *FBXO4, SUCGL2* and *ZFP42*, with all three genes being hypermethylated. Additionally, few non-imprinted genes were hypomethylated. Furthermore, the authors showed that overexpressed NLRP7 interacts, via its LRR and PYD domains, with overexpressed Yin Yang 1 (YY1), a ubiquitous transcription factor that can bind imprinted DMRs and affect imprinted gene expression (Kim, 2008) in transfected

HEK293T cells. In the same year, another study by Beygo et al. performed a high-throughput methylation analysis of blood DNA from an affected live-born offspring with multiple anomalies and whose mother carries a single heterozygous missense *NLRP7* mutation (Beygo et al., 2013). The analysis detected methylation changes at 85 non-imprinted loci, different from those described earlier by Mahadevan et al. and found that half of these aberrantly-methylated loci were hypomethylated while the other half were hypermethylated. In the same analyzed DNA, Beygo et al. also demonstrated the presence of aberrant methylation at 13 loci of known imprinted genes including *PEG10, H19* and *GNAS*. The latest investigation was from Singer et al. who looked at the methylation pattern at two paternally (*H19*, *NESP55*) and two maternally (*SNRPN*, *PEG3*) imprinted genes in HEK293 following *wtNLRP7* transient transfection (Singer et al., 2015). Methylation analysis did not reveal any significant differences in the tested regions which remained unaffected even after single transfection of HEK293 cells with constructs carrying either of two known HM mutations R693P and R693W. In this study, the authors identified ZBTB16, a transcription repressor protein, as an interacting partner of NLRP7 using the yeast two-hybrid system on a human ovarian cDNA library. The data of this study suggest that neither wtNLRP7 nor its mutants affect the methylation marks at the analyzed imprinted genes in transfected HEK293 cells.

The implication of NLRP7 in regulating the methylation pattern at non-imprinted genes remains inconclusive since no additional studies have so far replicated the results described by Mahadevan et al. or Beygo et al. Additionally, both studies did not find common non-imprinted genes with abnormal DNA methylation pattern, which raises some questions with respect to the reliability and significance of these findings. Collectively, these data accumulate more evidence of an abnormal DNA methylation pattern occurring only at imprinted genes of diploid biparental HMs. This trend of abnormal methylation could also occur at yet uncharacterized imprinted genes that are responsible for maintaining normal cellular proliferation and differentiation. Such abnormal methylation would allow either the biallellic overexpression upon loss of methylation or the silencing in case of acquiring methylation of these key genes and lead consequently to the manifestation of HM. Further investigations of the two NLRP7 interacting partners, YY1, and ZBTB16 (Mahadevan et al., 2014; Singer et al., 2015), would indeed contribute to provide new insight on the role of NLRP7 in regulating the methylation process at imprinted loci.

1.6.3.7. NLRP7 regulates the expression of CDKN1C/p57^{KIP2} in diploid biparental HMs

The implication of NLRP7 in genomic imprinting was also elucidated in a series of experiments looking for the expression of p57^{KIP2} in diploid biparental HMs from patients with recessive *NLRP7* mutations. p57^{KIP2} is a cyclin dependent kinase inhibitor encoded by the paternally imprinted, maternally expressed gene *CDKN1C* in the nuclei of various cells. Additionally, this marker is used routinely in the clinical diagnosis of HM to detect the presence of the maternal genome and consequently distinguish between partial and complete moles. The first study by Fisher et al. demonstrated a lack of p57^{KIP2} expression in diploid biparental complete moles from patients with recessive *NLRP7* mutations similar to that seen in androgenetic moles (Fisher et al., 2002). Successive studies confirmed these observations in additional biparental molar tissues from patients with *NLRP7* mutations (Brown et al., 2013; Fallahian et al., 2013; Sebire et al., 2013). Recently, our laboratory conducted a large study on a total of 36 POCs from patients with biallelic *NLRP7* mutations with the goal of investigating a possible correlation between the nature of *NLRP7* mutations in the patients and the various histopathological features of their moles including p57^{KIP2} immunohistochemistry (Nguyen et al., 2014). In this study, all the POCs were found to be diploid biparental. Interestingly, some POCs showed variable levels of positive p57^{KIP2} nuclear expression that was statistically associated with the presence of embryonic tissues of inner cell mass (ICM) origin, mild trophoblastic proliferation and missense mutations in the patients. On the other hand, the absence of p57^{KIP2} nuclear expression was associated with the absence of embryonic tissues, excessive trophoblastic proliferation and at least one protein truncating mutation in the coding region of *NLRP7* in the patients. Additionally, the authors point out the similarities observed between partial diploid biparental moles, caused by missense *NLRP7* mutations, and common sporadic partial triploid dispermic moles. Also, similarities were observed between complete diploid biparental moles, caused by severe *NLRP7* defective alleles, and common complete androgenetic moles. Altogether, these observations implicate NLRP7 in the regulation of p57^{KIP2} expression, the product of paternally imprinted gene, and consequently the balance between tissue differentiation and proliferation during early human development.

1.7. Role of maternal-effect genes in various processes during the initiation of development

1.7.1. Chromatin remodeling, histone modification and DNA methylation

Chromatin is made up of DNA that loops over the core histone proteins, to constitute structures known as nucleosomes, which in turn are bound together by histone linker proteins to establish compacted chromatin. In mammals, chromatin and its major components, DNA and histones, undergo structural (chromatin remodeling), posttranslational (histone modification) and molecular modifications (DNA methylation) in order to allow a successful initiation of development. Herein, I describe these modifications that occur from gametogenesis until after fertilization. These modifications appear to be partially regulated by the products of maternal-effect genes in mice.

During gametogenesis in mammalian species including mouse and human, one of the main changes that affect chromatin is termed packaging, and it involves the addition of protamine to the male genome and histones to the female genome (Balhorn, 1982; Wouters-Tyrou et al., 1998) in order to achieve a remarkable level of compaction that is maintained until after fertilization. Also during gametogenesis, histone proteins are subject to two main changes during gametogenesis. These core proteins are acetylated in fully grown GV oocytes. However, with the resumption of meiosis, histones are subject to deacetylation that continues until the metaphase II oocyte stage in some mammals, including mouse (Akiyama et al., 2004; Kageyama et al., 2007; Kim et al., 2003; Nagashima et al., 2007; Sarmento et al., 2004). Contrariwise, although it occurs, the methylation of histones appears to be relatively stable during oocyte maturation (Hou et al., 2008; Kageyama et al., 2007; Ooga et al., 2008; Park et al., 2009; Qiao et al., 2010; Racedo et al., 2009; Sarmento et al., 2004; Wang et al., 2008) in mammals, including humans and mice. At the DNA level both haploid genomes are also subject to methylation which persists until after fertilization (Reik et al., 2001). Finally, gametogenesis culminates in a global transcriptional quiescence (Clegg and Piko, 1983; De Leon et al., 1983). At this stage of development, DNA methyltransferase 3A, (encoded by *Dnmt3a)* (Kaneda et al., 2004) with its partner DNA methyltransferase 3-like (encoded by *Dnmt3l)* (Bourc'his et al., 2001), two maternal-effect proteins, are crucial for specifically establishing *de novo* methylation at DMRs of imprinted genes. Embryos from homozygous *Dnmt3a*- or *Dnmt3l*-null females fail to progress beyond 10.5 and 9.5 days post-fertilization, respectively (Bourc'his et al., 2001; Kaneda et al.,

2004). After fertilization in mouse, the highly condensed male genome decompacts and is then repacked replacing its arginine-rich protamines by oocyte-supplied histones. Such a process generates DNA damage that necessitates immediate repair in order to maintain the cell's ability to carry out its normal functions (Derijck et al., 2006). The proteins of two maternal-effect genes, of which ubiquitin-conjugating enzyme E2A (encoded by *Rad6* homologue, *Ube2a*, also known as *Hr6a/Rad6)* (Roest et al., 2004) and nucleoplasmin 2 (encoded by *Npm2)* (Burns et al., 2003) have been involved in maintaining appropriate DNA repair and histone modification in mouse oocytes. The fertilization of oocytes from *Ube2a*- or *Npm2*-null mice led to the embryos' arrest at 1-cell and 2-cell stages, respectively (Burns et al., 2003; Roest et al., 2004). Soon after, the paternal and maternal chromatins that are packaged with histones undergo another extensive decondensation within distinct pronuclei and proceed through DNA replication. At this level of development, histone acetylation takes place again and the histones of the male pronucleus are more acetylated than those of the female genome (Adenot et al., 1997). Additionally, while absent from the male pronucleus, histone methylation is however observed in the female counterpart. This asymmetry in histone methylation carries through to the 2-cell stage (Liu et al., 2004a). Moreover, the male pronucleus is demethylated through 5-methylcytosine oxidation (Iqbal et al., 2011) while the female pronucleus is passively demethylated and this pattern remains until the 2-cell embryo (Santos et al., 2002). The transcriptional activity at this stage of development becomes detected at low levels in both genomes but is more pronounced in the male pronucleus (Adenot et al., 1997). At syngamy, the DNA of both pronuclei fuse after degeneration of their nuclear membrane and the mitotic spindle forms preparing the 1-cell embryo for the first division (Schatten et al., 1986; Zamboni et al., 1972). Zygote arrest 1 (encoded by *Zar1)* (Wu et al., 2003) and transcription intermediary factor 1 alpha (encoded by *Tif1α* also known as *Trim24)* (Torres-Padilla and Zernicka-Goetz, 2006) are two maternal genes described at this point of intracellular modifications to be implicated mainly in safeguarding syngamy and early wave of gene activation, respectively, in mouse oocytes. Mice lacking *Zar1* or *Tif1α/Trim24* ovulate eggs that can be fertilized normally; however, the derived embryos arrest at the 1-cell and 2-4 cell stages, respectively (Torres-Padilla and Zernicka-Goetz, 2006; Wu et al., 2003). Following syngamy, minor embryonic activation starts to be detected; however, gene expression is not fully activated until after zygotic chromatin remodeling (Clapier and Cairns, 2009). These modifications should occur to allow the accessibility of transcription factors

and RNA polymerase to DNA and thereby gene transcription (Dillon and Festenstein, 2002). A set of ATP dependent chromatin remodeling complexes interferes in this process. Among these, the proteins of two maternal genes SWI/SNF related, matrix associated, actin dependent regulator of chromatin, subfamily a, member 4 (encoded by *Smarca4* also known as *Brg1)* (Bultman et al., 2006) and Bromodomain and WD repeat domain containing 1 (encoded by *Brwd1)* (Philipps et al., 2008) were found to ensure the overall transcription activity and chromatin de-condensation respectively in mouse oocytes. The proteins of additional maternal-effect genes act at more advanced stages of preimplantation development in maintaining DNA methylation at imprinted genes. However, at this stage, a global demethylation pattern is still dominating. Of these, are the DNA methyltransferase 1 *(*encoded by *Dnmt1)* with both its isoforms (Hirasawa et al., 2008; Howell et al., 2001) and the developmental pluripotency-associated 3 (encoded by *Dpp3a* also known as *Stella)* (Bortvin et al., 2004; Payer et al., 2003). Genetically altered mice that lack *Smarca4, Brwd1, Dnmt1o or Dpp3a* develop normally and give rise to oocytes that fertilize normally with the exception of *Brwd1*-null oocytes that arrest at the 2 pronuclei stage. However, the embryos derived from *Smarca4*- or *Dpp3a-null* females arrest at the 2-cell stage and those derived from *Dnmt1*-null females continue to develop but arrest between days 14 and 21 post-implantation (Bortvin et al., 2004; Bultman et al., 2006; Howell et al., 2001; Payer et al., 2003; Philipps et al., 2008) (Tables 1.2 and 1.3).

1.7.2. Degradation of maternal RNA and proteins and embryonic gene activation are regulated by maternal-effect genes

Oogenesis is an important process that occurs in order to prepare the meiotic matured oocyte for ovulation and then fertilization prior to the formation of the embryo and its early development. Both late oogenesis and early embryogenesis take place with a complete transcription quiescence and count exclusively on the maternal RNA and protein stores that accumulated during early oogenesis. This dowry that is loaded into the egg by the mother gradually degrades during oocyte development. The process of degradation continues until almost 30-40% of maternal poly A+ RNA (Baugh et al., 2003; De Renzis et al., 2007; Hamatani et al., 2004a) and 50% of the maternal proteins (Clegg and Piko, 1983; De Leon et al., 1983; Merz et al., 1981) only remain at the 2-cell mouse embryo. The presence of this maternal store is

crucial to support normal oocyte development until the activation of the zygotic genome and consequently its transcription and translation. Although crucial for the transition from oocyte to embryo, the mechanism underlying the clearance of maternal RNAs and proteins remains not fully understood. However, recent investigations on mice found that this mechanism appears to be partially regulated by the products of maternal-effect genes at different levels; these are described below.

RNA degradation in oocytes was shown to involve a molecular complex known as the RNA-induced silencing complex (RISC) formed by small noncoding RNAs, such as siRNA and microRNAs, and proteins (Ghildiyal and Zamore, 2009; Okamura and Lai, 2008; Svoboda and Flemr, 2010; Tam et al., 2008; Watanabe et al., 2008). Once formed, this complex recognizes a specific complementary messenger RNA (mRNA) transcript and promotes its cleavage or represses its translation (Svoboda, 2010; Walser and Lipshitz, 2011). *Dicer 1* (Murchison et al., 2007) and Argonaute subunit 2 *(Ago2)* (Morita et al., 2007) are two maternal-effect genes whose proteins appear to be implicated in this RNA decay process. While Dicer 1 cleaves small noncoding RNA precursors into their mature forms to constitute RISC (Murchison and Hannon, 2004), Argonaute 2 that has an endonucleolytic activity guides RISC to the target mRNA and promotes its cleavage (Liu et al., 2004b). Additionally, *Dicer 1*-null oocytes do not develop beyond meiosis I (Murchison et al., 2007) while *Ago2* null oocytes develop and fertilize normally but generate embryos that arrest at the 2-cell stage during early development (Lykke-Andersen et al., 2008). Another maternal-effect protein known as Zinc finger protein 36, C3H type-like 2 (encoded by *Zfp36l2*) (Ramos et al., 2004) also seems to be involved in regulating maternal RNA clearance through a process independent of the RISC complex. ZFP36L2 binds to the target mRNA at the AU-rich element (ARE) and promotes its deadenylation and degradation (Lai et al., 2000). The absence of *Zfp36l2* in female mice leads to impaired meiosis II in their oocytes and the derived embryos arrest at the 2-cell stage of development (Ball et al., 2014; Ramos et al., 2004).

On the other hand, the degradation of maternal proteins in the oocyte involves ubiquitin proteasome pathways (Roest et al., 2004; Suzumori et al., 2003; Verlhac et al., 2010) and macroautophagy, a process during which intracellular vesicles termed autophagosomes trap cellular organelles and proteins and then fuse with lysosomes for subsequent degradation. One maternal-effect protein known as Autophagy related 5 (encoded by *Atg5*), which is an E3

ubiquitin ligase, was documented to be essential for the formation of the autophagosome and consequently for maintaining autophagy in oocytes (Tsukamoto et al., 2008a; Tsukamoto et al., 2008b). The embryos whose mothers lack *Atg5* stop progression between the 4- and 8-cell stages (Tsukamoto et al., 2008a; Tsukamoto et al., 2008b).

The activation of the embryonic genome occurs in one minor and one major wave. Both waves occur at the same time as the overall chromatin remodeling during the first cleavage in mammalian embryos, including mouse and human. The minor and major waves occur at 1-cell (pronuclear stage) and 2-cell stages, respectively, in mice (Hamatani et al., 2004a) but at the 1-cell (Xue et al., 2013) and 4- to 8-cell (Braude et al., 1988; Dobson et al., 2004; Vassena et al., 2011; Zhang et al., 2009) stages, respectively, in humans. Several maternal-effect proteins were described to be implicated in the regulation of RNA transcription or embryonic genome activation in mouse. Of these, Heat shock factor 1 (encoded by *Hsf1)* (Christians et al., 2000), a DNA-binding protein that specifically binds heat shock promoter elements (HSE) and activates transcription (Guertin and Lis, 2010); Basonuclin 1 (encoded by *Bnc1*) (Ma et al., 2006), a regulator for ribosomal RNA transcription (Tian et al., 2001); CCCTC binding factor (encoded by *Ctcf*) (Wan et al., 2008), a transcription factor involved in transcriptional regulation by binding to chromatin insulators and preventing interaction between promoters with enhancers and silencers that are in close proximity (Cuddapah et al., 2009); and POU domain, class 5, transcription factor 1 (encoded by *Pou5f1* also known as *Oct4)* (Foygel et al., 2008), a transcription factor that plays a role in the maintenance of pluripotent ESC phenotype (Gifford and Meissner, 2012). Ovulated eggs from *Hsf1-, Bnc1-, Ctcf-* or *Pou5f1-* null mice can be fertilized but display various defects, with the exception of those from *Pou5-/-* (Foygel et al., 2008; Ma et al., 2006; Metchat et al., 2009; Wan et al., 2008). However, the derived embryos from all these maternal-effect gene-null mice stop developing between the 1-cell and 16-cell stages (Christians et al., 2000; Foygel et al., 2008; Ma et al., 2006; Wan et al., 2008) (Tables 1.2 and 1.3).

1.7.3. Cytoskeleton formation, integrity, dynamics, and stability are orchestrated by maternal-effect genes during fertilization

The oocyte cytoskeleton is mainly composed of actin filaments, microtubules and intermediate filaments and plays important roles during the process of fertilization. This role appears to be orchestrated by some cytoskeleton associated proteins and maternal-effect proteins (Tables 1.2 and 1.3).

1.7.3.1. Actin

Actin filaments are one of three major components of the oocyte cytoskeleton. Actin can be found either as a soluble monomer, designated as globular or G-actin, or as part of a linear polymer filaments termed filamentous or F-actin. Filamentous actin localizes throughout the egg cytoplasm and at the cortex. Two maternal-effect genes seem to be implicated in F-actin formation/maintenance. The first one is the Heat shock factor (encoded by *Hsf1)* (Christians et al., 2000) whose depletion in mouse oocytes causes less dense and disorganized F-actin proteins at the cortex (Bierkamp et al., 2010). The embryos derived from these deficient *Hsf1* oocytes arrest before the blastocyst stage mainly at the 1-cell embryo stage (Christians et al., 2000). The second one is Formin 2, (encoded by *Fmn2)* (Leader et al., 2002), without which mouse oocytes exhibit defects in cytoplasmic actin polymerization (Azoury et al., 2008; Li et al., 2008a; Schuh and Ellenberg, 2008). Fertilization of *Fmn2*-deficient oocytes leads to the formation of polyploid embryos and recurrent pregnancy loss in *Fmn2*-null mice (Leader et al., 2002).

The primary role of F-actin resides in its ability to surround and position the spindle apparatus perpendicularly to the oocyte membrane at the cortex prior to egg activation by the sperm in all mammals. However, an exception is made for rodents where the spindle apparatus is initially placed parallel to the egg cortex and then rotates 90 degrees before the extrusion of the second polar body (Labarrere et al., 1985; Longo and Chen, 1985; Maro et al., 1986; Maro et al., 1984; Webster and McGaughey, 1990). This process was recently subject to a thorough investigation in mouse oocytes and was demonstrated to be controlled by the following actin regulators a) spire-type actin nucleation factor 1 and 2 (encoded by *Spire 1/2*) (Pfender et al., 2011) and actin-related protein 2 and 3 (encoded by *Arp2/3*) (Sun et al., 2011), and b) small GTPase of the Rho

family such as cell division cycle 42 (encoded by *cdc42*) (Na and Zernicka-Goetz, 2006) and c) MAPKKK kinase protein (Choi et al., 1996; Verlhac et al., 2000; Yu et al., 2007).

During fertilization in mammals, the actin filaments, which constitute the backbone of the egg microvilli, trap the decapitated and incorporated sperm in a mesh-like pattern at the egg cortex and ensure normal fertilization (Le Guen et al., 1989; Maro et al., 1984; Webster and McGaughey, 1990). After fertilization, actin filaments continue to play an important role in the appropriate formation and emission of the second polar body (Le Guen et al., 1989; Longo and Chen, 1985; Maro et al., 1986). This role is driven by several signal transduction pathways mediated by kinases and actin associated proteins (Gallicano et al., 1997a; Gallicano et al., 1993; Gallicano et al., 1997b; Johnson et al., 1998; Longo and Chen, 1985). In addition, transducin-Like Enhancer of Split 6 (encoded by *Tle6)* is a third maternal-effect gene that seems to be involved in F-actin dynamics after fertilization since zygotes from *Tle6*-null mice do not form an F-actin meshwork and consequently arrest between the morula and blastocyst stages (Yu et al., 2014).

1.7.3.2. Microtubules

Microtubules are the second major element of the oocyte cytoskeleton. These structures are composed of the polymerization of alpha and beta tubulin proteins and can be observed either as wine-barrel shape structures during cell division, termed spindle apparatus, or as a filamentous network scattered all over the cytoplasm (Dutcher, 2001; Palacios et al., 1993). Microtubules are involved in two major processes during fertilization in mammalian eggs. The first role is in the formation of the spindle apparatus and segregation of half of the homologous chromosomes of the oocyte into the first polar body during meiosis I before fertilization. The second role is in the segregation of one sister chromatid of each chromosome into the second polar body upon the completion of meiosis II, i.e. following fertilization with the spermatozoon. At this stage, the resulting fertilized egg encompasses one copy of each maternal and paternal chromosome. This process is known to be regulated by intracellular free calcium concentrations, MAP kinases (Chesnel and Eppig, 1995; Hatch and Capco, 2001; Moos et al., 1995; Verlhac et al., 1994) and CamKinases 2 (Johnson et al., 1998). The second role of microtubules resides in the formation of a cytoplasmic network, which facilitates and controls the migration of the male and female

pronuclei after fertilization. Ten maternal-effect genes appear to be involved in maintaining the integrity of microtubules and the formation of microtubule spindles either before or after fertilization: KH domain containing 3 (encoded by *Khdc3 (Filia)*) (Zheng and Dean, 2009); NLR family, pyrin domain containing 5 (encoded by *Nlrp5 (Mater)*) (Tong et al., 2000); Peptidyl arginine deiminase, type VI (encoded by *Padi6*) (Esposito et al., 2007); Transducin-like enhancer of split 6 (encoded by *Tle6*) (Li et al., 2008b); Heat shock factor 1 (encoded by *Hsf1*) (Christians et al., 2000); Zygote arrest 1 (encoded by *Zar1*) (Wu et al., 2003); Argonaute RISC catalytic subunit 2 (encoded by *Ago2*) (Kaneda et al., 2009); Dicer 1 (encoded by *Dicer1*) (Murchison et al., 2007); Bromodomain and WD repeat domain containing 1 (encoded by *Brwd1*) (Philipps et al., 2008)*;* and Formin 2 (encoded by *Fmn2*) (Leader et al., 2002). Oocytes derived from null females display defects in the levels of synthetized tubulins, stability of microtubules, spindle assembly, migration and dynamics, and also kinetochore-microtubule attachment and consequently leads to impaired chromosome segregation (Dumont et al., 2007; Kan et al., 2011; Kaneda et al., 2009; Kim et al., 2014; Leader et al., 2002; Metchat et al., 2009; Murchison et al., 2007; Pattabiraman et al., 2015; Wu et al., 2003; Yu et al., 2014; Zheng and Dean, 2009). For instance, *Dicer 1* or *Fmn2* deficient oocytes arrest at meiosis I (Leader et al., 2002; Murchison et al., 2007); however, all the other maternal-effect-gene-deficient oocytes can be fertilized but lead to embryo arrest between the 1-cell and blastocyst stages (Christians et al., 2000; Esposito et al., 2007; Kaneda et al., 2009; Philipps et al., 2008; Tong et al., 2000; Wu et al., 2003; Yu et al., 2014; Zheng and Dean, 2009). Once cytoplasmic microtubules are nucleated, they come into contact with the newly formed female and male pronuclei and orient them side by side, awaiting the trigger of the first zygotic division. During this process, the nuclear envelope dissolves and both haploid genomes fuse (syngamy) with one another. The intracellular signal that is found to be implicated to some extent in this second role of microtubules is protein kinase C (PKC) and its cytosolic counterpart protein kinase M (PKM) (Boveri, 1901; Gallicano et al., 1993; Poueymirou and Schultz, 1987).

1.7.3.3. Intermediate filaments

Intermediate filaments are the third major component of the cytoskeleton. These structures constitute a highly cross-linked network covered with a layer of one or more proteins resembling sheets-like clusters, also termed cytoskeletal sheets or cytoplasmic lattices (CPLs) in mammalian eggs (Capco and McGaughey, 1986; Carson et al., 2000; Gallicano et al., 1994b; McGaughey and Capco, 1989). Recently, it has been shown that *Padi6* (Esposito et al., 2007) and *Nlrp5* (Tong et al., 2000), two maternal-effect genes, are indispensable for the formation of these lattices in mouse oocytes (Esposito et al., 2007). These sheets are mainly composed of keratins (Jackson et al., 1981) and are found in two types of configurations, fibrous and planar (Gallicano et al., 1992, 1994b; McGaughey and Capco, 1989). The fibrous sheets are detected in humans, bovines, canines, porcines and mice while the planar ones are found in rats and hamsters (Gallicano et al., 1992). Intermediate filaments undergo spatiotemporal changes in the mammalian egg cytoplasm (Gallicano et al., 1994a; Gallicano et al., 1991, 1995; McGaughey and Capco, 1989; Philipps et al., 2008). For instance, before fertilization, fibrous sheets are not detected at the cortical region; however, after fertilization, sheets of intermediate filaments redistribute to the cortex and are trapped in the cortical cytoskeleton. The planar sheets behave as the fibrous ones but appear to be organized in a coiled configuration prior to fertilization until the oocyte is activated, during which they become linearized. Restructuring of the sheets is found to be controlled by the PKC/PKM signaling pathway (Gallicano et al., 1995). There is no direct role attributed so far for these structures in the fertilization process (prior, during or after). However, recent investigations revealed that these sheets were found to constitute a storage site for ribosomes and to ensure appropriate de novo protein synthesis and therefore play a role in murine embryonic genome activation (Yurttas et al., 2008).

1.7.4. The role of the cytoskeleton in embryo compaction

The cytoskeleton also has major roles during embryo compaction mainly at the cell-to-cell junctions in the 8- to 16-cell stage embryos. These stages are characterized by two main changes in the embryo. The first one drives the blastomeres from a spherical to a flattened morphological pattern. The second one is the drastic modification of the shape of the embryo itself as a consequence of blastomeres flattening, and this leads to the formation of morula embryos. These changes seem to be controlled by some molecular signals and cytoskeleton-associated proteins. However, there are no described maternal-effect genes in the literature known to be implicated in regulating the cytoskeleton during embryo compaction.

1.7.4.1. Actin

During early development, actin functions primarily in cell adhesion where it associates with adherens junctions and protein complexes at cell-to-cell junctions, via alpha-catenin, which in turn binds to E-cadherin and beta-catenin. Once the association is established, actin filaments maintain the blastomeres of the embryos in a compacted configuration (Vasioukhin and Fuchs, 2001). Additionally, the actin cytoskeleton allows blastomeres to go through cytocortical microfilament polarization (Clayton et al., 1999) that is crucial for the establishment of trophoblast and inner cell mass lineages and subsequent development. This process occurs once the adherens junctions, along with tight junctions other junctional complexes of cell-cell adhesion, are formed. Although adhesion and polarization are both actin-based processes, the underlying regulatory mechanisms are different. The former is believed to be mediated by PKC signaling (Goval et al., 2000; Pey et al., 1998) while the latter is controlled by Rho GTPase (Clayton et al., 1999) and cofilin 1, which binds and depolymerizes actin filaments (Ma et al., 2009).

1.7.4.2. Microtubules

Microtubules are believed to be implicated in embryo compaction however their roles are poorly understood. Nonetheless, Eg5 (encoded by *KIF11*) which is a plus end directed kinesin related motor protein that associates with spindle microtubules, may partially regulate this process in mammalian embryos. Investigations uncovered that genetic ablation of *Eg5* in mouse resulted in improper spindle assembly and early arrested embryos with reduced cell numbers as well as failure of compaction and progression to the blastocyst stage (Castillo and Justice, 2007). Microtubules were shown to undergo posttranslational modifications and protein distribution in compacted blastomeres (Houliston and Maro, 1989). At compaction, alpha tubulins are either tyrosinated and located at the apical part of the blastomeres, or acetylated and detected at the basal part of the blastomeres. The acetylated form is also primarily found in blastomeres that are localized in the middle of the compacted embryo.

1.7.4.3. Intermediate filaments

Intermediate filaments or cytoskeletal sheets during embryo compaction undergo a significant morphological change (Capco et al., 1993; Gallicano et al., 1994a; Gallicano et al., 1991, 1994b; McGaughey and Capco, 1989) resulting in clear detectable filaments. During compaction, it appears that these sheets also bind to junctional complexes resembling desmosomes in order to maintain the structural integrity of the cell (Chan et al., 1994; Hesse et al., 2000; McGowan and Coulombe, 1998). These sheets were also found to associate with the nucleus of blastomeres (Albers and Fuchs, 1989; Capco et al., 1984; Georgatos and Blobel, 1987; Robson, 1989; Skalli and Goldman, 1991) and cooperate with actin and microtubules in order to regulate nuclear positioning in somatic cells (Dupin and Etienne-Manneville, 2011). Therefore, by analogy to somatic cells, it is plausible to suggest that these sheets may also be implicated, during embryonic compaction, in the positioning of the nuclei within the blastomeres to mediate cell fate specification of the preimplantation mammalian embryo, acting as an indicator of the outer /inner cell.

1.8. Maternal-effect genes and reproduction

1.8.1. *Padi6*

Padi6, Peptidylarginine deiminase 6, belongs to the PAD family (Chavanas et al., 2004; Wright et al., 2003) of calcium-dependent sulfhydryl enzyme proteins (Senshu, 1990) with role in citrullination also known as deimination, a post-translational modification converting arginine residues to citrulline (Rothnagel and Rogers, 1984). This modification is shown to affect the stability and degradation of the target protein and to play a cardinal role during development and cell differentiation (Akiyama and Senshu, 1999; Gyorgy et al., 2006). *Padi6* maps to chromosome 4 in mice, while its homologue in humans localizes to chromosome 1. PADI6 expression is primarily confined to the oocyte and early cleavage embryos with its protein being first detected in primordial follicles where it remains until at least the blastocyst stage (Wright et al., 2003). PADI6 localizes to the cytoplasm of the oocyte and is enriched at the cortex and absent from the cell-to-cell contact region in the early embryo stages (Morency et al., 2011). PADI6 is part of a specialized oocyte cytoskeletal structure called fibrous structure or CPLs (Wright et al., 2003). These structures are known to undergo reorganization at critical stages of development (Capco and McGaughey, 1986). To gain insight into the function of PADI6 in development, Esposito et al. generated and studied the reproduction of *Padi6*-null female mice. The authors found that these null females ovulated and their oocytes fertilized normally but lacked citrullination activity and displayed diffused cytoskeletal lattices (Esposito et al., 2007). Using the same system, Yurtas et al. demonstrated the requirement of PADI6 for the earliest stages of lattice formation in GV oocytes before maturation and fertilization. The authors showed that CPL-depleted *Padi6*$^{-/-}$ 2-cell embryos exhibited various defects that include low ribosomal storage, a global decrease of *de novo* protein synthesis and dysregulation of the translational program (Yurttas et al., 2008). Such defects were suggested to lead to partial activation of the embryonic genome and, subsequently, arrest at the 2-cell stage embryos (Esposito et al., 2007). Yet, Kan et al. revealed that the absence of PADI6-CPL structure in a *Padi6*-null GV oocyte affects the stability of cytoplasmic microtubules and consequently leads to altered mitochondria and endoplasmic reticulum positioning and redistribution during oocyte maturation. This study suggested that PADI6 and CPLs are involved in microtubule-mediated organelles redistribution (Kan et al., 2011). Altogether, these data point towards the fact that the defect leading to the

arrest of 2-cell embryos from *Padi6*-null mice actually starts from the GV stage and continues during oocyte growth.

1.8.2. *Tle6*

Tle6, Transducin-like enhancer of split 6, is a member of the Groucho/TLE transcriptional co-repressor family that lacks DNA-binding activity and plays roles in developmental signalling pathways (Notch, Wnt, Hedgehog and Dpp/BMP), and *Drosophila* neurogenesis and segmentation (Paroush et al., 1994). Additionally, members of this family were identified as targets of E2A-hepatic Leukaemia factor (Yeung et al., 2004). *Tle6* maps to chromosome 10 in mouse and its human homologue is found on chromosome 19. *Tle6* transcripts are abundantly found in growing murine oocytes but promptly degrade after oocyte maturation until almost no RNA is detected in 2-cell embryos. TLE6 protein expression begins during oocyte growth and remains until the blastocyst stage (Li et al., 2008b). TLE6 was originally described to physically interact with brain factor 1 (BF-1), a DNA binding protein in neural progenitors, and inhibit BF-1-mediated transcriptional repression (Marcal et al., 2005). TLE6 localizes exclusively to the cortex of oocytes and early cleavage stages and associates with MATER/NLRP5, OOEP/FLOPED and FILIA/KHDC3L to constitute a subcortical maternal complex (SCMC) in human and mouse oocytes (Li et al., 2008b; Zhu et al., 2015). To elucidate the role of *Tle6* in development, Yu et al. established *Tle6*-null mice and found that the number and morphology of oocytes from these mice not only were comparable to those of their wild type counterparts but that they can also be fertilized. However, these *Tle6*$^{-/-}$ oocytes clearly displayed diffused localization of all SCMC components (Yu et al., 2014). Additionally, the embryos derived from null females showed abnormal spindle formation and positioning due to altered F-actin dynamics. This defective actin cytoskeleton was attributed to the decreased levels of phosphorylated cofilin, a key regulator of F-actin assembly (Yu et al., 2014). These abnormalities lead to high incidence of asymmetrical divisions with the cytoplasm being fragmented into blebs and the embryos arrest between the morula and blastocyst stages (Yu et al., 2014). Recently, a new function for *Tle6* was established in mouse during oocyte maturation (Duncan et al., 2014). This study demonstrated that while co-localizing to the cortex at the germinal vesicle breakdown (GVBD) stage, TLE6 becomes phosphorylated by protein kinase A

(PKA), a critical physiological inhibitor of meiotic resumption in mammalian oocytes (Duncan et al., 2014). The implication of phosphorylation was speculated to be linked to the roles of *Nlrp5* and *Filia* in spindle assembly and migration during oocyte maturation (Zheng et al., 2013a). Altogether, these data uncover an important role of *Tle6* in regulating the oocytes cytoskeleton.

1.8.3. *Filia*

Filia, official name, *Khdc3,* KH domain containing 3, is a member of a family of proteins that contain a KH domain, which is known for its RNA binding ability (Dejgaard and Leffers, 1996; Krecic and Swanson, 1999; Musco et al., 1996; Ostareck-Lederer et al., 1998; Zhu and Chen, 2000). The KH domain binds preferentially to short pyrimidine-rich sequences (cytosine and uracil, *CUU*) in its target RNA (Amarasinghe et al., 2001). This family of KH-containing proteins is implicated in various physiological processes including early embryonic development (Herr et al., 2008), neuron degeneration (Buckanovich et al., 1996; Lewis et al., 2000), apoptosis (Krecic and Swanson, 1999; Shain et al., 2002) and cancer development (Mueller-Pillasch et al., 1997). *Filia* maps to chromosome 9 in mice (Ohsugi et al., 2008) and is the homologue of the human *KHDC3L* that maps to chromosome 6. *Filia* is a member of the oocyte/embryo expressed gene family in eutherian mammals along with *khdc1, dppa5,* and *floped (Ooep)* (Pierre et al., 2007), which are characterized by their atypical KH domain. This gene is transcribed into two isoforms of 1.6 kb and 1.2 kb. The former encodes a protein of 70 KDa and is mainly expressed in undifferentiated mouse ESCs (Mitsui et al., 2003) whereas the latter that encodes a protein of 50 KDa, is predominantly present in growing oocytes (Ohsugi et al., 2008). FILIA proteins (50 KDa) were found during oocyte growth and embryogenesis with levels falling off at the blastocyst stage. In the same cells, FILIA localizes within the SCMC and directly interacts with MATER but not with FLOPED or TLE6 (Li et al., 2008b). *Filia*$^{-/-}$ female mice are not completely sterile and their derived embryos progress to morula and blastocyst stages but display significant delays in their development. Additionally, depletion of maternal *Filia* promotes severe aneuploidy in cleavage-stage embryos due to a defect in the spindle assembly and the allocation of its key regulators to the centrosome, chromosome misalignment, and spindle assembly checkpoint (SAC) inactivation (Zheng and Dean, 2009). These abnormalities were also

reproducibly observed in mouse ESC lines (Zhao et al., 2015) where *Filia* was genetically ablated (Zhao et al., 2015). Consequently, these defects lead to cell transformation and tumorigenesis in *Filia*-deprived cells. Taken together, these data emphasize the role of FILIA as a safeguard for the cytoskeleton integrity.

1.8.4. *Floped*

Floped, Factor located in oocytes permitting embryonic development, also known as *Ooep* or *Moep19*, like *Filia* belongs to the oocyte/embryo expressed gene family (Pierre et al., 2007) and maps to chromosome 9 in mice and 6 in humans. *Floped* mRNAs are abundantly detected in undifferentiated ESCs (Miura et al., 2010), growing mouse oocytes (Li et al., 2008b) and unfertilized eggs with levels dropping off after fertilization (Tashiro et al., 2011). FLOPED localizes to the oocytes mainly to the cortex and is part of the SCMC where it interacts with MATER, TLE6, but not with FILIA (Li et al., 2008b). *Ooep*-null female mice formed well developed meiotically matured oocytes and mate successfully with wild type males; however, their oocytes lack the SCMC and display perturbed subcortical localization of MATER, FILIA and TLE6 (Li et al., 2008b). Additionally Ooep-null females are infertile as a result of early embryonic arrest at the 2- to 4-cell stages (Tashiro et al., 2011). Another novel role of *Floped* is that its loss by targeted mutation strategy does not affect ESC self-renewal under undifferentiated conditions but accelerates the differentiation pace of the induced ESCs (Miura et al., 2010) indicating that normal Floped is a negative regulator of ESC differentiation. In parallel, an investigation from Tang et al. was able to implicate *Floped* in the reprogramming process of ESCs since high mRNA expression of this gene at the resolution of single cells was detected during the conversion of ICM to ESCs (Tang et al., 2010).

1.8.5. *Nlrp2*

Nlrp2, NLR family, pyrin domain containing 2, is also a member of the NLRP family and maps to chromosome 7. It has a human orthologue on chromosome 19 that is considered to be the closest gene to *NLRP7*, with 64% amino acid identity at the protein level (Meyer et al.,

2009). NLRP2 is also an inhibitor of the NF-kappaB signaling pathway (Bruey et al., 2004) and its transcription was demonstrated to be regulated by NF-kappaB in various cellular models (Fontalba et al., 2007). A frameshift mutation in human *NLRP2* was identified in two siblings, with of Beckwith-Wiedemann syndrome (BWS), a rare genetic overgrowth and imprinting disorder (Meyer et al., 2009). The mutation was in a homozygous state in one child and in a heterozygous state in the other. Additionally, human *NLRP2* mRNA was shown to have a similar expression pattern as *NLRP7* during oocyte growth and embryogenesis (Zhang et al., 2008) suggesting a similar role in early development and imprinting establishment. *Nlrp2* is expressed at the RNA level in mouse oocytes and granulosa cells from the primary follicle and onwards; however, these transcripts are not present after 2-cell embryos (Peng et al., 2012). NLRP2 proteins were detected in the same cells at various follicular stages and persist until the blastocyst stages. NLRP2 was described to localize to the cytoplasm, nucleus, and to the nuclear pores in immature oocytes (Peng et al., 2012). Knocking down *Nlrp2* at the GV stage with siRNA did not affect the development or the maturation of murine oocytes. However, the embryos derived from these oocytes underwent a developmental arrest at the 2-cell stage (Peng et al., 2012). These data indicate that NLRP2 is dispensable for oocyte maturation and development but is indeed required for early embryonic development.

1.8.6. *Nlrp5*

Nlrp5 also called *Mater*, Maternal antigen that embryos require, is the first-described maternal-effect gene in mice (Tong et al., 2000) and also a member of the NLRP family. *Nlrp5* maps to chromosome 7 in mice and its orthologue to chromosome 19 in humans. Recently, variants in *NLRP5* were found to be associated with cases of reproductive loss and multilocus imprinting disorders in humans (Docherty et al., 2015). In humans, *NLRP5* transcripts and proteins are detected in oocytes from the GV until blastocyst stages (Zhang et al., 2008). *Nlrp5* murine transcripts accumulate during oogenesis, reach their highest levels at the GV stage, and then disappear in all stages of preimplantation embryos. *Nlrp5* protein was first detected in the cytoplasm of growing oocytes and persisted through late blastocyst stage (Tong et al., 2004). NLRP5 localizes to mitochondria, nucleoli, nuclear envelope, and the cortex in oocytes (Tong et al., 2004). Similar to PADI6, NLRP5 binds to CPLs and is required for their formation (Kim et

al., 2010). Kim et al. also went on to investigate the loss of *Nlrp5* in female mice and found that null-*Nlrp5* females are phenotypically normal and have normal folliculogenesis, ovulation, and fertilization. However oocytes from *Nlrp5*$^{-/-}$ oocytes lack CPLs (Kim et al., 2010) and exhibit abnormal mitochondrial localization and increased mitochondrial activity that lead to the accumulation of reactive oxygen species and consequently mitochondrial damage (Fernandes et al., 2012). Upon *in vitro* fertilization, the same oocytes had reduced amount of non-microtubule tubulin and displayed abnormal endoplasmic reticulum distribution and Ca2+ homeostasis, suggesting that NLRP5 regulates microtubules dynamics or stability and that its loss affects organelles positioning in oocytes (Kim et al., 2014). Furthermore, all embryos from *Nlrp5*$^{-/-}$ females do not progress beyond the 2-cell stage (Tong et al., 2000).

1.8.7. *Nlrp14*

Nlrp14, NLR Family, pyrin domain containing 14, is another member of the NLRPs, which maps to chromosome 7 in mice and 11 in humans. It is exclusively expressed in testes in humans (Westerveld et al., 2006) but is found in testes and ovaries in mice (Horikawa et al., 2005). A single study reported five male patients with spermatogenic failure; these patients each carried either a stop codon or one of four described missense mutations in *NlRP14* in a heterozygous state. The significance of these findings is not clear. Thus, identifying more mutations of *NLRP14* in additional cases with spermatogenic failure is needed in order to associate *NLRP14* with this condition. Interestingly, *Nlrp14* seems to affect female fertility since its inactivation using siRNA in murine fertilized oocytes led to early developmental arrest between the 2- to 4-cell stages in half of the embryos, while the other half continued to develop and arrested at the blastocyst stage (Hamatani et al., 2004b).

1.8.8. *Nlrp4e*

Nlrp4e is one of seven copies of *Nlrp4* with roles in the reproductive system in mice. *Nlrp4e* maps to chromosome 7 and has no orthologue in humans. Inactivating *Nlrp4e* in mouse

oocytes using siRNA did not affect their maturation or fertilization; however, the resulting embryos arrested their development between the 2- and 8-cell stages (Chang et al., 2013).

1.8.9. *Npm2*

Npm2, Nucleoplasmin 2 is a member of the nucleoplasmin (NPM) family of proteins implicated in ribosomal biogeneis, centrosome and DNA duplication, histone chaperoning, and chromatin assembly (Frehlick et al., 2007). *Npm2* maps to chromosome 14 in mice while its human orthologue maps to chromosome 8. In mice, *Npm2* transcripts and proteins are found in all stages of growing oocytes with the mRNA levels declining after fertilization and persisting to the 32-cell stage (Burns et al., 2003; Vitale et al., 2007). NPM2 protein localizes to the nuclei but not the nucleolei of GV oocytes until metaphase II, where it is solely cytoplasmic, with enrichment at the cortex of the oocyte (Burns et al., 2003; Vitale et al., 2007). Following metaphase II, the protein translocates back to the nucleus where it remains until the blastocyt stage. At metaphase II, NPM2 is phosphorylated and remains in the phosphorylated state until after fertilization, and then the protein is dephosphorylated and persists in this state throughout early developmental stages (Vitale et al., 2007). While *Npm2*$^{-/-}$ males are fertile, the females are subfertile with a 70% decrease in litter sizes as compared to wildtype. Oocytes from *Npm2*$^{-/-}$ females are apparently normal in terms of oogenesis, folliculogenesis, *in vitro* maturation, and fertilization. However, the DNA in *Npm2*$^{-/-}$ oocytes is amorphous and diffuse with disrupted nucleolar structure. Such abnormalities are also observed in *Npm2*$^{-/-}$ embryos along with defective transcriptional regulation and result in the development of only few embryos to blastocysts (Burns et al., 2003). In conclusion, NPM2 is required for nuclear and nucleolar organization and consequently compaction of chromatin from the oocyte till the early cleavage-stages. However, the mechanism(s) connecting NPM2 phosphorylation to its role in chromatin formation is/are not clear yet.

1.8.10. *Dnmt1o*

Dnmt1, DNA methyl transferase (cytosine-5) 1, is an enzyme that mainly methylates hemimethylated CpG residues of DNA in order to maintain epigenetic inheritance. *Dnmt1* maps to chromosome 9 in mice and 19 in humans. Homozygous mutations in *Dnmt1* were shown to be responsible for global genomic demethylation, X inactivation in mice (Li et al., 1993a; Li et al., 1993b; Panning and Jaenisch, 1996) and lethality around mid-gestation in embryos (Li et al., 1992). In mice, *Dnmt1* gives rise to three isoforms characterized by different 5' exons. The *Dnmt1o* isoform is expressed only in oocytes and early cleavage embryos; *Dnmt1s* is expressed in somatic cells and *Dnmt1p* is expressed only in spermatocytes at the pachytene stage (Mertineit et al., 1998). At the protein level, DNMT1o starts to appear in growing oocytes where it localizes both to the nucleus and to the cytoplasm. As the oocyte develops, the protein restricts its presence exclusively to the cytoplasm of GV and metaphase II. This cytoplasmic pattern with absence of signal at the cell-to-cell contact region remains until the 8-cell stage where the protein translocates from the cytoplasm to the nucleus and reappears only in the cytoplam at the morula and blastocyst stages (Howell et al., 2001). *Dnmt1o* null females were almost completely infertile, however, null males were fertile. Absence of maternal *Dnmt1o* did not affect oogenesis or preimplantation progress but led to embryos that all died between days 14 and 21 (Howell et al., 2001) except for a few pups that reached term and were successfully born. Of these few, some died later from severe abnormalities. Investigating the methylation pattern at 8-cell embryo, a stage during which DNMT1o translocates to the nucleus and comes into contact with the genome, revealed loss of methylation marks on normally imprinted, differentially methylated domains of several genes. This suggested that *Dnmt1o* is required to maintain appropriate DNA imprints at the fourth S phase of embryogenesis (Cirio et al., 2008; Howell et al., 2001).

RATIONALE AND OBJECTIVES OF THE PHD THESIS

In 2006, the identification of mutations within *NLRP7* in patients with RHMs led our group to conduct investigations that could provide insights on the role of NLRP7 in this rare condition. NLRP7 belongs to the NLRP family, members of which are known to mediate the activation of the innate immune response following various stimuli, which include pathogen-associated molecular patterns (PAMPs), such as bacterial lipopolysaccharides and fungal zymosan, as well as molecules associated with stress or danger such as crystals of uric acid and calcium pyrophosphatedihydrate (Tschopp et al., 2003). The activation of NLRPs leads to the formation of a multiprotein complex known as an inflammasome, which in turn promotes the maturation and secretion of the pro-inflammatory cytokine IL1B. Once secreted, the mature IL1B induces a complex network of other proinflammatory cytokines which in turn engage endothelial cells to capture leukocytes from the blood and recruit them to the site of infection or injury. In 2006, only one study by Kinoshita et al. about the functional role of this protein was reported and showed that NLRP7 inhibits caspase-1-dependent IL1B secretion in *NLRP7*-transfected THP1 cells in response to LPS stimulation (Kinoshita et al., 2005). Another study by Agostini et al. on NLRP3, another member of the NLRP family, had shown that this protein induces caspase-1-dependent IL1B processing and secretion in macrophages from PBMCs of a patient with Muckle-Wells Syndrome carrying a mutation in *NLRP3* (Agostini et al., 2004). In this patient, IL1B secretion was abnormally high in the supernatant of cells prior to stimulation and increased to a higher level after stimulation with LPS. Based on these two studies and before I joined the lab, our group went on investigating IL1B secretion by PBMCs isolated from patients with RHMs carrying either one or two *NLRP7* mutations or rare and low frequency variants. In collaboration with Dr. Salman Qureshi and using Enzyme-linked immunosorbent assay (ELISA), our group demonstrated that LPS-stimulated *ex vivo* PBMCs from patients with RHMs secrete lower levels of IL1B and tumor necrosis factor (TNF) than those of control subjects. Western blot analysis on the same stimulated cells revealed normal to slightly higher amounts of intracellular pro-IL1B synthesis and normal IL1B processing (Messaed et al., 2011a).

Hypothesis: We therefore hypothesized that *NLRP7* mutations do not alter IL1B synthesis or processing but affect the microtubules and consequently the trafficking of IL1B and other cytokines to the extra-cellular milieu.

The objectives described below reflect particularly the work I have done to answer our hypothesis

Objectives

1- Confirm the lower secretion of IL1B and of TNF, another cytokine, in PBMCs from additional patients with one or two *NLRP7* mutations and/or rare and low frequency variants (Chapter 2).

2- Check the expression and characterize the subcellular localization of NLRP7 in hematopoietic cells and particularly in monocytes, which are the main cells that secrete IL1B (Chapter2).

3- Characterize the expression and localization of KHDC3L, a second gene responsible for the same condition in hematopoietic cells (data not shown) (Reddy et al., 2013).

The above work led to the conclusion that both NLRP7 and KHDC3L co-localize to the microtubule organizing center (MTOC) suggesting their involvement in microtubule formation in hematopoietic cells. This raised the question whether these two proteins also co-localize in the oocytes, the cells that manifest the primary defect of this pathology, and whether NLRP7 and KHDC3L are implicated in the formation of the oocyte cytoskeleton and set the subsequent objectives of my thesis.

4- Investigate the subcellular localization of NLRP7 and KHDC3L in human oocytes and early cleavage embryos. This work led to the conclusion that NLRP7 and KHDC3L co-localize to a particular type of cytoskeleton in human oocytes. Also my extensive work on human oocytes and early embryos allowed me to learn how to preserve the integrity of the oocyte cytoskeleton and obtain high definition photos of its structure that have never been obtained before on human materials (Chapter 3).

5- Expand this analysis to other maternal-effect proteins known to bind to similar cytoskeletal structures in mice (Chapter 4).

6- Characterize the nature of the cytoskeleton to which NLRP7 and its possible connection to other oocyte cytoskeletal proteins (Chapter 4).

7- Review the reproductive history of patients with RHMs with the goal of investigating a possible correlation between the nature of *NLRP7* mutations in the patients and the exceptional occurrence of live births (Chapter 5).

FIGURES

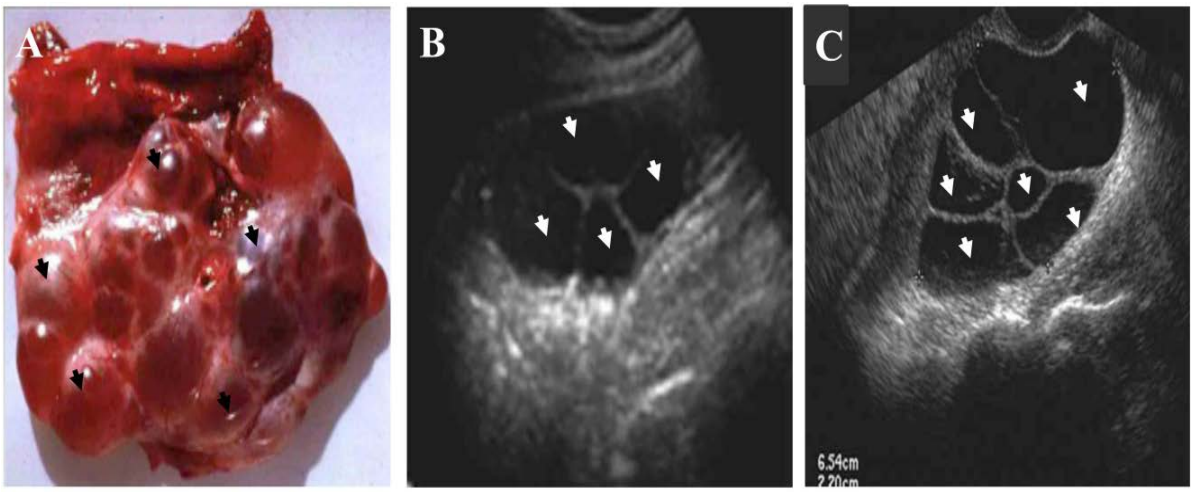

Figure 1.1. **Images of theca lutein cysts in an ovary**
(A) Gross appearance of one ovary showing multiple theca lutein cysts (black arrows). (B-C) Transabdominal scan of bilateral enlarged ovaries with multiple small theca lutein cysts, the left (B) measuring 6 cm and the right (C) measuring 9 cm in a 19-year old woman who is in her 11 weeks of molar pregnancy.
The Photo A is from from (https://quizlet.com/60102001/reproductive-flash-cards). Photos B and C are from Gloria Chiang and Deborah Levine. Imaging of Adnexal Masses in Pregnancy. The American Institute of Ultrasound in Medicine • J Ultrasound Med 2004; 23:805–819.

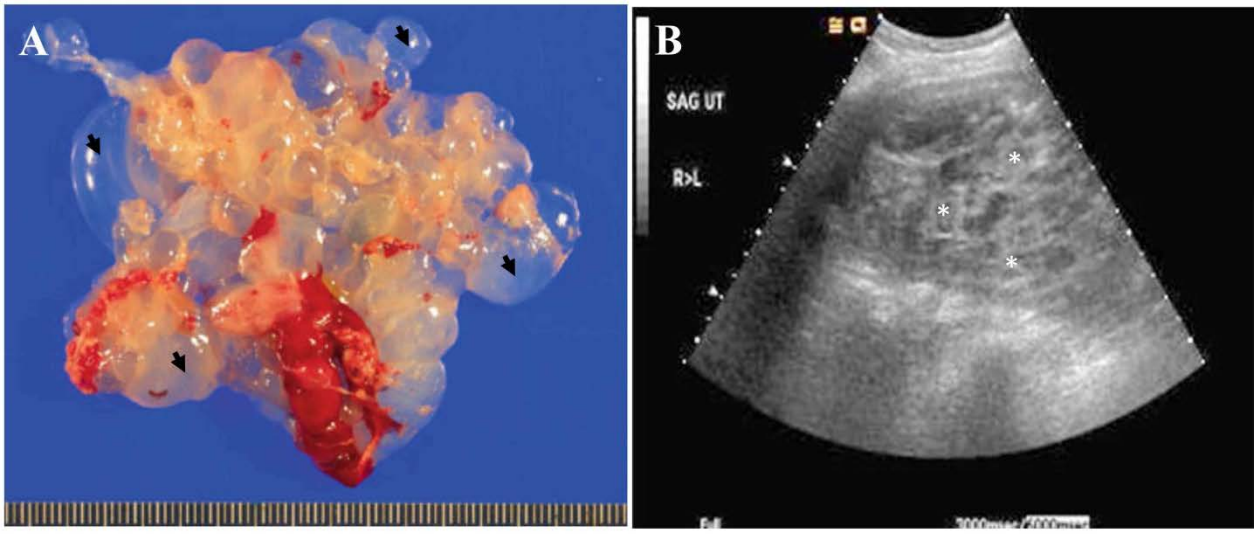

Figure 1.2. <u>Gross morphology (A) and ultrasound (B) photos of a complete hydatidiform mole</u>

(A) The chorionic villi are distinctly enlarged and hydropic (black arrows) and some covered with blood (Photo credit book of Pei Hu. Gestational trophoblastic disease: Diagnostic and molecular genetic pathology 2012). (B) The fetus is absent and the uterus is filled with mixed echogenic structures (asterisks). Credit to Dr. John Soper from the website: http://bestpractice.bmj.com/best-practice/monograph/1136/resources/image/bp/1.html.

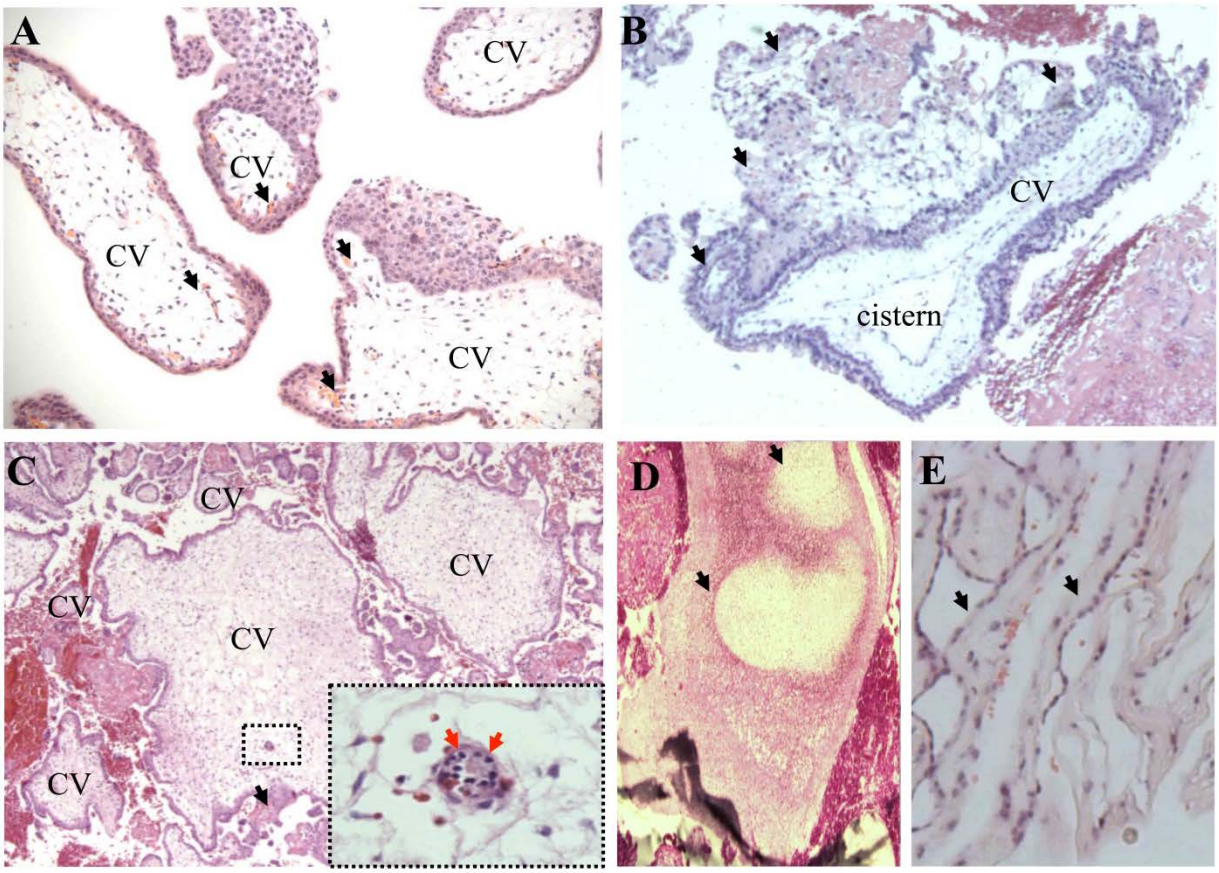

Figure 1.3. <u>Histopathological appearance of a normal placenta (A), a complete hydatidiform mole (B) and a partial hydatidiform mole (C)</u>
(A) The chorionic villus (CV) of a normal placenta displays two layers of cytotrophoblast and syncytiotrophoblast cells without abnormal proliferation. Note the presence of fetal blood vessels inside the CV (arrows). (B) The CV of a CHM displays enlarged hydropic villi with circumferential non-polar trophoblastic proliferation (arrows) and the presence of a cistern. (C) The CV of a PHM exhibits two populations of chorionic villi, large and small ones, with mild and focal trophoblastic proliferation (arrows). Inset in (C) shows a magnification of fetal nucleated red blood cells inside the CV of a PHM (red arrows). (D) A microscopic view of a fetal bone (arrows) in a PHM. (E) A microscopic view of fetal membranes (arrows) in a PHM. (Pictures were taken in Dr. Rima Slim's lab).

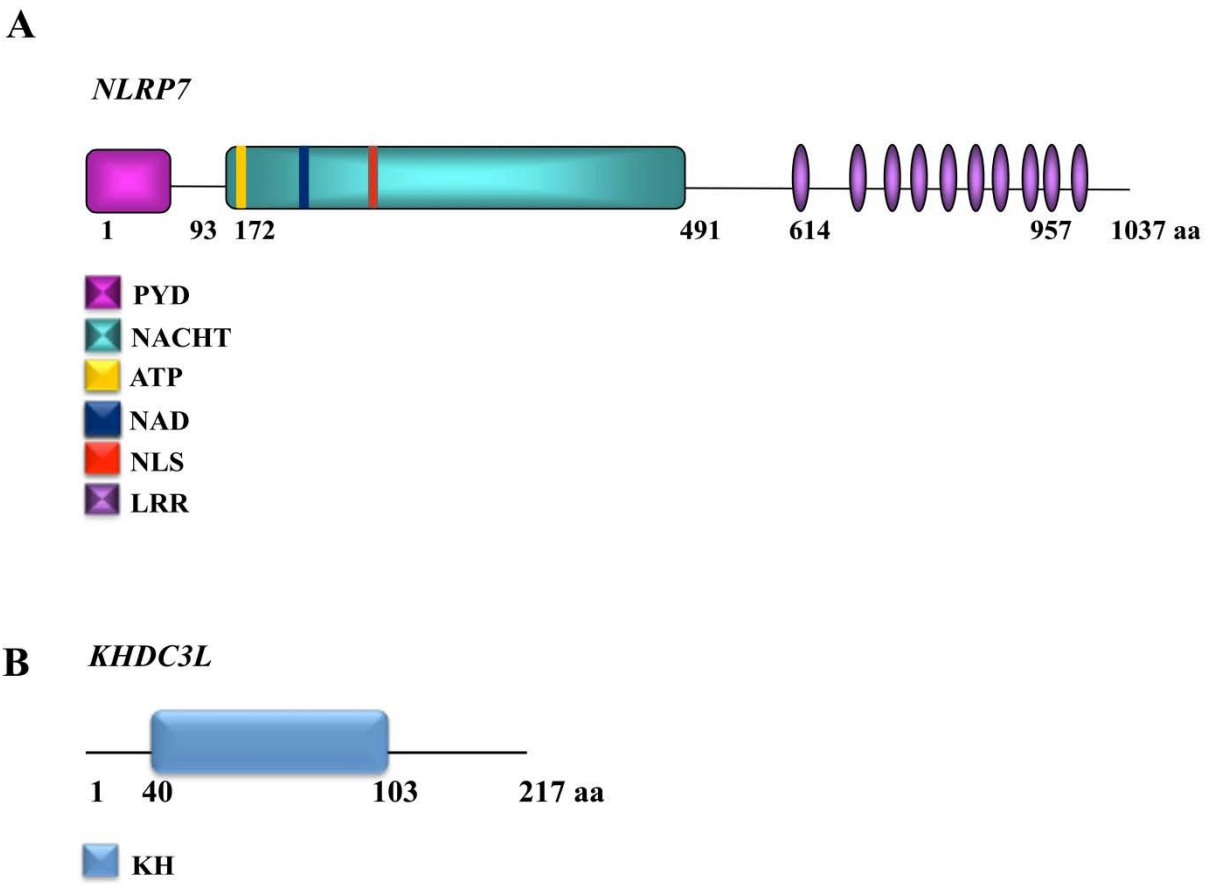

Figure 1.4. <u>Schematic representation of NLRP7 (A) and KHDC3L (B) protein domains</u>
PYD = pyrin domain; NACHT = the domain found in NAIP, CIITA, HET-E, and TP1 family of proteins; ATP = adenosine 5′-triphosphate binding motif; NAD, NACHT-associated domain; NLS, nuclear localization signal; LRR = leucine-rich repeats; KH = K homology domain (http://www.uniprot.org/).

TABLES

Table 1.1. Histopathological features of complete and partial hydatidiform moles

	CHM	**PHM**
Chorionic Villi	Diffuse with hydropic changes	Dismorphous: normal and hydropic with scalloped pattern
Cistern formation	Present	Present with maze-like pattern
Trophoblastic inclusions	Absent	Pseudo
Trophoblast proliferation	Severe; multifocal and circumferential	Mild to moderate and focal
Trophoblast nuclear and cytoplasmic enlargement known as cytological atypia	Present	Absent
Vasculature	Absent	May be present
Red blood cells and embryonic structures and tissues of inner cell mass origin	Absent	Present

Table 1.2. Maternal-effect genes in oocytes and early cleavage-stage embryos

A. *Group I* maternal-effect genes

MEG	Female/ Male	Abnormalities in		Wild type protein localization in		References
		Null oocytes	Null embryos	Oocytes	Early cleavage embryos	
Bnc1	Subfertile/ N/D	Abnormal oogeneis Abnormal oocyte morphology Impaired rate of RNA polymerase I-and II-mediated transcription	Nuclear structural abnormalities Reduction or block in DNA replication Embryo arrest at 2-cell with delayed progress	Nucleus and nucleolus in GV and Met II	Nucleus only in 1-cell but not detected afterwards	(Ma et al., 2006; Tian et al., 2001)
Brwd1	Sterile/ Sterile	Impaired meiosis progression Microtubules' defect Chromosomal congression defect	Embryo arrest at 2 pronuclei stage	N/D	N/D	(Pattabiraman et al., 2015; Philipps et al., 2008)

Ctcf	Subfertile/ N/D	Transcriptional misregulation Nucleolar abnormalities Delayed meiotic maturation Absence of polar body extrusion	Reduced zygotic genome activation Presence of apoptotic cells Embryo arrest 8- to 16-cell with delayed progress	Nucleus but not nucleolus	Nucleus but nucleolus until blastocyst	(Wan et al., 2008)
Dppa3 (Stella, Pgc7)	Subfertile/ Fertile	Nuclear and nucleolar structural defects Incomplete global transcription repression	Loss of methylation on maternal genome Loss of methylation on paternal genome Embryo arrest at 2- to 4-cell	Cytoplasm Nucleus	Cytoplasm Nucleus Trophectoderm	(Liu et al., 2012; Nakamura et al., 2007; Payer et al., 2003; Sato et al., 2002)
	Fertile/ Fertile	N/A	Embryo arrest at 4-cell	N/D	N/D	
	Bovine, N/A*/ N/A		Increased intensity of 5hmC staining in the maternal pronucleus Decreased in embryo developmental rates Fewer inner cell mass cells			(Bakhtari and Ross, 2014)

Dnmt1o	Sterile/ Fertile	N/D	Loss of methylation during 8-cell Embryo arrest between day 14 and 21 post-implantation	Nucleus at GV Cytoplasm at Met II	Cortex No cell-to-cell contact Nucleus 8-cell Cytoplasm at blastocyst Nucleus from 1-cell until blastocyst (independent study)	(Hirasawa et al., 2008; Howell et al., 2001; Petrussa et al., 2014)
Dnmt3l	Sterile/ Sterile	Loss of methylation on maternal imprinted loci	Loss of methylation on maternal imprinted loci Pericardial edema, exencephaly and other neural tube defects Embryo arrest at 9.5 days post-implantation	Nucleus at GV	Cytoplasm at morula and blastocyst	(Bourc'his et al., 2001; Petrussa et al., 2014),
Hsf1	Sterile/ Fertile	Impaired meiosis progression Low MAPK pathway activity	Nuclear structural abnormalities Impaired exocytosis	Cytoplasm Nucleus	Cytoplasm Nucleus	(Bierkamp et al., 2010; Christians et al., 2000; Kang et al., 2014; Metchat et al., 2009)

		Microtubules' and F-actin defects Abnormal organelles positioning Activation of apoptotic pathway	Impaired pronuclei formation Activation of apoptotic pathway Embryo arrest at 1-cell			
KHDC3 (Filia)	Subfertile/ Fertile	N/D	Aneuploidy Microtubules' defect Chromosome misalignment Embryo progress to morula and blastocyst with delays in development	Cortex SCMC	Cortex No cell-to-cell contact SCMC	(Zheng and Dean, 2009)
Mlh1	Sterile/ Sterile	N/D	Absence of second polar body formation Embryo arrest mainly at 1-cell	N/D	N/D	(Edelmann et al., 1996)
Nlrp2	N/A*/ N/A	N/A	Embryo arrest at 2- to 8-cell	Cytoplasm Nucleus Close to nuclear pores	Cytoplasm Nucleus Close to nuclear pores	(Peng et al., 2012)

Nlrp4e	N/A*/ N/A	N/D	Embryo arrest at 2- to 8-cell	N/D	N/D	(Chang et al., 2013)
Nlrp5 (Mater)	Sterile/ Fertile	Reduced levels of ribosomal RNA transcription Microtubules' defect Abnormal organelles positioning Abnormal Ca2+ homeostasis Absence of CPL	Reduced embryonic transcription Reduced embryonic translation Embryo arrest at 2-cell	Cortex Mitochondria Nucleolus Nuclear envelope CPL /SCMC	Cortex No cell-to-cell contact CPL /SCMC	(Fernandes et al., 2012; Kim et al., 2010; Kim et al., 2014; Tong et al., 2004; Tong et al., 2000)
	Pig, N/A*/ N/A	N/D	Embryo arrest 2- to 8-cell	Cortex Cytoplasm	Cortex Cytoplasm No cell-to-cell contact	(Peng et al., 2015)
	Monkey, N/A*/ N/A	N/D	Embryo arrest at 8- to 16-cell	N/D	N/D	(Wu, 2009)
Nlrp14	N/A*/ N/A	N/D	50% Embryo arrest at 2- to 4-cell and 50% at blastocyst	Cytoplasm	N/D	(Hamatani et al., 2004b)

Npm2	Subfertile/ Fertile	Nuclear and nucleolar structural abnormalities in GV	Nuclear and nucleolar structural abnormalities Defective transcriptional regulation Embryo arrest at 1-cell	Nucleus but not nucleolus at GV Cytoplasm at Met II Cortex at Met II	Nucleus but not nucleoli	(Burns et al., 2003; Vitale et al., 2007)
	Zebrafish, N/A*/ N/A		Low expression of first-wave zygotic genes Embryo arrest before gastrulation	Nucleus and weak signal in cytoplasm	Nucleus and weak signal in cytoplasm	(Bouleau et al., 2014)
Oas1a	Subfertile/ Fertile	Defects in ovarian follicle development and decreased ovulation efficiency	Embryo arrest at 8-cell	Cytoplasm and enriched at the Cortex	Not detected in 2-cell or later stages N/D in 1-cell	(Yan et al., 2005)
Ooep (Floped, Moep19)	Sterile/ N/D	Diffused SCMC	Embryo arrest at the 1- to 2-cell	Cortex SCMC	Cortex No cell-to-cell contact SCMC	(Li et al., 2008b; Tashiro et al., 2011)
Padi6	Sterile/ Fertile	Absence of citrullination	Reduced ribosomal RNA	Cytoplasm	Cortex	(Esposito et al., 2007; Kan et al., 2011; Morency et al., 2011; Wright et al., 2003; Yurttas et

		Absence of CPL Microtubules defect Abnormal organelles positioning	Dysregulation of translation Incomplete activation of embryonic genome Embryo arrest at 2-cell	Cortex CPL/SCMC	No cell-to-cell contact CPL/SCMC	al., 2008)
Pms2	Fertile/ Sterile	N/D	Microsatellite instability Deficiency in DNA mismatch repair activity in 1-cell Arrest at later stages of preimplantation	N/D	N/D	(Gurtu et al., 2002)
Sebox	N/A*/ N/A	N/D	Embryo arrest at 2-cell	N/D	N/D	(Kim et al., 2008)
	N/A*/ N/A	Decrease number of GV	N/D	N/D	N/D	(Moreno et al., 2014)
	N/A*/ N/A	Upregulation of some maternal-effect genes	Impaired maternal mRNAs degradation Incomplete expression of zygotic genome activation (ZGA) Diminished transcriptional activity	N/D	N/D	(Park et al., 2015)

	Pig, N/A*/ N/A		Upregulation of maternally expressed genes Upregulation of pluripotency genes Impaired early embryonic development	N/D	N/D	(Zheng et al., 2013b)
Tcl1a	Subfertile/ Fertile	N/D	Embryo arrest at 4- to 8-cell with delays in development	Cortex at Met II	Shuttles between pronuclei and cortex during the first three embryonic divisions No cell-to-cell contact	(Narducci et al., 2002)
Trim24 (Tif1a)	N/A*/ N/A	N/D	Mislocalization of RNA pol II and also of BRG-1, SNF2H, two chromatin remodelling proteins in the zygote Downregulation of specific gene Embryo arrest 2- to 4-cell	Cytoplasm at GV	Cytoplasm from zygote until 4-cell Nucleolar-like bodies from zygote until 4-cell	(Torres-Padilla and Zernicka-Goetz, 2006)
Tle6	Sterile/ Fertile	Diffused SCMC with Abs against NLRP5, FILIA, OOEP	Microtubules and F-actin defects	Cortex	Cortex	(Li et al., 2008b; Yu et al., 2014; Zhu et al., 2015),

			Embryo arrest at morula to blastocyst Abnormal spindle formation and positioning	SCMC	No cell-to-cell contact SCMC	
Ube2a (Hr6a)	Sterile/ Fertile	N/D	Embryo arrest at 2-cell	N/D	N/D	(Roest et al., 2004)
Zar1	Sterile/ Fertile	N/D	Incomplete fertilization Microtubules defect Reduction in the synthesis of the proteins of the transcription requiring complex Delayed cell cycle progression Embryo arrest primarily at 1-cell	Cytoplasm	Cytoplasm Diminishes by 2-cell embryo	(Wu et al., 2003)
Uchl1	Subfertile/ N/D	Polyspermy *in vitro* Low monoubiquitin levels	Embryo arrest at Zygote Polyploidy	Cortex	Cortex No cell-to-cell contact Trophectoderm	(Sekiguchi et al., 2006)
	Bovine, N/A*/ N/A	Increased abundance of K63-linked polyubiquitin chains	High rate of polyspermy	N/D	Cortex	(Susor et al., 2010)

		Impaired migration of CGs toward the cortex during oocyte maturation and fertilization-induced extrusion of CGs	Decreased levels in the monomeric ubiquitin and polyubiquitin pool		Nucleus	
Zfp36l2	Sterile/ Fertile	Reduced oocyte number	Embryo arrest at 2-cell	N/D	N/D	(Ramos et al., 2004)
	Sterile/ N/D	Impaired meiosis II progression Excessive PKA activation Increase cAMP levels Increase of adenyl cyclase activity	N/D	N/D	N/D	(Ball et al., 2014)

B. *Group II* maternal-effect genes

MEG	Female/ Male	Abnormalities in			Wild type protein localization in		References
		Null mice	**Null oocytes**	**Null embryos**	**Oocytes**	**Early cleavage embryos**	
Ago2 (Eif2c2)	Lethal/ Lethal	N/D	N/A	N/A	N/D	N/D	(Morita et al., 2007)
	N/A*/ N/A	N/A	N/D	Stabilization of some maternal mRNAs of a group of gene Reduction of zygotic transcripts of other genes Embryo arrest at 2-cell	N/D	RNA degradation polar bodies in 2-cell	(Lykke-Andersen et al., 2008)
	Sterile/ N/D	N/D	Microtubules' defect Chromosome organization defect Reduced expression levels of microRNA Deregulation of expression for some genes	Embryo arrest at zygote	N/D	N/D	(Kaneda et al., 2009)

Atg5	Lethal/ Lethal	N/D	N/A	N/A	N/D	N/D	(Kuma et al., 2004)
	Sterile/ N/D	N/D	Defective autophagy	Reduced overall protein synthesis Embryo arrest at 4- to 8-cell	N/D	N/D	(Tsukamoto et al., 2008a; Tsukamoto et al., 2008b)
Cdh1 (E-cad)	Lethal/ Lethal	N/D	N/A	Failure to form intact trophectoderm layer	N/D	N/D	(Larue et al., 1994)
	Fertile/ N/D	N/D	N/D	Absence of blastomeres adherence until late morula Delayed cell division Progressed compaction of individual blastomeres	N/D	Cortex Cell-to-cell contact	(De Vries et al., 2004)
Dicer 1	Sterile/	N/D	Microtubules' defect	N/A	N/D	N/D	(Murchison et al., 2007)

	N/D		Chromosomal congression defect Cohesion defect Affected transcriptome Arrest in meiosis I				
Dnmt3a	Lethal/ Lethal	N/D	N/A	N/A	N/D	N/D	(Okano et al., 1999)
	Sterile/ Sterile	N/D	N/D	Developmental defect Lack of methylation at all maternally imprinted loci Embryo arrest at E10.5 post-implantation	Cytoplasm	Cytoplasm Nucleus from one cell to 8-cell (Independent study)	(Hirasawa et al., 2008; Kaneda et al., 2004; Petrussa et al., 2014)
Ezh2	Lethal/ Lethal	Impaired histone methylation in the female	N/A	N/A	The ovary (cytoplasm and nucleus)	Both pronuclei Nuclear in all early embryonic stages Trophectoderm	(O'Carroll et al., 2001)

	Fertile/ N/D	N/D	N/D	N/D	N/D	N/D	(Erhardt et al., 2003)
	N/A*/ N/A	N/A	N/D	Reduced histone modification Increased apoptotic cells in blastocysts Upregulated expression of genes related to the differentiation of germ layers Severe growth retardation and reduced blastocyst formation	Nucleus Cytoplasm	Nucleus all early embryonic stages Inner cell mass	(Huang et al., 2014)
Fmn2	Subfertile/ Fertile	N/D	Impaired meiosis progression Microtubule and F-actin defects Polyploidy	Polyploidy in 2-cell and blastocysts	Cytoplasm Meoitic spindle	Cytoplasm of 2-cell	(Azoury et al., 2008; Dumont et al., 2007; Kwon et al., 2011; Leader et al., 2002; Li et al., 2008a; Schuh and Ellenberg, 2008),

			Inability to extrude the first polar body Defective chromosomal migration and cytokinesis during meiosis I Arrest at Met I				
Gas6	N/A*/ N/A	N/A	Change in MPF activity Reduced Ca2+ oscillation Absence of pronucleus formation Exocytosis at cortical granules Arrest at Met II	N/A	N/D	N/D	(Kim et al., 2011)
Pla2g4c	N/A*/ N/A	N/A	N/D	N/A	Cortex Nucleus MVA at GV Spindle poles in Met II	Cortex No cell-to-cell contact	(Vitale et al., 2005)

Pou5f1 (Oct-4)	N/A*/ N/A	N/A	N/D	Deregulation of genes encoding post-transcriptional regulators Embryo arrest 1-cell to morula	N/D	N/D	(Foygel et al., 2008)
	Lethal/ Lethal	Giant trophoblast cells and no ICM	N/A	N/A	Cytoplasm	Cytoplasm Nucleus of all cleavage-stages Inner cell mass	(Nichols et al., 1998; Palmieri et al., 1994)
Spin1	Lethal/ grafted oocytes/ N/A	N/A	Impaired meiosis progression and maternal transcript stability	N/D	Cytoplasm Meiotic spindle	N/D	(Chew et al., 2013; Oh et al., 1997)
Sox2	Lethal/ Lethal	Outgrowth and defective ICM	N/A	N/A	Cytoplasm	Cytoplasm Nucleus Trophectoderm	(Avilion et al., 2003; Keramari et al., 2010)
Smarca4 (Brg1)	Lethal/ Lethal	N/D	N/A	N/A	N/A	N/A	(Bultman et al., 2000)

	Subfertile/ N/D	N/D	N/D	Decreased levels of histone methylation Reduced overall transcription activity Embryo arrest at 2-cell	Cytoplasm Nucleus	Cytoplasm Nucleus	(Bultman et al., 2006; Kang et al., 2014)

The abnormalities in the oocytes and embryos derived from null organisms are described in mice unless otherwise indicated. MEG, stands for maternal-effect gene; N/A, not applicable; N/A*, not Applicable + the knockdown was done immediately on oocytes or zygotes using siRNA or morpholino antisense or protein inhibitor or an antibody/; N/D, not described; L, lethality; CL, cytoplasmic lattices; GV, germinal vesicle; Met I, metaphase I; Met II, metaphase II; ICM, inner cell mass; CG, cortical granules; MVA, multivesicular aggregates; MPF, maturation promoting factor, Abs, antibodies. The table of *Group I* MEG indicates the genes that upon genetic ablation or knockdown show various defects in oocytes and embryos and eventually lead to early embryonic arrest. The table of *Group II* MEG indicates the genes that upon genetic ablation or knockdown show either maternal lethality associated sometimes with abnormalities in the female mice and/or various defects in the derived oocytes and embryos.

Table1.3. Full names of maternal-effect genes, their HUGO symbols and aliases

Maternal-effect proteins	**Gene symbol**	**Aliases**
Argonaute RISC catalytic subunit 2	*Ago2*	1110029L17Rik, 2310051F07Rik, AI225898, AL022874, AW546247, ENSMUSG00000072493, Eif2c2, Gerp95, Gm10365, mKIAA4215
Autophagy related 5	*Atg5*	2010107M05Rik, 3110067M24Rik, AW319544, Apg5ll, C88337, Paddy
Basonuclin 1	*Bnc1*	AI047752, AW546376, Bnc
Bromodomain and WD repeat domain containing 1	*Brwd1*	5330419I02Rik, D530019K20Rik, G1-403-16, Wdr9, repro5
Cadherin 1	*Cdh1*	AA960649, ARC-1, E-cad, L-CAM, UVO, Um, E-cadherin
CCCTC-binding factor	*Ctcf*	AW108038
Developmental pluripotency-associated 3	*Dppa3*	2410075G02Rik, PCG7, PGC7, Stella
Dicer 1, ribonuclease type III	*Dicer 1*	1110006F08Rik, D12Ertd7e, mKIAA0928
DNA methyltransferase (cytosine-5) 1 oocyte	*Dnmt1o*	Cxxc9, Dnmto, MCMT, MTase, Met-1, Met1, MommeD2, m.MmuI, Dnmt1
DNA methyltransferase 3A	*Dnmt3a*	MmuIIIA
DNA methyltransferase (cytosine-5) 3-like	*Dnmt3l*	D6Ertd14e, ecat7
Enhancer of zeste 2 polycomb repressive complex 2 subunit	*Ezh2*	Enx-1, Enx1h, KMT6, mKIAA4065
Formin 2	*Fmn2*	AU024104
Growth arrest specific 6	*Gas6*	Gas-6
Heat shock factor 1	*Hsf1*	AA960185alpha, Hsf1beta
KH domain containing 3	*Khdc3*	2410004A20Rik, AI467128, OEEP48, *Filia, ECAT1*
MutL homologue 1	*Mlh1*	1110035C23Rik, AI317206, AI325952, AI561766
NLR family, pyrin domain containing 2	*Nlrp2*	E330007A02Rik, NBS1, Nalp2, PAN1, PYPAF2
NLR family, pyrin domain containing 4E	*Nlrp4e*	4930406H16Rik, Nalp-epsilon, Nalp4e, Nlrp4
NLR family, pyrin domain containing 5	*Nlrp5*	Mater, Nalp5, Op1, PAN11
NLR family, pyrin domain containing 14	*Nlrp14*	4921520L01Rik, GC-LRR, Nalp-iota, Nalp14, Nalp14l
Nucleoplasmin 2	*Npm2*	No aliases

2'-5' oligoadenylate synthetase 1A	*Oas1a*	L3
Oocyte expressed protein	*Ooep*	2410146L05Rik, Floped, Moep19, Sddr
Peptidyl arginine deiminase, type VI	*Padi6*	Pad6, Padi5, ePAD
Phospholipase A2, group IVC	*Pla2g4c*	D7Ertd445e
Postmeiotic segregation increased 2	*Pms2*	AW555130, Pmsl2
POU domain, class 5, transcription factor 1	*Pou5f1*	NF-A3, Oct-3, Oct-3/4, Oct-4, Oct3, Oct3/4, Oct4, Otf-3, Otf-4, Otf3, Otf3-rs7, Otf3g, Otf4
SEBOX homeobox	*Sebox*	OG9, Og9x
Spindlin 1	*Spin1*	Spin
SRY (sex determining region Y)-box 2	*Sox2*	Sox-2, lcc, ysb
SWI/SNF related, matrix associated, actin dependent regulator of chromatin, subfamily a, member 4	*Smarca4*	Brg1, HP1-BP72, SNF2beta, SW1/SNF, b2b508.1Clo, b2b692Clo
T-cell leukemia/lymphoma 1A	*Tcl1a*	No aliases
Transcription intermediary factor 1 alpha	*Tif1α*	A130082H20Rik, AI447469, D430004I05Rik, TIF1, TIF1-alpha, TIF1alpha, Tif1a,Trim24
Transducin-like enhancer of split 6	*Tle6*	1810057E06Rik, Grg6
Ubiquitin carboxy-terminal hydrolase L1	*Uchl1*	AW822034, C88048, PGP 9.5, PGP9.5, R75593, UCH-L1, UCHL-1, gad
Ubiquitin-conjugating enzyme E2A	*Ube2a*	HR6A; HHR6A; Mhr6a
Zinc finger protein 36, C3H type-like 2	*Zfp36l2*	Brf2, ERF2, Tis11d
Zygote arrest 1	*Zar1*	No aliases

CHAPTER 2

NLRP7, A NUCLEOTIDE OLIGOMERIZATION DOMAIN-LIKE RECEPTOR PROTEIN, IS REQUIRED FOR NORMAL CYTOKINE SECRETION AND CO-LOCALIZES WITH THE GOLGI AND THE MICROTUBULE-ORGANIZING CENTER

Christiane Messaed[1,2#], Elie Akoury[1,2#],Ugljesa Djuric[1,2], Jibin Zeng[1,2], Maya Saleh[3], Lucy Gilbert[1,2], Muhieddine Seoud[4], Salman Qureshi[3], and Rima Slim[1,2]

[#]Both authors contributed equally to this work.

[1]Departments of Human Genetics; [2]Obstetrics and Gynecology, McGill University Health Centre, Montreal H3G 1A4, Canada; [3]Department of Medicine and the Centre for the Study of Host Resistance, McGill University Health Centre, Montreal H3G 1A4, Canada; [4]Department of Obstetrics and Gynecology, American University of Beirut, Beirut, Lebanon.

Manuscript published in the Journal of Biological Chemistry December 16, 2011 volume 286 number 50 (PMID: 2202561).

2.1 ABSTRACT

A Hydatidiform mole is a human pregnancy with hyperproliferative placenta and abnormal embryonic development. Mutations in *NLRP7*, a member of the nucleotide oligomerization domain-like receptor family of proteins with roles in inflammation and apoptosis, are responsible for recurrent HMs. However, little is known about the functional role of NLRP7. Here, we demonstrate that PBMCs from patients with *NLRP7* mutations and rare variants secrete low levels of IL1B and TNF in response to LPS. We show that cells from patients, carrying mutations or rare variants, have variable levels of increased intracellular pro-IL1B indicating that normal NLRP7 downregulates pro-IL1B synthesis in response to LPS. Using transient transfections, we confirm the role of normal NLRP7 in inhibiting pro-IL1B and demonstrate that this inhibitory function is abolished by protein truncating mutations after the Pyrin domain. Within PBMCs, NLRP7 co-localizes with the Golgi and the microtubule-organizing center and is associated with microtubules. This suggests that *NLRP7* mutations may affect cytokine secretion by interfering, directly or indirectly, with their trafficking. We propose that the impaired cytokine trafficking and secretion caused by NLRP7 defects makes the patients tolerant to the growth of these earlier arrested conceptions with no fetal vessels and that the retention of these conceptions until the end of the first trimester contributes to the molar phenotype. Our data will impact our understanding of postmolar choriocarcinomas, the only allograft non-self-tumors that are able to invade maternal tissues.

2.2 INTRODUCTION

Hydatidiform moles are abnormal human pregnancies with excessive proliferation of trophoblast cells and abnormal embryonic development. The common form of HMs is sporadic, not recurrent, and occurs in 1 in every 250 pregnancies in Western countries (Seckl et al., 2010). Molar pregnancies are usually benign but may degenerate into gestational choriocarcinomas and invade maternal tissues outside the uterus (Altieri et al., 2003). Using linkage analysis and positional cloning on rare familial cases of recurrent moles in which the disease segregates as an autosomal recessive condition, our group identified a maternal gene, *NLRP7*, responsible for recurrent HMs and associated with reproductive wastage (Murdoch et al., 2006). To date, 60 *NLRP7* mutations have been reported by several groups in patients from different populations and are listed on Infevers (Deveault et al., 2009; Hayward et al., 2009; Kou et al., 2008; Milhavet et al., 2008; Puechberty et al., 2009; Qian et al., 2007; Wang et al., 2009a). Patients with recurrent HMs have usually two defective alleles. However, to date 14 patients with a single defective allele each have been reported and these patients have better reproductive outcomes, i.e. less recurrent moles, more spontaneous abortions, and more live births than patients with two defective alleles (Deveault et al., 2009; Hayward et al., 2009; Messaed et al., 2011b; Muhlstein et al., 2011). Moreover, we have shown that rare nonsynonymous (NSVs) *NLRP7* variants found in the general European population are associated with recurrent reproductive wastage in European patients (Deveault et al., 2009; Hayward et al., 2009).

NLRP7 is a member of the nucleotide oligomerization domain-like family, a series of cytoplasmic proteins characterized by an N-terminal PYD domain, followed by a NACHT domain, and a C-terminal LRR region. Although the Pyrin and the LRR domains are involved in protein-protein interactions, the NACHT is a NTPase domain found in apoptosis proteins as well as in proteins involved in the transactivation of the major histocompatibility complex (MHC) class II (Tschopp et al., 2003). Recent studies have shown increased *NLRP7* expression in testicular (Okada et al., 2004) and endometrial (Ohno et al., 2008) cancers. One *in vitro* study has shown that overexpressing wild-type NLRP7 inhibits caspase-1-dependent IL1B processing and secretion (Kinoshita et al., 2005).

In this study, we demonstrate that patients with *NLRP7* mutations and variants secrete significantly lower amounts of IL1B and TNF than control cells in response to LPS despite their higher intracellular pro-IL1B synthesis and normal pro-IL1B processing. Using transient transfections, we demonstrate that overexpression of wild-type NLRP7 inhibits primarily pro-

IL1B synthesis and consequently decreases the amount of intracellular mature IL1B. We then tested the functional consequences of different mutations and found that only protein-truncating mutations after the N-terminal Pyrin domain significantly increased pro-IL1B synthesis. Using constructs carrying the different NLRP7 domains, we demonstrate that the three domains are required to confer the full inhibitory activity of the protein with the LRR and the NACHT playing the major role. Within PBMCs, NLRP7 co-localizes with the Golgi apparatus and the MTOC, which indicates that mutations in this gene may impair cytokine trafficking and secretion. Altogether, our *ex vivo* and *in vitro* data demonstrate, first, that *NLRP7* mutations and variants impair cytokine secretion potentially by affecting their trafficking and, second, that mutations in *NLRP7* impair its capacity to down regulate pro-IL1B synthesis in response to LPS.

2.3 MATERIALS AND METHODS

Patients and mutation analysis

Mutations in patients 4, 723, 428, II.3, and 636, have been previously described (Deveault et al., 2009; Messaed et al., 2011b; Murdoch et al., 2006) and their *NLRP7* mutations and NSVs are shown in Figure 2.1 and Supplemental Table 2.1 Additional new patients were analyzed as described previously, and their reproductive history is shown in Supplemental Table 2.1. We use the term mutations to indicate DNA changes leading to protein truncating mutations or missense mutations that were not found in at least 100 controls of matching ethnicities to those of the patients. We use NSVs to indicate changes in amino acids that were also found in controls from the general population. This study was approved by the Institutional review Board of the McGill University. All patients provided written consent to provide blood samples and participate in the study.

Cytokine assay

Blood (on K_3EDTA) from patients 4, II-3, 428, 636 , 723 and 890 with mutations and patients 896, 747, 882, and 993 with rare variants were analyzed in parallel to one sample from a control subject (control 1) within 24 hours (h) from withdrawal. Blood from 15 additional controls from unrelated subjects (between 20 and 45 years) from various ethnic groups were later collected and analyzed with control 1. All the controls did not have family histories of immunological or inflammatory condition and had no family history of recurrent fetal losses. All patients and controls were not pregnant (except for patient 890) or under any type of treatment at the time of blood withdrawal. In addition, a complete white blood cell profile and count was performed on control and patient samples the day of the experiments to exclude any acquired temporary inflammation. PBMCs were isolated using Ficoll-Paque PLUS and $1.5x10^6$ cells were plated in 24-well plates and stimulated with LPS (100ng/ml) (Sigma, L6529, from *Escherichia coli* 055:B5) or ultrapure LPS (1 μg/ml (Cedarlane 423(LB) from E. coli 0552:B5).

Cloning and site-directed mutagenesis of human *NLRP7* or plasmid constructs

Human wt*NLRP7* cDNA was cloned into pCR-Blunt-II-TOPO vector (IMAGE ID: 40036028, Accession number BC109125; Open Biosystems). The *NLRP7* cDNA in the IMAGE clone contained three NSVs, Q310R, L311I, and A481T that were corrected by site directed mutagenesis and the corrected vector was considered as our wild-type for this study. The *NLRP7* cDNA was FLAG-tagged using the primer

5':GCGGCTTAAGCCACCATGGACTACAAAGACGACGATGACAAGGGTACCATGACAT CGCCCCAG and Primer 3':GCGGCTCGAGTCAGCAAAAAAAGTCACAGCACGGA. FLAG-*NLRP7* was inserted into a pcDNA 3.1 (+) vector (Invitrogen) using restriction sites AflII and Xho1. Missense mutations and base pair deletions in the *NLRP7* gene were generated by site-directed mutagenesis using PfuUltra High-fidelity DNA polymerase AD (Agilent Technologies) the QuikChange™ site-directed mutagenesis (Stratagene). The integrity of all clones was confirmed by direct sequencing of the whole insert.

Cell culture and transfection

One day prior to transfection HEK293 cells were seeded at a density of 1×10^5 cells per well using 24-well plates in 500µl of Dulbeco's modified Eagle's medium (DMEM) (Invitrogen) supplemented with 10% of fetal bovine serum (FBS) (Invitrogen). The cells were transfected with 400ng of total plasmid DNA, pre-complexed with the Plus Reagent, and diluted in Lipofectamine reagent according to manufacturer's instructions (Invitrogen). In co-transfection experiments, the pcDNA 3.1(+)-pro-IL1B vector encoding the human IL1B protein and the pcDNA 3.1(+)-FLAG-caspase-1 vector encoding the human caspace-1 protein (NM_033292.21) were co-transfected with pcDNA 3.1 (+)-FLAG-*NLRP7*.

Western blotting

Twenty-four hours post-transfection or stimulation, cells were lyzed, and proteins separated on 10% SDS–PAGE, transferred into PVDF membranes and immunodetected using a monoclonal antibody directed against FLAG (1:2000) (F3165 Sigma), monoclonal antibodies directed against human IL1B (2022, Cell Signaling technology) (1:1000), α-tubulin (2144, Cell Signaling Technology) (1:1000), and *β*-actin (MAB1501, Chemicon Intl.) (1:1000). Protein bands were revealed using the Hyperfilm ECL Western blotting detection reagents (GE Healthcare) and quantified by NIH ImageJ software (http://rsb.info.nih.gov/ij/).

Nocodazole treatment

EBV cells ($1.5x10^6$) from one control were plated in Four-well chamber slides (Ultident), stimulated or not with ultrapure LPS (1μg/ml) (Cedarlane 423(LB) from *E. coli* 0552:B5) for 24 h, and treated the next day with nocodazole 10μM (Sigma, M1404, dissolved in dimethyl sulfoxide (DMSO)), DMSO alone, or without nocodazole or DMSO. All treatments were at 37°C for 30 min in 5% CO_2 humidified atmosphere.

Immunofluorescence staining

Four-well chamber slides (Ultident) were pre-treated with poly-L-lysine (0.1 mg/ml) (Invitrogen) for 2 h at room temperature and 7.5×10^5 cells were seeded per well and incubated for 15 min at 4°C. PBMCs were then fixed with 95% alcohol 5% glacial acetic acid for 15 min at 4°C, permeabilized with 0.2% Triton X-100 (Sigma) in phosphate-buffered saline (PBS 1x) for 15 min at room temperature, blocked with 3% BSA in PBS 1x for 1 h, and then incubated with each of the primary antibodies: goat anti-NLRP7 (1:100) (sc-50642, Santa Cruz Biotechnology), mouse anti-IL1B (1:100) (MAB201, R&D systems), rabbit anti-giantin (1:100) (sc-67168, Santa Cruz Biotechnology), mouse anti-protein disulfide isomerase (PDI) (1:100; MA3-019, Thermo Scientific), mouse anti-γ-tubulin (1:100) (MA1-850, Thermo Scientific) overnight at 4°C, followed by incubation for 1 h at room temperature with their respective secondary antibodies: Alexa-Fluor-conjugated donkey anti-goat (1:500) (A11055, Invitrogen), donkey anti-mouse (1:500) (A10037, Invitrogen) and donkey anti-rabbit (1:500) (A10042, Invitrogen). Finally, the slides were mounted using Vectashield hard-set mounting medium with 4–6 diamidino-2-phenylindol-2-HCl (DAPI) (Vector Laboratories). The specificity of the NLRP7 primary antibody was tested after blocking with the NLRP7 peptide (sc-50642 P) according to the manufacturer's instructions. Fluorescence images were captured on an Axioskop 2 plus microscope. Cells were also examined and images were captured using a laser-scanning confocal microscope (Olympus FluoView^{TM} FV1000) with an oil immersion objective (UPLSAP, ×100).

Statistical analyses

Statistical analyses of ELISA measurements were performed using single factor analysis of variance (ANOVA). The frequencies of NLRP7 polar signals were calculated using two-by-two table on the Simple Interactive Statistical Analysis (SISA) website. *P* value <0.05 were considered as statistically significant.

2.4 RESULTS

Cells from patients with *NLRP7* mutations and variants secrete low levels of IL1B and TNF

Mutations in *NLRP3*, another member of the nucleotide oligomerization domain-like receptor proteins, have been shown to be associated with increased IL1B and TNF secretion from PBMCs of patients with Muckle-Wells and related autoinflammatory disorders (Agostini et al., 2004; Hoffman et al., 2001; Loock et al., 2010). To investigate the role of NLRP7 in the regulation of cytokine production in an *ex vivo* cellular model, PBMCs from six patients with previously reported mutations that are not present in the general population (Figure 2.1A) and 15 controls (c1 to c15) were stimulated with LPS for 24 h and the levels of IL1B and TNF released into the culture supernatants were measured by ELISA. This analysis revealed that the cells of the patients secrete lower amounts of both cytokines than control cells (p values ≤ 0.0004) (Figure 2.1B). Patients with *NLRP7* mutations are rare and most of the patients are referred to our laboratory from international collaborators. Consequently, it is difficult to have access to fresh blood cells from additional patients with mutations. We therefore assessed IL1B and TNF secretion by PBMCs from nine patients with rare NSVs in *NLRP7* that were found at higher frequencies in patients than in controls of European ancestry and are therefore associated with recurrent reproductive wastage in the European population (Messaed et al., 2011b). Data on four patients (754, 819, 821, and 830) have been reported previously and show statistically lower amounts of secreted IL1B and TNF. In the current study, we analyzed five additional European patients, 747, 840, 882, 896, and 993, three with variant G487E and two with variant K511R. Again, we found that cells from these patients secrete lower levels of IL1B and TNF than cells from controls without these variants (Figure 2.1C).

PBMCs from patient 636 with one mutation and one control were maintained in the presence of LPS for 48 h and then assayed for IL1B and TNF secretion. This analysis showed higher concentrations of IL1B accumulated after 48 h in the supernatants of both patient and control cells but the ratios of secreted IL1B by patient and control cells were almost the same (Figure 2.1D). For TNF, lower levels were noted after 48 h of stimulation in both patient and control cells and may be due to its degradation in the culture supernatants. Altogether, our data demonstrate that patients with *NLRP7* mutations and variants secrete statistically lower levels of IL1B and TNF than controls and are therefore hyporesponsive to LPS.

Normal IL1B processing in *ex vivo* stimulated patient's PBMCs

To investigate the causes of the reduced amounts of secreted IL1B by patients relative to controls cells, we measured the ratios of intracellular pro, mature, and secreted IL1B in two patients, 723 and 890, with *NLRP7* mutations (Figure 2.2A) and four patients, 747, 896 (Figure 2.2B), 882, and 993, with rare *NLRP7* variants versus controls without the mutations or the rare variants. We found variable amounts of synthesized pro-IL1B in the patients, with four of them having slightly higher amounts of intracellular pro-IL1B than controls (Figure 2.2C). Two patients with rare variants, 896 and 993, had lower and higher amounts of pro-IL1B than controls, respectively. In five of the six patients, the levels of mature IL1B mirrored those of pro-IL1B and none of the patients had defective pro-IL1B processing. In addition, all the analysed patients had lower levels of secreted IL1B than controls with the exception of patient, 890, who was pregnant at the time of blood drawing for LPS stimulation. These data lead us to two conclusions: first, *NLRP7* mutations do not affect IL1B processing but interfere, directly or indirectly, with its secretion in the extracellular milieu; second, *NLRP7* mutations and variants increase the levels of intracellular pro-IL1B synthesis in response to LPS stimulation, which indicates that normal NLRP7 inhibits pro-IL1B synthesis, and mutations and variants in this gene impair this function. We note that the decrease in cytokine secretion was relatively more important than the increase in pro-IL1B synthesis and seems to be the major defect of PBMCs from patients carrying *NLRP7* mutations and rare variants.

NLRP7 co-localizes with the Golgi and MTOC in *ex vivo* stimulated PBMCs with LPS

The fact that cells from patients with *NLRP7* mutations secrete lower amounts of IL1B and TNF implies that NLRP7 interferes, directly or indirectly, with the secretion of these cytokines and must be therefore expressed in cells that secrete these cytokines. In PBMCs, IL1B and TNF are mainly secreted by stimulated monocytes. Using immunofluorescence on PBMCs, we confirmed that IL1B and TNF expression is restricted to LPS-stimulated monocytes and showed *NLRP7* expression in monocytes expressing IL1B (Figure 2.3A-C). *NLRP7* expression was also detected in all the other PBMCs subpopulations, and in seven hematopoietic cell lines, EBV, BJAB, Raji and Ramos (all of B-cell origin), Jurkat (of T-cell origin), THP1 (Figure 2.3D and Supplemental Figure 2.1) and U937 (THP1 and U937 are of monocytic origin). In all LPS-stimulated PBMCs subpopulations, NLRP7 was not distributed homogeneously in the cytoplasm as reported previously in transiently transfected cells overexpressing wild-type *NLRP7* cDNA in

human embryonal carcinoma cell lines (Okada et al., 2004). The strongest NLRP7 signal was detected around the nucleus, restricted to a quarter of the cell circumference suggesting its presence in cellular organelles (Figure 2.3E-G). The polarity of the NLRP7 signal was more prominent after LPS stimulation, being observed in 73% of the cells compared to 42% of unstimulated cells (Figure 2.4). (Chi^2=52.98, $p<0.0001$). Using regular immunofluorescence microscopy and antibodies against protein disulphide isomerase, an endoplasmic reticulum resident protein; giantin, a *cis*-Golgi resident protein; and γ-tubulin, a marker of the MTOC, after LPS stimulation, NLRP7 was found to overlap partially with protein disulphide isomerase (Figure 2.3H-J), but co-localized exactly with giantin (Figure 3K-M) and γ-tubulin (Figure 2.3N-P). The co-localization of NLRP7 with giantin and γ-tubulin was also observed after sequential laser confocal microscopy scans (data not shown).

To further investigate the potential association of NLRP7 with cytoskeleton proteins, we looked at the NLRP7 signal in EBV cells from a control subject treated with nocodazole, a microtubule depolymerizing agent, for 30 minutes before fixation and immunofluorescence. We found that nocodazole treatment in the presence or the absence of LPS fragmented the NLRP7 signal and decreased significantly its polarity (Chi^2=86.34, $p<0.0001$) (Figure 2.4).

NLRP7 inhibits pro-IL1B synthesis *in vitro* and nonsense mutations impair this inhibitory function

To further characterize the second role of normal NLRP7 in inhibiting pro-IL1B synthesis, HEK293 cells were co-transfected with vectors expressing pro-IL1B, procaspase-1, and FLAG-tagged wild-type *NLRP7* (FLAG-wt*NLRP7*) or FLAG-tagged *NLRP7* mutants to induce inflammasome formation and IL1B processing. This analysis demonstrated that *in vitro* wtNLRP7 also inhibits primarily pro-IL1B synthesis and decreases the level of mature IL1B in a dose-dependent manner and only in the presence of caspase-1 (Figure 2.5A and B). We also found that an increased amount of caspase-1 counteracted the inhibitory effect of NLRP7 on pro-IL1B synthesis (Figure 2.5C and D) and completely abolished it at higher concentrations.

We then tested the effects of fourteen mutations and variants (Figure 2.1A), of which eight were analyzed in the *ex vivo* assay. Our data demonstrate that premature stop codons, mainly after the Pyrin domain, compromise significantly the inhibitory function of NLRP7 and lead to a significant increase in the amount of intracellular pro-IL1B synthesis and consequently the amount of mature IL1B ($p<0.01$) (Figure 2.6A and B). In contrast to nonsense mutations, all the

tested missense mutations in the three domains did not alter significantly the inhibitory activity of NLRP7 on pro-IL1B synthesis in this *in vitro* system (Figure 2.6C and D) (Supplemental Figure 2.2). We also looked at the NLRP7 subcellular localization in transfected HEK293 cells with FLAG-wt*NLRP7* and anti-FLAG antibody. However, in these cells, the level of *NLRP7* expression varied between cells and was very high in most of transfected cells, which masked somehow the polarity of the signal (Supplemental Figure 2.3).

NLRP7 domains act concomitantly to inhibit pro-IL1B synthesis

To determine which domain is responsible for inhibiting pro-IL1B synthesis, we generated constructs containing only the Pyrin, the NACHT or the LRR domain of NLRP7 and constructs with a deleted Pyrin, NACHT or LRR domain. We co-transfected each of these constructs with plasmids expressing pro-IL1B and pro-caspase-1 and assessed their effects. We show that the Pyrin, the NACHT, and the LRR domains act concomitantly to reduce the intracellular level of synthesized pro-IL1B and consequently the intracellular level of mature IL1B. We found that both the LRR and the NACHT contribute equally to the NLRP7 inhibitory function of pro-IL1B synthesis (Figure 2.7A and B).

2.5 DISCUSSION

Our knowledge about autoinflammatory diseases has expanded significantly in the last decade with the identification of several genes responsible for inflammatory conditions. Among NLRP genes, the most studied one is *NLRP3* responsible for three related autoinflammatory diseases. Patients with *NLRP3* mutations have constitutive inflammation and their PBMCs secrete higher amounts of IL1B and TNF than controls upon LPS stimulation (Agostini et al., 2004; Jeru et al., 2010; Kastner et al., 2010; Loock et al., 2010).

Here we demonstrate that PBMCs from patients with *NLRP7* mutations sense and respond to LPS, but secrete lower amounts of IL1B and TNF than PBMCs from controls. These results are not entirely unexpected because patients with recurrent HMs other than their reproductive problem are in good health and do not manifest inflammatory attacks, fever or any other clinical sign of inflammation as do patients with *NLRP3* mutations. Our cytokine secretion data on patients with *NLRP7* mutations and variants are in agreement with previous reports on women with sporadic moles showing their weak cellular mediated immunity in response to Phytohemagglutinin and Concanavalin A, and delayed skin hypersensitivity to dinitrochlorobenzene, purified protein derivatives and recall *Candida* antigens (Ho et al., 1980; Khanna et al., 1985; Tomoda et al., 1976).

In addition, we show that the impaired cytokine secretion is not due to an abnormal IL1B processing since none of the 11 patients with mutations or variants that we have analyzed to date, including those previously reported (Messaed et al., 2011b), has an abnormal pro-IL1B processing. On the contrary, our *ex vivo* data showed that cells of patients have normal to higher amounts of intracellular pro-IL1B ranging from 1.1 to 5.6 fold those of controls. This suggests that normal NLRP7, in addition to its role in cytokine secretion, has also another role in downregulating the intracellular level of pro-IL1B in response to toll-like receptor-4 signaling and that mutations and variants in this gene impair this function and consequently lead to higher amounts of pro-IL1B production. Among the patients analyzed in this study, one with a rare variant in *NLRP7*, K511R (patient 896), had a lower level of pro-IL1B. Similarly, among previously analyzed patients with rare *NLRP7* variants, one out of five patients (patient 754) (Messaed et al., 2011b) displayed lower amount of intracellular pro-IL1B as compared to control. This indicates that patients with rare *NLRP7* variants have mutations or variants in other genes affecting pro-IL1B synthesis and contributing to their disease phenotype.

The fact that the abnormal low secreted levels of IL-1B mirrored those of TNF suggested that the export pathways of these two cytokines overlap, or at least share common trafficking proteins that are affected, directly or indirectly, by *NLRP7* mutations and variants. We therefore looked at NLRP7 subcellular localization in *ex vivo* stimulated PBMCs from normal subjects or in THP1 cell line and found that NLRP7 co-localizes with the Golgi apparatus and with the MTOC. This localization was affected by nocodazole treatment, which fragmented the NLRP7 signal and decreased its polarization (Figure 2.4). This suggests that mutations and variants in *NLRP7* impair cytokine secretion by affecting their trafficking either through the classical secretory pathway via the Golgi apparatus or by disrupting the microtubule network known to play a role in the non-classical pathway of IL1B secretion. Our data are in line with a previous report showing reduced IL1B and TNF secretion by normal monocytes stimulated with LPS and treated with histone deacetylase inhibitors, which disrupt microtubules and impair vesicle transportation (Carta et al., 2006). Also, a defect in factors regulating microtubule and actin filaments organization has been suggested, a long time ago by Edwards et al. (Edwards et al., 1990) to underlie postzygotic abnormalities during *in vitro* culture of embryos from a patient with recurrent moles. This suggestion is in line with the postzygotic aneuploidies and mosaicisms that occur in patients with *NLRP7* mutations (Deveault et al., 2009) and the association of another gene from the NLRP family, *NLRP5*, with abnormal spindle assembly, chromosome misalignment, aneuploidies and mosaicisms (Tong et al., 2000; Zheng and Dean, 2009).

To confirm the role of NLRP7 in downregulating pro-IL1B synthesis, we developed an *in vitro* assay and assessed first the effect of wt*NLRP7*. Again, in this *in vitro* system, we found that wt*NLRP7* downregulates the intracellular level of pro-IL1B in a dose-dependent manner, which is in agreement with our *ex vivo* data and previously reported data by Kinoshita et al. (Kinoshita et al., 2005). However, under our experimental *in vitro* conditions, wt*NLRP7* reduced primarily the amount of pro-IL1B and subsequently the amount of mature IL1B. We then tested the effects of constructs containing 13 mutations and rare variants observed in patients, eight of which were analysed in the *ex vivo* assay. We found, *in vitro*, that only the two analysed nonsense mutations after the Pyrin domain alter significantly the NLRP7 inhibitory function and lead to higher amounts of pro-and mature IL1B whereas all analysed missense mutations and variants in the three domains did not affect significantly the intracellular level of pro-IL1B. The lack of impact of missense mutations on pro- IL1B production, *in vitro*, may be due to domain redundancy that acts as a compensation mechanism since both the NACHT and the LRR are able to individually

mediate an important inhibition of pro-IL1B synthesis (Figure 2.7). Also, it is possible that our *in vitro* system is not sensitive enough to detect milder defects caused by missense mutations and rare variants. The exact mechanism by which NLRP7 downregulates pro-IL1B synthesis in transiently transfected cells with vectors without regulatory promoter regions is not clear, but definitely must involve a number of cellular changes affecting the expression of several endogenous genes that altogether, with the transfected ones, contribute to the downregulation of pro-IL1B at the transcriptional or/and translational levels.

We have previously shown the occurrence of all genetic types of moles, diploid biparental (Helwani et al., 1999; Qian et al., 2007), diploid androgenetic monospermic (Deveault et al., 2009), and triploid dispermic (Slim et al., 2011), in patients with *NLRP7* mutations. We proposed a two-hit mechanism underlying mole occurrence (Deveault et al., 2009). The first hit is the occurring of various complex abnormalities around the time of fertilization or/and very early in the zygote. The second hit is the retention of these aberrant pregnancies to later gestational stages. Among the analyzed patients in the *ex vivo* cytokine secretion assay, patient 636 had had triploid dispermic moles (Slim et al., 2011), patient 428 had had a diploid androgenetic monospermic mole (Deveault et al., 2009), and patient 4 had had diploid biparental moles (Helwani et al., 1999). All genotypic types of moles are basically non-viable conceptions that had arrested earlier than the time of their clinical diagnosis before the differentiation of fetal vessels inside the chorionic villi and the establishment of fetal blood circulation. Despite these abnormalities, these conceptions are retained by the patients until the end of the first trimester of pregnancy. The abnormal retention of such pregnancies is an important feature of this pathology and is by itself an indication of the compromised immune response of the patients. Our data demonstrating the inability of the cells of the patients to secrete cytokines and consequently mount appropriate inflammatory response provide an explanation for their abnormal tolerance of moles, conceptions with no embryos. Our findings will impact our understanding of several forms of reproductive wastage and will also open new avenues of research to better understand the causes of gestational choriocarcinomas, aggressive and malignant tumors that originate generally from the placenta of androgenetic moles. In humans, gestational androgenetic choriocarcinomas are the only tumors of non-self origin that are able to grow for several months and invade several maternal tissues (lung, brain, liver, etc.) without being rejected by the maternal immune system. Our findings about the impaired cytokine secretion by cells from patients with *NLRP7* mutations and consequently their delayed rejection of abnormal conceptions

will open new avenues of therapeutic research aiming at enhancing the immune response of patients and helping them in rejecting these non-self tumors.

2.6 ACKNOWLEDGMENTS

We thank the patients and controls for cooperation. We also thank Catherine Deveault for technical assistance.

2.7 FIGURES

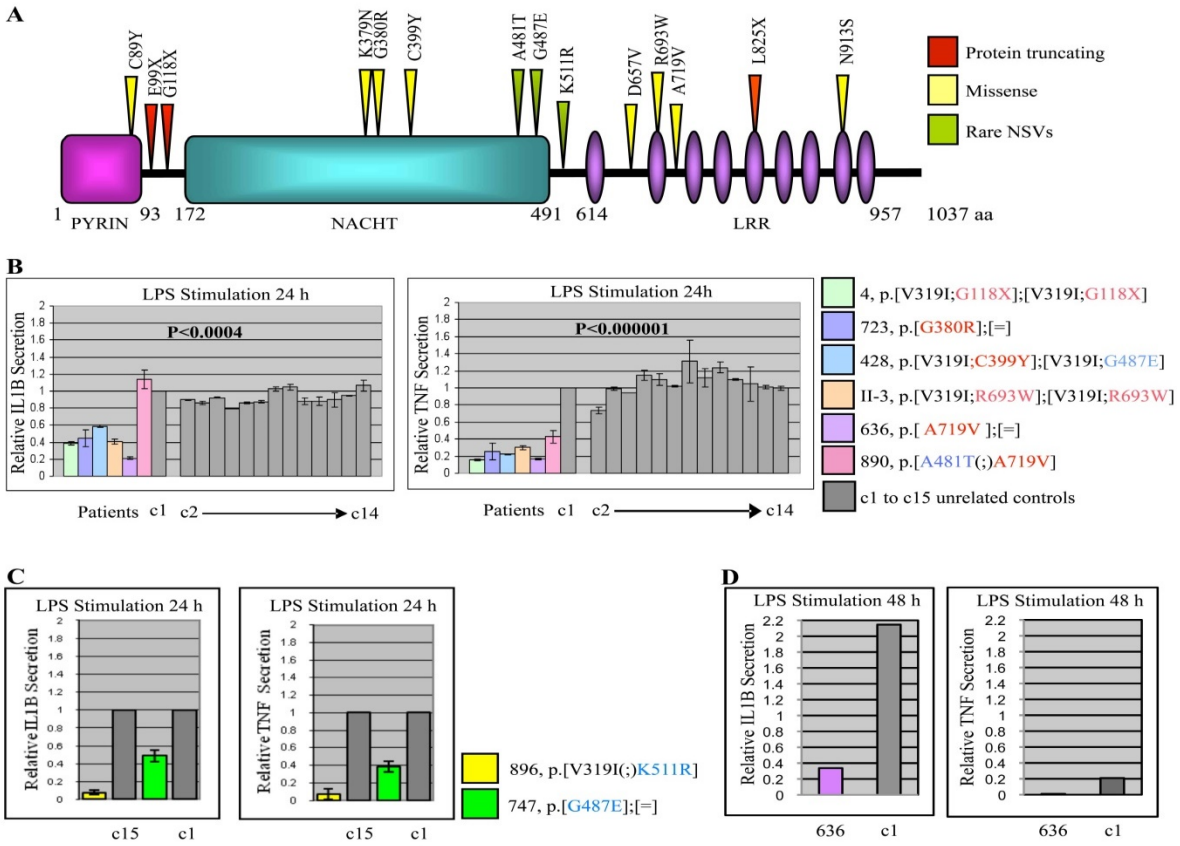
A
C89Y
E99X
G118X
K379N
G380R
C399Y
A481T
G487E
K511R
D657V
R693W
A719V
L825X
N913S
Protein truncating
Missense
Rare NSVs
1
PYRIN
93
172
NACHT
491
614
LRR
957
1037 aa
B
LPS Stimulation 24 h
P<0.0004
Relative IL1B Secretion
Patients c1 c2 → c14
LPS Stimulation 24h
P<0.000001
Relative TNF Secretion
Patients c1 c2 → c14
4, p.[V319I;G118X];[V319I;G118X]
723, p.[G380R];[=]
428, p.[V319I;C399Y];[V319I;G487E]
II-3, p.[V319I;R693W];[V319I;R693W]
636, p.[A719V];[=]
890, p.[A481T(;)A719V]
c1 to c15 unrelated controls
C
LPS Stimulation 24 h
Relative IL1B Secretion
c15 c1
LPS Stimulation 24 h
Relative TNF Secretion
c15 c1
896, p.[V319I(;)K511R]
747, p.[G487E];[=]
D
LPS Stimulation 48 h
Relative IL1B Secretion
636 c1
LPS Stimulation 48 h
Relative TNF Secretion
636 c1

Figure 2.1. Cytokine secretion by PBMCs from patients with *NLRP7* mutations and variants

(A) Schematic representation of the NLRP7 protein with the various mutations and rare variants analyzed in this study. NLRP7 protein shares three functional domains with several members of the Nod-like receptor (NLR) family, the PYD, the NACHT and the LRR. (B) PBMCs from patients with *NLRP7* mutations have an impaired IL1B and TNF secretion. Freshly isolated PBMCs ($1.5x10^6$cells) were stimulated with LPS for 24 h. The cells were centrifuged and supernatants were collected to measure the amount of IL1B and TNF released in the media by ELISA. Relative amounts of each cytokine refer to the secreted amounts by patients cells divided by those secreted by control cells. The averages and standard errors were calculated on two to three different ELISA assays on supernatants from the same LPS stimulation. (C) PBMCs from two patients with rare *NLRP7* variants show also lower IL1B and TNF secretion than controls. (D) IL1B and TNF secretion by PBMCs from patient 636 stimulated with LPS for 48 h. C1 after 24 h of stimulation was adopted as 1-fold. After 48 h of stimulation, the amount of IL1B was 2.2 times higher than the level after 24 h and was kept at 2.2 to highlight the accumulation of IL1B in both control and patient cells. aa, amino acids; NSV, nonsynonymous variants.

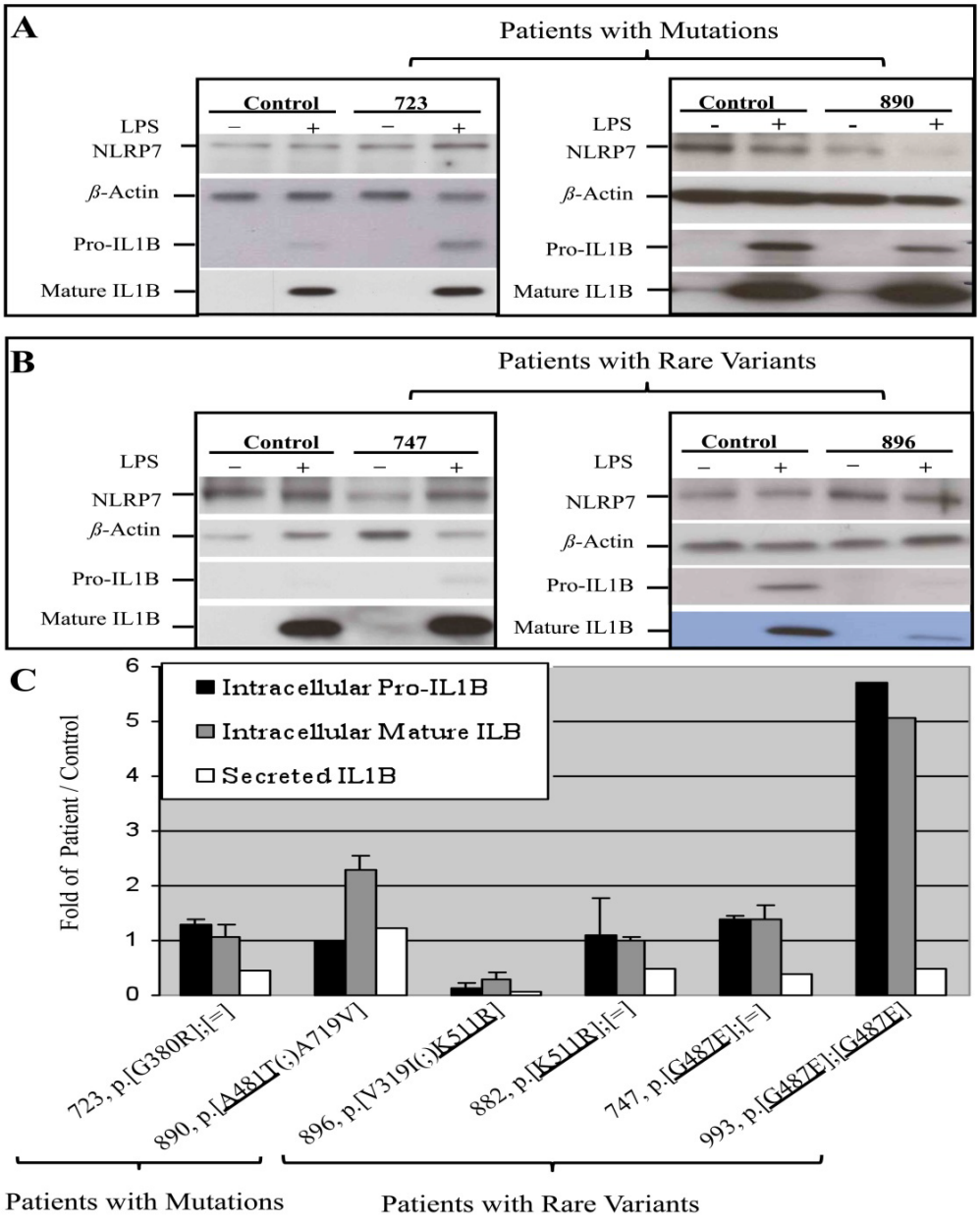
A
Patients with Mutations
Control
723
890
LPS
NLRP7
β-Actin
Pro-IL1B
Mature IL1B
B
Patients with Rare Variants
Control
747
896
C
Intracellular Pro-IL1B
Intracellular Mature ILB
Secreted IL1B
Fold of Patient / Control
723, p.[G380R];[=]
890, p.[A481T(;)A719V]
896, p.[V319I(;)K511R]
882, p.[K511R];[=]
747, p.[G487E];[=]
993, p.[G487E];[G487E]
Patients with Mutations
Patients with Rare Variants

Figure 2.2. Cells from patients with *NLRP7* mutations and rare variants display normal to higher pro-IL1B synthesis and normal processing

Freshly isolated PBMCs ($1.5x10^6$cells) were stimulated with LPS for 24 h. Immunoblots of whole cell lysates show the expression of intracellular pro, mature IL1B relative to β-actin in patients with *NLRP7* mutations (A) and rare variants (B). (C) Recapitulation of the ratios of pro, mature and secreted IL1B by the cells of patients divided by control cells (patient pro-IL1B /control pro-IL1B) after signal quantification using Image J software. When sufficient amount of cells from patients were available, the averages and standard deviations were calculated on two to three different western blots on cellular lysates from the same LPS stimulation.

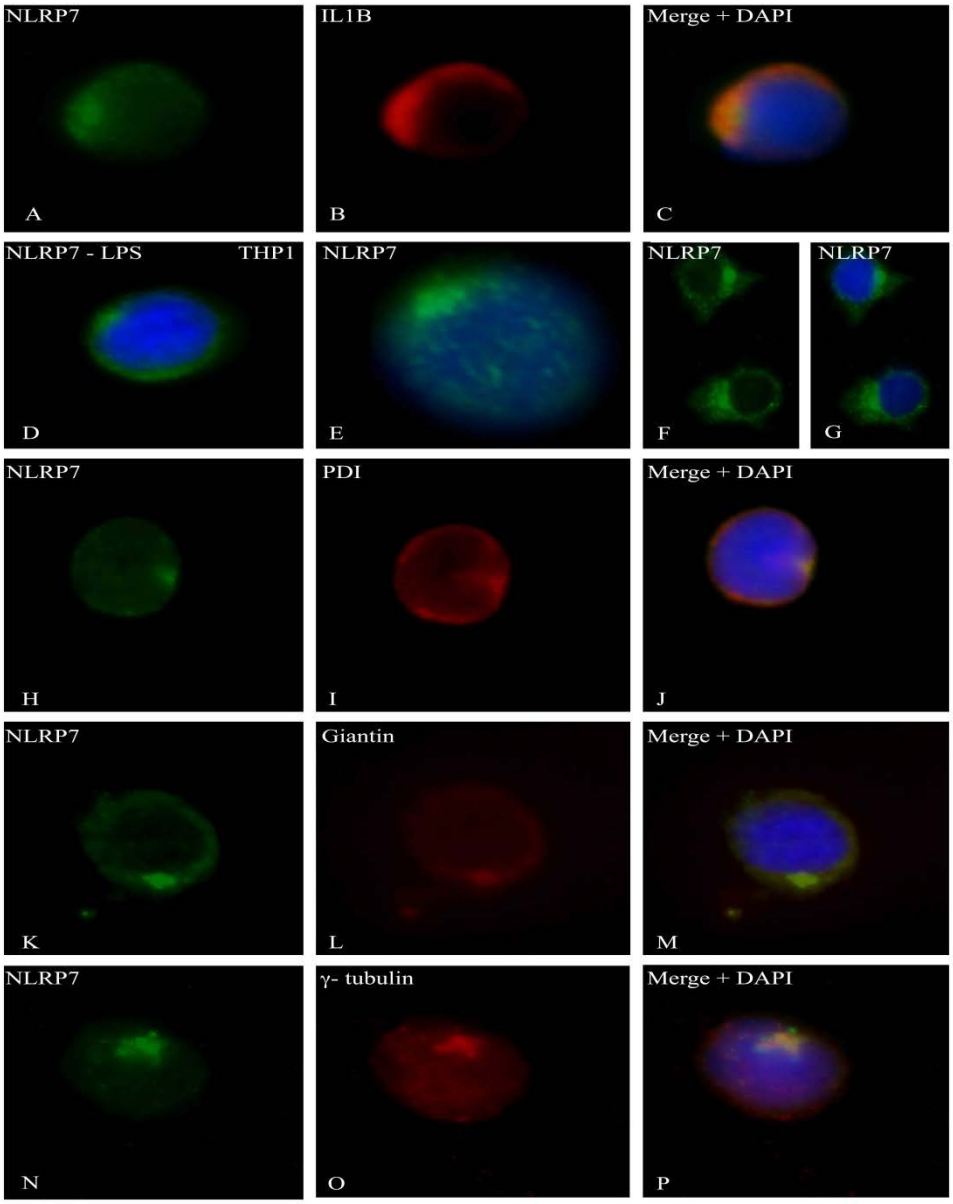

Figure 2.3. <u>Subcellular localization of NLRP7 and co-localizations</u>
(A-C) Expression of NLRP7 and IL1B in a monocyte after LPS stimulation. DNA was counterstained with DAPI (blue). (D) NLRP7 is distributed homogeneously in the cytoplasm of unstimulated THP1 cells, whereas it has predominantly a polar signal in stimulated PBMCs (E-G). In E, note the faint microtubule-like network staining emerging from the NLRP7 polar signal. Stimulated PBMCs show overlap between the localization of NLRP7 protein and PDI, a marker of the endoplasmic reticulum (H-J). Co-localization of NLRP7 protein in LPS-stimulated THP1 cells with giantin, a marker of the *cis*-Golgi (K-M). Co-localization in PBMCs of NLRP7 protein with γ-Tubulin, a marker of the MTOC (N-P).

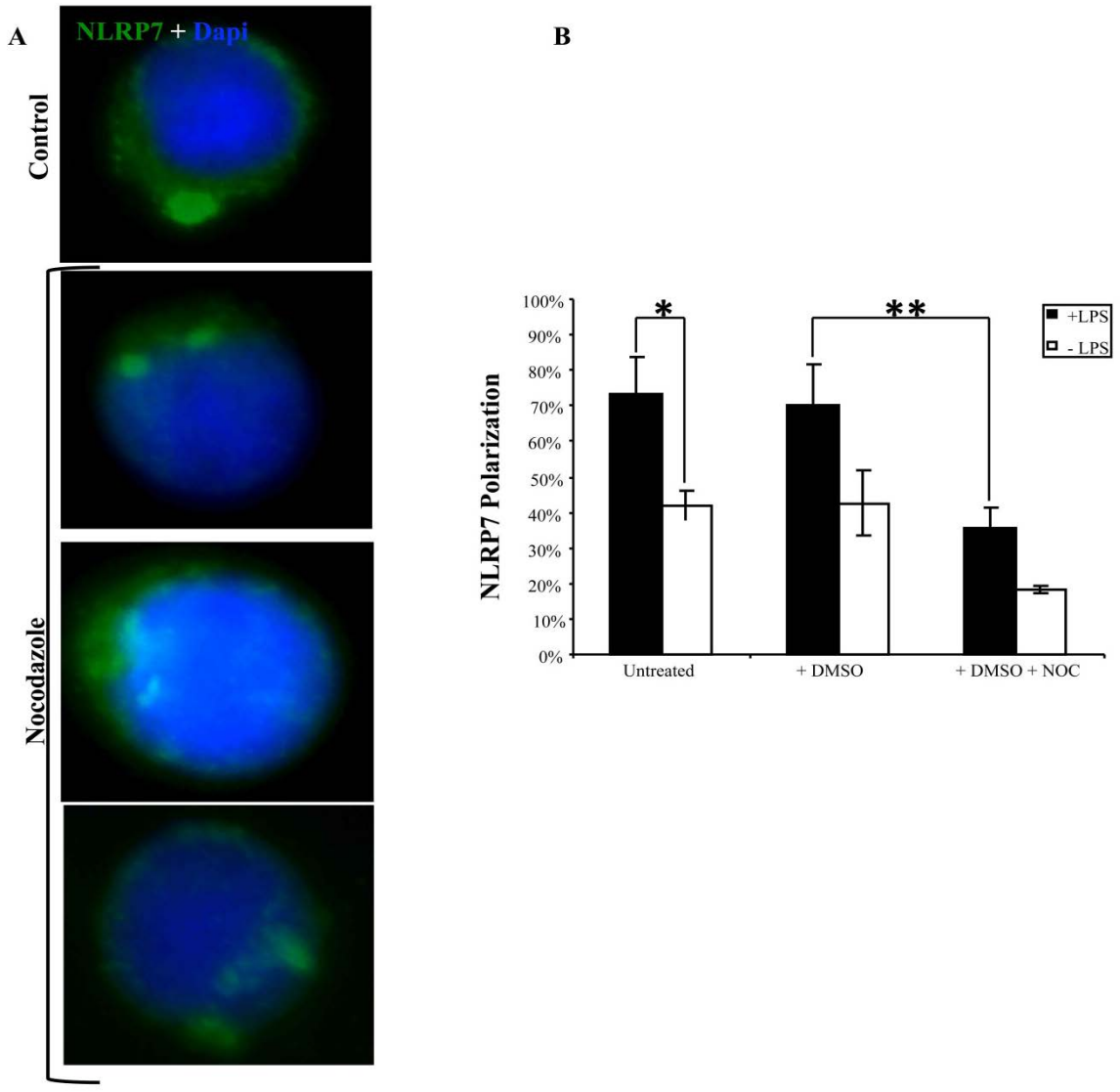

Figure 2.4. <u>Effect of LPS and nocodazole on NLRP7 polarization in EBV cells from a control subject</u>

(A) NLRP7 signal was polar in untreated cells; however, upon nocodazole treatment for 30 min NLRP7 signal was disrupted and became more diffuse and fragmented around the nucleus and less sequestered to one pole of the cells. (B) The results represent the percentage of EBV cells with polarized NLRP7 signal after each treatment. The averages and standard deviations in these histograms represent cell counts performed by two observers on 50 to 150 cells per condition. The indicated results are representative of data from three different experiments.

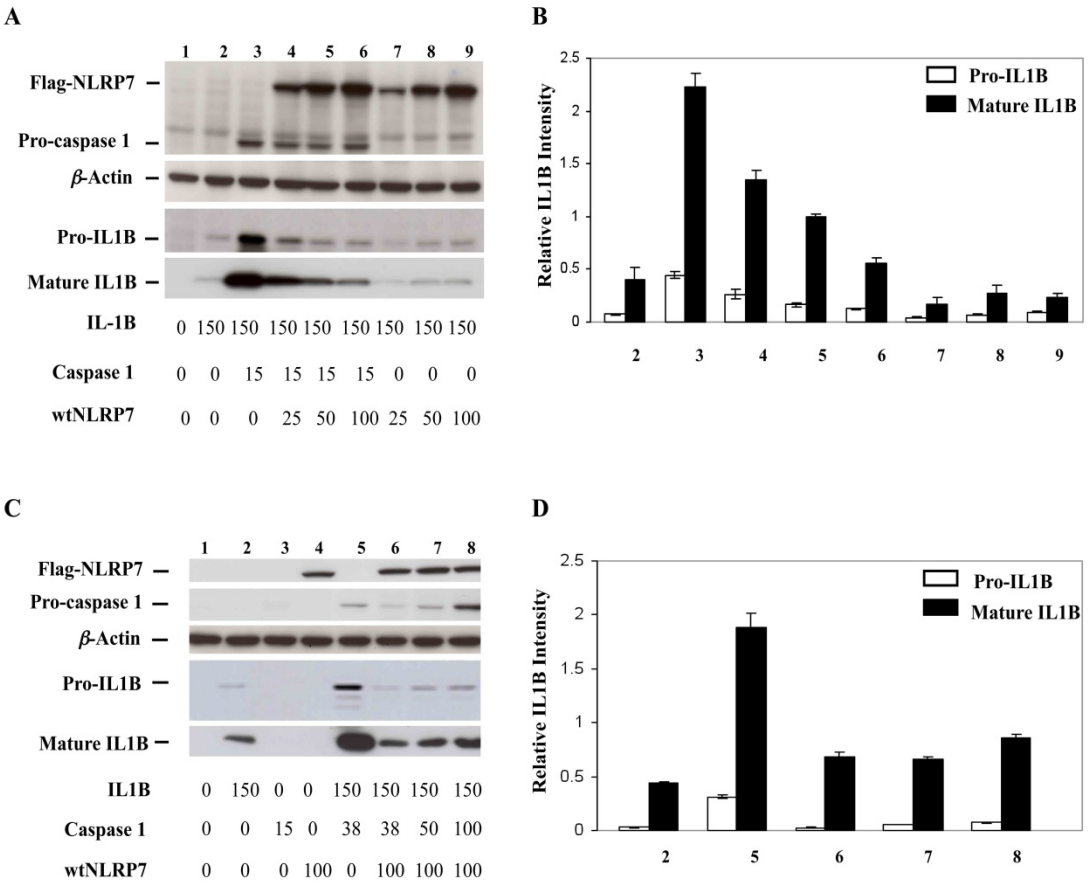

Figure 2.5. <u>Wild-type NLRP7 inhibits caspase-1 dependent IL1B production</u>
(A) Immunoblot of whole cell lysates of HEK293 cells that were transfected simultaneously with expression vectors encoding IL1B (150 ng), FLAG-caspase-1 (15 ng) and different amounts (25, 50, 100 ng) of FLAG-wt*NLRP7*. (B) Representation of the quantification of signals in panel A using Image J. This analysis shows that the level of pro-IL1B inversely correlates with the level of NLRP7 (lanes 3-6). (C) Immunoblot of whole cell lysates of HEK293 cells that were transfected simultaneously with expression vectors encoding IL1B (150 ng), different amount of FLAG-caspase-1 (15, 38, 50, 100 ng) and FLAG-wt*NLRP7* (100 ng). (D) Representation of the quantification of signals in panel C using Image J software. This analysis revealed that a dose-dependent increase of caspase-1 mitigates the inhibitory function of NLRP7 and correlates with an increase of pro-IL1B synthesis (lanes 6-8). In B and D, the averages and standard deviations were calculated on two different western blots on cellular lysates from different transfection experiments.

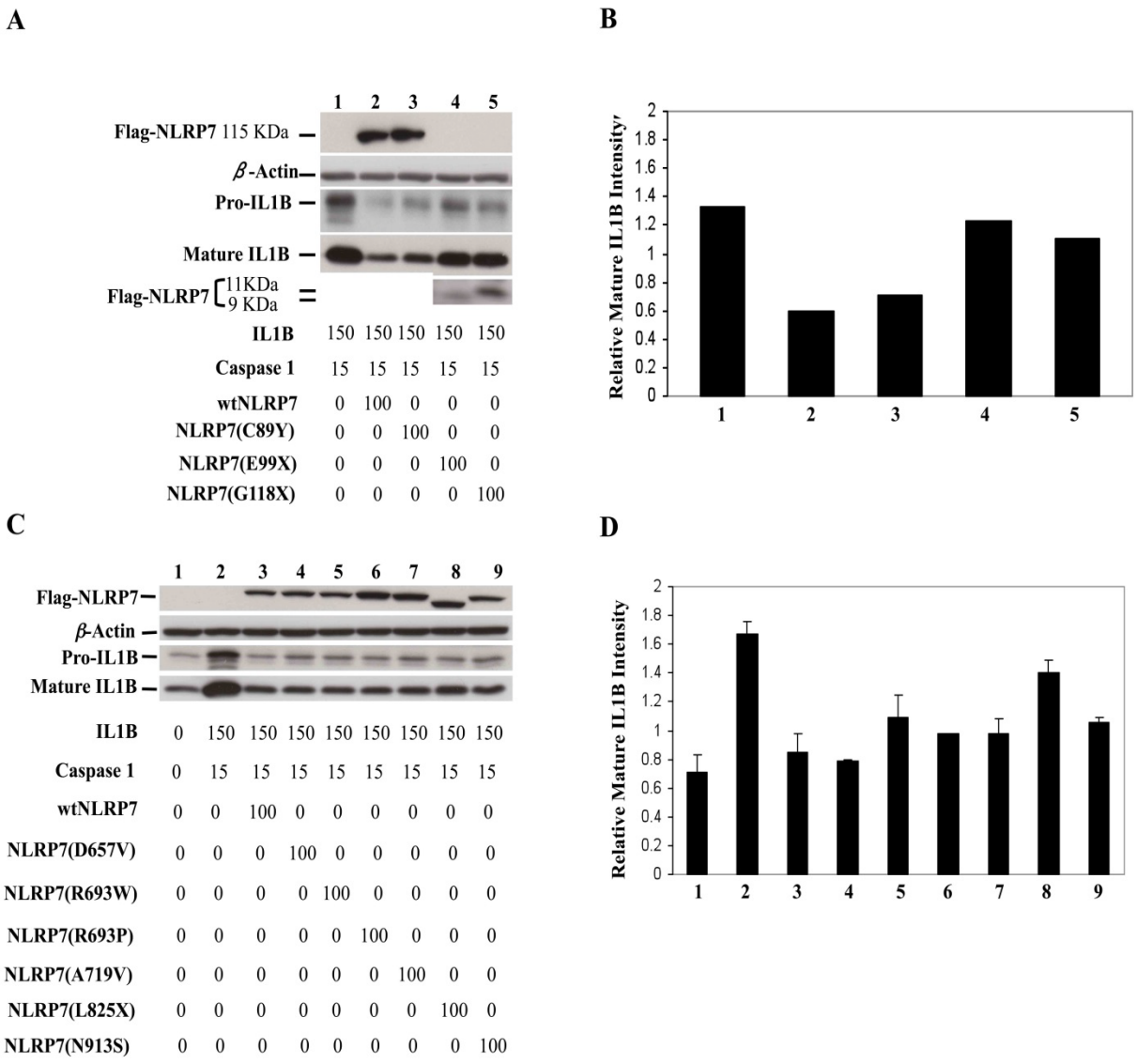

Figure 2.6. <u>Nonsense mutations in *NLRP7* abolish its inhibitory function</u>
(A and C) Immunoblots of whole cell lysates of HEK293 cells that were transfected simultaneously with expression vectors encoding IL1B (150 ng), FLAG-caspase-1 (15 ng) and FLAG-wt*NLRP7* (115KDa) or mutant *NLRP7* (100 ng) expression vectors. (B and D) Representations of the quantification of signals in panels A and C respectively using Image J software. This analysis showed that missense mutations in the Pyrin and the LRR domains do not alter significantly IL1B processing. However, nonsense mutations after the Pyrin domain, E99X (9KDa) and G118X (11KDa), and in the LRR domain, L825X, compromise significantly the inhibitory effect of NLRP7. In D, the averages and standard deviations were calculated on two different western blots on cellular lysates from different transfection experiments.

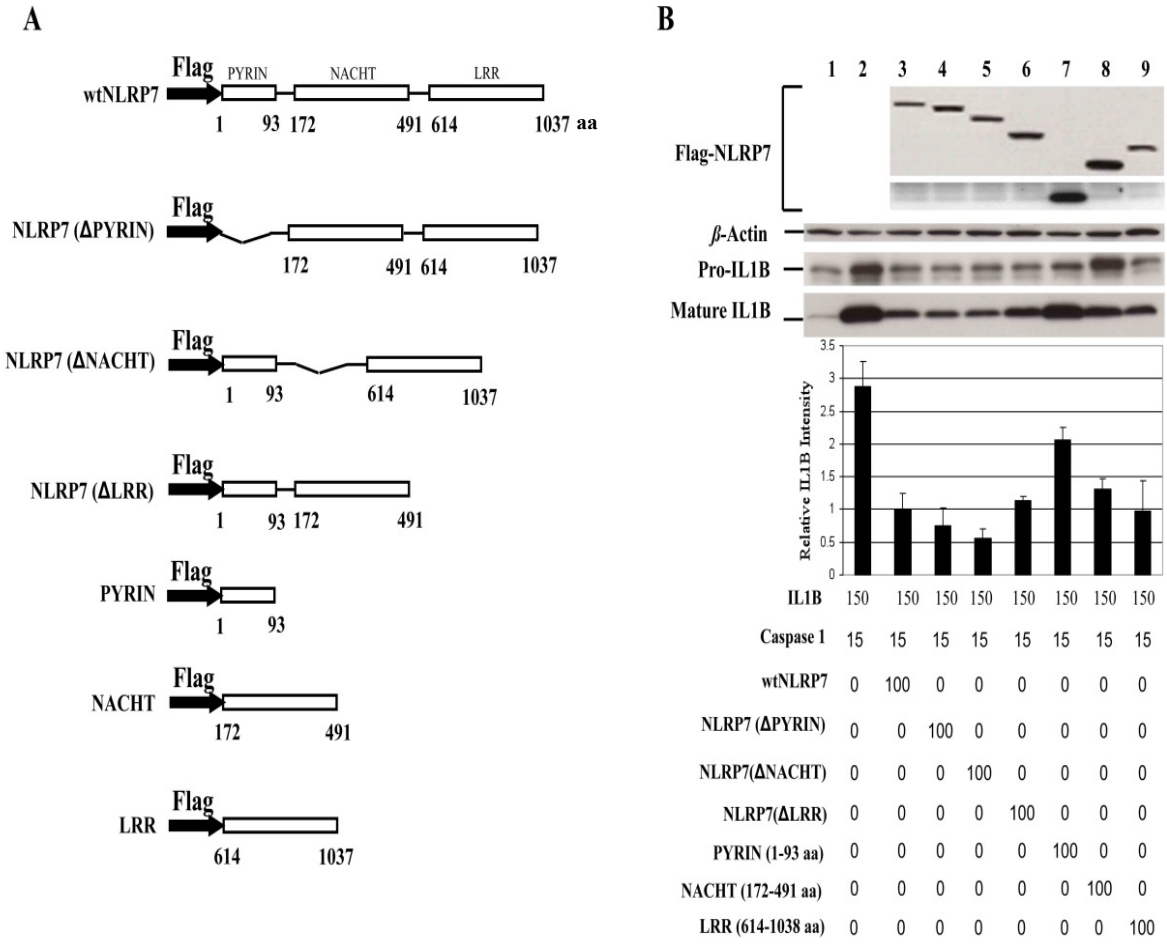

Figure 2.7. <u>NLRP7 domains work concomitantly to regulate caspase-1 dependent IL1B production</u>

(A) Schematic diagram of protein domain structures. (B) Immunoblot of whole cell lysates of HEK293 cells that were transfected simultaneously with expression vectors encoding IL1B (150 ng), FLAG-caspase-1 (15 ng), FLAG-wt*NLRP7* (100ng), FLAG-tagged NLRP7 domains constructs (100ng) and FLAG-tagged NLRP7 domain deletion constructs (100ng). Below the immunoblot is the representation of the quantification of signals using Image J software. This analysis revealed that the three NLRP7 domains contribute to the inhibition of IL1B processing, albeit to different extents. The strongest inhibitory effect is mediated by the NACHT and the LRR domains (lanes 7-9). In B, the averages and standard deviations were calculated on two different western blots on cellular lysates from different transfection experiments. aa, amino acids.

2.8 TABLES

Table 2.1. Mutation analysis and reproductive outcomes of patients with *NLRP7* mutations

Family ID	Patient ID	NLRP7	Reproductive Outcomes	Reference
Patients with Mutations				
MoLb1	4	p.[G118X;V319I];[G118X;V319I]	LB^{IUGR}, SB, END, PHM, 2 HM, CHM, SA, PHM	(Murdoch et al., 2006)
MoGe2	II-3	p.[R693W];[R693W]	CHM, CHM, CHM, HM	(Murdoch et al., 2006)
MoCa57	428	p.[V319I;G487E];[V319I;C399Y]	SB (21w), BO, twin (fetus+CHM), SA, SA, LB (28w) with malformations	(Deveault et al., 2009)
MoCa94	636	p.[A719V];[=]	EFL, NP, EFL, SA, EFL, PHM, NP	(Deveault et al., 2009)
MoBa169	723	p.[G380R];[=]	SA, SB (28w), HM	(Messaed et al., 2011b)
MoCa245	890	p.[A481T; A719V]	twin (EP+tubal), BO, SA, SA, Pregnant	(Messaed et al., 2011b)
Patients with Rare Variants				
MoCa247	896	p.[V319I(;)K511R]	TA (fetus with malformations), NP, CHM	This study
MoCa305	993	p.[G487E];[G487E]	SA, HM-GTD, SA	This study

Amino acid numbering of mutations and variants uses cDNA numbering with +1 corresponding to the A of the ATG translation initiation codon in the reference sequence, NM_001127255.1. NP, stands for normal pregnancy; LB, for live birth; IUGR, for intra-uterine growth restriction; SB, for stillbirth; END, for early neonatal death; PHM, for partial hydatidiform mole (HM); CHM, for complete HM; SA, for spontaneous abortion; BO, for blighted ovum; EP, ectopic pregnancy; EFL, for early fetal loss before a pregnancy test was performed; w, for weeks. Mutations that are not present in the general population are in red and rare variants found at lower frequencies in the general population and are associated with reproductive wastage are in blue. Common variants are in black.

2.9 APPENDIX

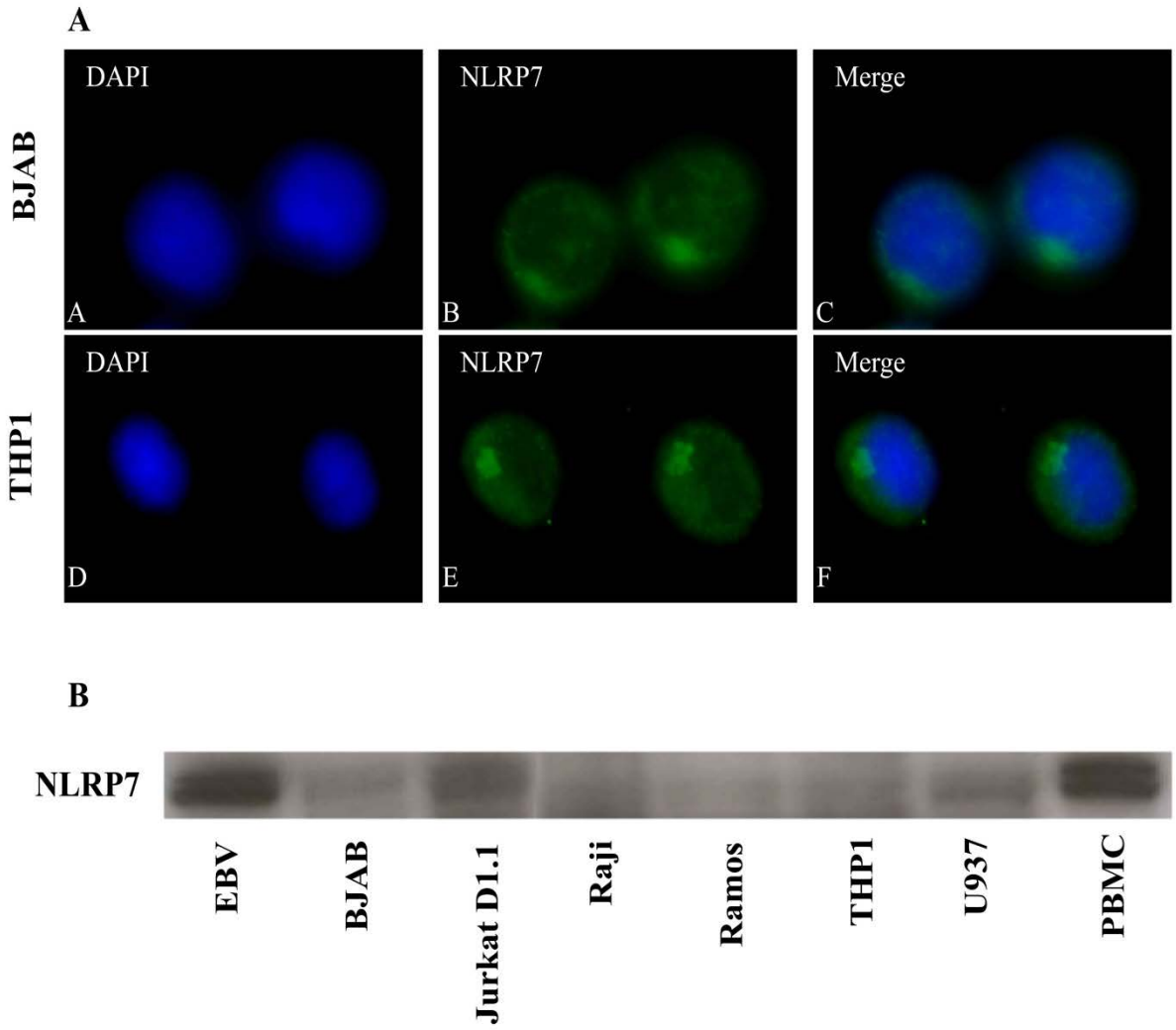

Supplemental Figure 2.1. <u>NLRP7 expression in different hematopoietic cell lines</u>
(A) Immunofluorescence photos showing NLRP7 expression in BJAB and THP1 cells. DNA was counterstained with DAPI (blue). (B) Different cell lines were seeded in supplemented RPMI 1640, collected, centrifuged, and the pellets were lyzed. Immunoblots of whole cell lysates showing NLRP7 expression in hematopoietic cell lines of different origins.

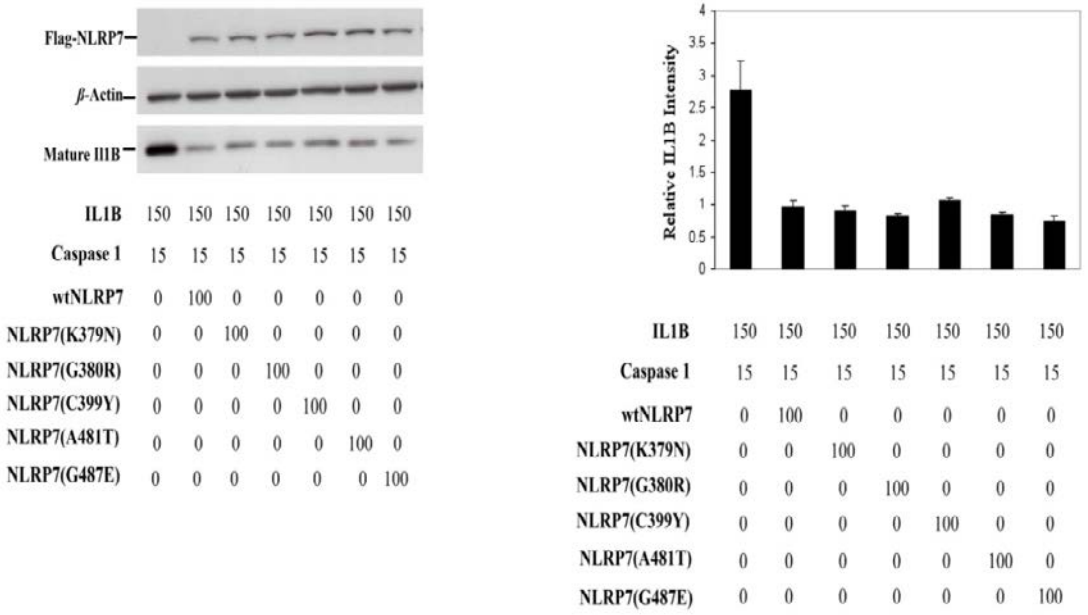

Supplemental Figure 2.2. <u>Missense mutations in the NLRP7 NACHT domain do not alter significantly the inhibitory function of the protein</u>

HEK293 cells were transfected simultaneously with expression vectors encoding IL1B (150 ng), FLAG-caspase-1 (15 ng) and FLAG-wtNLRP7 or mutant NLRP7 (100 ng) expression vectors. Left panel, immunoblots of whole cell lysates show that missense mutations in the NACHT domain do not affect the inhibitory function of NLRP7. Right panel, representation of the quantification of signals using Image J software showing that all NLRP7 mutants decrease IL1B production to the same extent as the wild-type protein.

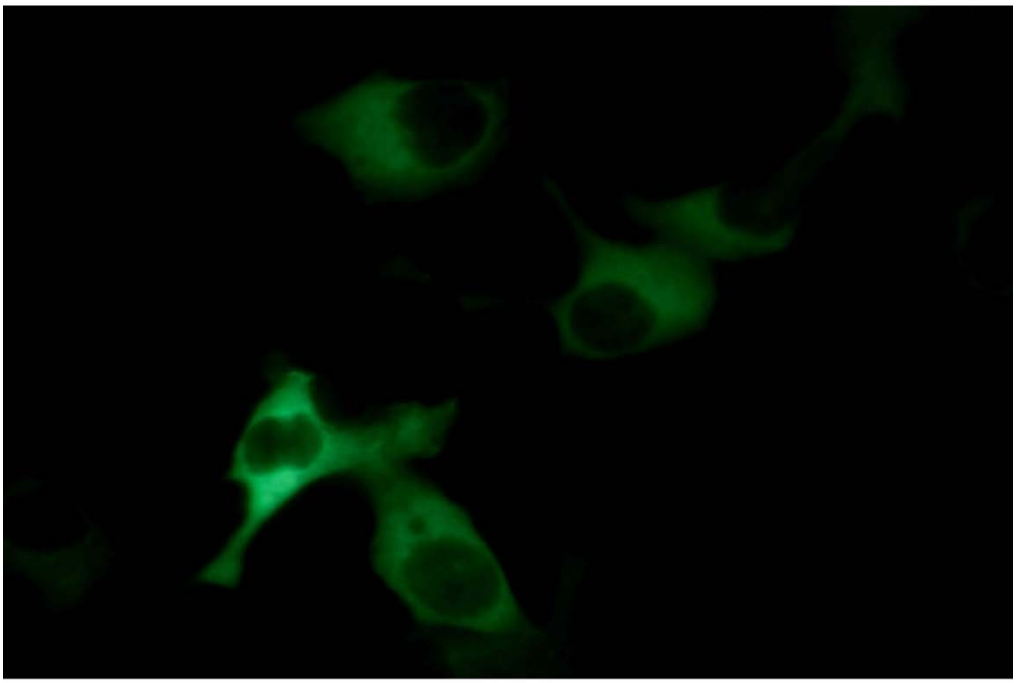

Supplemental Figure 2.3. <u>NLRP7 expression in HEK293 cells transfected with vector carrying wild type FLAG-NLRP7 and revealed with FLAG antibody</u>
Note the presence of the NLRP7 signal in one pole of the cells in three of the five shown cells.

Supplemental Table 2.1

N/A

PREFACE TO CHAPTER 3

The results described in Chapter 2 suggested that NLRP7 may impair IL1B secretion by affecting the microtubules and consequently the trafficking of IL1B-containing vesicles to the extra-cellular milieu. After the identification of *KHDC3L*, the second gene for HM, we decided to look at the subcellular localization of its protein in EBV cells. Within these cells, I found that KHDC3L co-localizes with NLRP7 to the MTOC and the Golgi apparatus (data not shown) (Reddy et al., 2013). This observation raised the question whether these two proteins also co-localize in the oocytes, the cells that manifest the primary defect of this pathology. Towards addressing this question and in collaboration with Dr. Asangla Ao, I carried out in Chapter 3 co-localization experiments of NLRP7 and KHDC3L on spare materials collected from patients undergoing reproductive assisted technologies.

CHAPTER 3

NLRP7 AND KHDC3L, THE TWO MATERNAL-EFFECT PROTEINS RESPONSIBLE FOR RECURRENT HYDATIDIFORM MOLES, CO-LOCALIZE TO THE OOCYTE CYTOSKELETON

Elie Akoury[1,2], Li Zhang[2], Asangla Ao[1,2], Rima Slim[1,2]

[1]Department of Human Genetics, McGill University Health Centre, Montreal, Quebec, Canada, [2]Obstetrics and Gynecology, McGill University Health Centre, Montreal, Quebec, Canada.

Manuscript published in the Human Reproduction, October 9, 2014 (PMID: 25358348).

3.1 ABSTRACT

Hydatidiform mole (HM) is an aberrant human pregnancy with abnormal embryonic development and excessive trophoblastic proliferation. Recessive mutations in the maternal-effect genes, *NLRP7* or *KHDC3L*, are responsible for recurrent HMs (RHMs). However, the exact roles of *NLRP7* and *KHDC3L* in this condition are not fully understood. To gain insights into their functions, we characterized their subcellular localizations in human oocytes and early embryos using regular and confocal immunofluorescence and electron microscopies. We found that in oocytes, from the germinal vesicle until the formation of the zygote, NLRP7 co-localized with KHDC3L mainly to the cortical region. Within this region, electron and high resolution confocal microscopies confirmed the co-localization of NLRP7 and KHDC3L between cortical granules, mitochondria, and other organelles on cytoskeletal structures that did not overlap exactly with the α-tubulin microtubule network or display similar pattern by immunofluorescence. As the embryo completed its first division, NLRP7 and KHDC3L became excluded from the cell-to-cell contact region, restricted to the outer cortical regions, and were part of some structural complexes that are not E-cadherin dependent. During early cleavage stages, the two proteins displayed different localization patterns. While NLRP7 maintained its polarity until the blastocyst stage where it became homogeneously distributed in the cytoplasm of cells from the inner cell mass and trophectoderm, KHDC3L translocated to the nuclei of cells from both the inner cell mass and trophectoderm at the morula stage. These data suggest that NLRP7 and KHDC3L could be involved in the integrity and organization of the oocyte cortical region.

3.2 INTRODUCTION

A hydatidiform mole is an abnormal human pregnancy characterized by absence of, or abnormal embryonic development, excessive trophoblastic proliferation, and hydropic degeneration of chorionic villi. The common form of this condition is sporadic, not recurrent, and occurs in 1 in every 600-1000 pregnancies in Western countries (Savage et al., 2010). Moles recur in 1-6% of patients with a prior mole and these cases are termed singleton cases of RHMs. Occasionally, patients with RHMs have relatives with HMs and these cases are designated as familial RHMs.

Owing to the fact that women with RHMs usually fail to have normal pregnancies and continue to have recurrent moles even after changing partners, we suggested that a maternal defective gene is responsible for this condition (Helwani et al., 1999). Maternal-effect genes encode mRNA and proteins that accumulate during oogenesis and govern the transition from oocyte to embryo (Dean, 2002). Such genes are not supposed to affect ovulation and fertilization but their absence would lead to early embryonic arrest. By studying rare familial cases of RHMs, two maternal-effect genes, *NLRP7* and *KHDC3L*, responsible for this condition have been identified (Murdoch et al., 2006; Parry et al., 2011). *NLRP7* is a major gene for RHMs and is mutated in 48-80% of patients depending on patients' ascertainment criteria (singleton or familial cases) and populations (Estrada et al., 2013; Qian et al., 2011; Sebire et al., 2013; Slim et al., 2009). *KHDC3L* is a minor gene for RHMs and is mutated in only 10-14% of patients with no *NLRP7* mutations (Fallahian et al., 2013; Parry et al., 2011; Reddy et al., 2013).

NLRP7 transcripts have been documented in all oocyte and preimplantation embryo stages (Murdoch et al., 2006) with levels decreasing from the GV to Day 3 embryos (Zhang et al., 2008). At the protein level, *NLRP7* expression in human oocytes has been documented in all follicular stages by immunohistochemistry (Wang et al., 2009a). *NLRP7* codes for a nucleotide oligomerization domain-like receptor protein and is a member of the NLRP family with roles in autoinflammation, apoptosis, and pathogen-induced inflammation (Tschopp et al., 2003). Three studies have tried to address the functional role of NLRP7 in inflammation and agree on the fact that NLRP7 downregulates inflammation in various cellular models (Khare et al., 2012; Kinoshita et al., 2005; Messaed et al., 2011a). Two of these studies also showed that *NLRP7* mutations and knockdown reduce the levels of secreted IL1B in peripheral mononuclear blood

cells from patients (Messaed et al., 2011a) and macrophages (Khare et al., 2012), respectively. In these cells, NLRP7 localizes to the MTOC, the Golgi apparatus, and associates with microtubules suggesting that it may impair IL1B secretion by affecting the microtubules and consequently the trafficking of IL1B-containing vesicles to the extra-cellular milieu (Messaed et al., 2011a). The role of NLRP7 in downregulating the inflammatory response is believed to play a secondary role in the pathology of RHMs that underlies the prolonged retention of these pregnancies, in which embryonic development had arrested earlier. However, the primary role of NLRP7 in the pathology of RHMs is believed to be in the oocyte by analogy to other maternal-effect genes and based on the fact that ovum donation has rescued the defect of three patients with recessive mutations in *NLRP7* (Fisher et al., 2011; Nguyen and Slim, 2014). *NLRP7* does not have an orthologue in mouse, but a paralogue, *Nlrp2*, from which *NLRP7* is believed to have emerged by gene duplication (Duenez-Guzman and Haig, 2014; Tian et al., 2009).

KHDC3L expression was documented at the RNA level in GV and metaphase II human oocytes and also at the protein level by immunohistochemistry during early folliculogenesis (Parry et al., 2011). KHDC3L is a member of the KH protein family characterized by the presence of an N-terminal KH domain, known to bind RNA (Garcia-Mayoral et al., 2007). Recently, we showed that KHDC3L co-localizes with NLRP7 in human hematopoietic cells (Reddy et al., 2013). In addition, *Filia*, the closest mouse gene to *KHDC3L*, has been reported to be part of a maternal protein complex confined to the oocyte cortex (Ohsugi et al., 2008).

Molar tissues from patients with two *NLRP7* or *KHDC3L* mutations are diploid biparental. Despite the normal biparental contribution to their genomes, these tissues lack maternal methylation marks on several maternally imprinted, paternally expressed genes. This has led to the suggestion that NLRP7 and KHDC3L play roles in establishing or maintaining maternal epigenetic marks during oogenesis or post-zygotic development (El-Maarri et al., 2003; Hayward et al., 2009; Judson et al., 2002; Kou et al., 2008). In line with these data, a recent study demonstrated the implication of NLRP7 in trophoblast lineage differentiation, chromatin reprogramming, and DNA methylation (Mahadevan et al., 2014).

Part of our understanding of the functions of NLRP7 and KHDC3L in the cells where these proteins play their primary roles is in the characterization of their exact subcellular localizations in human oocytes and early embryos. Towards this goal, we used a total of 164 spare human oocytes and embryos to characterize fully the expression of these two proteins. We

describe their localization to the oocyte cytoskeleton and show that both proteins redistribute at the 2-cell stage and become polar, restricted to the outer cortical region. Our full characterization of the subcellular localization of NLRP7 and KHDC3L will contribute to a better understanding of the roles of these proteins in the pathophysiology of RHMs.

3.3 MATERIALS AND METHODS

Collection of oocytes and early cleavage embryos

This study was approved by the Institutional Review Board of the McGill University. Patients undergoing IVF, intracytoplasmic sperm injection (ICSI), and/or pre-implantation genetic diagnosis (PGD) were treated with GnRH agonist or antagonists and FSH or hMG in a long- or short-treatment protocols. A single dose of 10,000 IU hCG was administered when two or more follicles reached a diameter above 18 mm. Oocytes were retrieved transvaginally 35 hours after hCG injection and were inseminated by either conventional IVF or ICSI. Oocytes and zygotes were cultured in cleavage medium (Cook Medical Inc., USA) in an atmosphere containing 6% CO_2, 5% O_2, and 89% N_2. Fertilization was assessed 17–19 h after insemination by examining the presence and number of pronuclei. Spare oocytes and embryos or those that were not of good quality were donated for research on days 1-3 from consenting patients. A total of 164 oocytes and embryos were used in this study and the detailed description of their stages is listed in Supplemental Table 3.1.

Disaggregation of cleavage-stage embryos

In some experiments, cleavage-stage embryos were disaggregated before immunofluorescence. In these experiments, the embryos were incubated for 20-30 seconds in Acidic Tyrode's Solution (T1788) (Sigma-Aldrich Inc., Saint Louis, MO, USA) in order to remove the zona pellucidae. Zona-free embryos were then incubated for 2 hours in Sydney IVF Cleavage Medium (G20720) (Cook Medical Inc., USA) and then 15-30 minutes in Sydney IVF Biopsy medium (Ca2+/Mg2+-free medium) (G26120) (Cook Medical Inc., USA) with 0.3% (w/v) polyvinylpyrrolidone (PVP) at 37°C. Embryos were disaggregated individually by gentle pipetting through an 80 µm tip in 50 µl drops of 0.5% (w/v) albumin in PBS 1x, transferred to glycine buffer (0.15M glycine in PBS 1x) and stored at 4°C until further processing.

Immunofluorescence and confocal microscopy

After collection, the oocytes and preimplantation embryos were fixed in 4% (v/v) para formaldehyde (catalogue number 15710) [Electron Microscopy Sciences (EMS), Hatfield, PA, USA] in PBS 1x for 30 min at room temperature, transferred to the glycine buffer, and stored at 4°C until further processing. The oocytes and embryos were then washed in immunofluorescence (IF) buffer [1% (w/v) bovine serum albumin (BSA), 0.5% (v/v) normal goat serum in PBS 1x], permeabilized with 0.5% (v/v) Triton X-100 in PBS 1x for 30 min, followed by three washes with IF buffer and blocked in 3% BSA (w/v) in PBS 1x for 1 h. In some experiments, a microtubule-stabilizing buffer was used to preserve microtubules structures. In these experiments, after collection the oocytes were fixed for 1 h at room temperature in the following microtubule-stabilizing buffer (0.1M Pipes, pH 6.9, 5 mM $MgCl_2$, 2.5mM EGTA) containing 2.0% (v/v) paraformaldehyde (PFA), 0.5% (v/v) Triton X-100, 1 μm taxol, 10 units/ml aprotinin and 50% (v/v) deuterium oxide (Messinger and Albertini, 1991), washed three times in IF buffer, and blocked in 5% (v/v) FBS, 1% (v/v) Triton X-100 in PBS 1x for 1 h.

The samples that were either fixed with 4% (v/v) PFA or with the microtubule-stabilizing buffer were incubated for an overnight at 4°C with one or two of the following primary antibodies: goat anti-NLRP7 (sc-50642, 1:100) (Santa Cruz Biotechnology, Inc., Dallas, Tx, USA); rabbit anti-NLRP7 (IMG- 6357A, 1:100) (Novus Biologicals, Littleton, CO, USA); rabbit anti-NLRP7 (GXT120931, 1:100) (GeneTex Inc., Irvine, CA, USA); rabbit anti-KHDC3L (AP11238a, 1:100) (Abgent Inc., San Diego, CA, USA); rabbit anti-KHDC3L (HPA043699, 1:100) (Sigma); mouse anti-α-tubulin that recognizes the protein coded by *TUBA4A* (T6074, 1:1000) (Sigma); mouse anti-E-cadherin (*CDH1*) (13-1700, 1:100) (Invitrogen Inc., Carlsbad, CA, USA) to visualize the transmembrane adhesion proteins at the cell-to-cell contact region; mouse anti-NANOG (4893, 1:100) (Cell signaling technology, Boston, MA, USA) to visualize the ICM cells. NLRP7 and/or KHDC3L antibodies used in most of the immunofluorescence experiments were sc-50642 and AP11238a, respectively, and in these cases, the catalog numbers and names of the suppliers are not indicated. Occasionally, when other antibodies to reveal NLRP7 and KHDC3L were used, the names of the suppliers or references are specified.

After an overnight incubation with the primary antibodies, the samples were washed with IF buffer and incubated with the following secondary antibodies, Alexa 488- or Alexa 568-conjugated secondary antibodies (1:500) (Invitrogen, Carlsbad, CA, USA) for 1 h at room

temperature and was followed by three washes in IF buffer. Finally, the oocytes or embryos were transferred onto slides, coverslipped and mounted using Vectashield hard-set mounting medium containing DAPI (H-1200) (Vector Laboratories, Burlingame, CA, USA) to visualize the nuclei. The specificity and validation of the main antibodies used to reveal NLRP7 and KHDC3L were reported previously (Messaed et al., 2011a; Reddy et al., 2013). Fluorescence images were captured using a laser scanning confocal microscope either Olympus FluoViewTM FV1000 or Leica SP8 (for Figure 3.3A). Optical sections of 1 μm were obtained and the imaging parameters were set using the greyscale function in the Olympus FluoViewTM FV1000 software. Figure 3.3A was generated using Volocity software (http://www.perkinelmer.co.uk). In order to ensure the highest possible quality images without saturation, confocal settings were adapted and the images were then exported as TIFF files and processed for final figure formatting.

Electron microscopy

Immunolabeling was performed before the embedding of the oocytes. After collection, oocytes were incubated with goat anti-NLRP7 (1:100) (sc-50642) followed by incubation with rabbit anti-Goat IgG (1:20) conjugated to 10 nm gold particles (G5402) (Sigma) for 30 minutes at room temperature and then fixed with 2.5% (v/v) glutaraldehyde [Electron Microscopy Sciences (EMS), Hatfield, PA, USA], in 0.1 M sodium cacodylate buffer (pH 7.3) for an overnight at 4°C. The oocytes were then post-fixed with 1% (v/v) osmium tetroxide (EMS), 1.5% (w/v) aqueous potassium ferrocyanide in 0.1 M sodium cacodylate buffer (EMS) for 2 h at 4°C, dehydrated through a graded series of ethanol baths, and then embedded in Epon (EMS). Ultrathin sections (80–95 nm) were cut with a diamond knife (Diatome) (EMS) on a Leica Microsystems UCT ultramicrotome (Vienna, Austria) and transferred onto Cu 200 mesh TEM grids with Formvar support film (EMS). Sections on the grids were contrast stained with 2% (w/v) uranyl acetate and Reynold's lead (EMS). Samples were imaged in a FEI Tecnai 12 TEM (FEI, Hillsboro, OR, USA) at an accelerating voltage of 120 kV and images were collected with an AMT XR80C CCD camera (Advanced Microscopy Techniques Corp, Woburn, MA, USA).

Statistical analysis

For the statistical analysis of immunofluorescence images, three different sections (at z=50 μm, section thickness=1μm) of either metaphase II oocytes or 2-cell embryos from three independent experiments were analyzed to measure NLRP7 signal intensities using AutoQuantX software (Media Cybernetics, Inc, USA; http://www.mediacy.com). Measurements were performed on three regions indicated in Figure 3.1F as the cortical (I and III) or central (II) regions for the metaphase II oocyte and in Figure 3.4B as the cortical (I and III) or the cell-to-cell contact region (II) for the 2-cell embryos. All the data points generated by the software in each region were averaged. Then the averages of NLRP7 signal in each region between all three images were calculated. Standard deviations were calculated for the averages generated for the three images. Statistical significance was performed using two-tailed t-test by comparing the average values obtained in regions I, II, and III in the oocytes and the 2-cell embryos. P-values <0.05 were considered statistically significant.

For the TEM image analysis, four different sections of a metaphase II oocyte (section thickness=95 nm) were used to count the number of immunogold particles from the cortex towards the center of the oocyte using Image J software (National Institutes of Health, USA; http://imagej.nih.gov/ij). The three regions in which the counts were performed are shown in Figure 3.2B where interval 1 represents the region between 1 nm and 1000 nm from the oocyte membrane, region 2 represents the interval between 1000 nm and 2000 nm, and region 3 represents the interval that goes beyond 2000 nm from the oocyte membrane. The total number of immunogold particles in each region was calculated for each image. Then the averages and standard errors of the means (SEM) in each region between all four images were calculated and represented in the histograms. Statistical significance was performed using two-tailed t-test by comparing the values obtained in each region for the four images. P-values <0.05 were considered statistically significant.

3.4 RESULTS

NLRP7 and KHDC3L localize to the oocyte cortical region

So far NLRP7 expression in oocytes has been documented only by immunohistochemistry, which does not provide information about its precise subcellular localization. To gain further information about NLRP7 protein localization in the cells where it plays its primary role, we performed an extensive analysis on spare oocytes that were collected from patients undergoing assisted reproductive technologies. Using immunofluorescence, NLRP7 was found to localize to the cortical region in the GV stage oocytes (Figure 3.1A), metaphase II oocytes (Figure 3.1B), and fertilized eggs (Figure 3.1C). In addition, NLRP7 was also detected in the polar bodies (Figure 3.1C). The specificity of NLRP7 signal was checked after neutralizing the primary antibody with the peptide used to raise it, according to the manufacturer's instructions, and subsequent revelation by immunofluorescence. We found that the peptide blocked completely NLRP7 signal (Supplemental Figure 3.1A-C), which demonstrates the specificity of the signal. In all oocyte stages, NLRP7's signal displayed a gradient of decreasing intensities from the cortical region toward the center of the oocytes. Measuring the intensity of the NLRP7 signal on three metaphase II oocytes from different experiments revealed that the intensity of the signal in the cortical region is ~ 3-fold higher than that observed in the center ($P<0.03$; Figure 3.1E and F).

We then checked whether NLRP7 intense cortical signal is caused by a technical artefact due to the incubation time and temperature with the primary antibody; the composition of the fixation buffer as previously shown for some proteins by Morency et al. (Morency et al., 2011); or the antibody itself by testing two additional ones. However, the NLRP7 cortical signal did not change significantly with all the tested conditions (Supplemental Figure 3.2 and 3.3). We note that NLRP7's signal in the zona pellucida was not revealed with the two additional antibodies, which indicates that the zona pellucida signal obtained with the main antibody (sc-50642) is most likely an artefact. We then extracted the oocytes with 0.1% (v/v) Triton X-100 1% (v/v) DMSO in PBS 1x for 5 minutes before fixation with PFA 4% (v/v) and performed double labeling experiments with NLRP7 and α-tubulin antibodies. We found that NLRP7 protein distribution was not affected by the treatment and remained mainly at the cortical region while α-tubulin antibody gave a clear filamentous network that was uniformly distributed throughout

the cytoplasm (Figure 3.2A-C), which demonstrate appropriate protein extraction before fixation. Altogether, our data demonstrate that NLRP7 intense cortical signal is unlikely to be due to an experimental artifact, but reflects the higher concentration of the protein at the cortical region.

We next investigated the localization of KHDC3L in human oocytes at the metaphase II stage using two commercially available antibodies. KHDC3L was found expressed at this stage, mainly in the cortical region (Figure 3.2D-F and Supplemental Figure 3.4) similar to NLRP7 (Figure 3.2B). KHDC3L was also expressed in the polar bodies (Supplemental Figure 3.5), and was completely absent from the zona pellucida with the two analyzed antibodies (Figure 3.2D-F and Supplemental Figure 3.4 and 3.5). The specificity of the KHDC3L primary antibody (AP11238a) was also tested after blocking with the KHDC3L peptide according to the manufacturer's instructions, which abolished completely its signal (Supplemental Figure 3.1D-F).

NLRP7 is part of the oocyte cytoskeleton structure

To gain further knowledge about NLRP7 localization in the oocytes, we fixed some oocytes with microtubule-stabilizing buffer, performed immunofluorescence, and analyzed the oocytes with high magnification confocal microscopy. This treatment preserved the microtubules and revealed a very nice cytoskeleton staining with NLRP7 antibody that was again more intense at the cortical region and was localized between some round structures that were not stained with NLRP7 antibody (Figure 3.3A). To identify these round structures and further refine the localization of NLRP7 at the cortical region, we performed ultrastructure analysis of metaphase II oocytes by transmission electron microscopy (Figure 3.3B-D) and first looked at the morphology of the oocyte with a particular interest to identify the different components and structures that are present in the cortical region. As previously reported (Van Blerkom and Henry, 1988), we found that this region is highly rich in cortical granules, mitochondria, smooth endoplasmic reticulum, and vacuoles (Figure 3.3B), which are embedded into some cytoskeletal structures. Immunostaining with NLRP7 antibody followed by electron microscopy revealed immunogold particles that were located between cortical granules, mitochondria, and other organelles (Figure 3.3C and D), on some structures that were not well preserved. These immunogold particles displayed a gradient of decreasing numbers from the membrane toward the center of the oocytes ($P<0.04$; Figure 3.3E). To reveal the nature of the structures on which

immunogold particles were bound, we fixed additional oocytes with the microtubule-stabilizing buffer, which allows simultaneous extraction and fixation and performed confocal microscopy using either NLRP7 or KHDC3L and α-tubulin antibodies (Figure 3.3F-K). This treatment preserved the structure of the oocyte microtubules and cytoskeleton and revealed with α-tubulin antibody a microtubule filamentous network that was evenly distributed in the cytoplasm (Figure 3.3G and H; J and K) while NLRP7 and KHDC3L antibodies stained some cytoskeletal structures that were again more intense at the cortical region (Figure 3.3F-K; L-N). In conclusion, these data suggest that NLRP7 and KHDC3L are part of the oocyte cytoskeleton and are more abundant at the cortical region.

NLRP7 is polar during early embryogenesis

Next, we investigated the distribution of NLRP7 in preimplantation embryos from 2-cell to blastocyst stages. In humans, the thickness of the 2-cell embryo is ~100 μm. In the middle section of 2-cell stage embryos (at 50 μm), NLRP7 signal was found polar with a gradient of decreasing intensities from the outer cortical region to the cell-to-cell contact region, where NLRP7 was completely absent ($P<0.006$) (Figure 3.4A and B). To investigate NLRP7 polarity throughout the three dimensional structure of the 2-cell embryo, we measured the intensities of its signal from the slide level (0 μm) to the top level (100 μm) using the z stack confocal option. At 40 μm and 60 μm, NLRP7 signal was present in the inner part of the cells but was less intense than in the cortical region (Figure 3.4C and D). At 30 μm and 70 μm, NLRP7 signal in the inner part was higher than at 40 μm and 60 μm, respectively (data not shown). This pattern was reproduced in three different experiments and on three different 2-cell embryos (Figure 3.4B), which demonstrates the three-dimensional polarity of NLRP7 in 2-cell embryos with a predominant location to the outer cortical part of the cells.

We next performed double labeling experiments with NLRP7 and E-cadherin, a transmembrane adhesion protein that attaches blastomeres one to another after the completion of the first cell division via calcium-dependent homotypic interactions (De Vries et al., 2004) (Figure 3.4E-G). This analysis showed the presence of E-cadherin at the cell-to-cell contact region demonstrating therefore that the absence of NLRP7 at the cell-to-cell contact is not due to incomplete permeabilization of the cells, inaccessibility of the antibody, or technical issues affecting the transmission and detection of fluorescence. Dissociation of blastomeres from 2- to

8-cell embryos using calcium-free culture media resulted in a quick re-distribution of NLRP7 to the same uniform, cortical localization observed in oocytes (Figure 3.4H-J). The same uniform and cortical distribution of NLRP7 was also observed in decompacted blastomeres of two degenerated embryos that were processed for immunofluorescence (Figure 3.4K and L). This indicates that NLRP7 protein is not soluble and free in the oocytes, but is part of some cytoskeletal structures that are maintained in good-quality embryos but lost upon embryo degeneration. We note that in several embryos, blastomeres undergoing apoptosis expressed higher amount of NLRP7. Three of these embryos are shown in Figures. 3.4H, 3.5F and I. The polarity of NLRP7 was maintained until the morula stage (Figure 3.5) but disappeared at the blastocyst stage where NLRP7 was homogenously distributed in the cytoplasm of cells from both the trophectoderm and the ICM (Figure 3.6). In this experiment, NANOG was used to identify ICM cells.

KHDC3L polarity was maintained until the morula stage where it started to become nuclear in some blastomeres but excluded from the nucleoli (Figure 3.5J-O). At the blastocyst stage, KHDC3L remained nuclear and was expressed in both the ICM and the trophoblast layer (Figure 3.6F-M). Our data on early embryos demonstrate that NLRP7 and KHDC3L are both polar localized to the outer part of the cortical region during early cleavage-stages.

3.5 DISCUSSION

To date, several maternal-effect genes have been identified in mice and the subcellular localization of some of their proteins, OOEP, NLRP5, TLE6, FILIA, PADI6, DNMT1O, and cPLA2γ, in the oocytes and early embryo cleavage-stages has been described (Howell et al., 2001; Kim et al., 2010; Li et al., 2008b; Morency et al., 2011; Ohsugi et al., 2008; Tashiro et al., 2011; Vitale et al., 2005; Yurttas et al., 2010; Yurttas et al., 2008). These studies have revealed that one of the main characteristics of these proteins is their cortical localization in the oocytes and their polar distribution toward the outer part of the cortical region from 2-cell to morula stages.

To gain insight about the subcellular localization of the proteins of the only two known maternal-effect genes in humans, *NLRP7* and *KHDC3L,* we performed extensive analysis on a total of 164 human oocytes and preimplantation embryos using confocal immunofluorescence and electron microscopies. We found that in oocytes, from the GV until the formation of the zygote, NLRP7 localized mainly to the cortical region along with KHDC3L. Modifying a range of experimental parameters did not significantly alter NLRP7 signal and validated its higher concentration at the cortical region of the oocytes. Within the cortical region, electron and high-resolution confocal microscopies confirmed the localization of NLRP7 between cortical granules, mitochondria, and other organelles on some cytoskeletal structures that did not overlap exactly with the α-tubulin microtubule network or display similar pattern by immunofluorescence. Similar cytoskeletal structures, called CPLs, were identified in mouse oocytes and consist of bundled fibers (Capco et al., 1993) to which five maternal-effect proteins, OOEP, FILIA, NLRP5, PADI6, TLE6, have been shown to localize (Li et al., 2008b; Wright et al., 2003). The exact roles of CPLs is not fully understood, but embryos from NLRP5, PADI6, OOEP (FLOPPED), TLE6, or FILIA null females arrest during preimplantation development due to various defects that include impaired embryonic transcription (Tong et al., 2000), dysregulation of *de novo* protein synthesis (Yurttas et al., 2008), mitotic spindle abnormalities (Zheng and Dean, 2009), asymmetric first-cell division (Zheng and Dean, 2009), delayed 1- to 2-cell division (Zheng and Dean, 2009). In addition, these CPLs were demonstrated to remain insoluble following treatment of oocytes with Triton X-100 (Capco et al., 1993; McGaughey and Capco, 1989), which is in agreement with our data on NLRP7 signal that persisted to be predominant at the cortical region even after extraction of the oocytes with Triton X-100. These

data suggest that NLRP7 is indeed part of these detergent-resistant cytoskeletal structures that are abundant at the oocyte cortical region.

As the embryo completed its first division, NLRP7 and KHDC3L became excluded from the cell-to-cell contact region, were asymmetrically restricted, to the outer cortical regions and were part of some structural complexes that are not E-cadherin dependent. During early cleavage-stages, NLRP7 was polar until the blastocyst stage where it lost its polarity and became homogeneously distributed in the cytoplasm of the ICM and the trophectoderm. KHDC3L was polar until the morula stage where it entered and remained in the nuclei of both the ICM and the trophectoderm layer. The fact that both *NLRP7* and *KHDC3L* are maternal-effect genes that cause the same disease suggests that stages displaying their identical subcellular localization, oocytes to morula, are the most critical ones for the development of RHMs. This suggestion is corroborated by the preimplantation abnormalities observed in patients with mutations in *KHDC3L* (Reddy et al., 2013) and rare variants in *NLRP7* (Deveault et al., 2009; Qian et al., 2011), and is further supported by data on other maternal-effect genes such as (i) *Nlrp2*, the closest gene to *NLRP7*, whose knockdown in mice leads to embryonic arrest between 2- and 8-cell stages (Peng et al., 2012); (ii) *Nlrp5*, whose knockout in mice leads to embryonic arrest at the 2-cell stage (Tong et al., 2000); and (iii) *Filia*, whose knockout leads to arrest of 50% of the embryos by the morula stage (Ohsugi et al., 2008). Because molar tissues from patients with *NLRP7* and *KHDC3L* mutations lack DNA methylation at several imprinted, maternally expressed genes (El-Maarri et al., 2003; Hayward et al., 2009; Judson et al., 2002; Kou et al., 2008), it was suggested that both NLRP7 and KHDC3L play a role in establishing or maintaining maternal methylation during oogenesis and/or early embryogenesis. The fact that KHDC3L translocates to the nuclei at the 8-cell stage similar to another maternal-effect protein in mice, DNMT1O (Howell et al., 2001), suggest some shared roles between the two proteins, perhaps in maintaining DNA methylation patterns at the 8-cell embryo stage and before lineage differentiation.

In conclusion, our study provides the first detailed and high resolution localization of the only two known maternal-effect proteins, NLRP7 and KHDC3L, in human oocytes and preimplantation embryos. We demonstrate their cytoskeletal localization in the oocytes and polarity throughout post-zygotic division. Our data suggest that NLRP7 and KHDC3L could be involved in the integrity and organization of the oocyte cortical region. In addition, their ability

to redistribute during early cleavage-stages indicate their possible involvement in sequestering macromolecules that may trigger, either directly or indirectly, the commitment of outer and inner cells to become, respectively, trophoblast and embryos, a process that was also suggested for FILIA and NLRP5 complex (Ohsugi et al., 2008).

3.6 ACKNOWLEDGMENTS

We thank the patients for their participation. We also thank Dr Hojattolah Vali, Jeannie Mui, Wejdan Alenezi, Adel R Moawad and Elke Küster-Schöck for technical assistance. We acknowledge the use of the Facility for Electron Microscopy Research (FEMR) and the Facility for Cell Imaging and Analysis Network (CIAN) at McGill University.

3.7 FIGURES

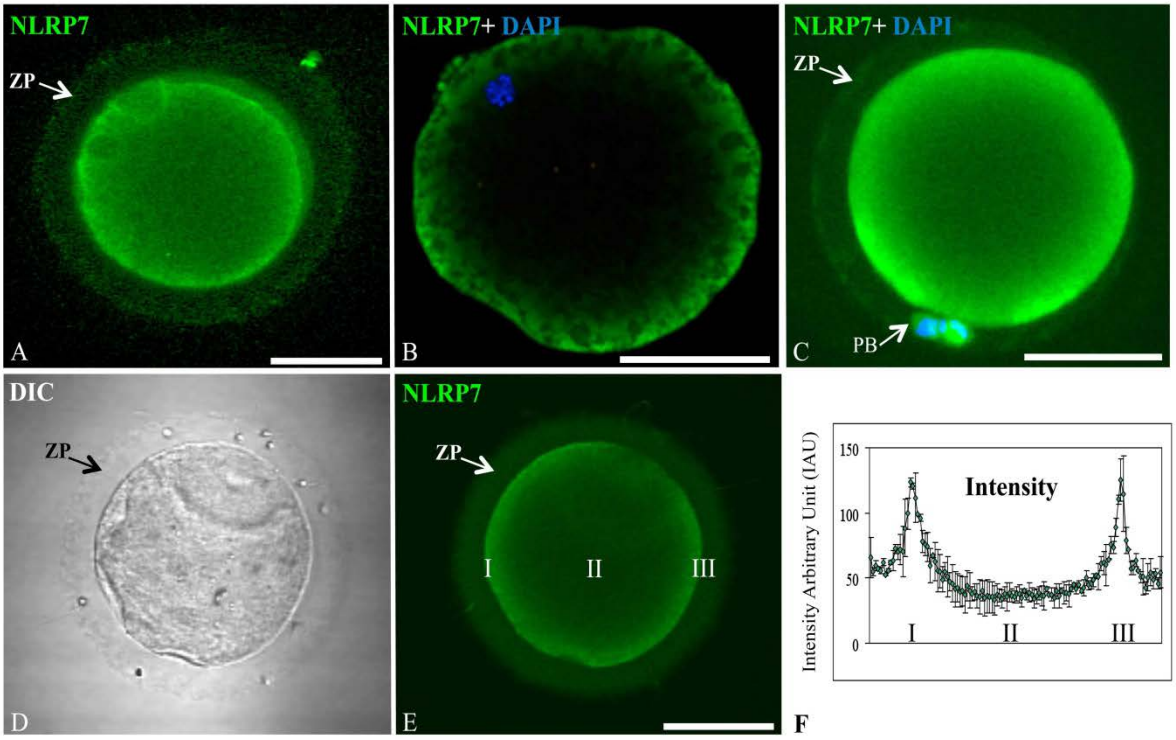

Figure 3.1. <u>NLRP7 localizes to the cortical region in human oocytes</u>
NLRP7 is expressed in the cortical region of GV (A) and metaphase II (B) oocytes. (C) NLRP7 expression in the cortical region and the polar bodies of a fertilized egg. (D) One section (at Z=50µm) of a different metaphase II oocyte visualized with differential interference contrast. (E) The same section of metaphase II oocyte shown in (D) is visualized with NLRP7 antibody and was used to measure the intensity of its signal in the cortical (I and III) or central (II) regions. (F) Intensity profile of NLRP7 signal showing averages and ± standard deviations of all the data points in the cortical (I and III) or central (II) regions of three different oocyte sections (at Z=50µm and thickness=1µm) from three different experiments. The values of the Y-axis are in arbitrary units. DAPI (blue) stains the nuclei of the oocyte and the polar bodies. Bars, 50 µm.

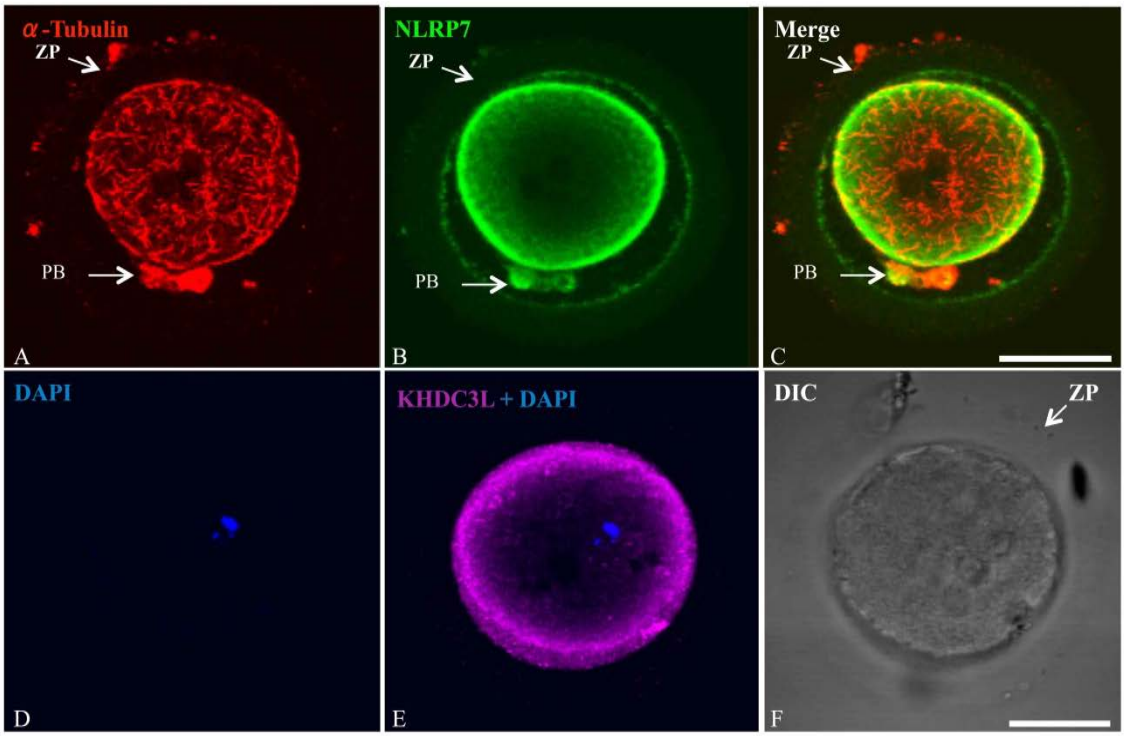

Figure 3.2. <u>NLRP7 and KHDC3L proteins localize to the oocyte cortical region</u>
(A-C) Double labeling of NLRP7 (green) and α-tubulin (red) of a fertilized egg after extraction with 0.1% (v/v) Triton 1% (v/v) DMSO in PBS 1x. α-tubulin antibody displays an evenly distributed filamentous network in the cytoplasm. (D-F) Single labeling of KHDC3L (magenta) showing its localization to the cortical region of a metaphase II oocyte. Note the absence of KHDC3L signal in the zona pellucida visualized with differential interference contrast. DAPI (blue) stains the nuclei of the oocyte. Bars, 50 μm.

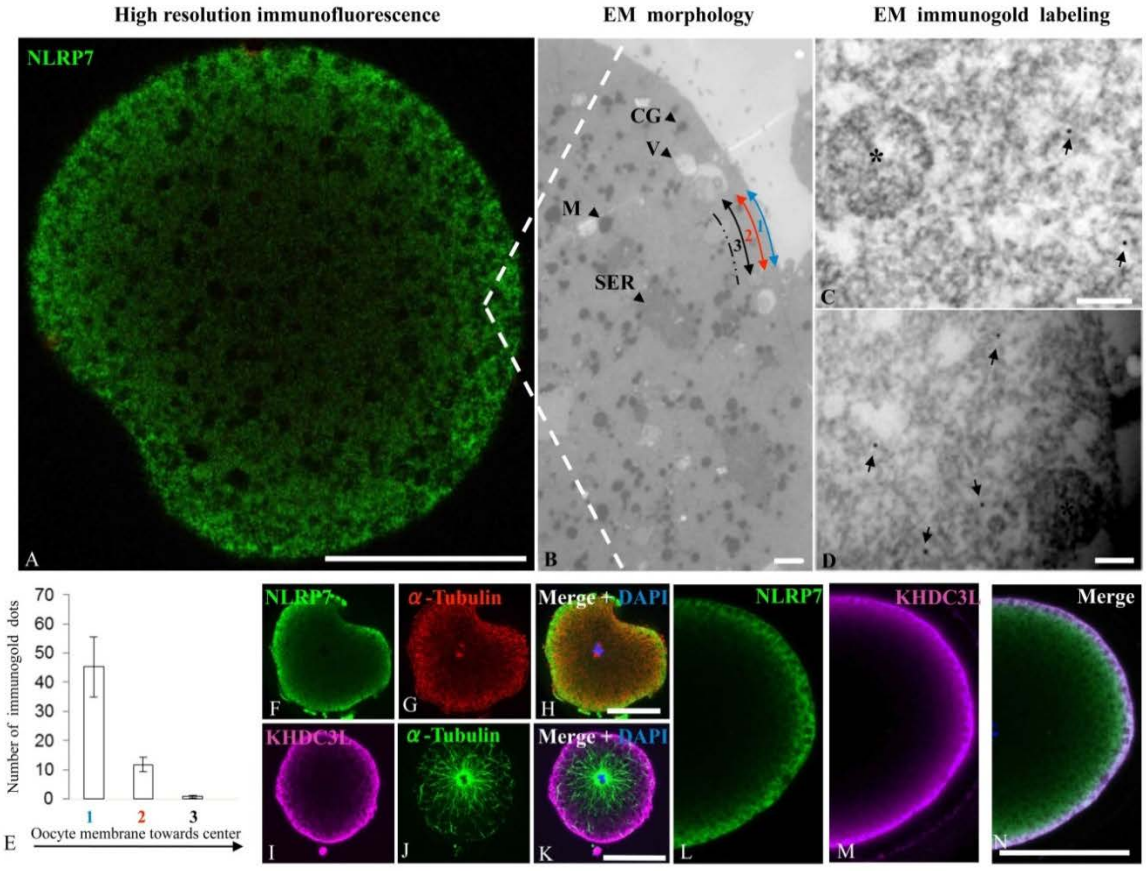
High resolution immunofluorescence
EM morphology
EM immunogold labeling
NLRP7
CG
V
M
SER
A
B
C
D
Number of immunogold dots
70
60
50
40
30
20
10
0
1
2
3
Oocyte membrane towards center
E
NLRP7
α-Tubulin
Merge + DAPI
NLRP7
KHDC3L
Merge
KHDC3L
α-Tubulin
Merge + DAPI
F
G
H
I
J
K
L
M
N

Figure 3.3: <u>Localization of NLRP7 within the human oocyte using confocal and electron microscopies</u>

(A) High resolution confocal microscopy image (1 μm thickness) showing NLRP7 expression in the cortical region of a denuded metaphase II oocyte at high magnification. Note the staining of a cytoskeletal-like network that is brighter at the cortical region. Bar, 50 μm. (B) Electron microscopy photo of an oocyte cortical region showing different organelles, cortical granules (CG), smooth endoplasmic reticulum (SER), mitochondria (M), and vacuoles (V) at low magnification. Bar, 2 μm. (C and D) Electron microscopy analysis with NLRP7 antibody showing immunogold signals (black dots) outside cortical granules (black asterisks) and organelles and on small grey filaments of the oocyte cytoskeleton (black arrows). Bars, 10 nm. (E) Histogram representing the number of immunogold particles in each of the three different regions shown in B. Each region is delimited by a double arrow curve. Interval 1 indicates the region from 1 nm to 1000 nm from the oocyte membrane, 2 indicates the region from 1000 nm to 2000 nm from the oocyte membrane, and 3 the region of more than 2000 nm from the membrane and toward the center of the oocyte. (F-K) Expression of NLRP7 (green) and KHDC3L (Sigma) (magenta) at the cortical region with α-tubulin in the cytoplasm of two different denuded metaphase II oocytes treated with a microtubule-stabilizing buffer. Bars, 50 μm. (L-N) Co-localization of NLRP7 (green) and KHDC3L (Sigma) (magenta) at the cortical region in a different denuded metaphase II oocyte treated with a microtubule-stabilizing buffer. DAPI (blue) stains the nuclei of the oocytes. Bar, 50 μm.

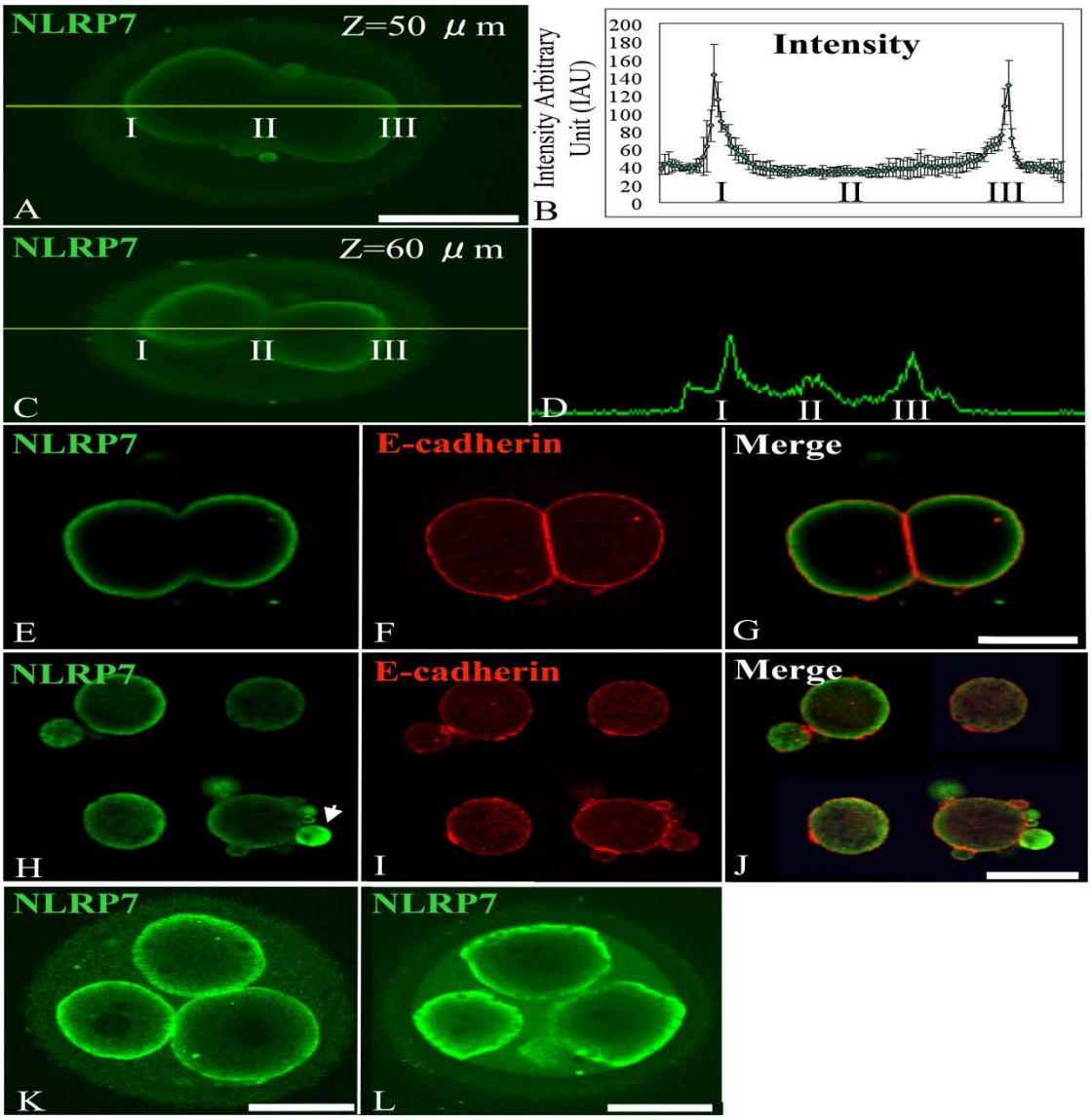
NLRP7
Z=50 μm
I
II
III
A
Intensity Arbitrary Unit (IAU)
200
180
160
140
120
100
80
60
40
20
0
Intensity
I
II
III
B
NLRP7
Z=60 μm
I
II
III
C
D
I
II
III
NLRP7
E
E-cadherin
F
Merge
G
NLRP7
H
E-cadherin
I
Merge
J
NLRP7
K
NLRP7
L

Figure 3.4. NLRP7 is polar in 2-cell embryos

(A) NLRP7 is expressed in the cortical zone (I and III) of a 2-cell embryo but not in the cell-to-cell contact region (II) at 50 μm. (B) Intensity profile of NLRP7 signal showing the averages and ± standard deviations of all the data points in the cortical (I and III) or cell-to-cell contact regions (II) of three different 2-cell embryo sections (at Z=50 μm and thickness=1 μm) from three different experiments. The values of the Y-axis are in arbitrary units. (C and D) NRLP7 signal reappears in the cell-to-cell contact region (II) of a 2-cell embryo at 60 μm. (E-G) Presence of E-cadherin (CDH1) (red) but absence of NLRP7 (green) from the cell-to-cell contact region. (H-J) Dissociated blastomeres from zona-free morulae embryo after incubation in a Ca^{2+}-free medium showing the redistribution of NLRP7 in disaggregated blastomeres. The photos of several blastomeres represented in this section were taken from different fields in the same experiment and gathered into a single image. White arrow in (H) indicates the presence of high NLRP7 signal in an apoptotic blastomere. (K and L) NLRP7 expression in two degenerated embryos that were processed for immunofluorescence. Bars, 50 μm.

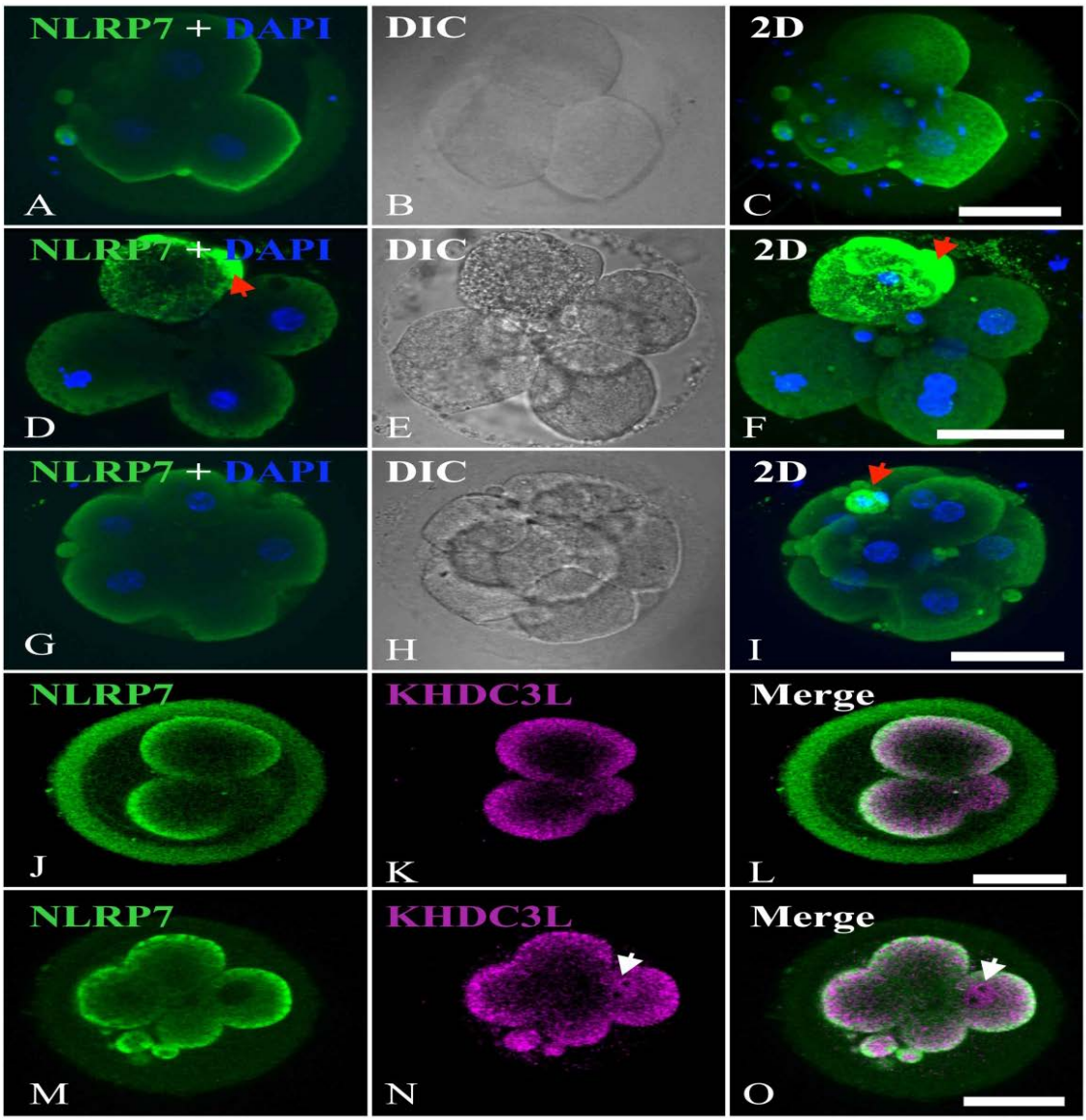
NLRP7 + DAPI
DIC
2D
A
B
C
NLRP7 + DAPI
DIC
2D
D
E
F
NLRP7 + DAPI
DIC
2D
G
H
I
NLRP7
KHDC3L
Merge
J
K
L
NLRP7
KHDC3L
Merge
M
N
O

Figure 3.5. NLRP7 and KHDC3L polarity in preimplantation embryos

NLRP7 polarity is maintained in 4-cell (A-C), 8-cell (D-F) and morula (G-I) embryos. NLRP7 (green) co-localizes with KHDC3L (magenta) in 3-cell (J-L) and 4-cell embryos (M-O). DIC indicates differential interference contrast images and 2D indicates two-dimensional reconstruction images from z stacks. Red arrows in (D), (F) and (I) indicate the presence of high NLRP7 signal in apoptotic blastomeres. White arrows in (N) and (O) indicate the presence of KHDC3L in the nucleus but not in the nucleoli of a 4-cell embryo. DAPI (blue) stains the nuclei of the blastomeres and the heads of the spermatozoa. Bars, 50 μm.

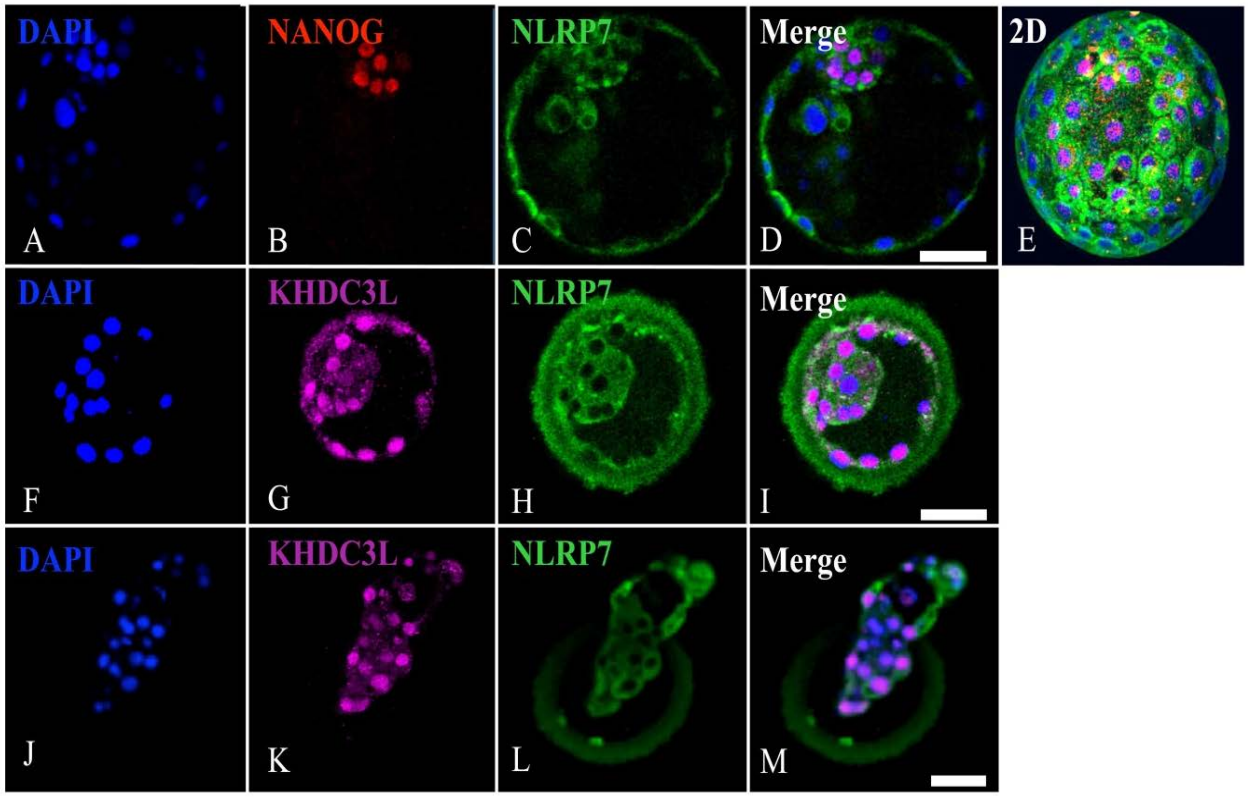

Figure 3.6. <u>NLRP7 and KHDC3L lose their polarity at the blastocyst stage</u>
(A-M) NLRP7 (green) and KHDC3L (magenta) are expressed in the ICM, where NANOG (red) is expressed too, and in the trophoblast layer. At the blastocyst stage, NLRP7 (green) is homogeneously distributed in the cytoplasm while KHDC3L (magenta) showed only nuclear staining. 2D indicates the two-dimensional reconstruction of the blastocyst image from z stacks. DAPI (blue) stains the nuclei of the embryos. Bars, 50 μm.

3.8 TABLES

N-A

3.9 APPENDIX

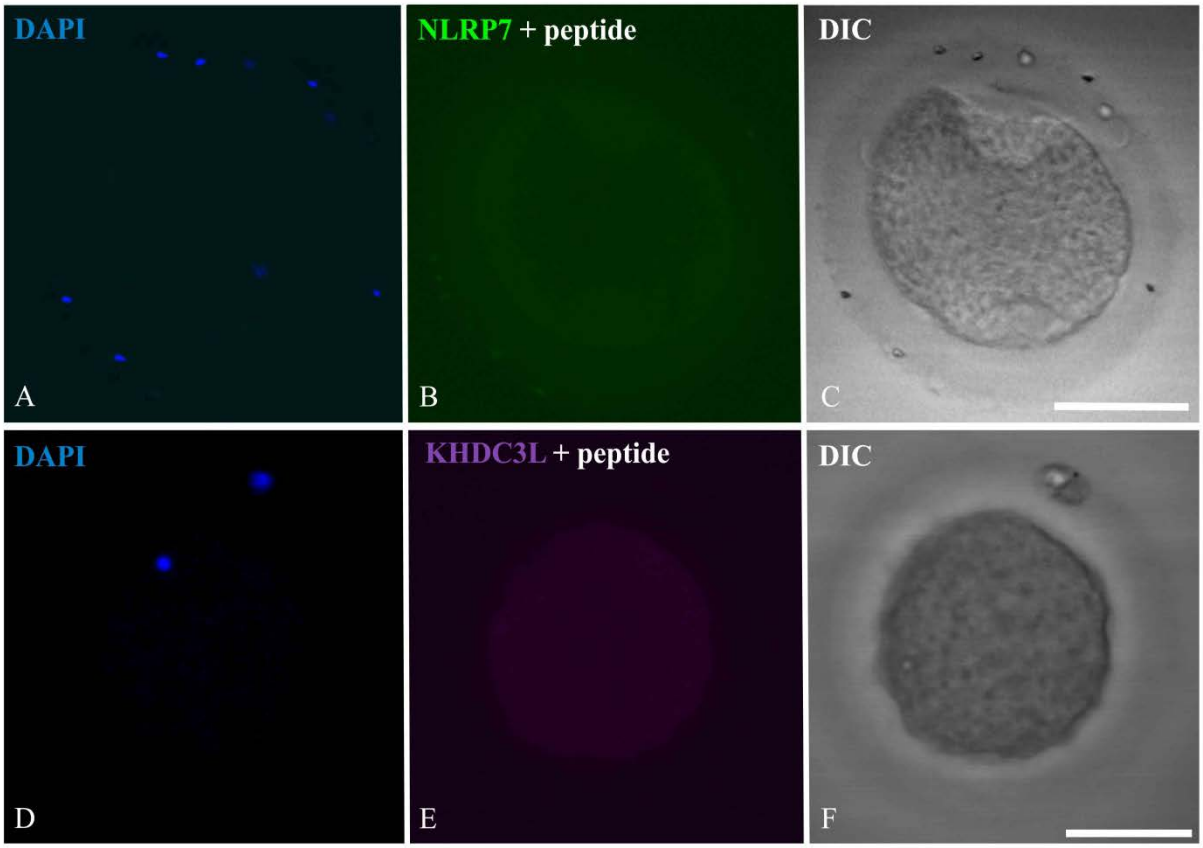

Supplemental Figure 3.1. NLRP7 (A-C, green) and KHDC3L (D-F, magenta) expressions are abolished in the metaphase II oocytes after incubating the primary antibodies of NLRP7 and KHDC3L with their respective blocking peptides

DAPI (blue) stains the heads of the spermatozoa and the nuclei of the oocyte and the polar bodies. Bars, 50 μm.

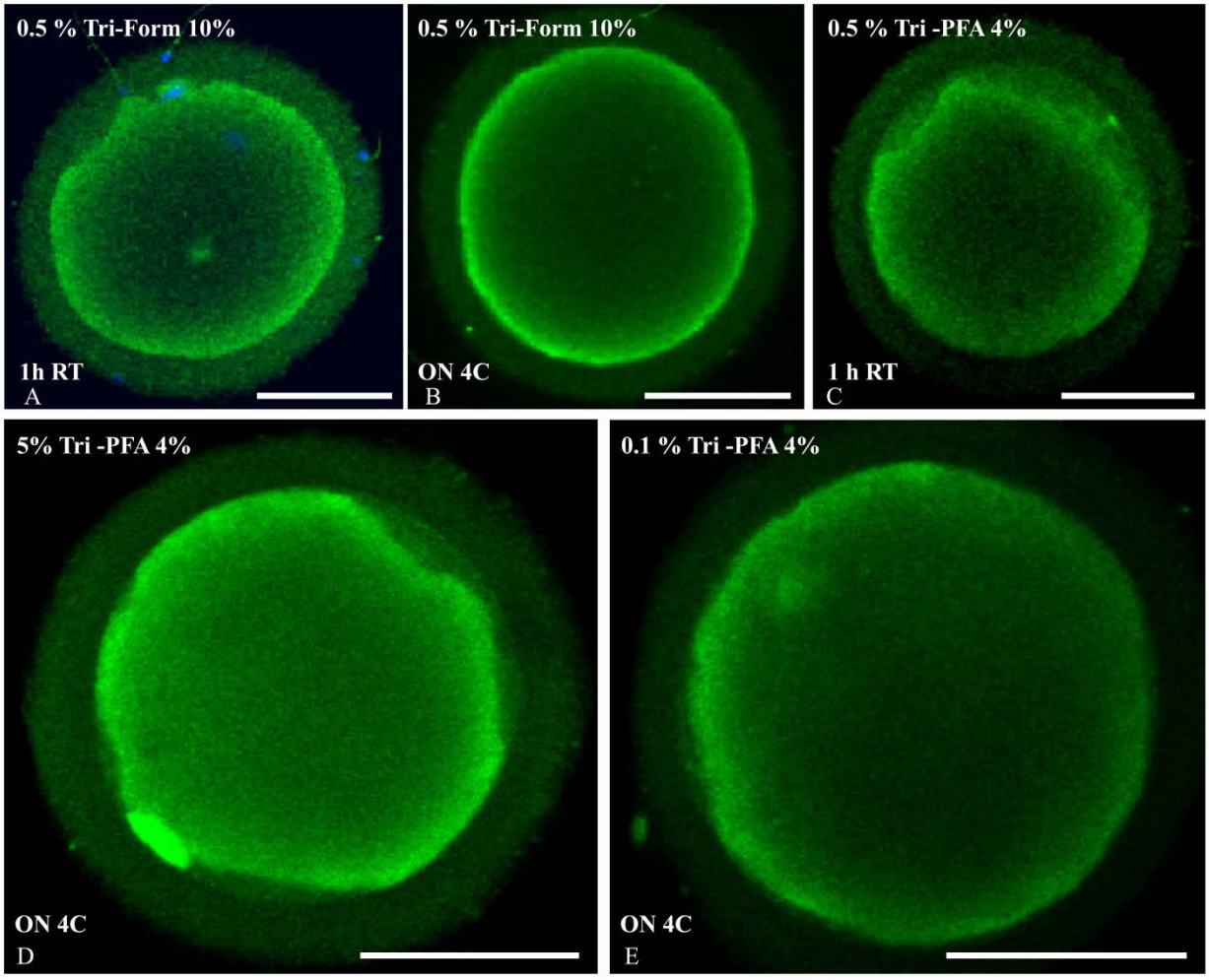
0.5 % Tri-Form 10%
1h RT
A
0.5 % Tri-Form 10%
ON 4C
B
0.5 % Tri -PFA 4%
1 h RT
C
5% Tri -PFA 4%
ON 4C
D
0.1 % Tri -PFA 4%
ON 4C
E

Supplemental Figure 3.2. <u>(A-E) NLRP7 signal (green) at the cortex of metaphase II oocytes was not significantly affected by testing a range of experimental parameters, incubation time and temperature with the primary antibody, fixation buffers and permeabilization conditions</u>

Permeabilization conditions are indicated at the top of the photos and incubation time at the bottom. All photos were obtained with the Santa Cruz primary NLRP7 antibody (sc-50642). RT, stands for room temperature; ON, for overnight; PFA 4%, for paraformaldehyde 4%; Tri, for triton; Form 10%, for formalin at 10%. DAPI (blue) stains the heads of the spermatozoa. Bars, 50 μm.

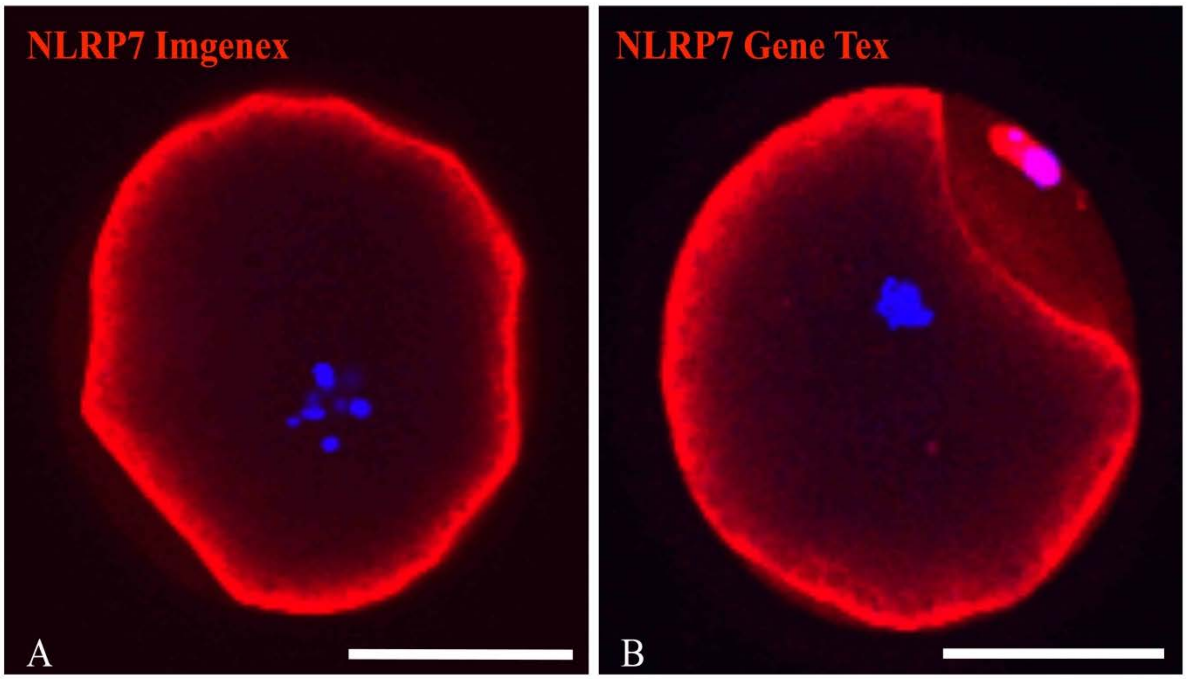

Supplemental Figure 3.3. <u>(A and B) NLRP7 (red) expression at the cortex in metaphase II oocytes with two additional antibodies Imgenex (IMG- 6357A) (A) and Genetex (GXT120931) (B)</u>

In these experiments, the main conditions described in the Materials and Methods were used. DAPI (blue) stains the nuclei of the oocytes and the polar bodies. Bars, 50 μm.

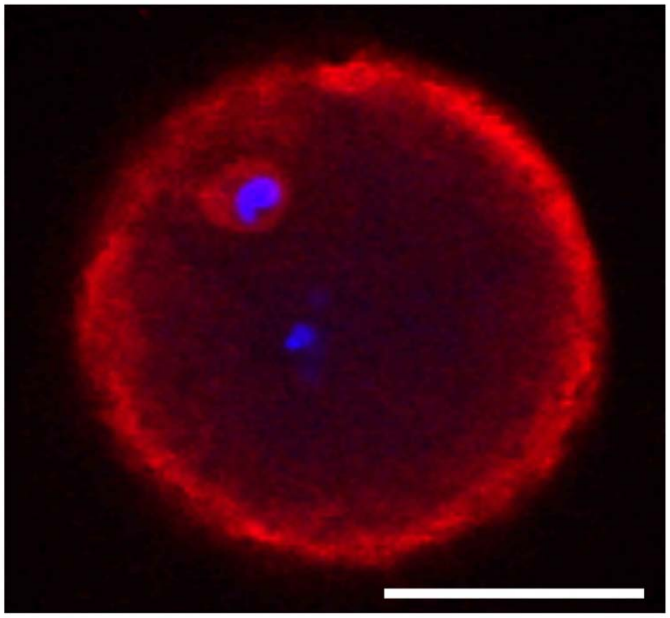

Supplemental Figure 3.4. KHDC3L (HPA043699) expression at the cortex in a metaphase II oocyte. In these experiments, the main conditions described in the Materials and Methods were used

DAPI (blue) stains the nuclei of the oocyte and the polar bodies. Bar, 50 μm.

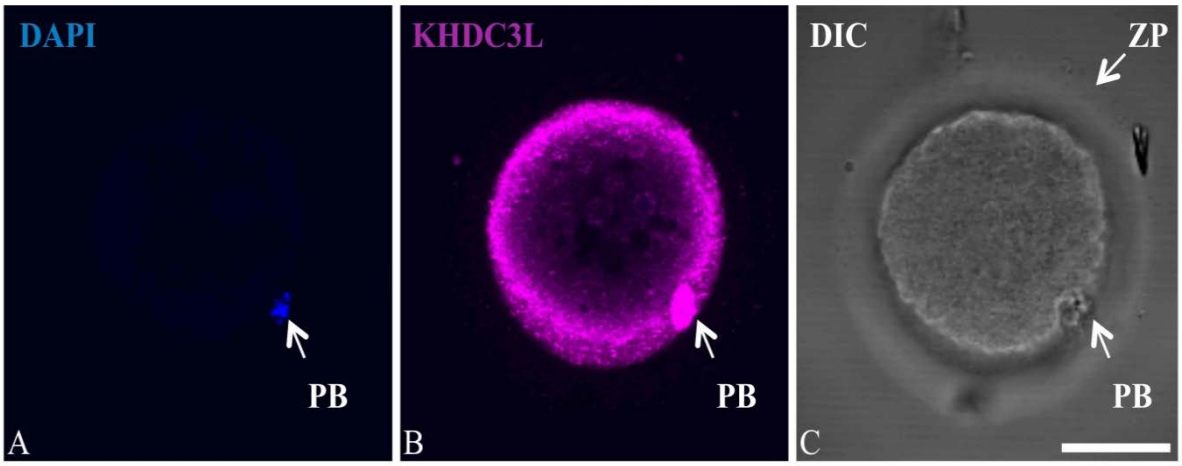

Supplemental Figure 3.5. <u>(A-C) KHDC3L(Abgent) is expressed in the polar bodies (PB) of a metaphase II oocyte (white arrows)</u>
Note the absence of KHDC3L expression in the zona pellucida (ZP). In these experiments, the main conditions described in the Materials and Methods were used. DAPI (blue) stains the nucleus of the polar bodies. Bar, 50 μm.

Supplemental Table 3.1. Detailed description of the number of oocytes and embryos on which conclusive results were obtained

	NLRP7 SC-50642	NLRP7 IMG- 6357A	NLRP7 GXT120931	NLRP7 SC-50642 + peptide	NLRP7 SC-50642 & Ecadherin	NLRP7 sc-50642 and Nanog		KHDC3L AP11238a & NLRP7 SC-50642	KHDC3L HPA043699	KHDC3L HPA043699 and NLRP7 SC-50642	KHDC3L AP11238a + Peptide		NLRP7 SC-50642 and Alpha Tubulin	KHDC3L HPA043699 and Alpha Tubulin	Total
In confocal microscopy															
Germinal vesicle - Metaphase I oocytes	11			2				4							17
Metaphase II oocyte	41	2	2	2				11	2	2	1			4	67
Fertilized egg													3		3
2-Cell embryo	3				1			1							5
3-Cell embryo	1							2					1		4
4-Cell embryo	7							1							8
8-Cell embryo	2														2
5-Cell embryo until 10-cell embryo	5							2	2	2			4		15
More than 10-cell embryo and Morula	4							2					2		8
Blastocyst	10			1	1	3		2							17
Hatching Blastocyst					1			3							4
Blastomere					6										6
In transmission electron microscopy															
Germinal vesicle to Metaphase II oocytes	7														7
2- to 4-cell embryos	1														1
Total															**164**

PREFACE TO CHAPTER 4

In Chapter 3, I showed that NLRP7 and KHDC3L localize to the oocyte cytoskeleton structures and are predominant at the cortical region in fully grown oocytes. After the first cellular division, these two maternal-effect proteins become asymmetrically confined to the outer cortical region and excluded from the cell-to-cell contact region until the blastocyst stage where NLRP7 and KHDC3L homogeneously redistribute to the cytoplasm and the nucleus, respectively. In Chapter 4, we sought to further investigate the nature of the structures to which NLRP7 localizes in human oocytes and early cleavage stage embryos and expand the localization analysis to KHDC3L and other maternal-effect proteins known to bind to similar cytoskeletal structures in mice

CHAPTER 4

NLRP7, RESPONSIBLE FOR RECURRENT HYDATIDIFORM MOLES, IS A POSSIBLE REGULATOR OF THE MICROTUBULES AND FILAMENTOUS ACTIN NETWORKS IN HUMAN OOCYTES

Elie Akoury[1,2], Asangla Ao[1,2], Rima Slim[1,2]

[1]Department of Human Genetics, McGill University Health Centre, Montreal, Quebec, Canada, [2]Obstetrics and Gynecology, McGill University Health Centre, Montreal, Quebec, Canada.

Manuscript in preparation.

4.1 ABSTRACT

Hydatidiform mole (HM) is an abnormal human pregnancy with excessive trophoblastic proliferation, hydropic chorionic villi, and abnormal embryonic development. NLRP7 and KHDC3L are associated recurrent HM (RHM). Using immunofluorescence and high resolution confocal microscopy, we showed that NLRP7 co-localizes with OOEP and TLE6, two components of the subcortical maternal complex (SCMC) in the mouse and human oocytes. Double labeling transmission electron microscopy confirmed the localization of NLRP7 with KHDC3L and OOEP to the same oocyte cytoskeletal structures. We also showed that the SCMC overlaps with alpha tubulin and F-actin cytoskeletons. In addition, treating oocytes with microtubule and filamentous actin depolymerizing agents, nocodazole and cytochalasin D, disrupts NLRP7 signal indicating therefore the dependence of the SCMC on alpha tubulin and F-actin networks. Our study is the first to characterize the nature of the human maternal complex in oocytes.

4.2 INTRODUCTION

Hydatidiform mole is an abnormal human conceptus characterized by an excessive trophoblastic proliferation, oedematous chorionic villi, and aberrant embryonic development. HMs are usually sporadic; however, in rare cases, HMs may be recurrent (RHM). Occasionally, HMs can also be recurrent and manifest in several related women of the same family; hence named familial recurrent HMs. Two genes, *NLRP7* and *KHDC3L,* have been reported to be associated with for RHMs (Murdoch et al., 2006; Parry et al., 2011). Homozygous or compound heterozygous mutations in either gene are associated with the HM phenotype through a maternal-effect mechanism (Helwani et al., 1999). *NLRP7* mutations are predominant in patients with RHMs and therefore *NLRP7* is considered the major gene for RHMs (Estrada et al., 2013; Qian et al., 2011; Sebire et al., 2013; Slim et al., 2009). NLRP7 and KHDC3L are expressed in human oocytes and embryos (Murdoch et al., 2006; Parry et al., 2011; Wang et al., 2009b; Zhang et al., 2008). At these stages, both proteins co-localize mainly at the cortex and are excluded from the cell-to-cell contact region from 2-cell embryos up to morula stages (Akoury et al., 2015b). At the blastocyst stage, NLRP7 and KHDC3L redistribute and occupy respectively the cytoplasm and the nucleus of both the inner cell mass and the trophectoderm layer (Akoury et al., 2015b). Using immunoelectron microscopy, we refined the localization of NLRP7 to the oocyte cytoskeletal structures (Akoury et al., 2015b). Subsequently, three maternal-effect proteins NLRP5, OOEP and TLE6 were reported to form a complex with KHDC3L and to localize to the human oocyte subcortical maternal complex (SCMC) (Zhu et al., 2015). These oocyte cytoskeletal structures exist also in mice and are also known as cytoplasmic lattices/sheets. SCMC are rich in keratins and are the storage site for RNAs and ribosomes (Capco et al., 1993; McGaughey and Capco, 1989; Yurttas et al., 2008). Another important characteristic of these structures is that they are resistant to extraction with Triton X-100-detergent in mouse oocytes (Capco et al., 1993; McGaughey and Capco, 1989). SCMC also constitutes the residence site of proteins of at least five maternal-effect genes in mice *Filia* (orthologue of the human *KHDC3L*), *Nlrp5*, *Flope/Ooep*, *Padi6,* and *Tle6* (Kim et al., 2010; Li et al., 2008b; Wright et al., 2003). Genetic ablation of any of these five genes in female mice leads to various defects in their null oocytes and in the embryos that include microtubules and/or actin abnormalities, reduced transcription and translation of the embryonic genome, and altered organelles positioning (Fernandes et al., 2012; Kan et al., 2011; Kim et al., 2014; Tong et al., 2000; Yu et al., 2014;

Zheng and Dean, 2009), and consequently restricted developmental capacity and embryonic arrest at the 2-cell stage (Esposito et al., 2007; Tashiro et al., 2011; Tong et al., 2000). However, few embryos derived from *Filia*- and *Tle6*-null mice progress to the morula and blastocyst with delays in the development of embryos from *Filia* knockout null mice (Yu et al., 2014; Zheng and Dean, 2009). Here, we report the co-localization of NLRP7, KHDC3L, OOEP and TLE6 to the same cytoskeletal structures and the dependence of NLRP7 on microtubules and filamentous actin in human oocytes.

4.3 MATERIALS AND METHODS

Collection of oocytes

This study was approved by the Institutional Review Board of the McGill University. A detailed description of this procedure is found in Chapter 3. Briefly, patients undergoing IVF, intracytoplasmic sperm injection (ICSI), and/or pre-implantation genetic diagnosis (PGD) were stimulated with hormones in a long- or short-treatment protocols. Oocytes were retrieved, inseminated by either conventional IVF or ICSI and cultured. Fertilization was assessed 17–19 h after insemination by examining the presence and number of pronuclei. Spare oocytes and embryos or those that were not of good quality or not fertilized were donated for research on days 1-3 from consenting patients.

Immunofluorescence and confocal microscopy

After collection, the oocytes were fixed with the microtubule-stabilizing and protein preserving buffer as previously described in Chapter 3 (Akoury et al., 2015b) and processed for immunofluorescence. The following primary antibodies were used for overnight at 4°C: goat anti-NLRP7 (sc-50642, 1:100) (Santa Cruz Biotechnology, Inc**.**, Dallas, TX, USA); rabbit anti-NLRP7 (IMG- 6357A, 1:100) (Novus Biologicals, Littleton, CO, USA); rabbit anti-KHDC3L (HPA043699, 1:500) (Sigma); mouse anti-α-tubulin that recognizes the protein encoded by *TUBA4A* (T6074, 1:1000) (Sigma); goat anti-Ooep (sc-241586, 1:100) (Santa Cruz Biotechnology, Inc.**,** Dallas, TX, USA); mouse anti-TLE6 (ab76858, 1:500) (Abcam, Toronto, On, Canada). The following secondary antibodies are used: Alexa 488- or Alexa 568-conjugated secondary antibodies (1:500) (Invitrogen, Carlsbad, CA, USA). Alexa Fluor® 568 phalloidin (A12380, 1:50) (Thermo Fisher scientific) was used to visualize filamentous actin (F-actin) and was applied on fixed oocytes for 1 hour at room temperature. For some experiments, the oocytes were treated for 1 hour at 37°C with either nocodazole (20 μM) (M1404, Sigma) to disrupt microtubules, or cytochalasin D (20 μM) (C8273, Sigma Aldrich) to inhibit/disrupt actin polymerization, before fixation with the microtubule-stabilizing buffer and processing for immunofluorescence. Fluorescence images were captured using a laser scanning confocal microscope ZEISS LSM880 of the Molecular Imaging Facility of the McGill University Health Centre. Optical sections of 1 μm were obtained and the imaging parameters were set using the greyscale function in the LSM software. In order to ensure the highest possible quality images without saturation, confocal settings were adapted and the images were then processed using the

LSM software for final figure formatting. Co-localization analysis (Pearson coefficient methods) was done using Coloc 2 option in Fiji software. A Pearson coefficient ≥ 0.8 indicates a strong correlation between the two studied channels (green and red) and therefore a strong co-localization between the two analyzed proteins.

Electron microscopy

Electron microscopy experiments are carried out as described in Chapter 3 with some exceptions. In this study, we performed a double labeling instead of a simple labeling and used the following primary antibodies: goat anti-NLRP7 (sc-50642, 1:100); rabbit anti-NLRP7 (IMG- 6357A, 1:100); rabbit anti-KHDC3L (HPA043699, 1:500); mouse anti-α-tubulin (T6074, 1:1000); goat anti-OOEP (sc-241586, 1:100). We also used the following secondary antibodies: donkey anti mouse (715-195-150, 1:50), donkey anti rabbit (711-205-152 or 711-195-152, 1:50), donkey anti goat (705-205-147, 1:50) (Jackson Immunoresearch, Baltimore, PA, USA).

Statistical analysis

The statistical tests used in this Chapter are two-tailed t-test as described in Chapter 3 and single factor Anova. P value of <0.05, is considered statistically significant in all experiments

4.4 RESULTS

High resolution confocal and electron microscopies: co-localization of four maternal-effect proteins in human oocytes

Previous work by Zhu et al. demonstrated the localization of KHDC3L, OOEP, NLRP5 and TLE6 to the human subcortical maternal complex (SCMC) by confocal microscopy (Zhu et al., 2015). However, in this study, these proteins displayed a ring-shape pattern at the cortex of the oocytes that was not connected to the center of the oocyte and the nucleus. Consequently, it was not clear from this study how these proteins are maintained at the cortical region. In addition, such staining may be obtained on oocytes with antibodies against various proteins and may result from fragmented non-preserved polymers of microtubules and actin fibers (Supplemental Figure 4.1). Therefore available data from this study were not optimal to demonstrate co-localization. To gain better knowledge about the real structure of the human SCMC complex and the relative localization of its four members, we used microtubule- and protein-preserving buffer before the fixation of the oocytes and incubation with antibodies and carried out using high resolution confocal microscopy. Immunostaining of NLRP7 and each of the following proteins, OOEP or TLE6, revealed that all these proteins co-localize at the cortex with a Pearson correlation coefficient reaching ~ 0.92 to 0.98. The measurements covered the area that starts from the oocyte membrane to 1 µm deep inward (Figure 4.1A-C and D-F). The same observation applies for any combination of two from the following proteins KHDC3L, OOEP, and TLE6 (Figure 4.2A-F and data not shown). We also detected NLRP7, KHDC3L, OOEP and TLE6 around the oocytes' nuclei after increasing the intensity of the signals at these regions (Figure 4.1A-B, 4.2.A-B and D-E, 4.7B and E). To validate our observations, we then performed ultrastructure analysis by transmission electron microscopy using the Tecnai 12 TEM, which provides a resolution significantly higher than that of the LSM 880 confocal microscopy. Immunostaining with KHDC3L antibody alone demonstrated the presence of KHDC3L immunogold particles to the oocyte cytoskeletal structures (Figure 4.3A-C) and which were more abundant at the cortex than the center of the oocyte ($p=0.043$). Double labeling using a combination of antibodies targeting NLRP7, KHDC3L or OOEP confirmed the co-localization of the three proteins NLRP7, KHDC3L, and OOEP to the same cytoskeletal structures (Figure 4.4A-C). Altogether our data demonstrate that NLRP7, KHDC3L, OOEP, and TLE6 are part of the same human maternal complex revealed by confocal and/or electron microscopies.

NLRP7 distribution depends on alpha tubulin network in the oocyte

We previously showed that NLRP7 and KHDC3L do not overlap exactly with alpha tubulin network or display similar localization pattern by confocal microscopy (Akoury et al., 2015b). Ultrastructure analysis by transmission electron microscopy after immunolabeling using NLRP7 or KHDC3L with alpha tubulin revealed that both proteins indeed do not co-localize, although they appear to be very close at the cortical region (Figure 4.5A and B). To investigate whether NLRP7 distribution depends on alpha tubulin network, we incubated human oocytes with nocodazole 20 µm, a microtubule disrupting drug, for 1 hour at 37°C before fixation and immunofluorescence. This treatment drastically altered the microtubule network which became disorganized and dispersed both at the cortex and in the center of the oocytes and also affected NLRP7 signal which became more diluted at the cortex and infiltrated towards the cytoplasm of the oocytes (Figure 4.6A-F). We then measured the intensity of the NLRP7 signal in oocytes (z=50 µm ±5 µm) in the region covering the area that starts from the oocyte membrane to 1 µm deep inward, from three different experiments. We found that the intensity of NLRP7 signal in the cortical region is decreased by 30% in the treated as compared to the untreated oocytes ($p=0.009$) (Figure 4.6G). This observation demonstrates that NLRP7 distribution in oocytes depends on alpha tubulin cytoskeleton.

NLRP7 distribution depends on filamentous actin network in the oocyte

We then checked whether NLRP7 co-localizes with filamentous actin, another major component of the oocyte cytoskeleton. Towards this goal, we incubated human oocytes with NLRP7 and Alexa Fluor® 568-phalloidin. Phalloidin is a product isolated from the death cap mushroom (*Amanita phalloides*) that binds and stabilizes F-actin. When phalloidin is conjugated to fluorophores, it serves to visualize F-actin. Following immunofluorescence, we found that NLRP7 and F-actin overlapped all over the oocyte and at the cortex; however, both proteins did not reveal similar patterns. While NLRP7 stained some cytoskeletal structures that were more abundant at the cortex, F-actin was evenly distributed in the cytoplasm and displayed a filamentous network that was not observed with NLRP7 (Figure 4.7A-C). The same observation was obtained following double labeling of F-actin with KHDC3L, OOEP, or TLE6

(Supplemental Figure 4.2A-F and data not shown). In order to check whether NLRP7 distribution depends on F-actin network, we incubated human oocytes with cytochalasin D, a potent inhibitor of actin polymerization for 1 hour at 37°C before fixation and immunofluorescence. Upon treatment, both F-actin and NLRP7 signals were affected. While F-actin detached from the cortex and aggregated towards the middle of the oocyte, NLRP7 became more diffused at the cortex and extended toward the cytoplasm (Figure 4.7D-F). We then measured the intensity of the NLRP7 signal on oocytes (z=50 μm ±5 μm) in the region covering the area that starts from the oocyte membrane to 1 μm deep inward, from three different experiments, before and after treatment. The analysis revealed that the intensity of NLRP7 signal in the cortical region is decreased by 23% in the treated oocytes compared to untreated oocytes p=0.0045 (Figure 4.7G). Altogether, these observations demonstrate that NLRP7 distribution in oocytes depends on the F-actin cytoskeleton.

4.5 DISCUSSION

In this study, using high resolution confocal and electron microscopies, we report the co-localization of NLRP7 with KHDC3L, OOEP, and TLE6 to the cytoskeletal structures also termed cytoplasmic lattices or the human subcortical maternal complex that are similar to the one characterized in mouse oocytes. These observations indicate that the human SCMC consists of at least NLRP7, KHDC3L, NLRP5, OOEP and TLE6, but do not demonstrate an interaction between NLRP7 and any founding member of the human SCMC. One could envision that NLRP7 and the other SCMC members play an important role in these structures perhaps in their organization or assembly in human oocytes. This hypothesis is corroborated by the fact that *Nlrp5* and *Padi6* are required for CPLs formation in mouse oocytes (Esposito et al., 2007; Kim et al., 2010). We previously documented that NLRP7 does not show a similar localization pattern or overlap exactly with alpha tubulin in human oocytes by confocal microscopy (Akoury et al., 2015b). Electron microscopy confirmed this observation but revealed that NLRP7 particles are relatively close to alpha tubulin at the oocyte cortex suggesting that the distribution of this maternal-effect protein could depend on alpha tubulin networks. Treating oocytes with nocodazole affected not only alpha tubulin but also NLRP7 whose signal decreased significantly at the cortex. In order to further characterize the nature of the structures to which NLRP7 binds, we performed double labeling of NLRP7 with F-actin/phalloidin in human oocytes. Our investigation revealed that these structures overlapped with F-actin network all over the oocyte. Treating oocytes with cytochalasin D disrupted both F-actin network and NLRP7 all over the oocyte. We could not check whether the same observations apply for KHDC3L or other members of the SCMC following any treatment due to unavailability of the materials. Nonetheless, altogether these observations indicate that NLRP7 distribution in the oocytes depends on the cytoskeleton of alpha tubulin and F-actin. This suggests that NLRP7 may play a role perhaps in the integrity of the microtubules and actin cytoskeletons in human oocytes and embryos. This suggestion is in line with data on other maternal-effect genes such as a) *Filia*, whose depletion in mice results in a defective spindle assembly and leads to higher rate of aneuploidy in cleavage-stage embryos (Zheng and Dean, 2009), b) *Padi6* whose knockout in GV oocytes affects the stability of cytoplasmic microtubules and consequently leads to altered mitochondria and endoplasmic reticulum positioning and redistribution during oocyte maturation (Kan et al., 2011), c) *Tle6*, whose absence in mouse leads to the formation of embryos with

abnormal spindle formation and positioning due to altered F-actin dynamics (Yu et al., 2014), and d) *Nlrp5* whose knockout in mice reduces the amount of non-microtubule tubulin and consequently affects organelles positioning in oocytes (Kim et al., 2014). In conclusion, our study is the first to provide a high resolution characterization of the four SCMC proteins, NLRP7, KHDC3L, OOEP and TLE6 in human oocytes and explore their association with the alpha tubulin and F-actin networks of human oocytes.

4.6 ACKNOWLEDGMENTS

We thank the patients for their participation. We also thank Dr. Min Fu, Dr. Isabelle Fernandez and Jeannie Mui for technical assistance. We would like also to thank Dr. Li Zhang and Xiao Yun Zhang for collecting the spare human oocytes from the patients. We acknowledge the use of the Facility for Electron Microscopy Research (FEMR) and the Facility for Molecular Imaging of the McGill University Health Centre Research Institute.

4.7 FIGURES

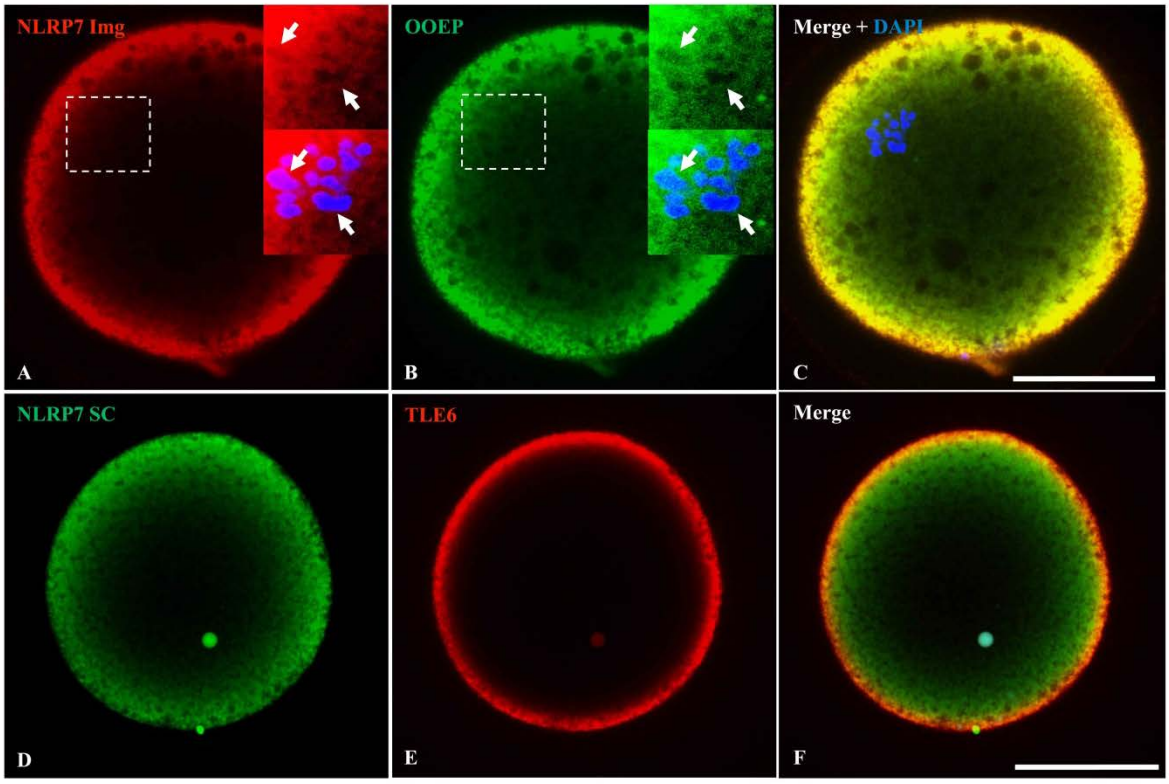

Figure 4.1. <u>NLRP7 co-localizes with OOEP and TLE6 at the cortex of human oocytes using confocal microscopy</u>
High resolution confocal microscopy images (section thickness=1 μm) showing the co-localization at the cortical region of NLRP7 (Imgenex, red) with OOEP (green) in a metaphase II oocyte (A-C) and NLRP7 (Santa Cruz, green) with TLE6 (red) in a metaphase I oocyte (D-F). DAPI (blue) stains the nucleus of the oocyte. Insets represent high magnification of the dashed squares. DNA localization (marked by arrows) in insets of A and B are stained by DAPI and surrounded by the analyzed protein. Bars, 50 μm.

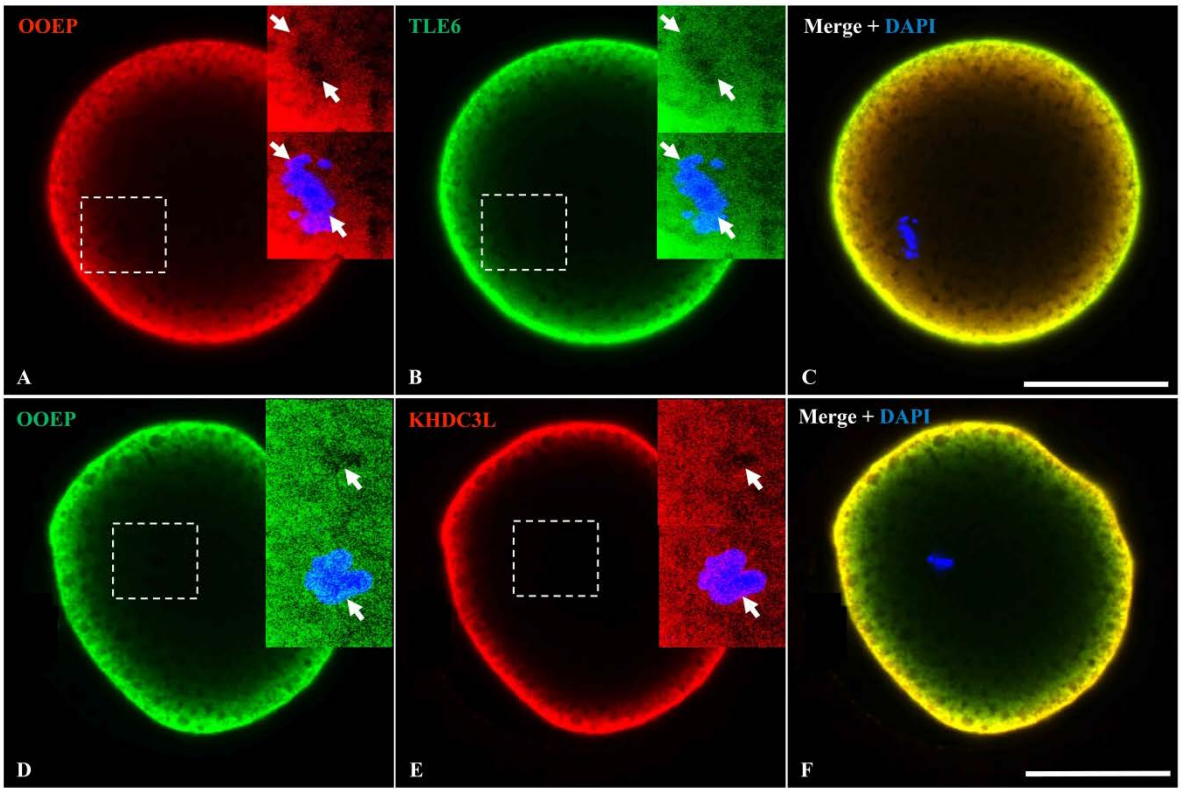

Figure 4.2. <u>OOEP co-localizes with KHDC3L and TLE6 at the cortex of human oocytes using confocal microscopy</u>

High resolution confocal microscopy image (section thickness=1 µm) showing the co-localization at the cortical region of OOEP (red) with TLE6 (green) in a metaphase I oocyte (A-C) and OOEP (green) with KHDC3L (red) in a metaphase II oocyte (D-F). DAPI (blue) stains the nuclei of oocytes. Insets represent high magnification of the dashed squares. DNA localization (marked by arrows) in insets of A, B, D, and E are stained by DAPI and surrounded by the analyzed protein. Bars, 50 µm.

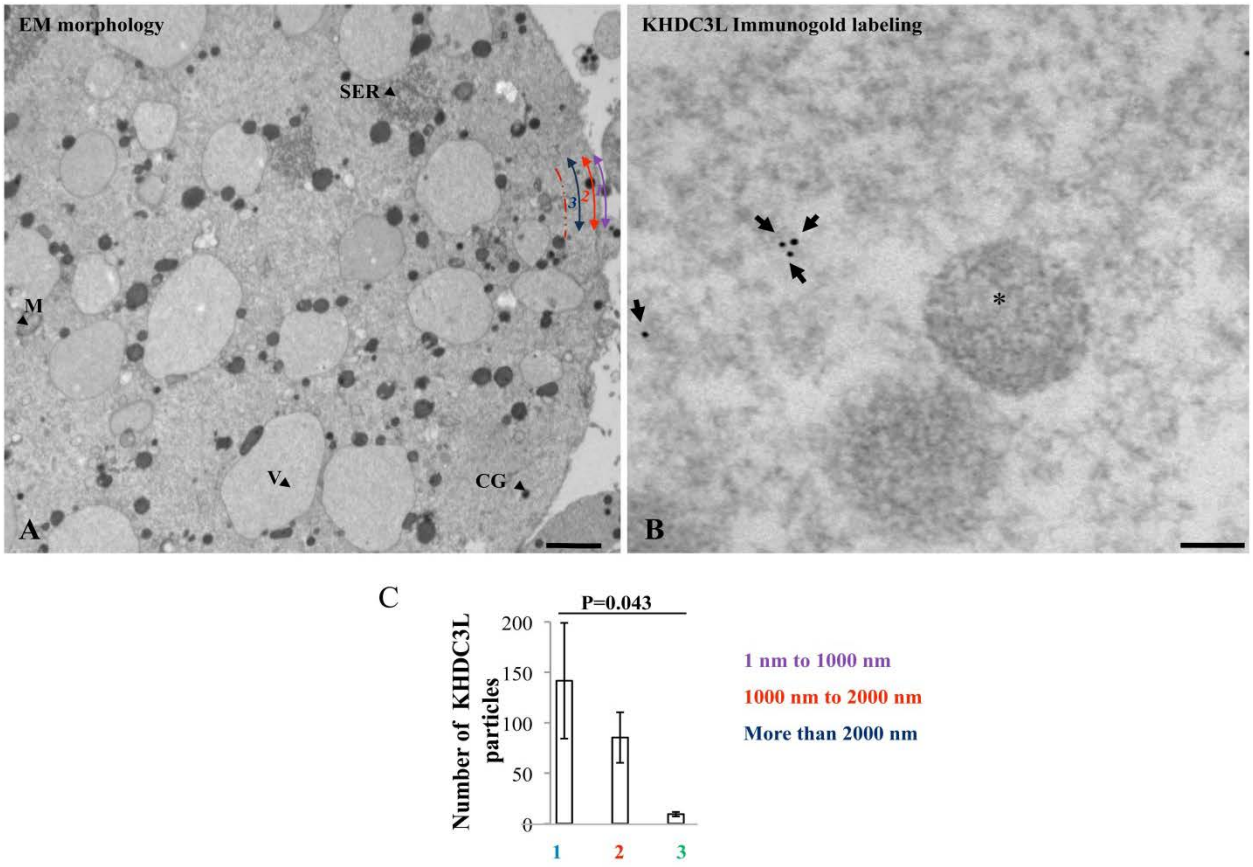

Figure 4.3. <u>KHDC3L subcellular localization by electron microscopy in a metaphase II human oocyte</u>

(A) Electron microscopy photo showing the morphology of a human oocyte and its different organelles, cortical granules (CG), smooth endoplasmic reticulum (SER), mitochondria (M), and vacuoles (V) at low magnification. Bar, 2 µm. (B) KHDC3L immunogold particles (12 nm black dots) are found outside cortical granules (black asterisks) and organelles and are bound to the oocyte cytoskeletal structures (black arrows). Bar, 100 nm. (C) Histogram representing the averages and standard errors of the means (SEM) of the number of immunogold particles in each of the three different regions (indicated by double-headed arrows in A) from three different sections (section thickness=95 nm) of a metaphase II oocyte.

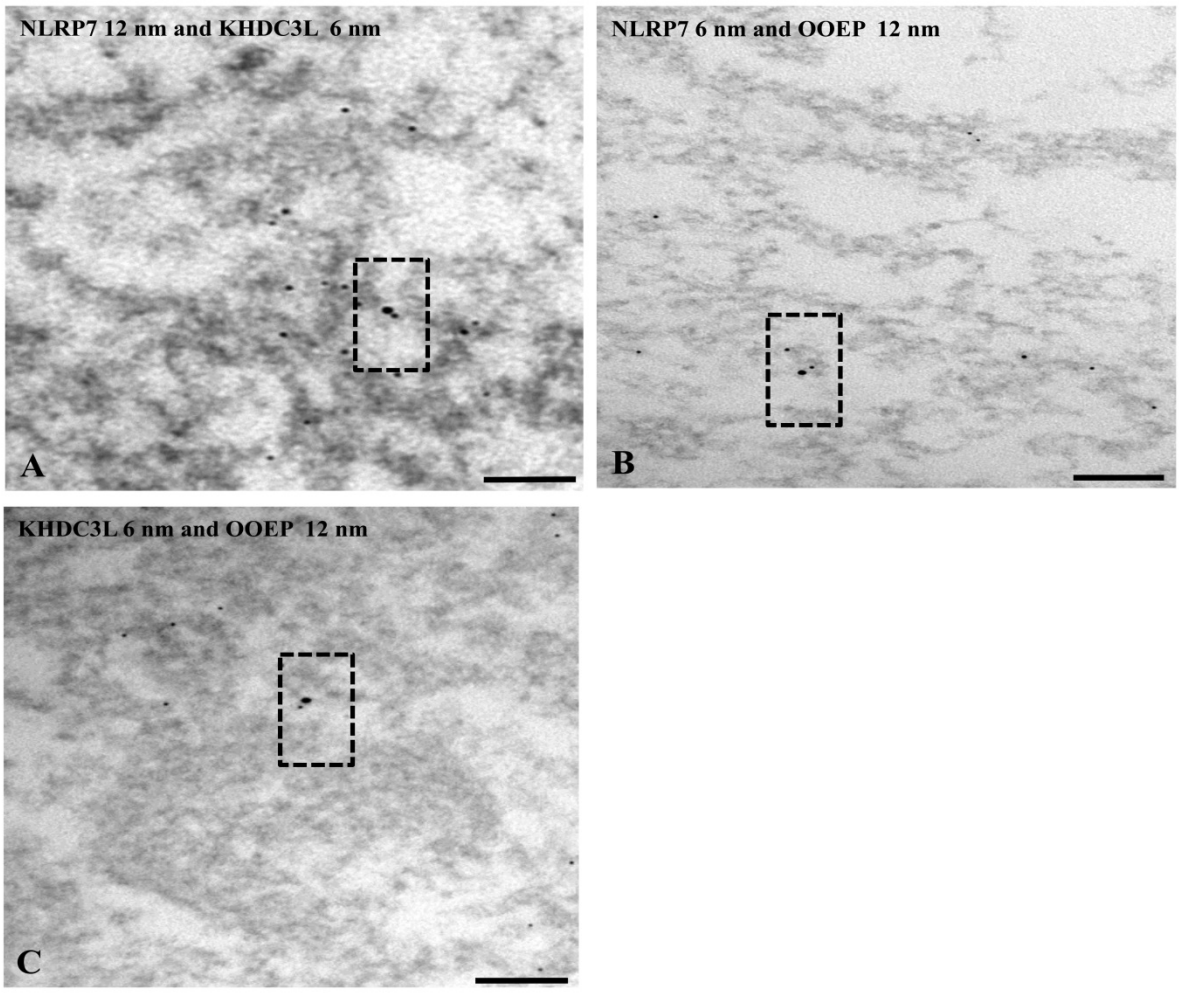

Figure 4.4. <u>NLRP7, KHDC3L and OOEP co-localize to the same cytoskeletal structures at the cortex of metaphase II oocyte by electron microscopy</u>
Co-localization of (A) NLRP7 12 nm (Santa Cruz) and KHDC3L 6 nm, (B) NLRP7 6 nm (Imgenex) and OOEP 12 nm, and (C) KHDC3L 6 nm and OOEP 12 nm. Bars, 100 nm.

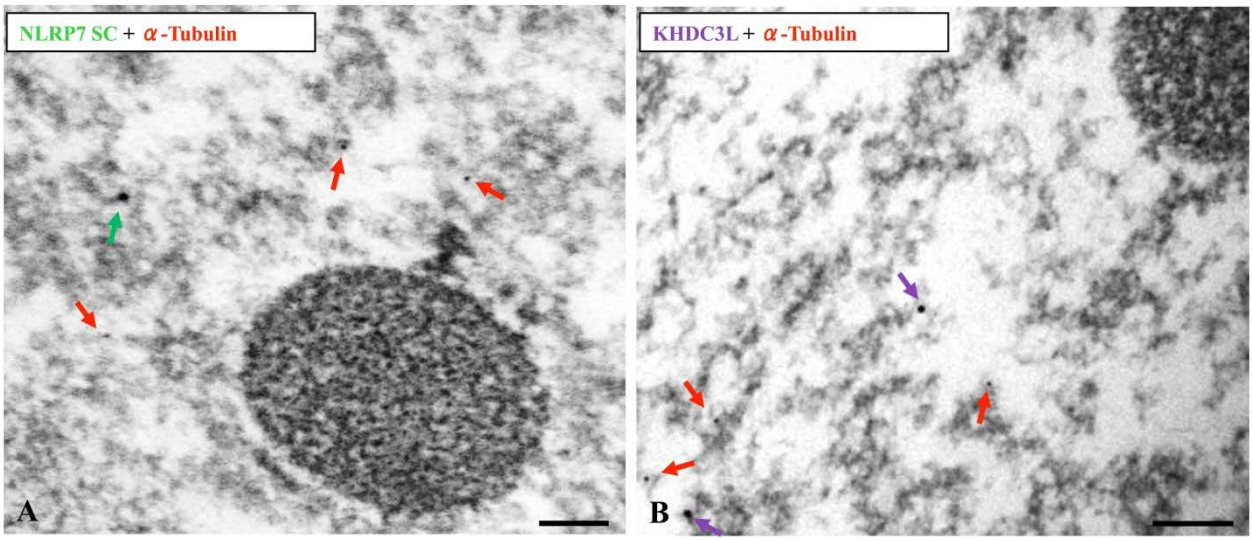

Figure 4.5. NLRP7 12 nm (Santa Cruz, green arrow) and KHDC3L 12 nm (magenta arrows) do not overlap exactly with α-Tubulin 6 nm (red arrows) at the cortex of a metaphase II oocyte by electron microscopy. Bars, 100 nm.

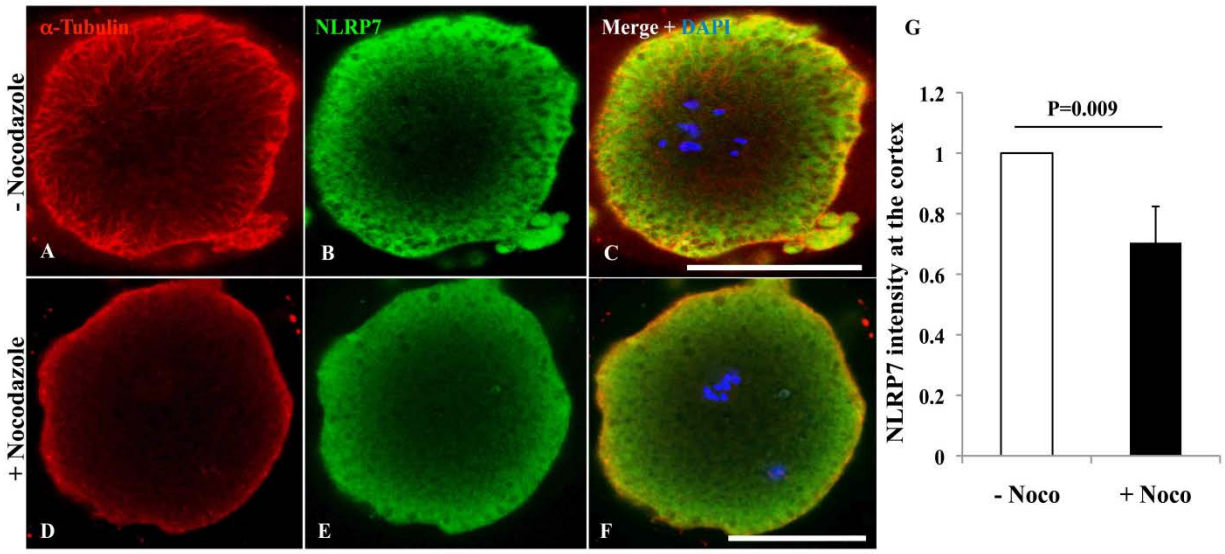

Figure 4.6. <u>Nocodazole treatment changes NLRP7 distribution in metaphase II oocytes</u>
(A-F) NLRP7 is in green (Santa Cruz) and alpha tubulin in red. DAPI (blue) stains the nuclei and the polar body of oocytes. Bars, 50 µm. (G) Histogram representing NLRP7 intensity which refers to the ratio of NLRP7 signal at the cortex in nocodazole-treated over untreated oocytes. The averages and standard deviations were calculated on at least two oocytes for each condition from three independent experiments. In each experiment, the oocytes were from the same patient and at the same stage.

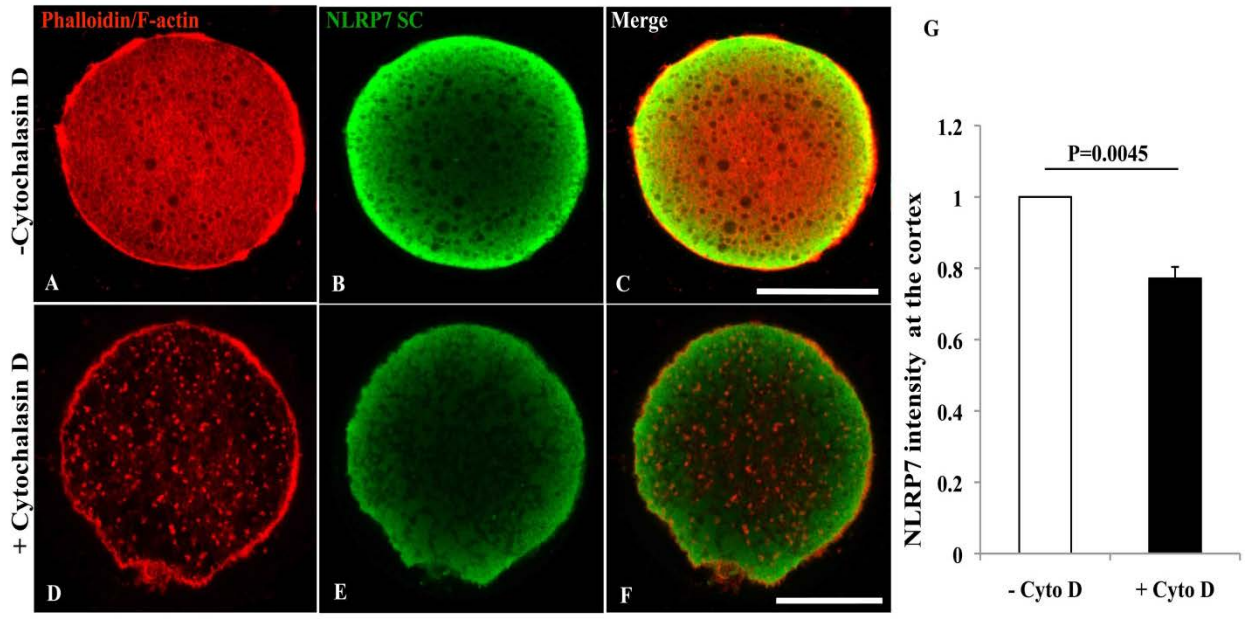

Figure 4.7. <u>Cytochalasin D treatment changes NLRP7 distribution in metaphase II oocytes</u>
(A-F) NLRP7 (Santa Cruz, green) and Phalloidin (F-actin, red). Bars, 50 µm. (G) Histogram representing NLRP7 intensity which refers to the ratio of NLRP7 signal at the cortex in cytochalasin D-treated over untreated oocytes. The averages and standard deviations were calculated on at least two oocytes for each condition from three independent experiments. In each experiment, the oocytes were from the same patient and at the same stage.

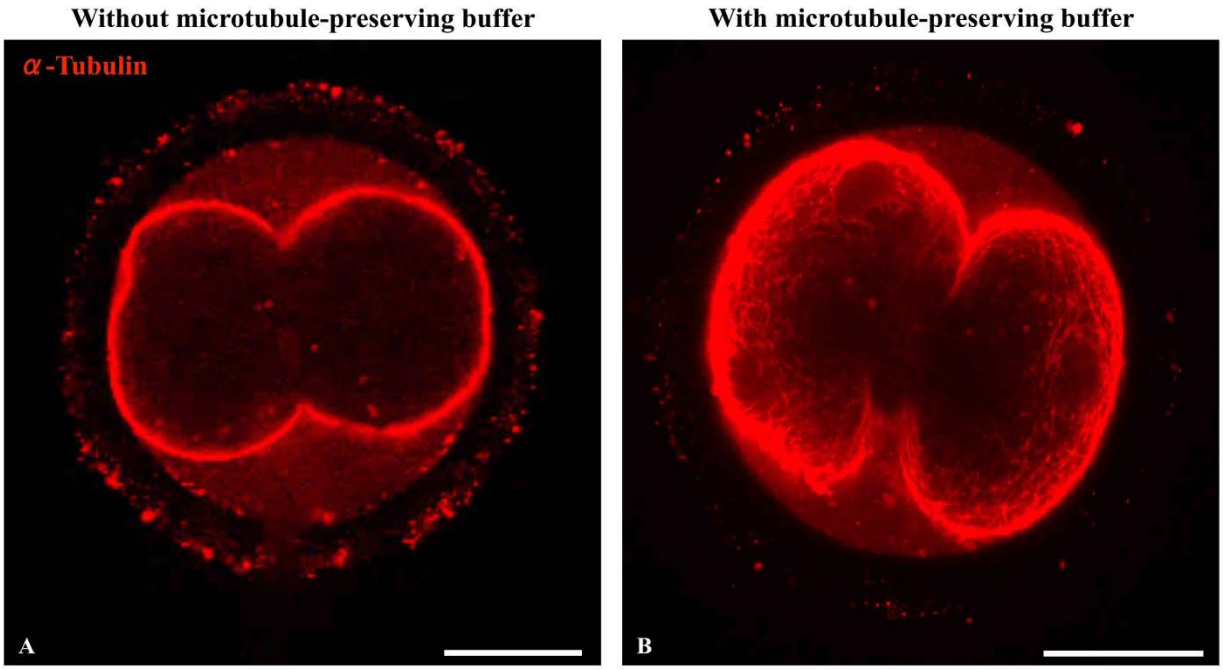

Supplemental Figure 4.1. α-Tubulin (red) distribution in a 2-cell embryo without (A) and with (B) the preservation of microtubules and proteins using confocal microscopy (section thickness=1 μm). Bars, 50 μm.

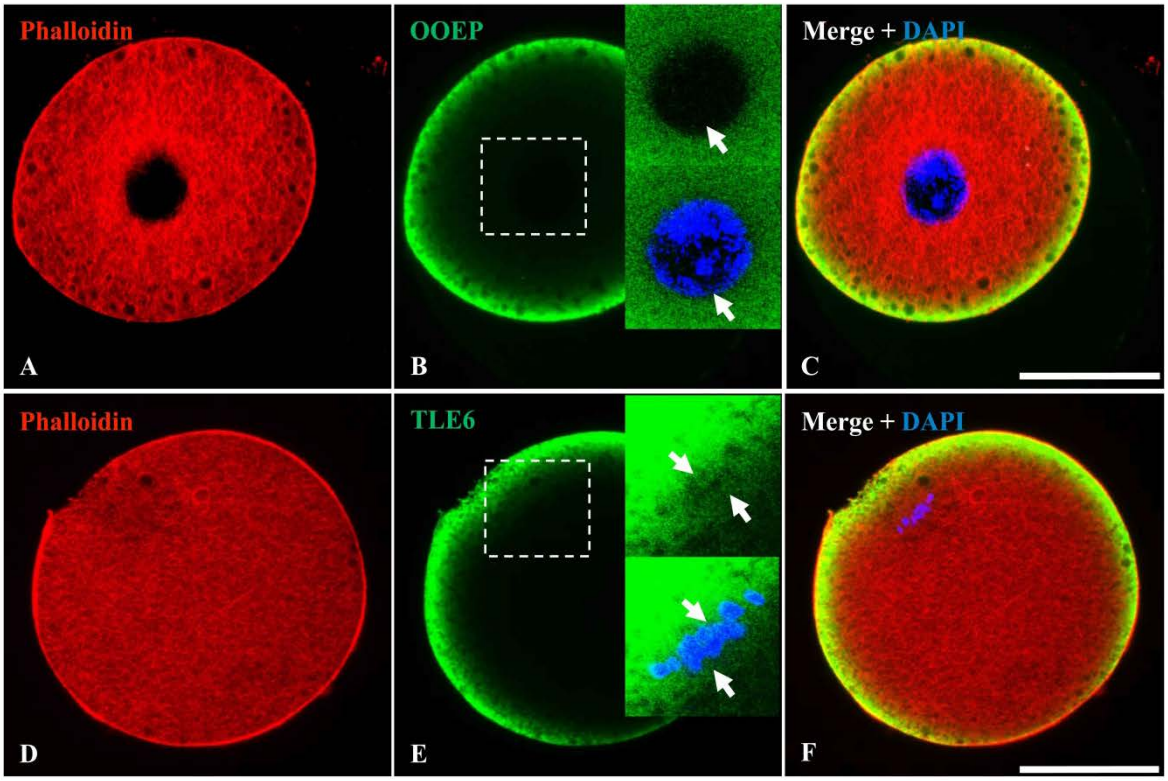

Supplemental Figure 4.2. <u>Distribution of Phalloidin (F-actin) with OOEP (green, A-C) and TLE6 (green, D-F) in metaphase II oocytes</u>
DAPI (blue) stains the nuclei of oocytes. Insets represent high magnification of the dashed squares. DNA localization (marked by arrows) in insets of A and E are stained by DAPI and surrounded by the analyzed protein. Bars, 50 μm.

4.8 TABLES

N-A

4.9 APPENDIX

N-A

PREFACE TO CHAPTER 5

In Chapter 4, I showed that NLRP7 co-localizes with KHDC3L, OOEP and TLE6, three components of the mouse and the human subcortical maternal cytoskeleton complex (SCMC), to the oocyte cytoskeletal structures. Additionally, I demonstrated that the SCMC depends, directly or indirectly, on alpha tubulin and F-actin cytoskeletal networks in human oocytes. These data suggest that *NLRP7* mutations could affect the microtubules and actin cytoskeleton and result in a defective oocyte and consequently lead to the manifestation of HM. The hypothesis of a defective oocyte is in line with a previous report documenting that the primary role of *NLRP7* lies within the oocyte and that ovum donation from unaffected women rescues the defects in patients with RHMs and allows the occurrence of successful pregnancies. In Chapter 5, we support this previous observation by reporting the occurrence of three additional live births from donated ova to two patients with two *NLRP7* mutations. Additionally, we reviewed the reproductive outcome and mutations of all reported patients with two *NLRP7* mutations either in homozygous or compound heterozygous state with the goal of investigating a possible correlation between the nature of *NLRP7* mutations in the patients and the exceptional occurrence of live births.

.

CHAPTER 5

LIVE BIRTHS IN WOMEN WITH RECURRENT HYDATIDIFORM MOLE AND TWO *NLRP7* MUTATIONS

Elie Akoury[1,2], Neerja Gupta[3], Rashmi Bagga[4], Stephen Brown[5], Christine Déry[1,2], Madhulika Kabra[3], Radhika Srinivasan[6], Rima Slim[1,2]

[1]Department of Human Genetics, McGill University Health Centre Research Institute, Glen site Montreal, H4A 3J1, Canada.
[2]Department of Obstetrics and Gynecology, McGill University Health Centre Research Institute, Glen site, Montreal, H4A 3J1, Canada.
[3]Genetic Unit, Department of Pediatrics, All India Institute of Medical Sciences in New Delhi (AIIMS), New Delhi, 110029, India.
[4]Department of Obstetrics and Gynecology, Post Graduate Institute of Medical Education and Research, PGIMER, Chandigarh-160012, India.
[5]Department of Obstetrics and Gynecology, University of Vermont, Given 263, 89 Beaumont Ave., Burlington, VT, 05405, USA.
[6]Cytology and Gynecological Pathology, Post Graduate Institute of Medical Education and Research, PGIMER, Chandigarh-160012, India.

Manuscript published in Reproductive Biomedicine online, April 16, 2015 (PMID: 25982095).

5.1 ABSTRACT

Hydatidiform mole (HM) is an aberrant human pregnancy with abnormal embryonic development and excessive proliferation of the trophoblast. Recessive mutations in *NLRP7* are responsible for recurrent HMs (RHMs). Women with recessive *NLRP7* mutations fail to have normal pregnancies from spontaneous conceptions with the exception of three out of 131 reported patients. Because there is no treatment for RHMs and maternal-effect genes are needed in the oocytes to sustain normal embryonic development until the activation of the embryonic genome, one patient with recessive *NLRP7* mutations tried ovum donation and achieved a successful pregnancy. This study reports three additional live births from donated ova to two patients with recessive *NLRP7* mutations. The occurrence of two live births from spontaneous conceptions to two other patients is also reported. The reproductive outcomes and mutations of all reported patients were reviewed and it was found that live births are associated with some missense mutations expected to have mild functional consequences on the protein. The data support a previous observation that ovum donation appears as the best management option for these patients to achieve normal pregnancies and provide an explanation for the rare occurrence of live births from natural spontaneous conceptions in patients with two *NLRP7* mutations.

5.2 INTRODUCTION

Hydatidiform mole (HM) is an aberrant human pregnancy characterized by abnormal embryonic development and hyperproliferation of the trophoblast. HM affects 1 in every 600 to 1000 pregnancies in western countries and most of them are not recurrent (Grimes, 1984; Savage et al., 2010). Recurrence of moles affects 1 to 9% of patients with a prior mole (Berkowitz et al., 1998; Boufettal et al., 2011; Horn et al., 2006; Kim et al., 1998; Kronfol et al., 1969; Sebire et al., 2003a) and few of these patients have a family history of moles [For reviews see (Fisher et al., 2004; Slim and Mehio, 2007)]. Two maternal-effect genes responsible for recurrent hydatidiform moles (RHMs), *NLRP7* and *KHDC3L*, have been identified (Murdoch et al., 2006; Parry et al., 2011). *NLRP7* encodes for a nucleotide oligomerization domain-like receptor pyrin containing protein 7 and is mutated in 48 to 80% of patients with RHMs (Estrada et al., 2013; Hayward et al., 2009; Qian et al., 2011; Sebire et al., 2013; Slim et al., 2009). *KHDC3L* encodes for a KH domain containing 3-like, a member of the subcortical maternal protein complex and is mutated in 10 to 14% of *NLRP7*-negative patients (Parry et al., 2011; Reddy et al., 2013).

To date, all reported women with RHMs and two defective alleles in either of the two known genes failed to have live births from spontaneous conceptions, with the exception of three patients with *NLRP7* mutations, two cousins from one family (MoLb1) (Moglabey et al., 1999) with a homozygous splice mutation, c.352+1G>A, p.G118Dfs*2 that leads to the inclusion of 4-bp of intron 3 in the mRNA and consequently creates a premature stop codon two amino acids after exon 3 (Murdoch et al., 2006), and a recently reported patient with a homozygous missense mutation, c.2248C>G, p.Leu750Val (Mahadevan et al., 2013). Three patients with two defective alleles in *NLRP7* have so far tried ovum donation (Deveault et al., 2009; Sensi et al., 2000) and only one successful pregnancy leading to a live birth has been reported (Fisher et al., 2011).

The study reports the occurrence of five live births, three from donated ova and two from spontaneous conceptions, in four patients with two *NLRP7* defective alleles.

5.3 MATERIALS AND METHODS

NLRP7 mutation analysis

This study was approved by the Institutional Review Board of the McGill University, (reference: A01-M07-03A) on 24 January 2003 and is renewed every year. Mutation analysis was performed as previously described by polymerase chain reaction (PCR) amplification of genomic DNA of the 11 exons of *NLRP7* followed by DNA sequencing in the two directions (Murdoch et al., 2006). Sequences were analyzed using DNASTAR. DNA mutations are numbered according to cDNA sequence reference NM_001127255 and UniProt reference sequences Q8WX94 for *NLRP7* (Murdoch et al., 2006).

DNA cloning and phase establishment

For patients with compound heterozygous mutations, the phase was established based on the analysis of other family members with the exception of patient 678 with one live birth and for whom no other family members were available for analysis. For this patient, the following PCR primers, N7Ex5-9ChF1: 5'-GAACTGGGCTCGGCAGGATCTTCGCTCTC and N7Ex5-9ChR1: 5'-AAACCAGCCCGGGAAAGATGACAAGACCTC, were designed to amplify a 7955-bp genomic DNA fragment that encompasses her two mutations, R693P and N913S. The 7955-bp PCR fragment was cloned into the pCR4-TOPO vector and DNA from five insert-containing vectors were sequenced and analyzed.

5.4 RESULTS

Three live births from donated ova in two patients with recessive *NLRP7* mutations

Patient 628 is of Indian origin. She presented at the age of 26 years with a history of four hydatidiform moles, of which one gave a gestational trophoblastic neoplasia (GTN). Because she had RHMs, this patient was referred to our laboratory for mutation analysis in *NLRP7,* which revealed that she is compound heterozygous for two founder mutations c.2078G>C, p.Arg693Pro, and c.2738A>G, p.Asn913Ser, in the Indian population (Slim et al., 2009). After genetic counselling and based on her own desire to have children, the patient sought assisted reproductive technologies, received a donated ovum from an unrelated woman, and had a normal singleton pregnancy that led to a normal live birth of a boy delivered by Caesarean section. The boy is now 5.2 years old and in good health.

Patient 748 is also of Indian origin. She presented at the age of 27 years with a history of three HMs. *NLRP7* mutation analysis revealed that she is homozygous for a missense mutation, c.2078G>C, p.Arg693Pro**.** After genetic counselling, the patient decided to attempt assisted reproductive technologies with donated ova and *in vitro* fertilization in the hope of achieving a normal pregnancy. Three embryos were transferred and resulted originally in a triplet pregnancy, of which one was spontaneously lost in the first trimester, and the pregnancy continued with two male embryos. The patient delivered two healthy boys at term by Caesarean section. The twins are now about 4 years old and in good health.

Two live births from spontaneous conceptions in two patients with recessive *NLRP7* mutations

Patient 1077 is a 24-year-old woman of European and Afro-Caribbean origin. She had a history of three pregnancy losses that consisted of one complete mole which developed into GTN, one partial mole with an embryo and fetal crown rump length compatible with a gestational age of 7 weeks, and another molar pregnancy with a non-viable embryo. The patient was referred to our laboratory for *NLRP7* mutation analysis and was found to carry a previously described missense mutation, c.2738A>G, p.Asn913Ser (N913S), in a homozygous state and this patient was previously described (Brown et al., 2013). Eight months later, the patient had a

spontaneous natural conception. At 39.5 weeks of gestation, she delivered a healthy boy (APGAR score 9/9) weighing at birth 3487 grams, who is now 1 year old and in good health. Histopathological evaluation of the placenta did not reveal any abnormalities.

Patient 678 is of Indian origin. She presented at the age of 30 years with a history of three pregnancy losses that consisted of a blighted ovum followed by two HMs that developed into GTNs. *NLRP7* mutation analysis revealed that the patient has two mutations, c.2078G>C, p.Arg693Pro, and c.2738A>G, p.Asn913Ser, and this patient was previously described (Slim et al., 2009). Three years later, the patient had a live birth from a spontaneous conception.
During the pregnancy that led to the live birth, the patient was on anti-epileptic medication, but the pregnancy was uncomplicated. At 37.5 weeks of gestation, the patient had pre-labour rupture of membranes and the foetus was in transverse position. She underwent an emergency Caesarean section and delivered a baby boy, who is currently healthy, attends nursery school, and has normal growth and development. The placenta of the live birth was normal with no histopathological abnormalities. Because her two mutations have been shown to be frequent in the Indian population (Slim et al., 2009) and to exclude their coincidental presence by chance on the same parental chromosome, a large genomic DNA fragment from the patient's DNA encompassing her two mutations was PCR-amplified, cloned and sequenced. Sequence analysis of five clones demonstrated the presence of N913S in all of them and none had the other mutation, R693P. Also, comparing the polymorphic variations observed in DNA in this patient, after direct PCR amplification of genomic DNA, and those observed in the clones showed the transmission of p.N913S, c.2738A>G, on the reference haplotype, NM_001127255.1:c.[2682T>C (rs269951); 2738A>G (rs104895503); 2775A>G (rs269950); 2810+98C>T (rs269949); 2810+123G>A (rs647845); 2810+126T>C (rs647844)] with the following alleles [T;G;A;C;G;T], which is identical to the previously reported haplotype carrying N913S (Slim et al., 2009). Therefore, these data demonstrate the presence of the two mutations in patient 678 on different parental chromosomes.

5.5 DISCUSSION

To date and including this report, three patients with two *NLRP7* defective alleles had a total of four live births from donated ova. The first case was previously described (Fisher et al., 2011) and three are included in this report. The occurrence of three live births from donated ova in two additional patients confirms the idea that the primary role of *NLRP7* in the pathology of RHM lies in the oocyte and that ovum donation from unaffected individuals rescued the defects of these patients and allowed them to have successful pregnancies. Because, it is not known how many patients with two *NLRP7* defective alleles have tried ovum donation, it is impossible to provide the frequency of live births with donated ova. However, given the complexity and high cost of such procedure, we believe that few patients with two defective alleles in *NLRP7* have tried donated ova.

So far, including the patients described in this report, there have been 48 distinct mutations reported (Figure 5.1), of which 17 missense and 31 leading to premature protein truncation (nonsense, splicing, small/gross deletion or insertion and complexe rearrangement) in a total of 131 patients with two defective alleles in *NLRP7* (Milhavet et al., 2008). Among these patients, five (3.8%) had six live births from spontaneous conceptions (Figure 5.1, Table 5.1) in a total of 612 pregnancies (Helwani et al., 1999; Mahadevan et al., 2013; Sunde et al., 1993). Therefore, patients with two defective alleles in *NLRP7* may have live births from spontaneous conceptions from their own oocytes in 1% of their pregnancies. Two of the patients with live births have a homozygous invariant splice mutation, c.352+1G>A, that affects the splicing of the main *NLRP7* isoform and results in the insertion of four bases between exons 3 and 4 and is expected to lead to a frameshift and premature protein truncation two amino acids after exon 3 (p.Gly118Aspfs*2). However, this mutation leaves another minor isoform without exon 3 intact (Figure 5.1) (Murdoch et al., 2006). The remaining three patients have one or two of the following missense mutations, p.Leu750Val (Mahadevan et al., 2013), p.Arg693Pro, and p.Asn913Ser, either in homozygous (Brown et al., 2013) or compound heterozygous state (Slim et al., 2009) (Figure 5.1).

The exact role of *NLRP7* in the pathology of molar pregnancies is not fully understood, but available data implicate its protein in inflammatory response (Khare et al., 2012; Kinoshita et al., 2005; Messaed et al., 2011a) and trophoblastic lineage differentiation (Mahadevan et al., 2014). This latter role is in agreement with a recent study from our laboratory demonstrating that

protein-truncating mutations, which are expected to have severe functional consequences on the protein, are associated with the absence of embryonic tissues in the conceptions of these patients while missense mutations, which are expected to have milder functional consequences on the protein, are associated with the differentiation of some embryonic tissues (Nguyen et al., 2014).

Similarly, three of the six live births observed in patients with two *NLRP7* defective alleles occurred in patients with missense mutations and the remaining three in patients with the splice mutation, c.352+1G>A, that leaves a minor isoform intact, which may have compensated for the loss of the other isoforms and attenuated the functional impact of the mutation. The same applies to one early neonatal death, six stillbirths, and five molar pregnancies with well-formed fetuses that occurred either in the same patients who had the live births or in other patients with only missense mutations (Figure 5.1).

In summary, the data corroborate a previous observation on the benefit of ovum donation to overcome the defects of these patients and provide an explanation of the possible, but very rare, occurrence of live births from spontaneous conceptions in patients with two *NLRP7* defective alleles. Based on this study's observations and data described by various groups that are recapitulated in this report, we believe that perhaps a more optimistic genetic counselling can be provided to patients with two defective alleles in *NLRP7* by explaining to them the following: first, ovum donation is the best management option for patients with two defective alleles in *NLRP7* who desire to have children based on three patients, of which two are included in this report; second, exceptionally, some of these patients may have live births from their own oocytes and this seems to be associated with some missense mutations. The most important advice to patients is the necessity of close follow-up and monitoring in the event of future pregnancies to prevent eventual complications of moles and the occurrence of stillbirths among their rare conceptions that may rarely reach term.

5.6 ACKNOWLEDGEMENTS

We thank the patients and their families for their cooperation. This study was supported by grants from the Canadian Institute of Health Research to RS (MOP-86546 and POP-122897). The funding agency had no involvement in the study design; the collection, analysis and interpretation of data, in the writing of the report; and in the decision to submit the article for publication.

5.7 FIGURES

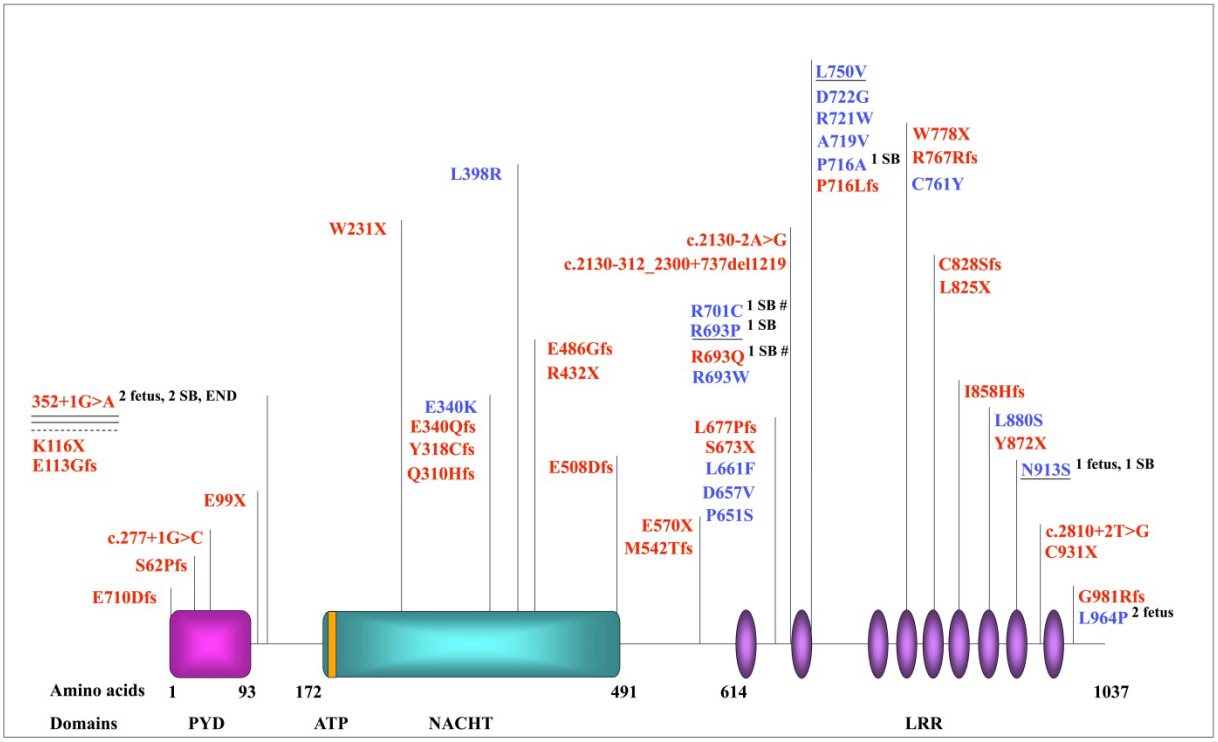

Figure 5.1. **A schematic representation showing the distribution of all recessive *NLRP7* mutations observed in patients with RHMs and highlighting those that are associated with live births from spontaneous natural conceptions**

Only mutations reported in PubMed are shown. Missense mutations are in blue and mutations (nonsense, splicing, small/gross deletion or insertion and complex rearrangement) leading to premature protein truncation are in red. Mutations in patients who had live births are underlined. Each line corresponds to one normal live birth and the dashed line corresponds to a live birth with several abnormalities. #, refers to one still-birth that occurred in a patient who is compound heterozygous for the two indicated mutations. ATP = 5′-triphosphate binding motif; END = early neonatal death; LRR = leucine-rich repeats; NACHT = the domain found in NAIP, CIITA, HET-E, and TP1 family of proteins; PYD = pyrin domain; SB = stillbirth. The superscript number before the reproductive outcome (e.g. fetus, SB, etc.) indicates the number of pregnancies with such entity. For instance, "2 fetus" refers to two pregnancies each with a fetus.

5.8 TABLES

Table 5.1. Summary of the reproductive outcomes of patients with two *NLRP7* defective alleles and the nature of their mutations

Mutation type	Live birth	END	Stillbirth	HM+fetus	RL (HM+SA)	Total Pregnancies
Missense on both alleles	3	0	4	3	313	323
G118Dfs*2 on both alleles	3	1	2	2	24	32
At least one protein truncating[a]	0	0	0	0	257	257
Total	6	1	6	5	594	612

END = early neonatal death; HM = hydatidiform mole; RL = reproductive loss; SA = spontaneous abortion. [a]indicates protein truncating mutations with the exception of G118Dfs*2.

5.9 APPENDIX

N-A

CHAPTER 6

GENERAL DISCUSSION OF THE THESIS

Hydatidiform mole (HM) is a decidedly mystifying disease of ancient recognition that has fascinated and puzzled mankind from the earliest times. Although scientists from all around the world have been studying the pathology of HM for centuries, our knowledge about its formation is not yet fully understood. This thesis describes studies designed to further our understanding on the role of *NLRP7*, a maternal-effect gene, in the pathology of recurrent HM (RHM). Through a series of experiments described herein, we were able to provide more pieces to the puzzle of HM formation and enhance its understanding.

6.1 Defective immune response in patients with *NLRP7* mutations

The defective IL1B and TNF secretion observed in PBMCs from patients carrying *NLRP7* mutations in response to stimulation with LPS underscores the importance of NLRP7 in the inflammatory response of women suffering from RHMs. This impaired cytokine secretion was not expected in patients with *NLRP7* mutations because PBMCs from patients with Muckle-Wells syndrome carrying mutations in *NLRP3*, another member of the NLRP family, were shown to have an abnormal cytokine secretion but in the opposite direction to that observed in cells from patients with *NLRP7* mutations (Agostini et al., 2004; Jeru et al., 2010; Kastner et al., 2010; Loock et al., 2010). Indeed PBMCs, from patients with *NLRP3* mutations secrete higher amounts of IL1B and TNF in response to LPS stimulation when compared to controls. However, patients with *NLRP7* mutations suffering from RHMs are in good health (except that they are unable to conceive) and do not reveal any clinical signs of inflammation (fever, rash…) as opposed to patients with *NLRP3* mutations.

To understand the role of NLRP7 in cytokine secretion, specifically IL1B, in patients with RHMs, another member in the laboratory assessed the intracellular protein levels of pro- and mature IL1B in the same PBMCs from patients with *NLRP7* mutations or rare/low frequency variants that were shown to have low IL1B secretion. We sought to conduct such an

investigation because the same approach was used on macrophages isolated from patients with Muckle-Wells syndrome and demonstrated increased intracellular IL1B processing (Agostini et al., 2004). Interestingly, we found that PBMCs from patients with *NLRP7* mutations have normal to slightly higher amounts of intracellular pro-IL1B and normal mature IL1B suggesting that the synthesis and processing of IL1B are normal. However, we were unable to detect intracellular levels of TNF by western blot analysis due to low amounts of TNF present in hematopoietic cells. We believe that this defective cytokine secretion could be at the origin of the abnormal retention of HMs in patients with *NLRP7* mutations and which may reflect impaired/compromised innate immunity in these patients. This is indeed in line with what is observed in patients suffering from the common sporadic non-recurrent HMs, which are not associated with recessive *NLRP7* mutations. Several reports have documented that these patients have defective cellular mediated immunity in response to phytohemagglutinin and concanavalin A and display delayed skin hypersensistivity to dinitrochlorobenzene, purified protein derivatives and *Candida* antigens (Ho et al., 1980; Khanna et al., 1985; Tomoda et al., 1976). Altogether, these observations concur with the fact that a defective immune response is a crucial factor that contributes to the manifestation of not only RHMs, but also of common, non-recurrent HMs. Therefore, characterizing the mechanism by which *NLRP7* mutations lead to an impaired cytokine secretion and consequently an altered immune response in patients with RHMs would clarify the mechanisms responsible not only for the formation of RHMs but also those responsible for the common form of HM.

6.2 Microtubules' defect could be leading to low cytokines' secretion

To better understand the mechanism underlying the defective IL1B secretion, we first sought to characterize the subcellular localization of NLRP7 in control PBMCs and found that this protein localizes mainly to the MTOC and Golgi apparatus. It is well established that TNF and IL1B have different release mechanisms. The former follows the conventional endoplasmic reticulum-Golgi route of secretion (Halban and Irminger, 1994), whereas the latter is secreted through five different unconventional secretory pathways, of which one mechanism involves the lysosomes in the secretion of IL1B through exocytosis, a process primarily dependent on microtubules (Holt et al., 2006). This suggestion is in line with previous data indicating the requirement of a functional microtubule network for IL1B secretion in human monocytes (Carta et al., 2006). We therefore hypothesized that an altered microtubules structure affects the trafficking and consequently secretion of IL1B-containing vesicles to the extracellular milieu. We then disrupted microtubules by treating control EBV cells with nocodazole before immunofluorescence and labeling with NLRP7. Upon treatment, we found that the NLRP7 signal was fragmented and dispersed within the cytoplasm. This suggested that *NLRP7* signal distribution depends on microtubules. We also tried to look for any possible defect in the structure of microtubules in EBV-transformed lymphoblastoid cells from patients with *NLRP7* mutations using immunofluorescence and confocal microscopy but did not notice any significant difference between cells from patients and controls. We attributed this failure to two main points: first, lymphoblastoid cells have a small cytoplasm which makes it hard to visualize the cytoskeleton well; second, these cells grow in suspension and are then adhered to poly-lysine-treated microscopic slides before immunofluorescence, which affects the shape of the cells and preclude the visualization of well-preserved microtubules structure, making it difficult to detect differences in structure between patients with *NLRP7* mutations and control cells.

6.3 NLRP7 and KHDC3L share the same localization to MTOC and Golgi apparatus

After the identification of *KHDC3L*, the second gene responsible for RHMs, we checked the subcellular localization of its protein in hematopoietic cells. KHDC3L and NLRP7 are two proteins that belong to two different families with different roles (Amarasinghe et al., 2001; Tschopp et al., 2003). My investigation in Reddy et al. demonstrated that KHDC3L localizes with NLRP7 to the MTOC and the Golgi apparatus in EBV cells from control subjects (Reddy et al., 2013). These observations indicate that KHDC3L may also have a role in the intracellular trafficking and secretion of cytokines, similarly to NLRP7 in PBMCs from patients with RHMs. To address this point, we organized an experiment in Tunisia, the country of origin of one patient with a homozygous mutation in *KHDC3L* and I went there for three days, performed the stimulation on freshly isolated PBMCs from the patient, collected the supernatants and brought them back to our laboratory where I assessed IL1B and TNF. Unfortunately, the results were not conclusive due to a high amount of secreted IL1B before stimulation. We believe this is due to the quality of the reagents used in the cell culture. Collectively, these data emphasize the similarities between NLRP7 and KHDC3L in their subcellular localization and indicate that both genes may be responsible for the same mechanism leading to molar formation.

6.4 NLRP7 and KHDC3L localizes to the oocyte cytoskeletal structures

The presence of maternal-effect genes in mice has proven indispensable for early embryonic development. These genes are not supposed to affect ovulation or fertilization but their absence would lead to embryonic arrest mostly between 2-cell and morulae stages (Kim and Lee, 2014). While almost 40 maternal-effect genes have been characterized in mice, NLRP7 and *KHDC3L* were the first two maternal-effect genes to be identified in humans. Recently, variants in *NLRP5,* a maternal-effect gene*,* were found to be associated with reproduction loss and multilocus imprinting disorders in humans (Docherty et al., 2015) (Tables 1.2 and 1.3). The proteins of some of these murine genes are characterized by a particular subcellular localization pattern such that they are confined to the oocyte cortex and are absent from the cell-to-cell contact region in 2-cell until up the morulae stage embryos (Howell et al., 2001; Kim et al., 2010; Li et al., 2008b; Morency et al., 2011; Narducci et al., 2002; Ohsugi et al., 2008; Sekiguchi

et al., 2006; Tong et al., 2004; Vitale et al., 2005). Furthermore, some of these proteins FILIA, PADI6, FLOPED, NLRP5 and TLE6 were shown to associate to specific structures termed cytoplasmic lattices or subcortical maternal complex. Since NLRP7 and KHDC3L are expressed at the RNA level in human oocytes, we decided to look at their subcellular localization in human oocytes and early cleavage embryos. We therefore collected spare oocytes and embryos from women undergoing assisted reproductive technologies and who most likely do not carry *NLRP7* and *KHDC3L* mutations since they do not suffer from RHMs. Using immunofluorescence and confocal microscopy, we demonstrated that NLRP7 and KHDC3L co-localize and are sequestered mainly to the cortex but are absent from the cell-to-cell contact region during early cleavage-stages (Akoury et al., 2015b). This particular localization suggested that NLRP7 and KHDC3L are part of the cortical complex or the human CPLs/SCMC similar to that found in murine oocytes (Kim et al., 2010; Morency et al., 2011). To our knowledge, there were no reports in the literature describing the CPLs/SCMC in humans. To investigate whether these structures exist in human oocytes, we performed high resolution and electron microscopies after immunolabeling with NLRP7 and found that NLRP7 binds to cytoskeletal structures that are similar to those characterized in murine oocytes. Soon after we published the Human Reproduction study, Zhu et al. reported the characterization of the subcortical maternal complex in human oocytes and which consisted of KHDC3L, OOEP, NLRP5 and TLE6, all of which physically co-interacted. However, Zhu's study lacked clear high-resolution structures of the SCMC and evidence of good preservation of the oocyte cytoskeleton (Zhu et al., 2015). The four described maternal-effect proteins exhibited a ring-shape pattern at the cortex of the oocyte that was not connected to the center of the oocyte and the nucleus. In order to gain more insights on the real structure of the human SCMC complex and the localization of its members, we used proteins- and microtubules-preserving buffer and performed immunofluorescence and high resolution confocal microscopy on oocytes. We chose to conduct these experiments on three founding members of the human cortical complex, KHDC3L, OOEP and TLE6. Immunostaining analysis revealed nice high-resolution structures of the three analyzed SCMC proteins at the cortex similar to that obtained previously for NLRP7. This observation prompted us to check for co-localization between NLRP7 and either of the three SCMC members. Confocal and electron microscopy analysis demonstrated that NLRP7 co-localizes with KHDC3L, OOEP and TLE6 to the same cytoskeletal structures. Based on our co-localization study and that of Zhu et al., we

therefore suggest that the human SCMC consists of at least NLRP7, KHDC3L, NLRP5, OOEP and TLE6. We thus do not know whether NLRP7 interacts with KHDC3L or any other member of the SCMC and further studies are required to address this point. We then sought to characterize the nature of the structures to which NLRP7 binds. Towards this goal, we performed double labeling of NLRP7 with alpha tubulin or F-actin/phalloidin. Our investigation revealed that although NLRP7 does not show a similar localization pattern or overlap exactly with alpha tubulin or F-actin by immunofluorescence, this maternal-effect protein depends directly or indirectly with alpha tubulin and F-actin in human oocytes. Our observation is in line with previous data demonstrating the disruption of NLRP7 signal in hematopoietic cells upon nocodazole treatment (Messaed et al., 2011a).

Murine oocytes or embryos of *Filia* (orthologue of human *KHDC3L*)*, Nlrp5, Padi6* and *Tle6* null females display various defects including abnormalities at the level of microtubules and F-actin networks (Kan et al., 2011; Kim et al., 2014; Yu et al., 2014; Zheng and Dean, 2009). Additionally, embryos derived from all these null-maternal gene mice arrest mainly between the 2-cell and morula stages with the exception of those derived from *Filia*-null mice, some of which continue to progress to the morula and blastocyst with delays in their development (Esposito et al., 2007; Tashiro et al., 2011; Tong et al., 2000; Yu et al., 2014; Zheng and Dean, 2009). One could envision that NLRP7 and KHDC3L are also involved in maintaining the integrity of the microtubules and actin cytoskeletons in human oocytes and embryos. Furthermore, NLRP7 contains a conserved ATP/GTPase binding site within its NACHT domain. It is therefore plausible to further suggest that NLRP7 regulates the cytoskeleton by interacting at the oocyte cortex with RhoA, a member of the Rho family GTPases, which is known to act in various cellular activities including actin filament organization (Hall, 1998; Ridley, 2001; Van Aelst and D'Souza-Schorey, 1997) and spindle assembly at mitosis (Bakal et al., 2005). Though the subcellular localization of RhoA has not been investigated in human oocytes, it could be that the human RhoA adopts a similar localization pattern to the spindle microtubules and the cortex as described in porcine oocytes (Zhang et al., 2014). KHDC3L does not contain a binding site for GTPases; however, this does not prevent KHDC3L from interacting indirectly with or intervening in the signaling pathway of RhoA. This explanation seems to be conceivable since *Filia*, the mouse orthologue of *KHDC3L*, has been shown to ensure proper spindle assembly partially through RhoA signaling in early cleavage mouse embryos (Zheng and Dean, 2009).

Alternatively, one could also suggest that NLRP7 and KHDC3L regulate the cytoskeleton by binding to or interfering with Ran, a small GTPase of the Ras superfamily, that is known to control the nucleo-cytoplasmic transport of mRNA and proteins, mitotic spindle assembly, and nuclear envelope formation (Dasso, 2001; Gorlich and Kutay, 1999; Heald and Weis, 2000; Hetzer et al., 2000; Zhang and Clarke, 2000). The subcellular localization of Ran GTPase is described to be at the cytoplasm and the spindle apparatus of murine oocytes (Cao et al., 2005). Regardless of the underlying mechanism that implicates NLRP7 and KHDC3L in the regulation of the oocyte cytoskeleton, we demonstrate that NLRP7 and by analogy KHDC3L depend on alpha tubulin and F-actin networks in human oocytes.

6.5 Ovum donation is the best reproductive management option for patients with RHMs

To date, there is no treatment that allows patients with *NLRP7* recessive mutations and RHMs to achieve successful pregnancies. However, ovum donation can be an effective fertility treatment for patients with RHMs. This suggestion has been proven few years back in a case report that established for the first time the occurrence of a normal live born in a patient after ovum donation (Fisher et al., 2011). Recently, we confirmed this observation by reporting three additional live births from donated ova to two patients with recessive *NLRP7* mutations. Although only four live births from donated ova have been so far reported, these data support the idea that the primary role of *NLRP7* and by analogy *KHDC3L* reside in the oocyte and that ovum donation from healthy women salvages the defects in patients with RHMs and give them the opportunity to achieve successful pregnancies. Patients with two *NLRP7* mutations can exceptionally achieve normal pregnancies from their own ova in 1% of their pregnancies (six live births occurred from a total of 612 pregnancies). We came up with this conclusion after we reviewed the reproductive outcomes of all reported patients in Pubmed. In an attempt to understand the occurrence of these spontaneous conceptions, we looked at the nature of the mutations carried by the patients with normal pregnancies. Our investigation showed that these live births are associated with one splice or some missense mutations in a recessive state. These observations indicate that some mild mutations have mild functional consequences on the protein and allow normal cellular differentiation and embryo development and consequently the

occurrence of successful pregnancies. This conclusion is in accordance with previous data from our group demonstrating that protein-truncating mutations, presumably resulting in severe functional consequences on the protein, are associated with the absence of embryonic tissues of ICM origin and excessive trophoblastic proliferation in the conceptions of these patients while missense mutations, supposedly entailing milder functional consequences on the protein, are associated with the differentiation of some embryonic tissues of ICM origin and mild trophoblastic proliferation (Nguyen et al., 2014).

6.6 Final conclusions

It is well established that hydatidiform mole can have three main genotypes, diploid androgenetic, triploid diandric and diploid biparental, all of which lead to somehow the same disease phenotype characterized by oedematous chorionic villi, excessive trophoblastic proliferation and abnormal embryonic development. Therefore, the underlying mechanism leading to HM appears to be independent of the genotype of the conceptions. Our series of experiments described in this thesis have provided key-pieces to complete part of the puzzle of RHMs (associated with *NLRP7* or *KHDC3L* mutations). We believe that the underlying mechanism for RHM is manifested at two levels and is based on a defective cytoskeleton mediated by *NLRP7* or *KHDC3L* mutations (Figure 6.1). An impaired cytoskeleton could also be at work for the common, sporadic HM (not associated with *NLRP7* or *KHDC3L* mutations) but through an uncharacterized upstream event without the presence of mutations in *NLRP7* or *KHDC3L*. Nonetheless, we believe that the primary defect is in the oocytes of patients with RHM. The oocyte defect could be at the level of establishment or maintenance of DNA methylation or at the level of the cytoskeleton. Such perturbations would disrupt several downstream processes including abnormal trophoblastic cellular proliferation and incomplete tissue differentiation and probably, an incomplete activation of the embryonic genome. Consequently, all these events would lead to early embryonic arrest. The same cytoskeletal defect has also an impact on the hematopoietic inflammatory cells present in the endometrium of the patient. These cells have impaired cytokine secretion and consequently mediate an altered maternal immune response. Such disruption may prevent patients with RHMs from

spontaneously eliminating these unviable pregnancies in which the fetal vascular system has not developed and leads to hydropic changes of chorionic villi and molar manifestation.

6.7 Limitations of the study and future directions and perspectives

In addition to providing novel information on the roles of *NLRP7* and *KHDC3L* in the manifestation of RHMs, the data presented in this thesis introduced a number of points that warrant further investigation and that could be pursued in future studies.

Using ELISA, we have demonstrated an impaired IL1B and TNF secretion in PBMCs from patients with *NLRP7* mutations. In collaboration with a laboratory in Denmark, we also checked the levels of other secreted cytokines in PBMCs from patients with RHMs and controls using a multiplex ELISA assay. However, these experiments did not yield conclusive results and we attributed this failure to the degradation of the analyzed cytokines in the supernatants following several freeze-thaw cycles. It would be worth repeating these experiments on new blood samples collected from either previous or new patients, and assessing cytokine secretion after LPS stimulation. This would generate a new list of cytokines that are abnormally secreted and allow us to better understand the role of *NLRP7* in the immune response and consequently in the pathology of RHMs. Since NLRP7 and KHDC3L co-localize in hematopoietic cells and at the cortex of human oocytes and early cleavage embryos, it would be worthwhile to demonstrate whether these two proteins physically interact in the described models using co-immunoprecipitation followed by western blotting.

We have speculated that NLRP7 and KHDC3L could be involved in trafficking of RNA and proteins. Therefore, it will be interesting to check whether these proteins bind, directly or indirectly, to RNA at the cortex of human oocytes. To this purpose, we could treat spare oocytes with RNAses and check if NLRP7 or KHDC3L signals are disrupted following the treatment.

Our work described in this thesis was mainly performed on hematopoietic cells from patients with *NLRP7* mutations and also on spare oocytes and embryos from women undergoing assisted reproductive technologies and who are most likely negative for *NLRP7* since they do not have RHMs. Although both models generated decent data, they presented some limitations. Fresh hematopoietic cells are not easy to get from patients with this rare condition because most of the patients are referred to Dr. Slim's laboratory from international collaborators and

hematopoietic cells cannot be maintained as primary cells for a long time in culture without viral transformation. Additionally, these cells have small cytoplasm which hampered their use in identifying cytoskeletal defects mediated by *NLRP7* or *KHDC3L* mutations. Human oocytes and mostly embryos are difficult to obtain for research purposes and are subject to stringent ethical regulations. For instance, embryos cannot be drug-treated before immunofluorescence; however, oocytes can be drug-treated, but not *in vitro* fertilized, and processed for immunofluorescence. Additionally, it is impossible to collect spare oocytes from patients with RHMs and investigate the effect of *NLRP7* or *KHDC3L* mutations on the cytoskeleton. An alternative would be the use of primary cells from patients with RHMs such as fibroblast cells isolated from skin biopsies. Although fibroblasts are not easy to request from patients, these cells are considered as the best alternative and Dr. Slim's lab was able to establish two primary fibroblast cells with the help of international collaborators from two patients with recessive *NLRP7* or *KHDC3L* mutations. Fibroblasts are known to express *NLRP7* and *KHDC3L* transcripts (http://biogps.org/). Additionally, I performed RT-PCR on RNA samples from these two cell lines and found that they express *NLRP7*. Using whole genome expression profiling, I analysed the transcriptome of primary fibroblasts of the patients with *NLRP7* mutations and two healthy individuals. I found 70 genes that were statistically differentially expressed, 23 up-regulated and 47 downregulated. (data not shown). Of these genes, some are involved in the cytoskeleton. Using real time quantitative PCR after reverse transcription, I validated the differential expression of a set of genes on the same RNA samples used in the microarrays and on four additional controls (data not shown). We recently collected two additional skin biopsies from two patients with *NLRP7* mutations. I used these biopsies to isolate fibroblasts and establish two primary cell lines in the lab. Our plan is to validate the transcriptome data by RT-PCR on these additional samples. It will be also worth to identify common pathways in which these genes are implicated using publicly available websites (STRING, IPA, DAVID, KEGG, etc.). One would also be interested in validating the expression of the identified genes at the protein level in the lysates prepared from fibroblasts of patients and controls.

I characterized the subcellular localization of NLRP7 and KHDC3L in fibroblasts from controls using immunofluorescence and confocal microscopy, assessed the impact of *NLRP7* mutations on the cytoskeleton, cell mobility and proliferation from patients and controls using mobility and proliferation assays. I already started this work and found differences between

fibroblasts from controls and patients (data not shown). Some of these data are still preliminary and require further validation.

Another alternative would also be the use of iPS cells generated from fibroblasts with *NLRP7* mutations and which can be induced to generate oocyte-like cells. The latter could be used to study the cytoskeletal defects mediated by *NLRP7* mutations and characterize the signalling pathways implicated downstream of NLRP7. One could also investigate possible role of *NLRP7* in DNA remodelling and epigenetic changes that could also contribute to a defective oocyte and consequently the manifestation of moles.

NLRP7 does not have an orthologue in mouse; however, using mouse oocytes can still be beneficial to study the role of *NLRP7*. One could transfect these oocytes with *NLRP7* mRNA and assess the effect of overexpressing *NLRP7* at many levels such as the oocyte cytoplasmic lattices and cytoskeleton (microtubules and actin), the localization of NLRP7 and other maternal-effect proteins, oocyte global transcriptional activity, DNA and histone methylation, etc. On the other hand, the second gene responsible for HM, *KHDC3L,* has an orthologue in mice, *Filia*. In order to study the function of *KHDC3L*, one could generate *Filia*-null oocytes in mice and apply the same experimental approaches described for *NLRP7.*

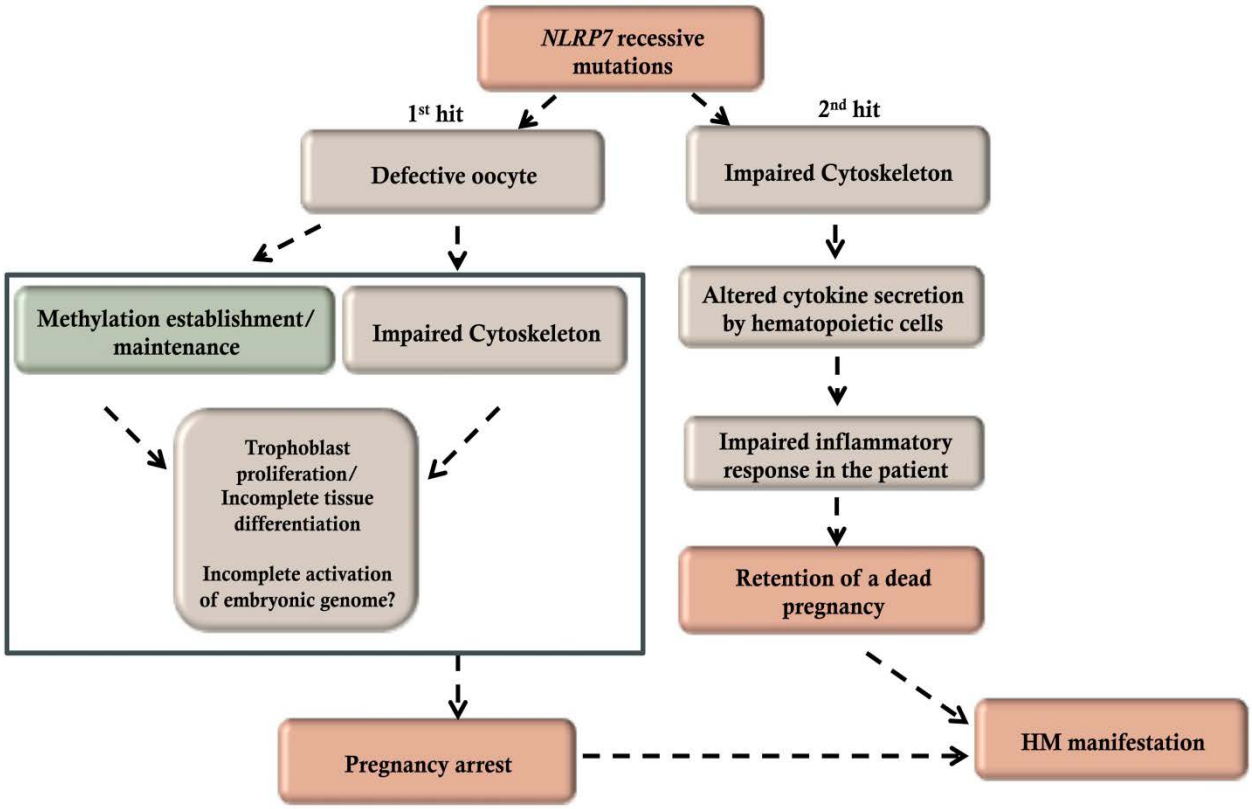

Figure.6.1. Two-hit mechanism for molar pregnancy formation

REFERENCES

Acaia, B., Parazzini, F., La Vecchia, C., Ricciardiello, O., Fedele, L., and Battista Candiani, G. (1988). Increased frequency of complete hydatidiform mole in women with repeated abortion. Gynecol Oncol *31*, 310-314.

Acosta-Sison, H. (1959). Observations which may indicate the etiology of hydatidiform mole and explain its high incidence in the Philippines and Asiatic countries. Philipp J Surg Surg Spec *14*, 290-293.

Adenot, P.G., Mercier, Y., Renard, J.P., and Thompson, E.M. (1997). Differential H4 acetylation of paternal and maternal chromatin precedes DNA replication and differential transcriptional activity in pronuclei of 1-cell mouse embryos. Development *124*, 4615-4625.

Agboola, A. (1979). Trophoblastic neoplasia in an African urban population. J Natl Med Assoc *71*, 935-937.

Agostini, L., Martinon, F., Burns, K., McDermott, M.F., Hawkins, P.N., and Tschopp, J. (2004). NALP3 forms an IL-1beta-processing inflammasome with increased activity in Muckle-Wells autoinflammatory disorder. Immunity *20*, 319-325.

Aguero, O., Kizer, S., and Pinedo, G. (1973). Hydatidiform mole in Concepcion Palacios Maternity Hospital. Am J Obstet Gynecol *116*, 1117-1120.

Akiyama, K., and Senshu, T. (1999). Dynamic aspects of protein deimination in developing mouse epidermis. Exp Dermatol *8*, 177-186.

Akiyama, T., Kim, J.M., Nagata, M., and Aoki, F. (2004). Regulation of histone acetylation during meiotic maturation in mouse oocytes. Mol Reprod Dev *69*, 222-227.

Akoury, E., Gupta, N., Bagga, R., Brown, S., Dery, C., Kabra, M., Srinivasan, R., and Slim, R. (2015a). Live births in women with recurrent hydatidiform mole and two NLRP7 mutations. Reprod Biomed Online *31*, 120-124.

Akoury, E., Zhang, L., Ao, A., and Slim, R. (2015b). NLRP7 and KHDC3L, the two maternal-effect proteins responsible for recurrent hydatidiform moles, co-localize to the oocyte cytoskeleton. Hum Reprod *30*, 159-169.

Albers, K., and Fuchs, E. (1989). Expression of mutant keratin cDNAs in epithelial cells reveals possible mechanisms for initiation and assembly of intermediate filaments. The Journal of cell biology *108*, 1477-1493.

Altieri, A., Franceschi, S., Ferlay, J., Smith, J., and La Vecchia, C. (2003). Epidemiology and aetiology of gestational trophoblastic diseases. Lancet Oncol *4*, 670-678.

Amarasinghe, A.K., MacDiarmid, R., Adams, M.D., and Rio, D.C. (2001). An in vitro-selected RNA-binding site for the KH domain protein PSI acts as a splicing inhibitor element. RNA *7*, 1239-1253.

Andrijono, A., and Muhilal, M. (2010). Prevention of post-mole malignant trophoblastic disease with vitamin A. Asian Pac J Cancer Prev *11*, 567-570.

Aravind, L., Dixit, V.M., and Koonin, E.V. (1999). The domains of death: evolution of the apoptosis machinery. Trends Biochem Sci *24*, 47-53.

Aschheim, S. (1930). The early diagnosis of pregnancy, chorionepithelioma and hydatidiform mole by the Aschheim-Zondek test. Am. J. Obstet. Gynec *10*, 335-342.

Atrash, H.K., Hogue, C.J., and Grimes, D.A. (1986). Epidemiology of hydatidiform mole during early gestation. Am J Obstet Gynecol *154*, 906-909.

Avilion, A.A., Nicolis, S.K., Pevny, L.H., Perez, L., Vivian, N., and Lovell-Badge, R. (2003). Multipotent cell lineages in early mouse development depend on SOX2 function. Genes & development *17*, 126-140.

Ayangade, O. (1979). Gestational trophoblastic disease in Nigeria- A 10 year review. East Afr Med J *56*, 278-282.

Azoury, J., Lee, K.W., Georget, V., Rassinier, P., Leader, B., and Verlhac, M.H. (2008). Spindle positioning in mouse oocytes relies on a dynamic meshwork of actin filaments. Curr Biol *18*, 1514-1519.

Azuma, C., Saji, F., Tokugawa, Y., Kimura, T., Nobunaga, T., Takemura, M., Kameda, T., and Tanizawa, O. (1991). Application of gene amplification by polymerase chain reaction to genetic analysis of molar

mitochondrial DNA: the detection of anuclear empty ovum as the cause of complete mole. Gynecol Oncol *40*, 29-33.
Baasanjav, B., Usui, H., Kihara, M., Kaku, H., Nakada, E., Tate, S., Mitsuhashi, A., Matsui, H., and Shozu, M. (2010). The risk of post-molar gestational trophoblastic neoplasia is higher in heterozygous than in homozygous complete hydatidiform moles. Hum Reprod *25*, 1183-1191.
Bagshawe, K.D., Dent, J., and Webb, J. (1986). Hydatidiform mole in England and Wales 1973-83. Lancet *2*, 673-677.
Bakal, C.J., Finan, D., LaRose, J., Wells, C.D., Gish, G., Kulkarni, S., DeSepulveda, P., Wilde, A., and Rottapel, R. (2005). The Rho GTP exchange factor Lfc promotes spindle assembly in early mitosis. Proc Natl Acad Sci U S A *102*, 9529-9534.
Bakhtari, A., and Ross, P.J. (2014). DPPA3 prevents cytosine hydroxymethylation of the maternal pronucleus and is required for normal development in bovine embryos. Epigenetics *9*, 1271-1279.
Balhorn, R. (1982). A model for the structure of chromatin in mammalian sperm. The Journal of cell biology *93*, 298-305.
Ball, C.B., Rodriguez, K.F., Stumpo, D.J., Ribeiro-Neto, F., Korach, K.S., Blackshear, P.J., Birnbaumer, L., and Ramos, S.B. (2014). The RNA-binding protein, ZFP36L2, influences ovulation and oocyte maturation. PLoS One *9*, e97324.
Bandy, L.C., Clarke-Pearson, D.L., and Hammond, C.B. (1984). Malignant potential of gestational trophoblastic disease at the extreme ages of reproductive life. Obstet Gynecol *64*, 395-399.
Barton, S.C., Surani, M.A., and Norris, M.L. (1984). Role of paternal and maternal genomes in mouse development. Nature *311*, 374-376.
Baugh, L.R., Hill, A.A., Slonim, D.K., Brown, E.L., and Hunter, C.P. (2003). Composition and dynamics of the Caenorhabditis elegans early embryonic transcriptome. Development *130*, 889-900.
Berkowitz, R., Ozturk, M., Goldstein, D., Bernstein, M., Hill, L., and Wands, J.R. (1989). Human chorionic gonadotropin and free subunits' serum levels in patients with partial and complete hydatidiform moles. Obstet Gynecol *74*, 212-216.
Berkowitz, R.S., Cramer, D.W., Bernstein, M.R., Cassells, S., Driscoll, S.G., and Goldstein, D.P. (1985). Risk factors for complete molar pregnancy from a case-control study. Am J Obstet Gynecol *152*, 1016-1020.
Berkowitz, R.S., and Goldstein, D.P. (1996). Chorionic Tumors. N Engl J Med *335*, 1740-1748.
Berkowitz, R.S., and Goldstein, D.P. (2009a). Clinical practice. Molar pregnancy. N Engl J Med *360*, 1639-1645.
Berkowitz, R.S., and Goldstein, D.P. (2009b). Current management of gestational trophoblastic diseases. Gynecol Oncol *112*, 654-662.
Berkowitz, R.S., Im, S.S., Bernstein, M.R., and Goldstein, D.P. (1998). Gestational trophoblastic disease. Subsequent pregnancy outcome, including repeat molar pregnancy. J Reprod Med *43*, 81-86.
Beygo, J., Ammerpohl, O., Gritzan, D., Heitmann, M., Rademacher, K., Richter, J., Caliebe, A., Siebert, R., Horsthemke, B., and Buiting, K. (2013). Deep bisulfite sequencing of aberrantly methylated loci in a patient with multiple methylation defects. PLoS One *8*, e76953.
Bierkamp, C., Luxey, M., Metchat, A., Audouard, C., Dumollard, R., and Christians, E. (2010). Lack of maternal Heat Shock Factor 1 results in multiple cellular and developmental defects, including mitochondrial damage and altered redox homeostasis, and leads to reduced survival of mammalian oocytes and embryos. Dev Biol *339*, 338-353.
Bird, A.P. (1986). CpG-rich islands and the function of DNA methylation. Nature *321*, 209-213.
Blackburn, P., and Gavilanes, J.G. (1982). Identification of lysine residues in the binding domain of ribonuclease A for the RNase inhibitor from human placenta. J Biol Chem *257*, 316-321.
Bortvin, A., Goodheart, M., Liao, M., and Page, D.C. (2004). Dppa3 / Pgc7 / stella is a maternal factor and is not required for germ cell specification in mice. BMC developmental biology *4*, 2.
Boufettal, H., Coullin, P., Mahdaoui, S., Noun, M., Hermas, S., and Samouh, N. (2011). [Complete hydatiforme mole in Morocco: epidemiological and clinical study]. J Gynecol Obstet Biol Reprod (Paris) *40*, 419-429.

Bouleau, A., Desvignes, T., Traverso, J.M., Nguyen, T., Chesnel, F., Fauvel, C., and Bobe, J. (2014). Maternally inherited npm2 mRNA is crucial for egg developmental competence in zebrafish. Biol Reprod *91*, 43.
Bourc'his, D., Xu, G.L., Lin, C.S., Bollman, B., and Bestor, T.H. (2001). Dnmt3L and the establishment of maternal genomic imprints. Science *294*, 2536-2539.
Boveri, T. (1901). Zellen-studien: Ueber die nature der centrosomen, Vol 4.
Bracken, M.B., Brinton, L.A., and Hayashi, K. (1984). Epidemiology of hydatidiform mole and choriocarcinoma. Epidemiol Rev *6*, 52-75.
Braude, P., Bolton, V., and Moore, S. (1988). Human gene expression first occurs between the four- and eight-cell stages of preimplantation development. Nature *332*, 459-461.
Brews, A. (1939). Hydatidiform mole and chorion-epithelioma. The Journal of Obstetrics & Gynaecology of the British Empire *46*.
Brinton, L.A., Wu, B.Z., Wang, W., Ershow, A.G., Song, H.Z., Li, J.Y., Bracken, M.B., and Blot, W.J. (1989). Gestational trophoblastic disease: a case-control study from the People's Republic of China. Am J Obstet Gynecol *161*, 121-127.
Brown, L., Mount, S., Reddy, R., Slim, R., Wong, C., Jobanputra, V., Clifford, P., Merrill, L., and Brown, S. (2013). Recurrent pregnancy loss in a woman with NLRP7 mutation: not all molar pregnancies can be easily classified as either "partial" or "complete" hydatidiform moles. Int J Gynecol Pathol *32*, 399-405.
Bruey, J.M., Bruey-Sedano, N., Newman, R., Chandler, S., Stehlik, C., and Reed, J.C. (2004). PAN1/NALP2/PYPAF2, an inducible inflammatory mediator that regulates NF-kappaB and caspase-1 activation in macrophages. J Biol Chem *279*, 51897-51907.
Buckanovich, R.J., Yang, Y.Y., and Darnell, R.B. (1996). The onconeural antigen Nova-1 is a neuron-specific RNA-binding protein, the activity of which is inhibited by paraneoplastic antibodies. J Neurosci *16*, 1114-1122.
Buckley, J.D. (1984). The epidemiology of molar pregnancy and choriocarcinoma. Clin Obstet Gynecol *27*, 153-159.
Bultman, S., Gebuhr, T., Yee, D., La Mantia, C., Nicholson, J., Gilliam, A., Randazzo, F., Metzger, D., Chambon, P., Crabtree, G.*, et al.* (2000). A Brg1 null mutation in the mouse reveals functional differences among mammalian SWI/SNF complexes. Molecular cell *6*, 1287-1295.
Bultman, S.J., Gebuhr, T.C., Pan, H., Svoboda, P., Schultz, R.M., and Magnuson, T. (2006). Maternal BRG1 regulates zygotic genome activation in the mouse. Genes & development *20*, 1744-1754.
Burns, K.H., Viveiros, M.M., Ren, Y., Wang, P., DeMayo, F.J., Frail, D.E., Eppig, J.J., and Matzuk, M.M. (2003). Roles of NPM2 in chromatin and nucleolar organization in oocytes and embryos. Science *300*, 633-636.
Cao, Y.K., Zhong, Z.S., Chen, D.Y., Zhang, G.X., Schatten, H., and Sun, Q.Y. (2005). Cell cycle-dependent localization and possible roles of the small GTPase Ran in mouse oocyte maturation, fertilization and early cleavage. Reproduction *130*, 431-440.
Capco, D.G., Gallicano, G.I., McGaughey, R.W., Downing, K.H., and Larabell, C.A. (1993). Cytoskeletal sheets of mammalian eggs and embryos: a lattice-like network of intermediate filaments. Cell Motil Cytoskeleton *24*, 85-99.
Capco, D.G., Krochmalnic, G., and Penman, S. (1984). A new method of preparing embeddment-free sections for transmission electron microscopy: applications to the cytoskeletal framework and other three-dimensional networks. The Journal of cell biology *98*, 1878-1885.
Capco, D.G., and McGaughey, R.W. (1986). Cytoskeletal reorganization during early mammalian development: analysis using embedment-free sections. Dev Biol *115*, 446-458.
Carson, D.D., Bagchi, I., Dey, S.K., Enders, A.C., Fazleabas, A.T., Lessey, B.A., and Yoshinaga, K. (2000). Embryo implantation. Dev Biol *223*, 217-237.
Carta, S., Tassi, S., Semino, C., Fossati, G., Mascagni, P., Dinarello, C.A., and Rubartelli, A. (2006). Histone deacetylase inhibitors prevent exocytosis of interleukin-1beta-containing secretory lysosomes: role of microtubules. Blood *108*, 1618-1626.

Castillo, A., and Justice, M.J. (2007). The kinesin related motor protein, Eg5, is essential for maintenance of pre-implantation embryogenesis. Biochem Biophys Res Commun *357*, 694-699.
Chan, Y., Anton-Lamprecht, I., Yu, Q.C., Jackel, A., Zabel, B., Ernst, J.P., and Fuchs, E. (1994). A human keratin 14 "knockout": the absence of K14 leads to severe epidermolysis bullosa simplex and a function for an intermediate filament protein. Genes & development *8*, 2574-2587.
Chang, B.H., Liu, X., Liu, J., Quan, F.S., Guo, Z.K., and Zhang, Y. (2013). Developmental expression and possible functional roles of mouse Nlrp4e in preimplantation embryos. In Vitro Cell Dev Biol Anim.
Chatenoud, L., Parazzini, F., di Cintio, E., Zanconato, G., Benzi, G., Bortolus, R., and La Vecchia, C. (1998). Paternal and maternal smoking habits before conception and during the first trimester: relation to spontaneous abortion. Annals of epidemiology *8*, 520-526.
Chavanas, S., Mechin, M.C., Takahara, H., Kawada, A., Nachat, R., Serre, G., and Simon, M. (2004). Comparative analysis of the mouse and human peptidylarginine deiminase gene clusters reveals highly conserved non-coding segments and a new human gene, PADI6. Gene *330*, 19-27.
Cheah, P.L., Looi, L.M., and Sivanesaratnam, V. (1993). Hydatidiform molar pregnancy in Malaysian women: a histopathological study from the University Hospital, Kuala Lumpur. Malays J Pathol *15*, 59-63.
Chesnel, F., and Eppig, J.J. (1995). Induction of precocious germinal vesicle breakdown (GVB) by GVB-incompetent mouse oocytes: possible role of mitogen-activated protein kinases rather than p34cdc2 kinase. Biol Reprod *52*, 895-902.
Chew, T.G., Peaston, A., Lim, A.K., Lorthongpanich, C., Knowles, B.B., and Solter, D. (2013). A tudor domain protein SPINDLIN1 interacts with the mRNA-binding protein SERBP1 and is involved in mouse oocyte meiotic resumption. PLoS One *8*, e69764.
Choi, T., Fukasawa, K., Zhou, R., Tessarollo, L., Borror, K., Resau, J., and Vande Woude, G.F. (1996). The Mos/mitogen-activated protein kinase (MAPK) pathway regulates the size and degradation of the first polar body in maturing mouse oocytes. Proc Natl Acad Sci U S A *93*, 7032-7035.
Christians, E., Davis, A.A., Thomas, S.D., and Benjamin, I.J. (2000). Maternal effect of Hsf1 on reproductive success. Nature *407*, 693-694.
Cirio, M.C., Martel, J., Mann, M., Toppings, M., Bartolomei, M., Trasler, J., and Chaillet, J.R. (2008). DNA methyltransferase 1o functions during preimplantation development to preclude a profound level of epigenetic variation. Dev Biol *324*, 139-150.
Clapier, C.R., and Cairns, B.R. (2009). The biology of chromatin remodeling complexes. Annual review of biochemistry *78*, 273-304.
Clayton, L., Hall, A., and Johnson, M.H. (1999). A role for Rho-like GTPases in the polarisation of mouse eight-cell blastomeres. Dev Biol *205*, 322-331.
Clegg, K.B., and Piko, L. (1983). Poly(A) length, cytoplasmic adenylation and synthesis of poly(A)+ RNA in early mouse embryos. Dev Biol *95*, 331-341.
Coulam, C.B. (1991). Epidemiology of recurrent spontaneous abortion. Am J Reprod Immunol *26*, 23-27.
Coullin, P., Diatta, A.L., Boufettal, H., Feingold, J., Leguern, E., and Candelier, J.J. (2015). The involvement of the trans-generational effect in the high incidence of the hydatidiform mole in Africa. Placenta *36*, 48-51.
Court, F., Martin-Trujillo, A., Romanelli, V., Garin, I., Iglesias-Platas, I., Salafsky, I., Guitart, M., Perez de Nanclares, G., Lapunzina, P., and Monk, D. (2013). Genome-wide allelic methylation analysis reveals disease-specific susceptibility to multiple methylation defects in imprinting syndromes. Hum Mutat *34*, 595-602.
Craighill, M.C., and Cramer, D.W. (1984). Epidemiology of complete molar pregnancy. J Reprod Med *29*, 784-787.
Cuddapah, S., Jothi, R., Schones, D.E., Roh, T.Y., Cui, K., and Zhao, K. (2009). Global analysis of the insulator binding protein CTCF in chromatin barrier regions reveals demarcation of active and repressive domains. Genome Res *19*, 24-32.
Dasso, M. (2001). Running on Ran: nuclear transport and the mitotic spindle. Cell *104*, 321-324.

De Leon, V., Johnson, A., and Bachvarova, R. (1983). Half-lives and relative amounts of stored and polysomal ribosomes and poly(A) + RNA in mouse oocytes. Dev Biol *98*, 400-408.
De Renzis, S., Elemento, O., Tavazoie, S., and Wieschaus, E.F. (2007). Unmasking activation of the zygotic genome using chromosomal deletions in the Drosophila embryo. PLoS biology *5*, e117.
De Vries, W.N., Evsikov, A.V., Haac, B.E., Fancher, K.S., Holbrook, A.E., Kemler, R., Solter, D., and Knowles, B.B. (2004). Maternal beta-catenin and E-cadherin in mouse development. Development *131*, 4435-4445.
Dean, J. (2002). Oocyte-specific genes regulate follicle formation, fertility and early mouse development. J Reprod Immunol *53*, 171-180.
Dejgaard, K., and Leffers, H. (1996). Characterisation of the nucleic-acid-binding activity of KH domains. Different properties of different domains. Eur J Biochem *241*, 425-431.
Delaval, K., and Feil, R. (2004). Epigenetic regulation of mammalian genomic imprinting. Current opinion in genetics & development *14*, 188-195.
Dembic, Z. (2005). Toll and Toll-Like Receptors: An Immunologic Perspective (Eureka.com and Kluwer Academic/Plenum Publishers).
Derijck, A.A., van der Heijden, G.W., Giele, M., Philippens, M.E., van Bavel, C.C., and de Boer, P. (2006). gammaH2AX signalling during sperm chromatin remodelling in the mouse zygote. DNA repair *5*, 959-971.
Deveault, C., Qian, J.H., Chebaro, W., Ao, A., Gilbert, L., Mehio, A., Khan, R., Tan, S.L., Wischmeijer, A., Coullin, P.*, et al.* (2009). NLRP7 mutations in women with diploid androgenetic and triploid moles: a proposed mechanism for mole formation. Hum Mol Genet *18*, 888-897.
Diejomaoh, F.M., Omu, A.E., Okpere, E.E., Ezimokhai, M., Tabowei, O., and Ajabor, L.N. (1984). The problems of management of gestational trophoblastic neoplasms at the University of Benin Teaching Hospital, Benin City, Nigeria. Adv Exp Med Biol *176*, 417-428.
Dillon, N., and Festenstein, R. (2002). Unravelling heterochromatin: competition between positive and negative factors regulates accessibility. Trends in genetics : TIG *18*, 252-258.
Dixon, P.H., Trongwongsa, P., Abu-Hayyah, S., Ng, S.H., Akbar, S.A., Khawaja, N.P., Seckl, M.J., Savage, P.M., and Fisher, R.A. (2012). Mutations in NLRP7 are associated with diploid biparental hydatidiform moles, but not androgenetic complete moles. J Med Genet *49*, 206-211.
Djuric, U., El-Maarri, O., Lamb, B., Kuick, R., Seoud, M., Coullin, P., Oldenburg, J., Hanash, S., and Slim, R. (2006). Familial molar tissues due to mutations in the inflammatory gene, *NALP7*, have normal postzygotic DNA methylation. Human genetics *120*, 390-395.
Dobson, A.T., Raja, R., Abeyta, M.J., Taylor, T., Shen, S., Haqq, C., and Pera, R.A. (2004). The unique transcriptome through day 3 of human preimplantation development. Hum Mol Genet *13*, 1461-1470.
Docherty, L.E., Rezwan, F.I., Poole, R.L., Turner, C.L., Kivuva, E., Maher, E.R., Smithson, S.F., Hamilton-Shield, J.P., Patalan, M., Gizewska, M.*, et al.* (2015). Mutations in *NLRP5* are associated with reproductive wastage and multilocus imprinting disorders in humans. Nat Commun *6*, 8086.
Douglas, G.W. (1957). The diagnosis and management of hydatidiform mole. Surg Clin North Am *37*, 379-392.
Duenez-Guzman, E.A., and Haig, D. (2014). The evolution of reproduction-related NLRP genes. Journal of molecular evolution *78*, 194-201.
Duff, G.B. (1989). Gestational trophoblastic disease in New Zealand, 1980-1986. Aust N Z J Obstet Gynaecol *29*, 139-142.
Dumont, J., Million, K., Sunderland, K., Rassinier, P., Lim, H., Leader, B., and Verlhac, M.H. (2007). Formin-2 is required for spindle migration and for the late steps of cytokinesis in mouse oocytes. Dev Biol *301*, 254-265.
Duncan, F.E., Padilla-Banks, E., Bernhardt, M.L., Ord, T.S., Jefferson, W.N., Moss, S.B., and Williams, C.J. (2014). Transducin-like enhancer of split-6 (TLE6) is a substrate of protein kinase A activity during mouse oocyte maturation. Biol Reprod *90*, 63.
Dupin, I., and Etienne-Manneville, S. (2011). Nuclear positioning: mechanisms and functions. Int J Biochem Cell Biol *43*, 1698-1707.

Dutcher, S.K. (2001). The tubulin fraternity: alpha to eta. Current opinion in cell biology *13*, 49-54.
Eagles, N., Sebire, N.J., Short, D., Savage, P.M., Seckl, M.J., and Fisher, R.A. (2015). Risk of recurrent molar pregnancies following complete and partial hydatidiform moles. Hum Reprod *30*, 2055-2063.
Edelmann, W., Cohen, P.E., Kane, M., Lau, K., Morrow, B., Bennett, S., Umar, A., Kunkel, T., Cattoretti, G., Chaganti, R.*, et al.* (1996). Meiotic pachytene arrest in MLH1-deficient mice. Cell *85*, 1125-1134.
Edwards, R., Crow, J., Dale, S., Macnamee, M., Hartshorne, G., and Brinsden, P. (1990). Preimplantation diagnosis and recurrent hydatidiform mole. Lancet *335*, 1030-1031.
Edwards, Y.H., Jeremiah, S.J., McMillan, S.L., Povey, S., Fisher, R.A., and Lawler, S.D. (1984). Complete hydatidiform moles combine maternal mitochondria with a paternal nuclear genome. Ann Hum Genet *48*, 119-127.
Egwuatu, V.E., and Ozumba, B.C. (1989). Observations on molar pregnancy in Enugu, Nigeria. Int J Gynaecol Obstet *29*, 219-225.
El-Maarri, O., Seoud, M., Coullin, P., Herbiniaux, U., Oldenburg, J., Rouleau, G., and Slim, R. (2003). Maternal alleles acquiring paternal methylation patterns in biparental complete hydatidiform moles. Hum Mol Genet *12*, 1405-1413.
Elias, K.M., Goldstein, D.P., and Berkowitz, R.S. (2010). Complete hydatidiform mole in women older than age 50. J Reprod Med *55*, 208-212.
Elliott, J. (1971). Outlines of greek and roman medicine (Boston: Milford House Inc).
Erhardt, S., Su, I.H., Schneider, R., Barton, S., Bannister, A.J., Perez-Burgos, L., Jenuwein, T., Kouzarides, T., Tarakhovsky, A., and Surani, M.A. (2003). Consequences of the depletion of zygotic and embryonic enhancer of zeste 2 during preimplantation mouse development. Development *130*, 4235-4248.
Esposito, G., Vitale, A.M., Leijten, F.P., Strik, A.M., Koonen-Reemst, A.M., Yurttas, P., Robben, T.J., Coonrod, S., and Gossen, J.A. (2007). Peptidylarginine deiminase (PAD) 6 is essential for oocyte cytoskeletal sheet formation and female fertility. Molecular and cellular endocrinology *273*, 25-31.
Estrada, H., Buentello, B., Zenteno, J.C., Fiszman, R., and Aguinaga, M. (2013). The p.L750V mutation in the NLRP7 gene is frequent in Mexican patients with recurrent molar pregnancies and is not associated with recurrent pregnancy loss. Prenat Diagn, 1-4.
Fallahian, M., Sebire, N.J., Savage, P.M., Seckl, M.J., and Fisher, R.A. (2013). Mutations in NLRP7 and KHDC3L confer a complete hydatidiform mole phenotype on digynic triploid conceptions. Hum Mutat *34*, 301-308.
Fernandes, R., Tsuda, C., Perumalsamy, A.L., Naranian, T., Chong, J., Acton, B.M., Tong, Z.B., Nelson, L.M., and Jurisicova, A. (2012). NLRP5 mediates mitochondrial function in mouse oocytes and embryos. Biol Reprod *86*, 138, 131-110.
Fett, J.W., Strydom, D.J., Lobb, R.R., Alderman, E.M., Bethune, J.L., Riordan, J.F., and Vallee, B.L. (1985). Isolation and characterization of angiogenin, an angiogenic protein from human carcinoma cells. Biochemistry *24*, 5480-5486.
Fisher, R.A., Hodges, M.D., and Newlands, E.S. (2004). Familial recurrent hydatidiform mole: a review. J Reprod Med *49*, 595-601.
Fisher, R.A., Hodges, M.D., Rees, H.C., Sebire, N.J., Seckl, M.J., Newlands, E.S., Genest, D.R., and Castrillon, D.H. (2002). The maternally transcribed gene p57(KIP2) (CDNK1C) is abnormally expressed in both androgenetic and biparental complete hydatidiform moles. Hum Mol Genet *11*, 3267-3272.
Fisher, R.A., Lavery, S.A., Carby, A., Abu-Hayyeh, S., Swingler, R., Sebire, N.J., and Seckl, M.J. (2011). What a difference an egg makes. Lancet *378*, 1974.
Flam, F., Lundstrom-Lindstedt, V., and Rutqvist, L.E. (1992). Incidence of gestational trophoblastic disease in Stockholm County, 1975-1988. Eur J Epidemiol *8*, 173-177.
Fontalba, A., Gutierrez, O., and Fernandez-Luna, J.L. (2007). NLRP2, an inhibitor of the NF-kappaB pathway, is transcriptionally activated by NF-kappaB and exhibits a nonfunctional allelic variant. J Immunol *179*, 8519-8524.

Foygel, K., Choi, B., Jun, S., Leong, D.E., Lee, A., Wong, C.C., Zuo, E., Eckart, M., Reijo Pera, R.A., Wong, W.H., *et al.* (2008). A novel and critical role for Oct4 as a regulator of the maternal-embryonic transition. PLoS One *3*, e4109.
Franke, H.R., Risse, E.K., Kenemans, P., Vooijs, G.P., and Stolk, J.G. (1983). Epidemiologic features of hydatidiform mole in the Netherlands. Obstet Gynecol *62*, 613-616.
Frehlick, L.J., Eirin-Lopez, J.M., and Ausio, J. (2007). New insights into the nucleophosmin/nucleoplasmin family of nuclear chaperones. Bioessays *29*, 49-59.
Fukunaga, M., Katabuchi, H., Nagasaka, T., Mikami, Y., Minamiguchi, S., and Lage, J.M. (2005). Interobserver and intraobserver variability in the diagnosis of hydatidiform mole. Am J Surg Pathol *29*, 942-947.
Furtado, L.V., Paxton, C.N., Jama, M.A., Tripp, S.R., Wilson, A.R., Lyon, E., Jarboe, E.A., Thaker, H.M., and Geiersbach, K.B. (2013). Diagnostic utility of microsatellite genotyping for molar pregnancy testing. Arch Pathol Lab Med *137*, 55-63.
Gallicano, G.I., Larabell, C.A., McGaughey, R.W., and Capco, D.G. (1994a). Novel cytoskeletal elements in mammalian eggs are composed of a unique arrangement of intermediate filaments. Mech Dev *45*, 211-226.
Gallicano, G.I., McGaughey, R.W., and Capco, D.G. (1991). Cytoskeleton of the mouse egg and embryo: reorganization of planar elements. Cell Motil Cytoskeleton *18*, 143-154.
Gallicano, G.I., McGaughey, R.W., and Capco, D.G. (1992). Cytoskeletal sheets appear as universal components of mammalian eggs. J Exp Zool *263*, 194-203.
Gallicano, G.I., McGaughey, R.W., and Capco, D.G. (1994b). Ontogeny of the cytoskeleton during mammalian oogenesis. Microsc Res Tech *27*, 134-144.
Gallicano, G.I., McGaughey, R.W., and Capco, D.G. (1995). Protein kinase M, the cytosolic counterpart of protein kinase C, remodels the internal cytoskeleton of the mammalian egg during activation. Dev Biol *167*, 482-501.
Gallicano, G.I., McGaughey, R.W., and Capco, D.G. (1997a). Activation of protein kinase C after fertilization is required for remodeling the mouse egg into the zygote. Mol Reprod Dev *46*, 587-601.
Gallicano, G.I., Schwarz, S.M., McGaughey, R.W., and Capco, D.G. (1993). Protein kinase C, a pivotal regulator of hamster egg activation, functions after elevation of intracellular free calcium. Dev Biol *156*, 94-106.
Gallicano, G.I., Yousef, M.C., and Capco, D.G. (1997b). PKC-a pivotal regulator of early development. Bioessays *19*, 29-36.
Garcia-Mayoral, M.F., Hollingworth, D., Masino, L., Diaz-Moreno, I., Kelly, G., Gherzi, R., Chou, C.F., Chen, C.Y., and Ramos, A. (2007). The structure of the C-terminal KH domains of KSRP reveals a noncanonical motif important for mRNA degradation. Structure *15*, 485-498.
Genest, D.R. (2001). Partial hydatidiform mole: clinicopathological features, differential diagnosis, ploidy and molecular studies, and gold standards for diagnosis. Int J Gynecol Pathol *20*, 315-322.
Georgatos, S.D., and Blobel, G. (1987). Two distinct attachment sites for vimentin along the plasma membrane and the nuclear envelope in avian erythrocytes: a basis for a vectorial assembly of intermediate filaments. The Journal of cell biology *105*, 105-115.
Ghildiyal, M., and Zamore, P.D. (2009). Small silencing RNAs: an expanding universe. Nat Rev Genet *10*, 94-108.
Giakoumelou, S., Wheelhouse, N., Cuschieri, K., Entrican, G., Howie, S.E., and Horne, A.W. (2015). The role of infection in miscarriage. Human reproduction update.
Gifford, C.A., and Meissner, A. (2012). Epigenetic obstacles encountered by transcription factors: reprogramming against all odds. Current opinion in genetics & development *22*, 409-415.
Goldstein, D.P., and Berkowitz, R.S. (1994). Current management of complete and partial molar pregnancy. J Reprod Med *39*, 139-146.
Golubovsky, M.D. (2003). Postzygotic diploidization of triploids as a source of unusual cases of mosaicism, chimerism and twinning. Hum Reprod *18*, 236-242.

Gorlich, D., and Kutay, U. (1999). Transport between the cell nucleus and the cytoplasm. Annual review of cell and developmental biology *15*, 607-660.
Goval, J.J., Van Cauwenberge, A., and Alexandre, H. (2000). Respective roles of protein tyrosine kinases and protein kinases C in the upregulation of beta-catenin distribution, and compaction in mouse preimplantation embryos: a pharmacological approach. Biol Cell *92*, 513-526.
Grimes, D.A. (1984). Epidemiology of gestational trophoblastic disease. Am J Obstet Gynecol *150*, 309-318.
Gruss, O.J., and Vernos, I. (2004). The mechanism of spindle assembly: functions of Ran and its target TPX2. The Journal of cell biology *166*, 949-955.
Guertin, M.J., and Lis, J.T. (2010). Chromatin landscape dictates HSF binding to target DNA elements. PLoS Genet *6*, e1001114.
Gupta, M., Vang, R., Yemelyanova, A.V., Kurman, R.J., Li, F.R., Maambo, E.C., Murphy, K.M., DeScipio, C., Thompson, C.B., and Ronnett, B.M. (2012). Diagnostic reproducibility of hydatidiform moles: ancillary techniques (p57 immunohistochemistry and molecular genotyping) improve morphologic diagnosis for both recently trained and experienced gynecologic pathologists. Am J Surg Pathol *36*, 1747-1760.
Gurtu, V.E., Verma, S., Grossmann, A.H., Liskay, R.M., Skarnes, W.C., and Baker, S.M. (2002). Maternal effect for DNA mismatch repair in the mouse. Genetics *160*, 271-277.
Gyorgy, B., Toth, E., Tarcsa, E., Falus, A., and Buzas, E.I. (2006). Citrullination: a posttranslational modification in health and disease. Int J Biochem Cell Biol *38*, 1662-1677.
Halban, P.A., and Irminger, J.C. (1994). Sorting and processing of secretory proteins. The Biochemical journal *299 (Pt 1)*, 1-18.
Hall, A. (1998). Rho GTPases and the actin cytoskeleton. Science *279*, 509-514.
Hamatani, T., Carter, M.G., Sharov, A.A., and Ko, M.S. (2004a). Dynamics of global gene expression changes during mouse preimplantation development. Dev Cell *6*, 117-131.
Hamatani, T., Falco, G., Carter, M.G., Akutsu, H., Stagg, C.A., Sharov, A.A., Dudekula, D.B., VanBuren, V., and Ko, M.S. (2004b). Age-associated alteration of gene expression patterns in mouse oocytes. Hum Mol Genet *13*, 2263-2278.
Harel, A., and Forbes, D.J. (2004). Importin beta: conducting a much larger cellular symphony. Molecular cell *16*, 319-330.
Hatch, K.R., and Capco, D.G. (2001). Colocalization of CaM KII and MAP kinase on architectural elements of the mouse egg: potentiation of MAP kinase activity by CaM KII. Mol Reprod Dev *58*, 69-77.
Hayashi, K., Bracken, M.B., Freeman, D.H., Jr., and Hellenbrand, K. (1982). Hydatidiform mole in the United States (1970-1977): a statistical and theoretical analysis. Am J Epidemiol *115*, 67-77.
Hayward, B.E., De Vos, M., Talati, N., Abdollahi, M.R., Taylor, G.R., Meyer, E., Williams, D., Maher, E.R., Setna, F., Nazir, K.*, et al.* (2009). Genetic and Epigenetic Analysis of Recurrent Hydatidiform Mole. Hum Mutat *30*, E629-639.
Heald, R., and Weis, K. (2000). Spindles get the ran around. Trends in cell biology *10*, 1-4.
Helwani, M.N., Seoud, M., Zahed, L., Zaatari, G., Khalil, A., and Slim, R. (1999). A familial case of recurrent hydatidiform molar pregnancies with biparental genomic contribution. Human genetics *105*, 112-115.
Herr, J.C., Chertihin, O., Digilio, L., Jha, K.N., Vemuganti, S., and Flickinger, C.J. (2008). Distribution of RNA binding protein MOEP19 in the oocyte cortex and early embryo indicates pre-patterning related to blastomere polarity and trophectoderm specification. Dev Biol *314*, 300-316.
Hertig, A.T., and Sheldon, W.H. (1947). Hydatidiform mole; a pathologico-clinical correlation of 200 cases. Am J Obstet Gynecol *53*, 1-36.
Hesse, M., Franz, T., Tamai, Y., Taketo, M.M., and Magin, T.M. (2000). Targeted deletion of keratins 18 and 19 leads to trophoblast fragility and early embryonic lethality. EMBO J *19*, 5060-5070.
Hetzer, M., Bilbao-Cortes, D., Walther, T.C., Gruss, O.J., and Mattaj, I.W. (2000). GTP hydrolysis by Ran is required for nuclear envelope assembly. Molecular cell *5*, 1013-1024.

Hetzer, M., Gruss, O.J., and Mattaj, I.W. (2002). The Ran GTPase as a marker of chromosome position in spindle formation and nuclear envelope assembly. Nat Cell Biol *4*, E177-184.
Hirasawa, R., Chiba, H., Kaneda, M., Tajima, S., Li, E., Jaenisch, R., and Sasaki, H. (2008). Maternal and zygotic Dnmt1 are necessary and sufficient for the maintenance of DNA methylation imprints during preimplantation development. Genes & development *22*, 1607-1616.
Ho, P.C., Mak, L.W., Lawton, J.W., and Ma, H.K. (1980). Immunological parameters in gestational trophoblastic neoplasia. J Reprod Immunol *1*, 307-319.
Hodges, M.D., Rees, H.C., Seckl, M.J., Newlands, E.S., and Fisher, R.A. (2003). Genetic refinement and physical mapping of a biparental complete hydatidiform mole locus on chromosome 19q13.4. J Med Genet *40*, e95.
Hoffman, H.M., Mueller, J.L., Broide, D.H., Wanderer, A.A., and Kolodner, R.D. (2001). Mutation of a new gene encoding a putative pyrin-like protein causes familial cold autoinflammatory syndrome and Muckle-Wells syndrome. Nat Genet *29*, 301-305.
Hofsteenge, J., Matthies, R., and Stone, S.R. (1989). Primary structure of a ribonuclease from porcine liver, a new member of the ribonuclease superfamily. Biochemistry *28*, 9806-9813.
Holt, O.J., Gallo, F., and Griffiths, G.M. (2006). Regulating secretory lysosomes. Journal of biochemistry *140*, 7-12.
Honda, J., Yanagida, K., Sato, E., Sugawara, N., Munakata, S., and Fukushima, T. (1982). [Incidence of hydatidiform mole and aging of mothers (author's transl)]. Nihon Sanka Fujinka Gakkai Zasshi *34*, 915-919.
Horikawa, M., Kirkman, N.J., Mayo, K.E., Mulders, S.M., Zhou, J., Bondy, C.A., Hsu, S.-Y.T., King, G.J., and Adashi, E.Y. (2005). The Mouse Germ-Cell-Specific Leucine-Rich Repeat Protein NALP14: A Member of the NACHT Nucleoside Triphosphatase Family. Biol Reprod *72*, 879-889.
Horn, L.C., Kowalzik, J., Bilek, K., Richter, C.E., and Einenkel, J. (2006). Clinicopathologic characteristics and subsequent pregnancy outcome in 139 complete hydatidiform moles. Eur J Obstet Gynecol Reprod Biol *128*, 10-14.
Hoshina, M., Boothby, M.R., Hussa, R.D., Pattillo, R.A., Camel, H.M., and Boime, I. (1984). Segregation patterns of polymorphic restriction sites of the gene encoding the alpha subunit of human chorionic gonadotropin in trophoblastic disease. Proc Natl Acad Sci U S A *81*, 2504-2507.
Hou, J., Liu, L., Zhang, J., Cui, X.H., Yan, F.X., Guan, H., Chen, Y.F., and An, X.R. (2008). Epigenetic modification of histone 3 at lysine 9 in sheep zygotes and its relationship with DNA methylation. BMC developmental biology *8*, 60.
Houliston, E., and Maro, B. (1989). Posttranslational modification of distinct microtubule subpopulations during cell polarization and differentiation in the mouse preimplantation embryo. The Journal of cell biology *108*, 543-551.
Howat, A.J., Beck, S., Fox, H., Harris, S.C., Hill, A.S., Nicholson, C.M., and Williams, R.A. (1993). Can histopathologists reliably diagnose molar pregnancy? J Clin Pathol *46*, 599-602.
Howell, C.Y., Bestor, T.H., Ding, F., Latham, K.E., Mertineit, C., Trasler, J.M., and Chaillet, J.R. (2001). Genomic imprinting disrupted by a maternal effect mutation in the Dnmt1 gene. Cell *104*, 829-838.
Huang, X.J., Wang, X., Ma, X., Sun, S.C., Zhou, X., Zhu, C., and Liu, H. (2014). EZH2 is essential for development of mouse preimplantation embryos. Reprod Fertil Dev *26*, 1166-1175.
Illingworth, R.S., and Bird, A.P. (2009). CpG islands-'a rough guide'. FEBS Lett *583*, 1713-1720.
Iqbal, K., Jin, S.G., Pfeifer, G.P., and Szabo, P.E. (2011). Reprogramming of the paternal genome upon fertilization involves genome-wide oxidation of 5-methylcytosine. Proc Natl Acad Sci U S A *108*, 3642-3647.
Jackson, B.W., Grund, C., Winter, S., Franke, W.W., and Illmensee, K. (1981). Formation of cytoskeletal elements during mouse embryogenesis. II. Epithelial differentiation and intermediate-sized filaments in early postimplantation embryos. Differentiation *20*, 203-216.
Jacobs, P.A., Hunt, P.A., Matsuura, J.S., Wilson, C.C., and Szulman, A.E. (1982a). Complete and partial hydatidiform mole in Hawaii: cytogenetics, morphology and epidemiology. Br J Obstet Gynaecol *89*, 258-266.

Jacobs, P.A., Szulman, A.E., Funkhouser, J., Matsuura, J.S., and Wilson, C.C. (1982b). Human triploidy: relationship between parental origin of the additional haploid complement and development of partial hydatidiform mole. Ann Hum Genet *46*, 223-231.
Jacobs, P.A., Wilson, C.M., Sprenkle, J.A., Rosenshein, N.B., and Migeon, B.R. (1980). Mechanism of origin of complete hydatidiform moles. Nature *286*, 714-716.
Jeru, I., Marlin, S., Le Borgne, G., Cochet, E., Normand, S., Duquesnoy, P., Dastot-Le Moal, F., Cuisset, L., Hentgen, V., Fernandes Alnemri, T.*, et al.* (2010). Functional consequences of a germline mutation in the leucine-rich repeat domain of NLRP3 identified in an atypical autoinflammatory disorder. Arthritis Rheum *62*, 1176-1185.
Johnson, J., Bierle, B.M., Gallicano, G.I., and Capco, D.G. (1998). Calcium/calmodulin-dependent protein kinase II and calmodulin: regulators of the meiotic spindle in mouse eggs. Dev Biol *204*, 464-477.
Judson, H., Hayward, B.E., Sheridan, E., and Bonthron, D.T. (2002). A global disorder of imprinting in the human female germ line. Nature *416*, 539-542.
Kageyama, S., Liu, H., Kaneko, N., Ooga, M., Nagata, M., and Aoki, F. (2007). Alterations in epigenetic modifications during oocyte growth in mice. Reproduction *133*, 85-94.
Kajii, T. (1986). The road to diploid androgenesis (the Japan Society of Human Genetics award lecture). Jinrui Idengaku Zasshi *31*, 61-71.
Kajii, T., and Niikawa, N. (1977). Origin of triploidy and tetraploidy in man: 11 cases with chromosomes markers. Cytogenetics and cell genetics *18*, 109-125.
Kajii, T., and Ohama, K. (1977). Androgenetic origin of hydatidiform mole. Nature *268*, 633-634.
Kan, R., Yurttas, P., Kim, B., Jin, M., Wo, L., Lee, B., Gosden, R., and Coonrod, S.A. (2011). Regulation of mouse oocyte microtubule and organelle dynamics by PADI6 and the cytoplasmic lattices. Dev Biol *350*, 311-322.
Kaneda, M., Okano, M., Hata, K., Sado, T., Tsujimoto, N., Li, E., and Sasaki, H. (2004). Essential role for de novo DNA methyltransferase Dnmt3a in paternal and maternal imprinting. Nature *429*, 900-903.
Kaneda, M., Tang, F., O'Carroll, D., Lao, K., and Surani, M.A. (2009). Essential role for Argonaute2 protein in mouse oogenesis. Epigenetics & chromatin *2*, 9.
Kang, E., Wu, G., Ma, H., Li, Y., Tippner-Hedges, R., Tachibana, M., Sparman, M., Wolf, D.P., Scholer, H.R., and Mitalipov, S. (2014). Nuclear reprogramming by interphase cytoplasm of two-cell mouse embryos. Nature *509*, 101-104.
Kastner, D.L., Aksentijevich, I., and Goldbach-Mansky, R. (2010). Autoinflammatory disease reloaded: a clinical perspective. Cell *140*, 784-790.
Keramari, M., Razavi, J., Ingman, K.A., Patsch, C., Edenhofer, F., Ward, C.M., and Kimber, S.J. (2010). Sox2 is essential for formation of trophectoderm in the preimplantation embryo. PLoS One *5*, e13952.
Khanna, A., Khanna, S., Gupta, R.M., Gupta, S., and Khanna, A.K. (1985). Immunological status of trophoblastic neoplasia. J Surg Oncol *28*, 4-6.
Khare, S., Dorfleutner, A., Bryan, N.B., Yun, C., Radian, A.D., de Almeida, L., Rojanasakul, Y., and Stehlik, C. (2012). An NLRP7-containing inflammasome mediates recognition of microbial lipopeptides in human macrophages. Immunity *36*, 464-476.
Khoo, S.K., Sidhu, M., Baartz, D., Yip, W.L., and Tripcony, L. (2010). Persistence and malignant sequelae of gestational trophoblastic disease: Clinical presentation, diagnosis, treatment and outcome. Aust N Z J Obstet Gynaecol *50*, 81-86.
Kim, B., Kan, R., Anguish, L., Nelson, L.M., and Coonrod, S.A. (2010). Potential role for MATER in cytoplasmic lattice formation in murine oocytes. PLoS One *5*, e12587.
Kim, B., Zhang, X., Kan, R., Cohen, R., Mukai, C., Travis, A.J., and Coonrod, S.A. (2014). The role of MATER in endoplasmic reticulum distribution and calcium homeostasis in mouse oocytes. Dev Biol *386*, 331-339.
Kim, J. (2008). Multiple YY1 and CTCF binding sites in imprinting control regions. Epigenetics *3*, 115-118.
Kim, J.H., Park, D.C., Bae, S.N., Namkoong, S.E., and Kim, S.J. (1998). Subsequent reproductive experience after treatment for gestational trophoblastic disease. Gynecol Oncol *71*, 108-112.

Kim, J.M., Liu, H., Tazaki, M., Nagata, M., and Aoki, F. (2003). Changes in histone acetylation during mouse oocyte meiosis. The Journal of cell biology *162*, 37-46.
Kim, K.H., Kim, E.Y., Kim, Y., Kim, E., Lee, H.S., Yoon, S.Y., and Lee, K.A. (2011). Gas6 downregulation impaired cytoplasmic maturation and pronuclear formation independent to the MPF activity. PLoS One *6*, e23304.
Kim, K.H., Kim, E.Y., and Lee, K.A. (2008). SEBOX is essential for early embryogenesis at the two-cell stage in the mouse. Biol Reprod *79*, 1192-1201.
Kim, K.H., and Lee, K.A. (2014). Maternal effect genes: Findings and effects on mouse embryo development. Clinical and experimental reproductive medicine *41*, 47-61.
Kinoshita, T., Wang, Y., Hasegawa, M., Imamura, R., and Suda, T. (2005). PYPAF3, a PYRIN-containing APAF-1-like Protein, Is a Feedback Regulator of Caspase-1-dependent Interleukin-1{beta} Secretion. J Biol Chem *280*, 21720-21725.
Ko, T.M., Hsieh, C.Y., Ho, H.N., Hsieh, F.J., and Lee, T.Y. (1991). Restriction fragment length polymorphism analysis to study the genetic origin of complete hydatidiform mole. Am J Obstet Gynecol *164*, 901-906.
Kobe, B., and Deisenhofer, J. (1996). Mechanism of ribonuclease inhibition by ribonuclease inhibitor protein based on the crystal structure of its complex with ribonuclease A. J Mol Biol *264*, 1028-1043.
Kokanali, M.K., Ozturkkan, D., Unsal, N., Moroy, P., Gungor, T., and Mollamahmutoglu, L. (2008). Plasma homocysteine, vitamin B12 and folate levels in hydatidiform moles and histopathological subtypes. Arch Gynecol Obstet *278*, 531-534.
Koonin, E., and Galperin, M. (2003). Sequence - Evolution - Function: Computational Approaches in Comparative Genomics (Boston: Kluwer Academic).
Kou, Y.C., Shao, L., Peng, H.H., Rosetta, R., del Gaudio, D., Wagner, A.F., Al-Hussaini, T.K., and Van den Veyver, I.B. (2008). A recurrent intragenic genomic duplication, other novel mutations in NLRP7 and imprinting defects in recurrent biparental hydatidiform moles. Mol Hum Reprod *14*, 33-40.
Kovacs, B.W., Shahbahrami, B., Tast, D.E., and Curtin, J.P. (1991). Molecular genetic analysis of complete hydatidiform moles. Cancer genetics and cytogenetics *54*, 143-152.
Krecic, A.M., and Swanson, M.S. (1999). hnRNP complexes: composition, structure, and function. Current opinion in cell biology *11*, 363-371.
Kronfol, N.M., Iliya, F.A., and Hajj, S.N. (1969). Recurrent hydatidiform mole: a report of five cases with review of the literature. J Med Liban *22*, 507-520.
Kuma, A., Hatano, M., Matsui, M., Yamamoto, A., Nakaya, H., Yoshimori, T., Ohsumi, Y., Tokuhisa, T., and Mizushima, N. (2004). The role of autophagy during the early neonatal starvation period. Nature *432*, 1032-1036.
Kwon, S., Shin, H., and Lim, H.J. (2011). Dynamic interaction of formin proteins and cytoskeleton in mouse oocytes during meiotic maturation. Mol Hum Reprod *17*, 317-327.
La Vecchia, C., Franceschi, S., Parazzini, F., Fasoli, M., Decarli, A., Gallus, G., and Tognoni, G. (1985). Risk factors for gestational trophoblastic disease in Italy. Am J Epidemiol *121*, 457-464.
Labarrere, C., Manni, J., Salas, P., and Althabe, O. (1985). Intrauterine growth retardation of unknown etiology. I. Serum complement and circulating immune complexes in mothers and infants. Am J Reprod Immunol Microbiol *8*, 87-93.
Lai, C.Y., Chan, K.Y., Khoo, U.S., Ngan, H.Y., Xue, W.C., Chiu, P.M., Tsao, S.W., and Cheung, A.N. (2004). Analysis of gestational trophoblastic disease by genotyping and chromosome in situ hybridization. Mod Pathol *17*, 40-48.
Lai, W.S., Carballo, E., Thorn, J.M., Kennington, E.A., and Blackshear, P.J. (2000). Interactions of CCCH zinc finger proteins with mRNA. Binding of tristetraprolin-related zinc finger proteins to Au-rich elements and destabilization of mRNA. J Biol Chem *275*, 17827-17837.
Lamzweerde, J.B.V. (1686). The Historia Naturalis Molarum Uteri.
Landolsi, H., Rittore, C., Philibert, L., Hmissa, S., Gribaa, M., Touitou, I., and Yacoubi, M.T. (2012). NLRP7 mutation analysis in sporadic hydatidiform moles in Tunisian patients: NLRP7 and sporadic mole. Arch Pathol Lab Med *136*, 646-651.

Langhans, T. (1901). Syncytium und Zellschicht. Placentarreste nach Aborten. Chorionepitheliome. Hydatidenmole. Hegars Beitr z Geb u Gyn *5*.
Larue, L., Ohsugi, M., Hirchenhain, J., and Kemler, R. (1994). E-cadherin null mutant embryos fail to form a trophectoderm epithelium. Proc Natl Acad Sci U S A *91*, 8263-8267.
Lawler, S.D., Fisher, R.A., and Dent, J. (1991). A prospective genetic study of complete and partial hydatidiform moles. Am J Obstet Gynecol *164*, 1270-1277.
Lawler, S.D., Fisher, R.A., Pickthall, V.J., Povey, S., and Evans, M.W. (1982). Genetic studies on hydatidiform moles. I. The origin of partial moles. Cancer genetics and cytogenetics *5*, 309-320.
Le Guen, P., Crozet, N., Huneau, D., and Gall, L. (1989). Distribution and role of microfilaments during early events of sheep fertilization. Gamete Res *22*, 411-425.
Leader, B., Lim, H., Carabatsos, M.J., Harrington, A., Ecsedy, J., Pellman, D., Maas, R., and Leder, P. (2002). Formin-2, polyploidy, hypofertility and positioning of the meiotic spindle in mouse oocytes. Nat Cell Biol *4*, 921-928.
Lewis, H.A., Musunuru, K., Jensen, K.B., Edo, C., Chen, H., Darnell, R.B., and Burley, S.K. (2000). Sequence-specific RNA binding by a Nova KH domain: implications for paraneoplastic disease and the fragile X syndrome. Cell *100*, 323-332.
Li, E., Beard, C., Forster, A.C., Bestor, T.H., and Jaenisch, R. (1993a). DNA methylation, genomic imprinting, and mammalian development. Cold Spring Harb Symp Quant Biol *58*, 297-305.
Li, E., Beard, C., and Jaenisch, R. (1993b). Role for DNA methylation in genomic imprinting. Nature *366*, 362-365.
Li, E., Bestor, T.H., and Jaenisch, R. (1992). Targeted mutation of the DNA methyltransferase gene results in embryonic lethality. Cell *69*, 915-926.
Li, H., Guo, F., Rubinstein, B., and Li, R. (2008a). Actin-driven chromosomal motility leads to symmetry breaking in mammalian meiotic oocytes. Nat Cell Biol *10*, 1301-1308.
Li, L., Baibakov, B., and Dean, J. (2008b). A subcortical maternal complex essential for preimplantation mouse embryogenesis. Dev Cell *15*, 416-425.
Lipata, F., Parkash, V., Talmor, M., Bell, S., Chen, S., Maric, V., and Hui, P. (2010). Precise DNA genotyping diagnosis of hydatidiform mole. Obstet Gynecol *115*, 784-794.
Liu, H., Kim, J.M., and Aoki, F. (2004a). Regulation of histone H3 lysine 9 methylation in oocytes and early pre-implantation embryos. Development *131*, 2269-2280.
Liu, J., Carmell, M.A., Rivas, F.V., Marsden, C.G., Thomson, J.M., Song, J.J., Hammond, S.M., Joshua-Tor, L., and Hannon, G.J. (2004b). Argonaute2 is the catalytic engine of mammalian RNAi. Science *305*, 1437-1441.
Liu, Y.J., Nakamura, T., and Nakano, T. (2012). Essential role of DPPA3 for chromatin condensation in mouse oocytogenesis. Biol Reprod *86*, 40.
Llewellyn-Jones, D. (1965). Trophoblastic Tumors; Geographical Variations In Incidence And Possible Aetiological Factors. J Obstet Gynaecol Br Commonw *72*, 242-248.
Longo, F.J., and Chen, D.Y. (1985). Development of cortical polarity in mouse eggs: involvement of the meiotic apparatus. Dev Biol *107*, 382-394.
Loock, J., Lamprecht, P., Timmann, C., Mrowietz, U., Csernok, E., and Gross, W.L. (2010). Genetic predisposition (NLRP3 V198M mutation) for IL-1-mediated inflammation in a patient with Schnitzler syndrome. J Allergy Clin Immunol *125*, 500-502.
Lorigan, P.C., Sharma, S., Bright, N., Coleman, R.E., and Hancock, B.W. (2000). Characteristics of women with recurrent molar pregnancies. Gynecol Oncol *78*, 288-292.
Lurain, J.R. (2011). Gestational trophoblastic disease II: classification and management of gestational trophoblastic neoplasia. Am J Obstet Gynecol *204*, 11-18.
Lykke-Andersen, K., Gilchrist, M.J., Grabarek, J.B., Das, P., Miska, E., and Zernicka-Goetz, M. (2008). Maternal Argonaute 2 is essential for early mouse development at the maternal-zygotic transition. Molecular biology of the cell *19*, 4383-4392.
Ma, J., Zeng, F., Schultz, R.M., and Tseng, H. (2006). Basonuclin: a novel mammalian maternal-effect gene. Development *133*, 2053-2062.

Ma, M., Zhou, L., Guo, X., Lv, Z., Yu, Y., Ding, C., Zhang, P., Bi, Y., Xie, J., Wang, L.*, et al.* (2009). Decreased cofilin1 expression is important for compaction during early mouse embryo development. Biochim Biophys Acta *1793*, 1804-1810.
Macara, I.G. (2001). Transport into and out of the nucleus. Microbiology and molecular biology reviews : MMBR *65*, 570-594, table of contents.
MacGregor, C., Ontiveros, E., Vargas, E., and Valenzuela, S. (1969). Hydatidiform mole. Analysis of 145 patients. Obstet Gynecol *33*, 343-351.
Mahadevan, S., Wen, S., Balasa, A., Fruhman, G., Mateus, J., Wagner, A., Al-Hussaini, T., and Van den Veyver, I.B. (2013). No evidence for mutations in NLRP7 and KHDC3L in women with androgenetic hydatidiform moles. Prenat Diagn *33*, 1242-1247.
Mahadevan, S., Wen, S., Wan, Y.W., Peng, H.H., Otta, S., Liu, Z., Iacovino, M., Mahen, E.M., Kyba, M., Sadikovic, B.*, et al.* (2014). NLRP7 affects trophoblast lineage differentiation, binds to overexpressed YY1 and alters CpG methylation. Hum Mol Genet *23*, 706-716.
Mann, M.R., and Bartolomei, M.S. (2002). Epigenetic reprogramming in the mammalian embryo: struggle of the clones. Genome biology *3*, REVIEWS1003.
Marcal, N., Patel, H., Dong, Z., Belanger-Jasmin, S., Hoffman, B., Helgason, C.D., Dang, J., and Stifani, S. (2005). Antagonistic effects of Grg6 and Groucho/TLE on the transcription repression activity of brain factor 1/FoxG1 and cortical neuron differentiation. Mol Cell Biol *25*, 10916-10929.
Marchand, F. (1895). Über die sogenannten dezidualen GeschwÜlste im Anschluß an normale Geburt, Blasenmole und Extrauterinschwangerschaft. Monatsschr Geburtshilfe Gynaekol
pp. 419-513.
Maro, B., Howlett, S.K., and Houliston, E. (1986). Cytoskeletal dynamics in the mouse egg. J Cell Sci Suppl *5*, 343-359.
Maro, B., Johnson, M.H., Pickering, S.J., and Flach, G. (1984). Changes in actin distribution during fertilization of the mouse egg. J Embryol Exp Morphol *81*, 211-237.
Martin, P.M. (1978). High frequency of hydatidiform mole in native Alaskans. Int J Gynaecol Obstet *15*, 395-396.
Matalon, M., and Modan, B. (1972). Epidemiologic aspects of hydatidiform mole in Israel. Am J Obstet Gynecol *112*, 107-112.
Matalon, M., Modan, M., Paz, B., and Modan, B. (1972). [Trophoblastic disorders in Istael]. Harefuah *83*, 566-568.
Matsui, H., Iitsuka, Y., Suzuka, K., Seki, K., and Sekiya, S. (2001). Subsequent pregnancy outcome in patients with spontaneous resolution of HCG after evacuation of hydatidiform mole: comparison between complete and partial mole. Hum Reprod *16*, 1274-1277.
Matsuura, J., Chiu, D., Jacobs, P.A., and Szulman, A.E. (1984). Complete hydatidiform mole in Hawaii: an epidemiological study. Genet Epidemiol *1*, 271-284.
Mazzanti, P., La Vecchia, C., Parazzini, F., and Bolis, G. (1986). Frequency of hydatidiform mole in Lombardy, Northern Italy. Gynecol Oncol *24*, 337-342.
McCorriston, C.C. (1968). Racial incidence of hydatidiform mole. A study in a contained polyracial community. Am J Obstet Gynecol *101*, 377-382.
McGaughey, R.W., and Capco, D.G. (1989). Specialized cytoskeletal elements in mammalian eggs: structural and biochemical evidence for their composition. Cell Motil Cytoskeleton *13*, 104-111.
McGowan, K., and Coulombe, P.A. (1998). The wound repair-associated keratins 6, 16, and 17. Insights into the role of intermediate filaments in specifying keratinocyte cytoarchitecture. Subcell Biochem *31*, 173-204.
Mertineit, C., Yoder, J.A., Taketo, T., Laird, D.W., Trasler, J.M., and Bestor, T.H. (1998). Sex-specific exons control DNA methyltransferase in mammalian germ cells. Development *125*, 889-897.
Merz, E.A., Brinster, R.L., Brunner, S., and Chen, H.Y. (1981). Protein degradation during preimplantation development of the mouse. Journal of reproduction and fertility *61*, 415-418.
Messaed, C., Akoury, E., Djuric, U., Zeng, J., Saleh, M., Gilbert, L., Seoud, M., Qureshi, S., and Slim, R. (2011a). NLRP7, a nucleotide oligomerization domain-like receptor protein, is required for normal

cytokine secretion and co-localizes with Golgi and the microtubule-organizing center. J Biol Chem *286*, 43313-43323.
Messaed, C., Chebaro, W., Di Roberto, R.B., Rittore, C., Cheung, A., Arseneau, J., Schneider, A., Chen, M.F., Bernishke, K., Surti, U.*, et al.* (2011b). NLRP7 in the spectrum of reproductive wastage: rare non-synonymous variants confer genetic susceptibility to recurrent reproductive wastage. J Med Genet *48*, 540-548.
Messinger, S.M., and Albertini, D.F. (1991). Centrosome and microtubule dynamics during meiotic progression in the mouse oocyte. J Cell Sci *100 (Pt 2)*, 289-298.
Metchat, A., Akerfelt, M., Bierkamp, C., Delsinne, V., Sistonen, L., Alexandre, H., and Christians, E.S. (2009). Mammalian heat shock factor 1 is essential for oocyte meiosis and directly regulates Hsp90alpha expression. J Biol Chem *284*, 9521-9528.
Meyer, E., Lim, D., Pasha, S., Tee, L.J., Rahman, F., Yates, J.R., Woods, C.G., Reik, W., and Maher, E.R. (2009). Germline mutation in NLRP2 (NALP2) in a familial imprinting disorder (Beckwith-Wiedemann Syndrome). PLoS Genet *5*, e1000423.
Meyer, R. (1930). In Berichte aus gynäkologischen Gesellschaften. Zentbl f Gynäk *54*, 431.
Milhavet, F., Cuisset, L., Hoffman, H.M., Slim, R., El-Shanti, H., Aksentijevich, I., Lesage, S., Waterham, H., Wise, C., Sarrauste de Menthiere, C.*, et al.* (2008). The infevers autoinflammatory mutation online registry: update with new genes and functions. Hum Mutat *29*, 803-808.
Mitsui, K., Tokuzawa, Y., Itoh, H., Segawa, K., Murakami, M., Takahashi, K., Maruyama, M., Maeda, M., and Yamanaka, S. (2003). The homeoprotein Nanog is required for maintenance of pluripotency in mouse epiblast and ES cells. Cell *113*, 631-642.
Miura, M., Ueda, A., Takao, Y., Nishimura, E.K., Koide, H., and Yokota, T. (2010). A stem cell-derived gene (Sddr) negatively regulates differentiation of embryonic stem cells. Int J Dev Biol *54*, 33-39.
Moglabey, Y.B., Kircheisen, R., Seoud, M., El Mogharbel, N., Van den Veyver, I., and Slim, R. (1999). Genetic mapping of a maternal locus responsible for familial hydatidiform moles. Hum Mol Genet *8*, 667-671.
Moos, J., Visconti, P.E., Moore, G.D., Schultz, R.M., and Kopf, G.S. (1995). Potential role of mitogen-activated protein kinase in pronuclear envelope assembly and disassembly following fertilization of mouse eggs. Biol Reprod *53*, 692-699.
Morency, E., Anguish, L., and Coonrod, S. (2011). Subcellular localization of cytoplasmic lattice-associated proteins is dependent upon fixation and processing procedures. PLoS One *6*, e17226.
Moreno, D.L., Salazar, Z., Betancourt, M., Casas, E., Ducolomb, Y., Gonzalez, C., and Bonilla, E. (2014). Sebox plays an important role during the early mouse oogenesis in vitro. Zygote *22*, 64-68.
Morita, S., Horii, T., Kimura, M., Goto, Y., Ochiya, T., and Hatada, I. (2007). One Argonaute family member, Eif2c2 (Ago2), is essential for development and appears not to be involved in DNA methylation. Genomics *89*, 687-696.
Mueller-Pillasch, F., Lacher, U., Wallrapp, C., Micha, A., Zimmerhackl, F., Hameister, H., Varga, G., Friess, H., Buchler, M., Beger, H.G.*, et al.* (1997). Cloning of a gene highly overexpressed in cancer coding for a novel KH-domain containing protein. Oncogene *14*, 2729-2733.
Muhlstein, J., Golfier, F., Rittore, C., Hajri, T., Philibert, L., Abel, F., Beneteau, C., and Touitou, I. (2011). The spectrum of NLRP7 mutations in French patients with recurrent hydatidiform mole. Eur J Obstet Gynecol Reprod Biol *157*, 197-199.
Murchison, E.P., and Hannon, G.J. (2004). miRNAs on the move: miRNA biogenesis and the RNAi machinery. Current opinion in cell biology *16*, 223-229.
Murchison, E.P., Stein, P., Xuan, Z., Pan, H., Zhang, M.Q., Schultz, R.M., and Hannon, G.J. (2007). Critical roles for Dicer in the female germline. Genes & development *21*, 682-693.
Murdoch, S., Djuric, U., Mazhar, B., Seoud, M., Khan, R., Kuick, R., Bagga, R., Kircheisen, R., Ao, A., Ratti, B.*, et al.* (2006). Mutations in NALP7 cause recurrent hydatidiform moles and reproductive wastage in humans. Nat Genet *38*, 300-302.

Musco, G., Stier, G., Joseph, C., Castiglione Morelli, M.A., Nilges, M., Gibson, T.J., and Pastore, A. (1996). Three-dimensional structure and stability of the KH domain: molecular insights into the fragile X syndrome. Cell *85*, 237-245.
Na, J., and Zernicka-Goetz, M. (2006). Asymmetric positioning and organization of the meiotic spindle of mouse oocytes requires CDC42 function. Curr Biol *16*, 1249-1254.
Nagashima, T., Maruyama, T., Furuya, M., Kajitani, T., Uchida, H., Masuda, H., Ono, M., Arase, T., Ozato, K., and Yoshimura, Y. (2007). Histone acetylation and subcellular localization of chromosomal protein BRD4 during mouse oocyte meiosis and mitosis. Mol Hum Reprod *13*, 141-148.
Nakamura, T., Arai, Y., Umehara, H., Masuhara, M., Kimura, T., Taniguchi, H., Sekimoto, T., Ikawa, M., Yoneda, Y., Okabe, M.*, et al.* (2007). PGC7/Stella protects against DNA demethylation in early embryogenesis. Nat Cell Biol *9*, 64-71.
Nakano, R., Sasaki, K., Yamoto, M., and Hata, H. (1980). Trophoblastic disease: analysis of 342 patients. Gynecol Obstet Invest *11*, 237-242.
Narducci, M.G., Fiorenza, M.T., Kang, S.M., Bevilacqua, A., Di Giacomo, M., Remotti, D., Picchio, M.C., Fidanza, V., Cooper, M.D., Croce, C.M.*, et al.* (2002). TCL1 participates in early embryonic development and is overexpressed in human seminomas. Proc Natl Acad Sci U S A *99*, 11712-11717.
Natoli, W.J., and Rashad, M.N. (1972). Hawaiian moles. Am J Roentgenol Radium Ther Nucl Med *114*, 142-144.
Ness, R.B., Grisso, J.A., Hirschinger, N., Markovic, N., Shaw, L.M., Day, N.L., and Kline, J. (1999). Cocaine and tobacco use and the risk of spontaneous abortion. N Engl J Med *340*, 333-339.
Nguyen, N.M., and Slim, R. (2014). Genetics and Epigenetics of Recurrent Hydatidiform Moles: Basic Science and Genetic Counselling. Current obstetrics and gynecology reports *3*, 55-64.
Nguyen, N.M., Zhang, L., Reddy, R., Dery, C., Arseneau, J., Cheung, A., Surti, U., Hoffner, L., Seoud, M., Zaatari, G.*, et al.* (2014). Comprehensive genotype-phenotype correlations between NLRP7 mutations and the balance between embryonic tissue differentiation and trophoblastic proliferation. J Med Genet *51*, 623-634.
Nichols, J., Zevnik, B., Anastassiadis, K., Niwa, H., Klewe-Nebenius, D., Chambers, I., Scholer, H., and Smith, A. (1998). Formation of pluripotent stem cells in the mammalian embryo depends on the POU transcription factor Oct4. Cell *95*, 379-391.
O'Carroll, D., Erhardt, S., Pagani, M., Barton, S.C., Surani, M.A., and Jenuwein, T. (2001). The polycomb-group gene Ezh2 is required for early mouse development. Mol Cell Biol *21*, 4330-4336.
Ogunbode, O. (1978). Benign hydatidiform mole in Ibadan, Nigeria. Int J Gynaecol Obstet *15*, 387-390.
Oh, B., Hwang, S.Y., Solter, D., and Knowles, B.B. (1997). Spindlin, a major maternal transcript expressed in the mouse during the transition from oocyte to embryo. Development *124*, 493-503.
Ohama, K., Okamoto, E., Nomura, K., Fujiwara, A., and Fukuda, Y. (1981). [Genetic studies of hydatidiform mole with 46,XY karyotype (author's transl)]. Nihon Sanka Fujinka Gakkai Zasshi *33*, 1664-1668.
Ohno, S., Kinoshita, T., Ohno, Y., Minamoto, T., Suzuki, N., Inoue, M., and Suda, T. (2008). Expression of NLRP7 (PYPAF3, NALP7) protein in endometrial cancer tissues. Anticancer Res *28*, 2493-2497.
Ohsugi, M., Zheng, P., Baibakov, B., Li, L., and Dean, J. (2008). Maternally derived FILIA-MATER complex localizes asymmetrically in cleavage-stage mouse embryos. Development *135*, 259-269.
Okada, K., Hirota, E., Mizutani, Y., Fujioka, T., Shuin, T., Miki, T., Nakamura, Y., and Katagiri, T. (2004). Oncogenic role of NALP7 in testicular seminomas. Cancer Sci *95*, 949-954.
Okamura, K., and Lai, E.C. (2008). Endogenous small interfering RNAs in animals. Nature reviews *9*, 673-678.
Okano, M., Bell, D.W., Haber, D.A., and Li, E. (1999). DNA methyltransferases Dnmt3a and Dnmt3b are essential for de novo methylation and mammalian development. Cell *99*, 247-257.
Olesnicky, G., Long, A.R., Quinn, M.A., Pepperell, R.J., Fortune, D.W., and Kneale, B.L. (1985). Hydatidiform mole in Victoria: aetiology and natural history. Aust N Z J Obstet Gynaecol *25*, 1-7.
Ooga, M., Inoue, A., Kageyama, S., Akiyama, T., Nagata, M., and Aoki, F. (2008). Changes in H3K79 methylation during preimplantation development in mice. Biol Reprod *78*, 413-424.

Ostareck-Lederer, A., Ostareck, D.H., and Hentze, M.W. (1998). Cytoplasmic regulatory functions of the KH-domain proteins hnRNPs K and E1/E2. Trends Biochem Sci *23*, 409-411.
Paksoy, N., and Reich, B. (1989). The occurrence of trophoblastic disease in Western Samoa. N Z Med J *102*, 162-163.
Palacios, M.J., Joshi, H.C., Simerly, C., and Schatten, G. (1993). Gamma-tubulin reorganization during mouse fertilization and early development. J Cell Sci *104 (Pt 2)*, 383-389.
Palmer, J.R. (1994). Advances in the epidemiology of gestational trophoblastic disease. J Reprod Med *39*, 155-162.
Palmer, J.R., Driscoll, S.G., Rosenberg, L., Berkowitz, R.S., Lurain, J.R., Soper, J., Twiggs, L.B., Gershenson, D.M., Kohorn, E.I., Berman, M.*, et al.* (1999). Oral contraceptive use and risk of gestational trophoblastic tumors. J Natl Cancer Inst *91*, 635-640.
Palmieri, S.L., Peter, W., Hess, H., and Scholer, H.R. (1994). Oct-4 transcription factor is differentially expressed in the mouse embryo during establishment of the first two extraembryonic cell lineages involved in implantation. Dev Biol *166*, 259-267.
Panning, B., and Jaenisch, R. (1996). DNA hypomethylation can activate Xist expression and silence X-linked genes. Genes & development *10*, 1991-2002.
Parazzini, F., La Vecchia, C., Mangili, G., Caminiti, C., Negri, E., Cecchetti, G., and Fasoli, M. (1988). Dietary factors and risk of trophoblastic disease. Am J Obstet Gynecol *158*, 93-99.
Parazzini, F., Mangili, G., La Vecchia, C., Negri, E., Bocciolone, L., and Fasoli, M. (1991). Risk factors for gestational trophoblastic disease: a separate analysis of complete and partial hydatidiform moles. Obstet Gynecol *78*, 1039-1045.
Park, K.E., Magnani, L., and Cabot, R.A. (2009). Differential remodeling of mono- and trimethylated H3K27 during porcine embryo development. Mol Reprod Dev *76*, 1033-1042.
Park, M.W., Kim, K.H., Kim, E.Y., Lee, S.Y., Ko, J.J., and Lee, K.A. (2015). Associations among Sebox and other MEGs and its effects on early embryogenesis. PLoS One *10*, e0115050.
Paroush, Z., Finley, R.L., Jr., Kidd, T., Wainwright, S.M., Ingham, P.W., Brent, R., and Ish-Horowicz, D. (1994). Groucho is required for Drosophila neurogenesis, segmentation, and sex determination and interacts directly with hairy-related bHLH proteins. Cell *79*, 805-815.
Parry, D.A., Logan, C.V., Hayward, B.E., Shires, M., Landolsi, H., Diggle, C., Carr, I., Rittore, C., Touitou, I., Philibert, L.*, et al.* (2011). Mutations causing familial biparental hydatidiform mole implicate c6orf221 as a possible regulator of genomic imprinting in the human oocyte. Am J Hum Genet *89*, 451-458.
Pascasio, F.M., Suarez, R., Manuel-Limson, G.A., and Gonzales-Germar, E.G. (1970). Serum protein changes in hydatidiform moles. Am J Obstet Gynecol *107*, 972-973.
Pattabiraman, S., Baumann, C., Guisado, D., Eppig, J.J., Schimenti, J.C., and De La Fuente, R. (2015). Mouse BRWD1 is critical for spermatid postmeiotic transcription and female meiotic chromosome stability. The Journal of cell biology *208*, 53-69.
Payer, B., Saitou, M., Barton, S.C., Thresher, R., Dixon, J.P., Zahn, D., Colledge, W.H., Carlton, M.B., Nakano, T., and Surani, M.A. (2003). Stella is a maternal effect gene required for normal early development in mice. Curr Biol *13*, 2110-2117.
Peng, H., Chang, B., Lu, C., Su, J., Wu, Y., Lv, P., Wang, Y., Liu, J., Zhang, B., Quan, F.*, et al.* (2012). Nlrp2, a maternal effect gene required for early embryonic development in the mouse. PLoS One *7*, e30344.
Peng, H., Liu, F., Li, W., and Zhang, W. (2015). Knockdown of NLRP5 arrests early embryogenesis in sows. Animal reproduction science *163*, 151-156.
Petrussa, L., Van de Velde, H., and De Rycke, M. (2014). Dynamic regulation of DNA methyltransferases in human oocytes and preimplantation embryos after assisted reproductive technologies. Mol Hum Reprod *20*, 861-874.
Pey, R., Vial, C., Schatten, G., and Hafner, M. (1998). Increase of intracellular Ca2+ and relocation of E-cadherin during experimental decompaction of mouse embryos. Proc Natl Acad Sci U S A *95*, 12977-12982.

Pfender, S., Kuznetsov, V., Pleiser, S., Kerkhoff, E., and Schuh, M. (2011). Spire-type actin nucleators cooperate with Formin-2 to drive asymmetric oocyte division. Curr Biol *21*, 955-960.
Philipps, D.L., Wigglesworth, K., Hartford, S.A., Sun, F., Pattabiraman, S., Schimenti, K., Handel, M., Eppig, J.J., and Schimenti, J.C. (2008). The dual bromodomain and WD repeat-containing mouse protein BRWD1 is required for normal spermiogenesis and the oocyte-embryo transition. Dev Biol *317*, 72-82.
Pierre, A., Gautier, M., Callebaut, I., Bontoux, M., Jeanpierre, E., Pontarotti, P., and Monget, P. (2007). Atypical structure and phylogenomic evolution of the new eutherian oocyte- and embryo-expressed KHDC1/DPPA5/ECAT1/OOEP gene family. Genomics *90*, 583-594.
Poueymirou, W.T., and Schultz, R.M. (1987). Differential effects of activators of cAMP-dependent protein kinase and protein kinase C on cleavage of one-cell mouse embryos and protein synthesis and phosphorylation in one- and two-cell embryos. Dev Biol *121*, 489-498.
Pour-Reza, M., Agheli, N., and Vaghefi, S.B. (1974). Serum creatinine, urea, and protein level changes in hydatidiform mole. JAMA *230*, 580-581.
Prickett, A.R., and Oakey, R.J. (2012). A survey of tissue-specific genomic imprinting in mammals. Mol Genet Genomics *287*, 621-630.
Puechberty, J., Rittore, C., Philibert, L., Lefort, G., Burlet, G., Benos, P., Reyftmann, L., Sarda, P., and Touitou, I. (2009). Homozygous NLRP7 mutations in a Moroccan woman with recurrent reproductive failure. Clin Genet *75*, 298-300.
Qian, J., Cheng, Q., Murdoch, S., Xu, C., Jin, F., Chebaro, W., Zhang, X., Gao, H., Zhu, Y., Slim, R.*, et al.* (2011). The Genetics of Recurrent Hydatidiform Moles in China: Correlations between NLRP7 Mutations, Molar Genotypes, and Reproductive Outcomes. Mol Hum Reprod *17*, 612-619.
Qian, J., Deveault, C., Bagga, R., Xie, X., and Slim, R. (2007). Women heterozygous for NALP7/NLRP7 mutations are at risk for reproductive wastage: report of two novel mutations. Hum Mutat *28*, 741.
Qiao, J., Chen, Y., Yan, L.Y., Yan, J., Liu, P., and Sun, Q.Y. (2010). Changes in histone methylation during human oocyte maturation and IVF- or ICSI-derived embryo development. Fertility and sterility *93*, 1628-1636.
Racedo, S.E., Wrenzycki, C., Lepikhov, K., Salamone, D., Walter, J., and Niemann, H. (2009). Epigenetic modifications and related mRNA expression during bovine oocyte in vitro maturation. Reprod Fertil Dev *21*, 738-748.
Radian, A.D., Khare, S., Chu, L.H., Dorfleutner, A., and Stehlik, C. (2015). ATP binding by NLRP7 is required for inflammasome activation in response to bacterial lipopeptides. Molecular immunology *67*, 294-302.
Ramos, S.B., Stumpo, D.J., Kennington, E.A., Phillips, R.S., Bock, C.B., Ribeiro-Neto, F., and Blackshear, P.J. (2004). The CCCH tandem zinc-finger protein Zfp36l2 is crucial for female fertility and early embryonic development. Development *131*, 4883-4893.
Reddy, R., Akoury, E., Phuong Nguyen, N.M., Abdul-Rahman, O.A., Dery, C., Gupta, N., Daley, W.P., Ao, A., Landolsi, H., Ann Fisher, R.*, et al.* (2013). Report of four new patients with protein-truncating mutations in C6orf221/KHDC3L and colocalization with NLRP7. Eur J Hum Genet *21*, 957-964.
Redline, R.W., Hassold, T., and Zaragoza, M.V. (1998). Prevalence of the partial molar phenotype in triploidy of maternal and paternal origin. Human pathology *29*, 505-511.
Reik, W., Dean, W., and Walter, J. (2001). Epigenetic reprogramming in mammalian development. Science *293*, 1089-1093.
Reik, W., and Walter, J. (2001). Genomic imprinting: parental influence on the genome. Nat Rev Genet *2*, 21-32.
Reyes, M.B.a.J. (1993). Gestational trophoblastic disease among adolescents. Journal of pediatric and adolescent gynecology *6*, 220-222.
Reynolds, S.R. (1976). Hydatidiform mole: a vascular congenital anomaly. Obstet Gynecol *47*, 244-250.
Ricci, J.V. (1950). Aetios of Amida: The Gynaecology and Obstetrics of the VIth Century, A.D., Vol 1 (Philadelphia: The Blakiston Company).
Ridley, A.J. (2001). Rho family proteins: coordinating cell responses. Trends in cell biology *11*, 471-477.

Ringertz, N. (1970). Hydatidiform mole, invasive mole and choriocarcinoma in Sweden 1958-1965. Acta Obstet Gynecol Scand *49*, 195-203.
Robson, R.M. (1989). Intermediate filaments. Current opinion in cell biology *1*, 36-43.
Roest, H.P., Baarends, W.M., de Wit, J., van Klaveren, J.W., Wassenaar, E., Hoogerbrugge, J.W., van Cappellen, W.A., Hoeijmakers, J.H., and Grootegoed, J.A. (2004). The ubiquitin-conjugating DNA repair enzyme HR6A is a maternal factor essential for early embryonic development in mice. Mol Cell Biol *24*, 5485-5495.
Rolon, P.A., and de Lopez, B.H. (1977). Epidemiological aspects of hydatidiform mole in the Republic of Paraguay (South America). Br J Obstet Gynaecol *84*, 862-864.
Rolon, P.A., Hochsztajn, B., and Llamosas, F. (1990). Epidemiology of complete hydatidiform mole in Paraguay. J Reprod Med *35*, 15-18.
Rothnagel, J.A., and Rogers, G.E. (1984). Citrulline in proteins from the enzymatic deimination of arginine residues. Methods Enzymol *107*, 624-631.
Sanchez-Delgado, M., Martin-Trujillo, A., Tayama, C., Vidal, E., Esteller, M., Iglesias-Platas, I., Deo, N., Barney, O., Maclean, K., Hata, K.*, et al.* (2015). Absence of Maternal Methylation in Biparental Hydatidiform Moles from Women with NLRP7 Maternal-Effect Mutations Reveals Widespread Placenta-Specific Imprinting. PLoS Genet *11*, e1005644.
Sand, P.K., Lurain, J.R., and Brewer, J.I. (1984). Repeat gestational trophoblastic disease. Obstet Gynecol *63*, 140-144.
Santos, F., Hendrich, B., Reik, W., and Dean, W. (2002). Dynamic reprogramming of DNA methylation in the early mouse embryo. Dev Biol *241*, 172-182.
Sarmento, O.F., Digilio, L.C., Wang, Y., Perlin, J., Herr, J.C., Allis, C.D., and Coonrod, S.A. (2004). Dynamic alterations of specific histone modifications during early murine development. J Cell Sci *117*, 4449-4459.
Sato, M., Kimura, T., Kurokawa, K., Fujita, Y., Abe, K., Masuhara, M., Yasunaga, T., Ryo, A., Yamamoto, M., and Nakano, T. (2002). Identification of PGC7, a new gene expressed specifically in preimplantation embryos and germ cells. Mech Dev *113*, 91-94.
Savage, P., Williams, J., Wong, S.L., Short, D., Casalboni, S., Catalano, K., and Seckl, M. (2010). The demographics of molar pregnancies in England and Wales from 2000-2009. J Reprod Med *55*, 341-345.
Savage, P.M., Sita-Lumsden, A., Dickson, S., Iyer, R., Everard, J., Coleman, R., Fisher, R.A., Short, D., Casalboni, S., Catalano, K.*, et al.* (2013). The relationship of maternal age to molar pregnancy incidence, risks for chemotherapy and subsequent pregnancy outcome. J Obstet Gynaecol *33*, 406-411.
Schatten, H., Schatten, G., Mazia, D., Balczon, R., and Simerly, C. (1986). Behavior of centrosomes during fertilization and cell division in mouse oocytes and in sea urchin eggs. Proc Natl Acad Sci U S A *83*, 105-109.
Schuh, M., and Ellenberg, J. (2008). A new model for asymmetric spindle positioning in mouse oocytes. Curr Biol *18*, 1986-1992.
Sebastian, A. (1999). A dictionary of the history of medicine (New york: The Parthenon Publishing Group Inc).
Sebire, N.J., Fisher, R.A., Foskett, M., Rees, H., Seckl, M.J., and Newlands, E.S. (2003a). Risk of recurrent hydatidiform mole and subsequent pregnancy outcome following complete or partial hydatidiform molar pregnancy. BJOG: An International Journal of Obstetrics and Gynaecology *110*, 22-26.
Sebire, N.J., Fisher, R.A., and Rees, H.C. (2003b). Histopathological diagnosis of partial and complete hydatidiform mole in the first trimester of pregnancy. Pediatr Dev Pathol *6*, 69-77.
Sebire, N.J., Savage, P.M., Seckl, M.J., and Fisher, R.A. (2013). Histopathological features of biparental complete hydatidiform moles in women with NLRP7 mutations. Placenta *34*, 50-56.
Seckl, M.J., Sebire, N.J., and Berkowitz, R.S. (2010). Gestational trophoblastic disease. Lancet.
Sekiguchi, S., Kwon, J., Yoshida, E., Hamasaki, H., Ichinose, S., Hideshima, M., Kuraoka, M., Takahashi, A., Ishii, Y., Kyuwa, S.*, et al.* (2006). Localization of ubiquitin C-terminal hydrolase L1 in

mouse ova and its function in the plasma membrane to block polyspermy. The American journal of pathology *169*, 1722-1729.
Senshu, T. (1990). [Recent progress in peptidylarginine deiminase research]. Seikagaku *62*, 192-196.
Sensi, A., Gualandi, F., Pittalis, M.C., Calabrese, O., Falciano, F., Maestri, I., Bovicelli, L., and Calzolari, E. (2000). Mole maker phenotype: possible narrowing of the candidate region. Eur J Hum Genet *8*, 641-644.
Shain, K.H., Landowski, T.H., and Dalton, W.S. (2002). Adhesion-mediated intracellular redistribution of c-Fas-associated death domain-like IL-1-converting enzyme-like inhibitory protein-long confers resistance to CD95-induced apoptosis in hematopoietic cancer cell lines. J Immunol *168*, 2544-2553.
Shang, E.R. (1982). [A retrospective investigation on the incidence of hydatidiform mole in 20,548 fertile women]. Zhonghua Yi Xue Za Zhi *62*, 282-285.
Shapiro, R., and Vallee, B.L. (1991). Interaction of human placental ribonuclease with placental ribonuclease inhibitor. Biochemistry *30*, 2246-2255.
Singer, H., Biswas, A., Nuesgen, N., Oldenburg, J., and El-Maarri, O. (2015). NLRP7, Involved in Hydatidiform Molar Pregnancy (HYDM1), Interacts with the Transcriptional Repressor ZBTB16. PLoS One *10*, e0130416.
Singer, H., Biswas, A., Zimmer, N., Messaed, C., Oldenburg, J., Slim, R., and El-Maarri, O. (2014). NLRP7 inter-domain interactions: the NACHT-associated domain is the physical mediator for oligomeric assembly. Mol Hum Reprod *20*, 990-1001.
Skalli, O., and Goldman, R.D. (1991). Recent insights into the assembly, dynamics, and function of intermediate filament networks. Cell Motil Cytoskeleton *19*, 67-79.
Slim, R., Ao, A., Surti, U., Zhang, L., Hoffner, L., Arseneau, J., Cheung, A., Chebaro, W., and Wischmeijer, A. (2011). Recurrent triploid and dispermic conceptions in patients with NLRP7 mutations. Placenta *32*, 409-412.
Slim, R., Bagga, R., Chebaro, W., Srinivasan, R., and Agarwal, N. (2009). A strong founder effect for two NLRP7 mutations in the Indian population: an intriguing observation. Clin Genet *76*, 292-295.
Slim, R., and Mehio, A. (2007). The genetics of hydatidiform moles: new lights on an ancient disease. Clinical Genetics *71*, 25-34.
Slocumb, J.C., and Lund, C.J. (1969). Incidence of trophoblastic disease: increased rate in youngest age group. Am J Obstet Gynecol *104*, 421-423.
Smith, H., and Kim, S. (2003). Epidemiology. In Gestational Trophoblastic Disease, B. Hancock, E. Newlands, R. Berkowitz, and L. Cole, eds. (http://www.isstd.org/index.html).
Solter, D. (1988). Differential imprinting and expression of maternal and paternal genomes. Annu Rev Genet *22*, 127-146.
Song H, W.B., Tang M, (1981). Trophoblastic tumors: diagnosis and treatment (Beijing, China: Capital Hospital).
Song, H.Z., and Wu, P.C. (1987). Hydatidiform mole in China: a preliminary survey of incidence on more than three million women. Bull World Health Organ *65*, 507-511.
Steigrad, S.J. (1969). The incidence of neoplastic trophoblastic disease in Australia. Aust N Z J Obstet Gynaecol *9*, 100-102.
Steigrad, S.J. (2003). Epidemiology of gestational trophoblastic diseases. Best Pract Res Clin Obstet Gynaecol *17*, 837-847.
Stevenson, A.C., Dudgeon, M.Y., and Mc, C.H. (1959). Observations on the results of pregnancies in women resident in Belfast. II. Abortions, hydatidiform moles and ectopic pregnancies. Ann Hum Genet *23*, 395-414.
Stone, M., and Bagshawe, K.D. (1976). Letter: Hydatidiform mole: two entities. Lancet *1*, 535.
Sun, S.C., Wang, Z.B., Xu, Y.N., Lee, S.E., Cui, X.S., and Kim, N.H. (2011). Arp2/3 complex regulates asymmetric division and cytokinesis in mouse oocytes. PLoS One *6*, e18392.
Sunde, L., Vejerslev, L.O., Jensen, M.P., Pedersen, S., Hertz, J.M., and Bolund, L. (1993). Genetic analysis of repeated, biparental, diploid, hydatidiform moles. Cancer genetics and cytogenetics *66*, 16-22.

Surani, M.A., Barton, S.C., Howlett, S.K., and Norris, M.L. (1988). Influence of chromosomal determinants on development of androgenetic and parthenogenetic cells. Development *103*, 171-178.
Susor, A., Liskova, L., Toralova, T., Pavlok, A., Pivonkova, K., Karabinova, P., Lopatarova, M., Sutovsky, P., and Kubelka, M. (2010). Role of ubiquitin C-terminal hydrolase-L1 in antipolyspermy defense of mammalian oocytes. Biol Reprod *82*, 1151-1161.
Suzumori, N., Burns, K.H., Yan, W., and Matzuk, M.M. (2003). RFPL4 interacts with oocyte proteins of the ubiquitin-proteasome degradation pathway. Proc Natl Acad Sci U S A *100*, 550-555.
Svoboda, P. (2010). Why mouse oocytes and early embryos ignore miRNAs? RNA biology *7*, 559-563.
Svoboda, P., and Flemr, M. (2010). The role of miRNAs and endogenous siRNAs in maternal-to-zygotic reprogramming and the establishment of pluripotency. EMBO reports *11*, 590-597.
Szulman, A.E. (1984). Syndromes of hydatidiform moles. Partial vs. complete. J Reprod Med *29*, 788-791.
Szulman, A.E., and Surti, U. (1978a). The syndromes of hydatidiform mole. I. Cytogenetic and morphologic correlations. Am J Obstet Gynecol *131*, 665-671.
Szulman, A.E., and Surti, U. (1978b). The syndromes of hydatidiform mole. II. Morphologic evolution of the complete and partial mole. Am J Obstet Gynecol *132*, 20-27.
Takeuchi, S. (1987). Incidence of gestational trophoblastic disease by regional registration in Japan. Hum Reprod *2*, 729-734.
Tam, O.H., Aravin, A.A., Stein, P., Girard, A., Murchison, E.P., Cheloufi, S., Hodges, E., Anger, M., Sachidanandam, R., Schultz, R.M.*, et al.* (2008). Pseudogene-derived small interfering RNAs regulate gene expression in mouse oocytes. Nature *453*, 534-538.
Tang, F., Barbacioru, C., Bao, S., Lee, C., Nordman, E., Wang, X., Lao, K., and Surani, M.A. (2010). Tracing the derivation of embryonic stem cells from the inner cell mass by single-cell RNA-Seq analysis. Cell Stem Cell *6*, 468-478.
Tashiro, F., Kanai-Azuma, M., Miyazaki, S., Kato, M., Tanaka, T., Toyoda, S., Yamato, E., Kawakami, H., Miyazaki, T., and Miyazaki, J. (2011). Maternal-effect gene Ces5/Ooep/Moep19/Floped is essential for oocyte cytoplasmic lattice formation and embryonic development at the maternal-zygotic stage transition. Genes Cells *15*, 813-828.
Taussig, F.J. (1907). The History of mole pregnancy (Medical library and historical journal).
Teoh, E.S., Dawood, M.Y., and Ratnam, S.S. (1971). Epidemiology of hydatidiform mole in Singapore. Am J Obstet Gynecol *110*, 415-420.
Tian, Q., Kopf, G.S., Brown, R.S., and Tseng, H. (2001). Function of basonuclin in increasing transcription of the ribosomal RNA genes during mouse oogenesis. Development *128*, 407-416.
Tian, X., Pascal, G., and Monget, P. (2009). Evolution and functional divergence of NLRP genes in mammalian reproductive systems. BMC Evol Biol *9*, 202.
Tomoda, Y., Fuma, M., Saiki, N., Ishizuka, N., and Akaza, T. (1976). Immunologic studies in patients with trophoblastic neoplasia. Am J Obstet Gynecol *126*, 661-667.
Tong, Z.B., Gold, L., De Pol, A., Vanevski, K., Dorward, H., Sena, P., Palumbo, C., Bondy, C.A., and Nelson, L.M. (2004). Developmental expression and subcellular localization of mouse MATER, an oocyte-specific protein essential for early development. Endocrinology *145*, 1427-1434.
Tong, Z.B., Gold, L., Pfeifer, K.E., Dorward, H., Lee, E., Bondy, C.A., Dean, J., and Nelson, L.M. (2000). Mater, a maternal effect gene required for early embryonic development in mice. Nat Genet *26*, 267-268.
Torres-Padilla, M.E., and Zernicka-Goetz, M. (2006). Role of TIF1alpha as a modulator of embryonic transcription in the mouse zygote. The Journal of cell biology *174*, 329-338.
Tschopp, J., Martinon, F., and Burns, K. (2003). NALPs: a novel protein family involved in inflammation. Nature reviews *4*, 95-104.
Tsukamoto, S., Kuma, A., and Mizushima, N. (2008a). The role of autophagy during the oocyte-to-embryo transition. Autophagy *4*, 1076-1078.
Tsukamoto, S., Kuma, A., Murakami, M., Kishi, C., Yamamoto, A., and Mizushima, N. (2008b). Autophagy is essential for preimplantation development of mouse embryos. Science *321*, 117-120.

Van Aelst, L., and D'Souza-Schorey, C. (1997). Rho GTPases and signaling networks. Genes & development *11*, 2295-2322.
Van Blerkom, J., and Henry, G. (1988). Cytogenetic analysis of living human oocytes: cellular basis and developmental consequences of perturbations in chromosomal organization and complement. Hum Reprod *3*, 777-790.
Vargas, R., Barroilhet, L.M., Esselen, K., Diver, E., Bernstein, M., Goldstein, D.P., and Berkowitz, R.S. (2014). Subsequent pregnancy outcomes after complete and partial molar pregnancy, recurrent molar pregnancy, and gestational trophoblastic neoplasia: an update from the New England Trophoblastic Disease Center. J Reprod Med *59*, 188-194.
Vasioukhin, V., and Fuchs, E. (2001). Actin dynamics and cell-cell adhesion in epithelia. Current opinion in cell biology *13*, 76-84.
Vassena, R., Boue, S., Gonzalez-Roca, E., Aran, B., Auer, H., Veiga, A., and Izpisua Belmonte, J.C. (2011). Waves of early transcriptional activation and pluripotency program initiation during human preimplantation development. Development *138*, 3699-3709.
Vassilakos, P., and Kajii, T. (1976). Letter: Hydatidiform mole: two entities. Lancet *1*, 259.
Vassilakos, P., Riotton, G., and Kajii, T. (1977). Hydatidiform mole: two entities. A morphologic and cytogenetic study with some clinical consideration. Am J Obstet Gynecol *127*, 167-170.
Vejerslev, L.O., Sunde, L., Hansen, B.F., Larsen, J.K., Christensen, I.J., and Larsen, G. (1991). Hydatidiform mole and fetus with normal karyotype: support of a separate entity. Obstet Gynecol *77*, 868-874.
Verlhac, M.H., Kubiak, J.Z., Clarke, H.J., and Maro, B. (1994). Microtubule and chromatin behavior follow MAP kinase activity but not MPF activity during meiosis in mouse oocytes. Development *120*, 1017-1025.
Verlhac, M.H., Lefebvre, C., Guillaud, P., Rassinier, P., and Maro, B. (2000). Asymmetric division in mouse oocytes: with or without Mos. Curr Biol *10*, 1303-1306.
Verlhac, M.H., Terret, M.E., and Pintard, L. (2010). Control of the oocyte-to-embryo transition by the ubiquitin-proteolytic system in mouse and C. elegans. Current opinion in cell biology *22*, 758-763.
Vitale, A., Perlin, J., Leonelli, L., Herr, J., Wright, P., Digilio, L., and Coonrod, S. (2005). Mouse cPLA2gamma, a novel oocyte and early embryo-abundant phospholipase A2 gamma-like protein, is targeted to the nuclear envelope during germinal vesicle breakdown. Dev Biol *282*, 374-384.
Vitale, A.M., Calvert, M.E., Mallavarapu, M., Yurttas, P., Perlin, J., Herr, J., and Coonrod, S. (2007). Proteomic profiling of murine oocyte maturation. Mol Reprod Dev *74*, 608-616.
Wake, N., Takagi, N., and Sasaki, M. (1978). Androgenesis as a cause of hydatidiform mole. J Natl Cancer Inst *60*, 51-57.
Wallace, D.C., Surti, U., Adams, C.W., and Szulman, A.E. (1982). Complete moles have paternal chromosomes but maternal mitochondrial DNA. Human genetics *61*, 145-147.
Walser, C.B., and Lipshitz, H.D. (2011). Transcript clearance during the maternal-to-zygotic transition. Current opinion in genetics & development *21*, 431-443.
Wan, L.B., Pan, H., Hannenhalli, S., Cheng, Y., Ma, J., Fedoriw, A., Lobanenkov, V., Latham, K.E., Schultz, R.M., and Bartolomei, M.S. (2008). Maternal depletion of CTCF reveals multiple functions during oocyte and preimplantation embryo development. Development *135*, 2729-2738.
Wang, C.M., Dixon, P.H., Decordova, S., Hodges, M.D., Sebire, N.J., Ozalp, S., Fallahian, M., Sensi, A., Ashrafi, F., Repiska, V.*, et al.* (2009a). Identification of 13 novel NLRP7 mutations in 20 families with recurrent hydatidiform mole; missense mutations cluster in the leucine-rich region. J Med Genet *46*, 569-575.
Wang, M., Dixon, P.H., Decordova, S., Hodges, M., Sebire, N.J., Ozalp, S., Fallahian, M., Sensi, A., Ashrafi, F., Repiska, V.*, et al.* (2009b). Identification of 13 novel NLRP7 mutations in 20 families with recurrent hydatidiform mole; missense mutations cluster in the leucine rich region. J Med Genet *46*, 569-555.

Wang, Q., Ai, J.S., Idowu Ola, S., Gu, L., Zhang, Y.Z., Chen, D.Y., and Sun, Q.Y. (2008). The spatial relationship between heterochromatin protein 1 alpha and histone modifications during mouse oocyte meiosis. Cell Cycle *7*, 513-520.
Watanabe, T., Totoki, Y., Toyoda, A., Kaneda, M., Kuramochi-Miyagawa, S., Obata, Y., Chiba, H., Kohara, Y., Kono, T., Nakano, T.*, et al.* (2008). Endogenous siRNAs from naturally formed dsRNAs regulate transcripts in mouse oocytes. Nature *453*, 539-543.
Webster, S.D., and McGaughey, R.W. (1990). The cortical cytoskeleton and its role in sperm penetration of the mammalian egg. Dev Biol *142*, 61-74.
Wei, P.Y., and Ouyang, P.C. (1963). Trophoblastic diseases in Taiwan. A review of 157 cases in a 10 year period. Am J Obstet Gynecol *85*, 844-849.
Westerveld, G.H., Korver, C.M., van Pelt, A.M.M., Leschot, N.J., van der Veen, F., Repping, S., and Lombardi, M.P. (2006). Mutations in the testis-specific NALP14 gene in men suffering from spermatogenic failure. Hum Reprod *21*, 3178-3184.
Womack, C., and Elston, C.W. (1985). Hydatidiform mole in Nottingham: a 12-year retrospective epidemiological and morphological study. Placenta *6*, 93-105.
Wouters-Tyrou, D., Martinage, A., Chevaillier, P., and Sautiere, P. (1998). Nuclear basic proteins in spermiogenesis. Biochimie *80*, 117-128.
Wright, P.W., Bolling, L.C., Calvert, M.E., Sarmento, O.F., Berkeley, E.V., Shea, M.C., Hao, Z., Jayes, F.C., Bush, L.A., Shetty, J.*, et al.* (2003). ePAD, an oocyte and early embryo-abundant peptidylarginine deiminase-like protein that localizes to egg cytoplasmic sheets. Dev Biol *256*, 73-88.
Wu, X. (2009). Maternal depletion of NLRP5 blocks early embryogenesis in rhesus macaque monkeys (Macaca mulatta). Hum Reprod *24*, 415-424.
Wu, X., Viveiros, M.M., Eppig, J.J., Bai, Y., Fitzpatrick, S.L., and Matzuk, M.M. (2003). Zygote arrest 1 (Zar1) is a novel maternal-effect gene critical for the oocyte-to-embryo transition. Nat Genet *33*, 187-191.
Xue, Z., Huang, K., Cai, C., Cai, L., Jiang, C.Y., Feng, Y., Liu, Z., Zeng, Q., Cheng, L., Sun, Y.E.*, et al.* (2013). Genetic programs in human and mouse early embryos revealed by single-cell RNA sequencing. Nature *500*, 593-597.
Yamashita, K., Wake, N., Araki, T., Ichinoe, K., and Makoto, K. (1979). Human lymphocyte antigen expression in hydatidiform mole: androgenesis following fertilization by a haploid sperm. Am J Obstet Gynecol *135*, 597-600.
Yan, W., Ma, L., Stein, P., Pangas, S.A., Burns, K.H., Bai, Y., Schultz, R.M., and Matzuk, M.M. (2005). Mice deficient in oocyte-specific oligoadenylate synthetase-like protein OAS1D display reduced fertility. Mol Cell Biol *25*, 4615-4624.
Yen, S., and MacMahon, B. (1968). Epidemiologic features of trophoblastic disease. Am J Obstet Gynecol *101*, 126-132.
Yeung, J., O'Sullivan, E., Hubank, M., and Brady, H.J. (2004). E4BP4 expression is regulated by the t(17;19)-associated oncoprotein E2A-HLF in pro-B cells. Br J Haematol *125*, 560-567.
Yoder, J.A., Walsh, C.P., and Bestor, T.H. (1997). Cytosine methylation and the ecology of intragenomic parasites. Trends in genetics : TIG *13*, 335-340.
Yu, L.Z., Xiong, B., Gao, W.X., Wang, C.M., Zhong, Z.S., Huo, L.J., Wang, Q., Hou, Y., Liu, K., Liu, X.J.*, et al.* (2007). MEK1/2 regulates microtubule organization, spindle pole tethering and asymmetric division during mouse oocyte meiotic maturation. Cell Cycle *6*, 330-338.
Yu, X.J., Yi, Z., Gao, Z., Qin, D., Zhai, Y., Chen, X., Ou-Yang, Y., Wang, Z.B., Zheng, P., Zhu, M.S.*, et al.* (2014). The subcortical maternal complex controls symmetric division of mouse zygotes by regulating F-actin dynamics. Nat Commun *5*, 4887.
Yurttas, P., Morency, E., and Coonrod, S.A. (2010). Use of proteomics to identify highly abundant maternal factors that drive the egg-to-embryo transition. Reproduction *139*, 809-823.
Yurttas, P., Vitale, A.M., Fitzhenry, R.J., Cohen-Gould, L., Wu, W., Gossen, J.A., and Coonrod, S.A. (2008). Role for PADI6 and the cytoplasmic lattices in ribosomal storage in oocytes and translational control in the early mouse embryo. Development *135*, 2627-2636.

Zamboni, L., Chakraborty, J., and Smith, D.M. (1972). First cleavage division of the mouse zygot. An ultrastructural study. Biol Reprod *7*, 170-193.
Zhang, C., and Clarke, P.R. (2000). Chromatin-independent nuclear envelope assembly induced by Ran GTPase in Xenopus egg extracts. Science *288*, 1429-1432.
Zhang, P., Dixon, M., Zucchelli, M., Hambiliki, F., Levkov, L., Hovatta, O., and Kere, J. (2008). Expression analysis of the NLRP gene family suggests a role in human preimplantation development. PLoS ONE *3*, e2755.
Zhang, P., Zucchelli, M., Bruce, S., Hambiliki, F., Stavreus-Evers, A., Levkov, L., Skottman, H., Kerkela, E., Kere, J., and Hovatta, O. (2009). Transcriptome profiling of human pre-implantation development. PLoS One *4*, e7844.
Zhang, Y., Duan, X., Cao, R., Liu, H.L., Cui, X.S., Kim, N.H., Rui, R., and Sun, S.C. (2014). Small GTPase RhoA regulates cytoskeleton dynamics during porcine oocyte maturation and early embryo development. Cell Cycle *13*, 3390-3403.
Zhao, B., Zhang, W.D., Duan, Y.L., Lu, Y.Q., Cun, Y.X., Li, C.H., Guo, K., Nie, W.H., Li, L., Zhang, R., *et al.* (2015). Filia Is an ESC-Specific Regulator of DNA Damage Response and Safeguards Genomic Stability. Cell Stem Cell *16*, 684-698.
Zheng, P., Baibakov, B., Wang, X.H., and Dean, J. (2013a). PtdIns(3,4,5)P3 is constitutively synthesized and required for spindle translocation during meiosis in mouse oocytes. J Cell Sci *126*, 715-721.
Zheng, P., and Dean, J. (2009). Role of Filia, a maternal effect gene, in maintaining euploidy during cleavage-stage mouse embryogenesis. Proceedings of the National Academy of Sciences *106*, 7473-7478.
Zheng, Z., Zhao, M.H., Jia, J.L., Heo, Y.T., Cui, X.S., Oh, J.S., and Kim, N.H. (2013b). Knockdown of maternal homeobox transcription factor SEBOX gene impaired early embryonic development in porcine parthenotes. The Journal of reproduction and development *59*, 557-562.
Zhu, J., and Chen, X. (2000). MCG10, a novel p53 target gene that encodes a KH domain RNA-binding protein, is capable of inducing apoptosis and cell cycle arrest in G(2)-M. Mol Cell Biol *20*, 5602-5618.
Zhu, K., Yan, L., Zhang, X., Lu, X., Wang, T., Yan, J., Liu, X., Qiao, J., and Li, L. (2015). Identification of a human subcortical maternal complex. Mol Hum Reprod *21*, 320-329.
Zondek, B. (1929). Hypophysenvorderlappen und Schwangerschaft Endokrinologie *5*, 425-434.

LIST OF WEBSITES

http://bestpractice.bmj.com/best-practice/monograph/1136/resources/image/bp/1.html
http://biogps.org
http://imagej.nih.gov/ij
http://quizlet.com/60102001/reproductive-flash-cards
http://rsb.info.nih.gov/ij
http://www.genecards.org
http://www.hgmd.org
http://www.mediacy.com
http://www.perkinelmer.co.uk
http://www.uniprot.org

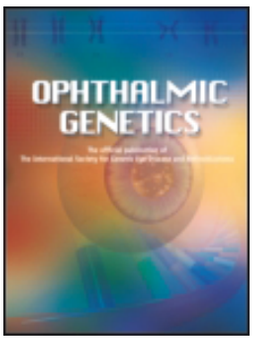

Ophthalmic Genetics

ISSN: 1381-6810 (Print) 1744-5094 (Online) Journal homepage: http://www.tandfonline.com/loi/iopg20

A novel 5-bp deletion in Clarin 1 in a family with Usher syndrome

Elie Akoury, Elie El Zir, Ahmad Mansour, André Mégarbané, Jacek Majewski & Rima Slim

To cite this article: Elie Akoury, Elie El Zir, Ahmad Mansour, André Mégarbané, Jacek Majewski & Rima Slim (2011) A novel 5-bp deletion in Clarin 1 in a family with Usher syndrome, Ophthalmic Genetics, 32:4, 245-249

To link to this article: http://dx.doi.org/10.3109/13816810.2011.587083

Published online: 15 Jun 2011.

Ophthalmic Genetics, 32(4), 245–249, 2011

ISSN: 1381-6810 print/ 1744-5094 online
DOI: 10.3109/13816810.2011.587083

informa
healthcare

CASE REPORT

A novel 5-bp deletion in Clarin 1 in a family with Usher syndrome

Elie Akoury[1], Elie El Zir[2], Ahmad Mansour[3], André Mégarbané[4], Jacek Majewski[5], and Rima Slim[1]

[1]Departments of Human Genetics and Obstetrics-Gynecology, McGill University Health Centre, Montreal, Canada, [2]Department of Otorhinolaryngology, Hôpital Sacré-Coeur, Baabda, Lebanon, [3]Department of Ophthalmology, American University of Beirut, Lebanon, [4]Unité de génétique médicale, Faculté de médecine, Université Saint Joseph, Beirut, Lebanon, and [5]McGill University and Genome Quebec Innovation Centre and Department of Human Genetics, McGill University Health Centre, Montreal, Canada

ABSTRACT

Background: To identify the genetic defect in a Lebanese family with two sibs diagnosed with Usher Syndrome.

Materials and Methods: Exome capture and sequencing were performed on DNA from one affected member using Agilent in solution bead capture, followed by Illumina sequencing.

Results: This analysis revealed the presence of a novel homozygous 5-bp deletion, in Clarin 1 (*CLRN1*), a known gene responsible for Usher syndrome type III. The deletion is inherited from both parents and segregates with the disease phenotype in the family. The 5-bp deletion, c.301_305delGTCAT, p.Val101SerfsX27, is predicted to result in a frameshift and protein truncation after 27 amino acids. Sequencing all the coding regions of the *CLRN1* gene in the proband did not reveal any other mutation or variant.

Conclusion: Here we describe a novel deletion in *CLRN1*. Our data support previously reported intra familial variability in the clinical features of Usher syndrome type I and III.

Keywords: clarin 1, mutation, Usher syndrome, exome sequencing, deletion

INTRODUCTION

Usher syndrome (USH) is an autosomal recessive disorder combining sensorineural hearing loss and retinitis pigmentosa (RP). It is the leading cause of deaf-blindness in humans with a prevalence estimated to range from 2–6.2 per 100,000 (for reviews see[1,2]). Three distinct clinical subtypes have been described. USH type 1 (USH1) represents the most severe form and is characterized by a profound hearing loss, a vestibular dysfunction and a prepubertal onset of RP. USH type II (USH2) is characterized by a milder hearing loss with no vestibular function impairment and RP. Usher type III (USH3) is defined by the association of a postlingual progressive hearing loss, occasional vestibular dysfunction, and RP (for reviews see [3,4]). To date, mutations in nine genes are known to be responsible for Usher syndrome, of which five genes, *MYO7A*, harmonin, *CDH23*, *PCDH15*, and *USH1G*, are responsible for USH1 and one gene, *CLRN1*, is responsible for USH3[5]. Several *CLRN1* splice isoforms have been described with the main one being formed by three exons, named 0, 2, and 3, encoding a 232 amino acid protein.[6–8] CLRN1 belongs to a large family of transmembrane proteins including both the tetraspanin and the claudin families. Members of this family have several roles including regulating cell morphology, motility, invasion, fusion, and signaling.[9–11] Here we describe a new family with USH in which a novel homozygous 5-bp deletion in *CLRN1* was found.

MATERIALS AND METHODS

Family data

Patient recruitment was done at the American University of Beirut, had the approval of its Ethics

Received 03 March 2011; revised 18 April 2011; accepted 01 May 2011

Correspondence: Rima Slim, Montreal General Hospital Research Institute, L3-121, 1650 Cedar Avenue, Montreal, P.Q., Canada H3G 1A4. Tel: +1 514 934 1934 Ext: 44550. Fax: +1 514 934 8261. E-mail: rima.slim@muhc.mcgill.ca

Committee, and conformed to the Declaration of Helsinki. Audiometric examination of the two patients included air conduction, bone conduction and discrimination thresholds. Electronystagmography was used to assess spontaneous and positional nystagmus. A standard caloric test (30°C and 44°C) was performed using an ICS caloric irrigation system and observation of the nystagmus using Frenzel's glasses. Ocular examinations included measurement of visual acuity, funduscopy, visual field examination, color vision testing, and retinoscopy. Blood samples were taken from all members of this family, USHLB3,[12] and DNA was extracted according to standard methods.

Exome capture and sequencing

The strategy employed here was similar to that described earlier.[13] Briefly, exome capture was performed using the Agilent in solution bead capture, all-exon v1 kits, on genomic DNA from one affected member, III-5. Sequencing was carried out using one lane, single end 76 base reads, on the Illumina GAIIx sequencer. This resulted in an approximately 30X average genome-wide coverage of the targeted coding exons. The reads were aligned to the reference genome (hg19) using BWA.[14] Variants were called using the SAMTools[15] software. The list of variants was filtered against more than 30 of individual exomes previously sequenced by the McGill University and Genome Quebec Innovation Centre. All variants that have previously appeared in two or more samples were discarded. This procedure removes systematic false positives, as well as common polymorphisms. The remaining variants were annotated using ANNOVAR,[16] and visualized using Integrative Genomics Viewer.[17]Additional analyses– such as the identification of regions of homozygosity were performed using custom PERL scripts.

Mutation analysis

The three exons of the main splice isoform of the *CLRN1* gene were PCR amplified on genomic DNA from the proband using previously described primers[18] and sequenced in one direction. Sequence analysis was performed using DNASTAR and compared with Reference Sequence. Mutation nomenclature is according to the Human Genome Variation Society guidelines and uses the A of the ATG translation initiating methionine as number 1. Reference sequences NM_174878.2 and NP_777367 are used for nucleotide and protein numberings, respectively (https://research.cchmc.org/LOVD/). A 144-bp PCR fragment spanning the 5-bp deletion was amplified with another pair of primers, forward, 5′-AAGCAATCCCAGTGAGCATCCAC and reverse, 5′-GGTACAGCCCTAGGGGACCATG and used to investigate the familial segregation of the deletion and its presence in control subjects on 4 % NuSieve: agarose (3:1) gels.

RESULTS

Clinical assessment

At the time of the clinical evaluation, the two affected children were 12 and 17 years old.

Retinitis pigmentosa was diagnosed in both of them based on the presence of mid peripheral bone *spicule*-like pigmentary degeneration, peripheral pigment epithelial atrophy, cellophane epiretinal membrane, and macular pigmentary abnormalities. Both patients reported pre-pubertal signs of RP.

Patients were subjected to a pure tone audiometry with aerial and bone conduction analysis, which revealed severe to profound bilateral neurosensory hearing loss (Figure 1). Hearing loss was slightly milder in the younger sib. An earlier audiogram for the older sib, performed at the age of 6 years, was also available and showed similar hearing impairment (80–85dB), which excluded the progressive nature of the hearing loss. Family history revealed that the older sib pronounced his first words at the age of 3.5 years, which is indicative of a congenital hearing loss. At the time of clinical examination, both patients had had hearing aids since the age of 5–6 years. While the older patient did not benefit much from hearing aids and did not have intelligible speech, his younger brother wore hearing aids all the time, had intelligible speech, and had attended regular school since the age of 5 years. The 17-year-old boy had complete bilateral vestibular areflexia upon caloric stimulation while his younger brother had a mild response in the right ear (17%) and severe hyporeflexia in the left ear (7%).

Based on vestibular abnormalities, Usher type II was excluded in this family, but we could not determine whether the patients have USH1 or USH3. The congenital occurrence of the hearing loss and the absence of its progression in the older patient (III-7) were in favor of Usher type I while the postlingual hearing impairment in the younger sib (III-5) was in favor of USH3, but the absence of a second audiological evaluation for this sib (III-5) prevented us from assessing the progressive nature of the hearing loss. Also, at the time of clinical assessment, in 1995, USH3 was believed to be very rare and restricted to the Finish population. In addition, the clinical overlap between USH1 and USH3 was not documented.

Patient III-7 had an isolated postaxial polydactyly of the upper limbs that were removed by surgery at birth.

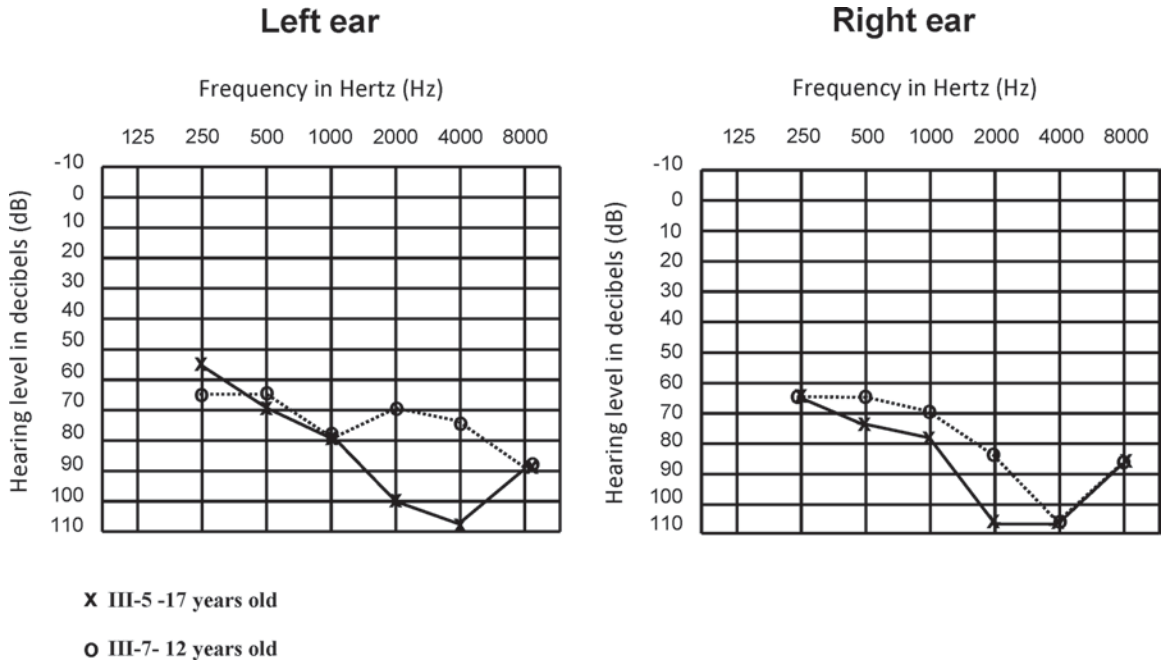

FIGURE 1 Audiograms of the two patients III-5 and III-7 showing degree of hearing loss at the age of 12 and 17 years, respectively.

Exclusion of linkage to four USH loci

Linkage analysis with microsatellite markers around four loci or genes responsible for Usher syndrome type 1, *MYO7A* (locus USH1B on 11q13.5), harmonin (locus USH1C on 11p14.3), *CDH23* (locus USH1D on 10q22), and USH1E (21q) were previously reported and excluded the involvement of these four USH1 loci in the disease phenotype in this family.[19]

Exome capture, sequencing, and mutation analysis

To identify the mutated gene in this family, exome sequencing was performed on DNA from only the proband, III-5. This analysis excluded the causal involvement of two other USH1 genes, *PCDH15* and *USH1G* that were not excluded by linkage analysis based (i) on the absence of homozygosity spanning them, and (ii) the absence of non-synonymous changes, in homozygous or heterozygous states, that are not present in controls. In addition, Exome sequencing revealed the presence of a 5-bp deletion, c.301_305delGTCAT, p.Val101SerfsX27, in exon 2 of the *CLRN1* gene. This deletion was found within a region of 10.3 Mb of homozygosity on chromosome 3 and is predicted to lead to a frameshift and protein truncation after 27 amino acids. The mutation was then confirmed by PCR amplification and direct DNA sequencing of exon 2 in the proband, III-5 (Figure 2). A smaller PCR fragment spanning the deletion was also amplified in all family members, separated by electrophoresis, and used to trace the segregation of the deletion in the family (Figure 2). Sequencing of the two other *CLRN1* exons, 0 and 3, did not reveal any other DNA change in the proband confirming therefore that this 5-bp deletion is responsible for the Usher phenotype in this family. The 5-bp deletion was not found in 93 Lebanese subjects from the general population.

DISCUSSION

To date, only 14 different mutations or variants in *CLRN1* have been identified in a total of 156 patients (http://www.umd.be/USH3A/). Half of these mutations lead to premature termination codons and are likely to result in nonfunctional proteins.[20] Here we describe a novel 5-bp deletion in *CLRN1*, c.301_305delGTCAT, p.Val101SerfsX27, in a Lebanese family with Usher syndrome. The novel mutation is predicted to lead to a frameshift in the second transmembrane domain and result in protein truncation after 27 amino acids.

The differential diagnosis of USH3 and its distinction from the two other types relies mainly on the postlingual occurrence of the hearing loss and its progressive nature. However, patient III-7 pronounced his first words at the age of 3.5 years which is indicative of a prelingual profound hearing loss preventing language development. Moreover, his hearing impairment was stable between the age of 6 and 17 years. The second affected sib, III-5, had intelligible speech which indicates a postlingual hearing loss. Based on these features, the diagnosis of the older sib, III-7, was compatible with USH1 while the diagnosis of the younger sib, III-5, was more compatible with USH3. Therefore, the family could not be classified into USH1 or USH3. Our data are in agreement with a previous report describing

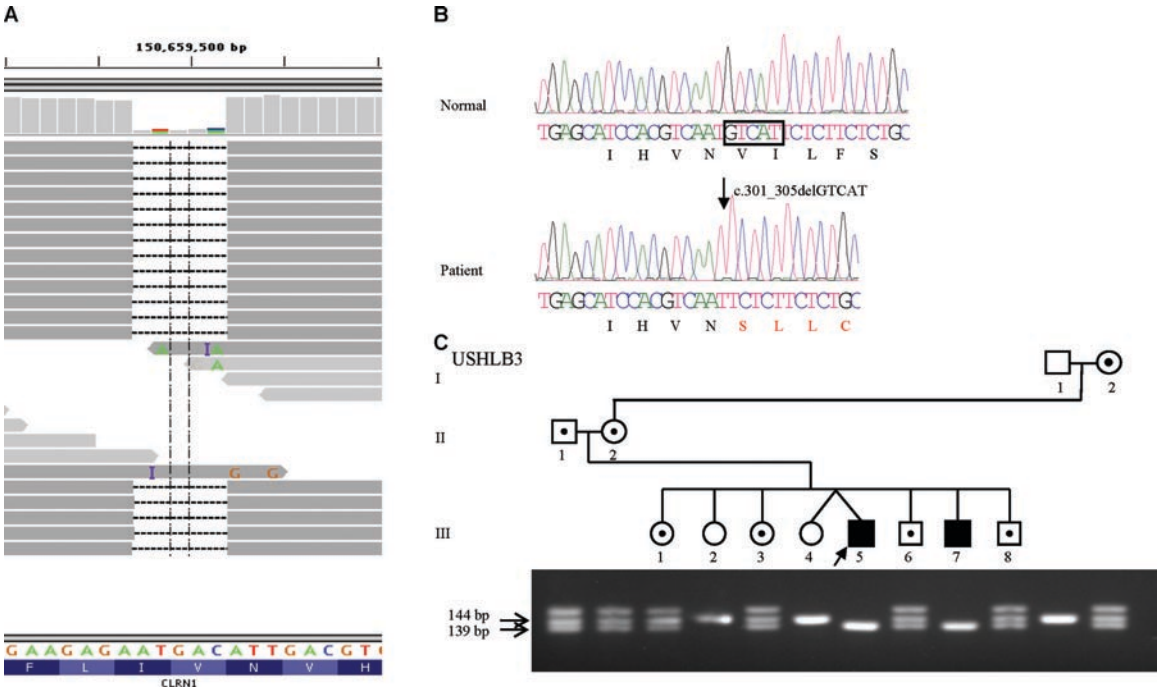

FIGURE 2 Genetic study on the analyzed family. (A) Exome capture and sequencing results in the proband, III-5, showing a 5 bp deletion read aligned on the negative DNA strand. (B) Electropherograms of wild type and mutated clarin 1 showing the 5-bp deletion, c.301_305delGTCAT, p.Val101SerfsX27, on the positive strand of exon 2 of the proband. (C) Pedigree of the family showing the segregation of the mutated (139 bp) and normal (144 bp) alleles. Heterozygous subjects display a third band due to heteroduplex formation between PCR fragments containing wild type and mutated alleles.

a homozygous protein-truncating mutation in *CLRN1*, Y63X, in three patients who had been diagnosed with USH1[21] and suggest that severe *CLRN1* mutations are sometimes associated with severe clinical presentation and can be misdiagnosed as USH1. Also, intra familial and intersubjects (between subjects carrying the same mutation) variability in patients with *CLRN1* mutations has been previously reported[22–24] and may explain differences in the clinical features observed in the two sibs.

USH3 is a rare form of Usher syndrome affecting about 2% of Usher cases in several populations with the exception of the Finnish population and the Ashkenazi Jewish populations where USH3 accounts for 40% of all Usher cases.[23,25] Previous studies from our group and collaborators have described several Lebanese families with linkage to USH2A[12] and one family with mutation in harmonin (USH1C).[26] While the former is a common cause of Usher syndrome in several populations, USH1C is a relatively rare form underlying approximately 7% of all USH1 cases in the US (http://www.ncbi.nlm.nih.gov/books/NBK1265/). Now, we report another rare form of Usher syndrome, caused by defect in *CLRN1*, in a Lebanese family. The presence of the same mutation in the two unrelated parents indicates its inheritance from a common ancestor, which was not completely unexpected since the two parents originate from a small village and the Lebanese population is known to have a high rate of consanguinity, 21%.[27] This 5-bp deletion was absent in 93 Lebanese controls indicating that this mutation is a recent event and is unlikely to be caused by an ancestral widespread founder mutation in this population. Our data highlight the mosaic structure of the Lebanese population and the diversity of the genetic causes underlying its patients with Usher syndrome.

Usher syndrome is a genetically heterogeneous condition with 9 different causative genes, most of which, such as Usherin, *CDH23*, and *MYO7A*, are large and have many exons. Consequently, microarrays have been developed to facilitate mutation screening and reduce its cost, but still this approach allows the detection of less than 40% of mutations depending on the clinical types.[28] In cases with no detected mutations on the microarray, other approaches are needed such us linkage analysis followed by sequencing of all coding exons, which is not possible in small uninformative families. Nowadays the cost of exome sequencing in Canada is approximately $1600 and is expected to go down in the near future. The identification of this novel mutation using exome capture and sequencing of DNA from only the proband illustrates the importance of this new approach as the easiest and fastest approach that may become soon the less expensive one for molecular diagnosis of heterogeneous conditions caused by mutations in large genes.

ACKNOWLEDGMENTS

We thank the patients, their families, and control subjects for their cooperation. We would also like to thank the

staff of the Genome Quebec sequencing platforms for expert help and personal involvement in the exome capture and sequencing. R.S. is supported by a Chercheur Boursier Salary Award, Senior from the FRSQ. This work is supported by the CIHR (grant number MOP 86546) and by internal pilot funding from the McGill University Health Centre Research Institute.

***Declaration of interest*:** The authors report no conflicts of interest. The authors alone are responsible for the content and writing of the paper.

REFERENCES

1. Ahmed ZM, Riazuddin S, Riazuddin S, Wilcox ER. The molecular genetics of Usher syndrome. Clin Genet 2003;63(6):431–44.
2. Keats BJ, Corey DP. The Usher syndromes. Am J Med Genet 1999;89(3):158–66.
3. Petit C. Usher syndrome: from genetics to pathogenesis. Annu Rev Genomics Hum Genet 2001;2:271–97.
4. Kremer H, van Wijk E, Marker T, Wolfrum U, Roepman R. Usher syndrome: molecular links of pathogenesis, proteins and pathways. Hum Mol Genet 2006;15(Spec No. 2):R262–70.
5. Joensuu T, Hamalainen R, Yuan B, Johnson C, Tegelberg S, Gasparini P, et al . Mutations in a novel gene with transmembrane domains underlie Usher syndrome type 3. Am J Hum Genet 2001;69(4):673–84.
6. Vastinsalo H, Jalkanen R, Dinculescu A, Isosomppi J, Geller S, Flannery JG, et al . Alternative splice variants of the USH3A gene Clarin 1 (CLRN1). Eur J Hum Genet 2010;19(1):30–5.
7. Adato A, Vreugde S, Joensuu T, Avidan N, Hamalainen R, Belenkiy O, et al . USH3A transcripts encode clarin-1, a four-transmembrane-domain protein with a possible role in sensory synapses. Eur J Hum Genet 2002;10(6):339–50.
8. Fields RR, Zhou G, Huang D, Davis JR, Moller C, Jacobson SG, et al . Usher syndrome type III: revised genomic structure of the USH3 gene and identification of novel mutations. Am J Hum Genet 2002;71(3):607–17.
9. Hemler ME. Tetraspanin proteins mediate cellular penetration, invasion, and fusion events and define a novel type of membrane microdomain. Annu Rev Cell Dev Biol 2003;19:397–422.
10. Hemler ME. Tetraspanin functions and associated microdomains. Nat Rev Mol Cell Biol 2005;6(10):801–11.
11. Hubner K, Windoffer R, Hutter H, Leube RE. Tetraspan vesicle membrane proteins: synthesis, subcellular localization, and functional properties. Int Rev Cytol 2002;214:103–59.
12. Saouda M, Mansour A, Bou Moglabey Y, El Zir E, Mustapha M, Chaib H, et al . The Usher syndrome in the Lebanese population and further refinement of the USH2A candidate region. Hum Genet 1998;103(2):193–8.
13. Lalonde E, Albrecht S, Ha KC, Jacob K, Bolduc N, Polychronakos C, et al . Unexpected allelic heterogeneity and spectrum of mutations in Fowler syndrome revealed by next-generation exome sequencing. Hum Mutat 2010;31(8):918–23.
14. Li H, Handsaker B, Wysoker A, Fennell T, Ruan J, Homer N, et al . The Sequence Alignment/Map format and SAMtools Bioinformatics 2009;25(16):2078–9.
15. Li H, Durbin R. Fast and accurate short read alignment with Burrows-Wheeler transform. Bioinformatics 2009;25(14):1754–60.
16. Wang K, Li M, Hakonarson H. ANNOVAR: functional annotation of genetic variants from high-throughput sequencing data. Nucleic Acids Res 2010;38(16):e164.
17. Robinson JT, Thorvaldsdottir H, Winckler W, Guttman M, Lander ES, Getz G, et al . Integrative genomics viewer. Nat Biotechnol. 2011;29(1):24–6.
18. Ebermann I, Wilke R, Lauhoff T, Lubben D, Zrenner E, Bolz HJ. Two truncating USH3A mutations, including one novel, in a German family with Usher syndrome. Mol Vis 2007;13:1539–47.
19. Chaib H, Kaplan J, Gerber S, Vincent C, Ayadi H, Slim R, et al . A newly identified locus for Usher syndrome type I, USH1E, maps to chromosome 21q21. Hum Mol Genet 1997;6(1):27–31.
20. Isosomppi J, Vastinsalo H, Geller SF, Heon E, Flannery JG, Sankila EM. Disease-causing mutations in the CLRN1 gene alter normal CLRN1 protein trafficking to the plasma membrane. Mol Vis 2009;15:1806–18.
21. Aller E, Jaijo T, Oltra S, Alio J, Galan F, Najera C, et al . Mutation screening of USH3 gene (clarin-1) in Spanish patients with Usher syndrome: low prevalence and phenotypic variability. Clin Genet 2004;66(6):525–9.
22. Plantinga RF, Kleemola L, Huygen PL, Joensuu T, Sankila EM, Pennings RJ, Cremers CW. Serial audiometry and speech recognition findings in Finnish Usher Syndrome Type III patients. Audiol Neurootol 2005;10:79–89.
23. Ness SL, Ben-Yosef T, Bar-Lev A, Madeo AC, Brewer CC, Avraham KB, et al . Genetic homogeneity and phenotypic variability among Ashkenazi Jews with Usher syndrome type III. J Med Genet 2003;40(10):767–72.
24. Pennings RJ, Fields RR, Huygen PL, Deutman AF, Kimberling WJ, Cremers CW. Usher syndrome type III can mimic other types of Usher syndrome. Ann Otol Rhinol Laryngol 2003;112(6):525–30.
25. Pakarinen L, Karjalainen S, Simola KO, Laippala P, Kaitalo H. Usher's syndrome type 3 in Finland. Laryngoscope 1995;105(6):613–7.
26. Verpy E, Leibovici M, Zwaenepoel I, Liu XZ, Gal A, Salem N, et al . A defect in harmonin, a PDZ domain-containing protein expressed in the inner ear sensory hair cells, underlies Usher syndrome type 1C. Nat Genet 2000;26(1):51–5.
27. Kaloustian VM. Genetic disorders in Lebanon. In: Teebi AS, editor. Genetic disorders among Arab populations, 2nd edn. Berlin Heidelberg: Springer, 2010; 377–441.
28. Jaijo T, Aller E, Garcia-Garcia G, Aparisi MJ, Bernal S, Avila-Fernandez A, et al . Microarray-based mutation analysis of 183 Spanish families with Usher syndrome. Invest Ophthalmol Vis Sci 2010;51(3):1311–7.